Black Holes

Volker Perlick (perlick@zarm.uni-bremen.de)

Summer Term 2022, University of Bremen

Lectures: Thu 10-12, NW1, N3130
Fr 14–15, NW1, N1250
Tutorials: Fr 15–16, NW1, N1250

General Relativity text-books with detailed sections on black holes:

L. Ryder: "Introduction to General Relativity" Cambridge University Press (2009)

N. Straumann: "General Relativity and Relativistic Astrophysics" Springer (1984)

C. Misner, K. Thorne and J. Wheeler: "Gravitation" Freeman (1973)

R. Wald: "General Relativity" Chicago University Press (1984)

Monographs:

V. Frolov and I. Novikov: "Black Hole Physics" Kluwer (1998)

S. Hawking and G. Ellis: "The Large-Scale Structure of Space-time" Cambridge University Press (1973)

B. O'Neill: "The Geometry of Kerr Black Holes" A. K. Peters (1995)

S. Chandrasekhar: "The Mathematical Theory of Black holes" Oxford University Press (1984)

Contents

1 Historic introduction

1783 J. Michell speculates in a letter to H. Cavendish if there might exist "dark bodies" that are so dense that light cannot escape from their surface (see Worksheet 1).

1796 P. S. Laplace calculates, independently of J. Michell, on what condition the escape velocity from the surface of a body is bigger than the velocity of light. (Laplace's calculation can be found in an Appendix of the book by Hawking and Ellis.)

1915 A. Einstein publishes the field equation of general relativity.

1916 K. Schwarzschild finds the spherically symmetric (and static) solution to Einstein's vacuum field equation. The same solution is also found, independently and only a little later, by J. Droste. It features a "singularity" at the *Schwarzschild radius* $r_S = 2GM/c^2$ which is not understood for decades.

1916 H. Reissner and two years later G. Nordström find the spherically symmetric (and static) solution to the Einstein-Maxwell equations. The same solution is found independently by H. Weyl. It is usually called the Reissner-Nordström solution.

1918 F. Kottler finds the unique spherically symmetric (and static) solution to Einstein's vacuum field equation with a cosmological constant.

1939 R. Oppenheimer and H. Snyder calculate the gravitational collapse of a spherically symmetric ball of dust. They find that a curvature singularity is formed within a finite time.

1958 D. Finkelstein explains the character of the sphere $r = r_S$ in the Schwarzschild solution as a "one-way membrane", nowadays called an "event horizon". Related articles appear in the years 1958 to 1960 by G. Szekeres, M. Kruskal and C. Frønsdal. The notion of an (event) horizon had been introduced already in 1955 by W. Rindler in the context of cosmology.

1963 R. Kerr finds a solution to Einstein's vacuum field equation that describes, in modern terminology, a rotating black hole.

1965 E. Newman and collaborators find the solution to the Einstein-Maxwell equations that describes rotating charged black holes, known as the Kerr-Newman solution.

1963-1969 R. Penrose and S. Hawking prove a series of theorems to the effect that the formation of a singularity is inevitable once a collapse process has started in a spacetime that solves Einstein's field equation with an energy-momentum tensor that satisfies certain "energy conditions". In 2020 R. Penrose receives 50 % of the Nobel Prize in Physics for this work.

1967 J. Wheeler uses the word "black hole", supposedly for the first time, in a talk in New York. The first page of the written version of this talk, with Wheeler's annotations, can be found in the book by Frolov and Novikov.

1967-1984 For black holes with mass, angular momentum and electric charge, uniqueness theorems ("no-hair theorems") are proven.

1969 R. Penrose formulates the "cosmic censorship hypothesis", saying that under certain physically reasonable assumptions gravitational collapse will never result in a naked singularity, i.e., a singularity without a horizon.

1973-1974 J. Bekenstein and S. Hawking formulate the thermodynamical laws of black holes. S. Hawking predicts that black holes decay by emitting black-body radiation ("Hawking radiation").

Observational evidence for the existence of black holes:

- Supermasive black holes ($10^6 - 10^{10} M_\odot$): There is very good evidence for their existence, as we will discuss later. The best known candidates are the object at the centre of our Galaxy, associated with the radio source Sgr A*, with $4 \times 10^6 M_\odot$ and the object at the centre of the galaxy M87, associated with the radio source M87*, with $6 \times 10^9 M_\odot$. It is widely believed that most, if not all, galaxies host black holes at their centres. For the observation with infrared telescopes of stars in the neighbourhood of Sgr A* R. Genzel and A. Ghez won 50 % of the Nobel Prize in Physics 2020. In 2017 the Event Horizon Telescope Collaboration produced a picture of the "shadow" of the object at the centre of M87, which was released with a lot of media covering in 2019.

- Intermediate black holes ($10^2 - 10^3 M_\odot$): They are much more hypothetical than supermassive black holes. They may exist at the centres of some globular clusters, possibly also near the centres of galaxies.

- Stellar black holes ($3 - 100\, M_\odot$): For this class of black holes the observational evidence for their existence is also very good. The oldest candidate for a stellar black hole is associated with the X-ray source Cyg X-1, believed to be a black hole of about $12 M_\odot$ in a binary system. Moreover, since 2015 the gravitational wave detectors LIGO and Virgo have observed about hundred events (as of spring 2022) most of which are assumed to have been produced by the merger of two stellar black holes. Some of them are thought to result from the merger of a stellar black hole with a neutron star, some others from the merger of two neutron stars. For the observation of gravitational waves with the LIGO detectors R. Weiss, K. Thorne and B. Barrish won the Nobel Prize in Physics 2017.

- Mini black holes (less than $1\, M_\odot$, possibly down to the Planck mass of approx. 10^{-8} kg): They are hypothetical. They may have been produced at a very early stage of the universe, in which case they are called "primordial black holes". Even more speculative is the idea that they may be produced from cosmic rays in our atmosphere or in accelerators. If they exist, they are expected to decay quickly by emitting Hawking radiation.

2 Brief review of general relativity

A general-relativistic spacetime is a pair (M, g) where:

- M is a four-dimensional manifold; local coordinates will be denoted (x^0, x^1, x^2, x^3) and Einstein's summation convention will be used for greek indices $\mu, \nu, \sigma, \ldots = 0, 1, 2, 3$ and for latin indices $i, j, k, \ldots = 1, 2, 3$.
- g is a Lorentzian metric on M, i.e. a covariant second-rank tensor field, $g = g_{\mu\nu} dx^\mu \otimes dx^\nu$, that is
  (a) symmetric, $g_{\mu\nu} = g_{\nu\mu}$, and
  (b) non-degenerate with Lorentzian signature, i.e., for any $p \in M$ there are coordinates defined near p such that $g|_p = -(dx^0)^2 + (dx^1)^2 + (dx^2)^2 + (dx^3)^2$.

As the metric is non-degenerate, we may introduce contravariant metric components by

$$g^{\mu\nu} g_{\nu\sigma} = \delta^\mu_\sigma \,. \tag{1}$$

We use $g^{\mu\nu}$ and $g_{\sigma\tau}$ for raising and lowering indices, e.g.

$$g_{\rho\tau} A^\tau = A_\rho \,, \qquad B_{\mu\nu} g^{\nu\tau} = B_\mu{}^\tau \,. \tag{2}$$

The metric contains all information about the spacetime geometry and thus about the gravitational field. In particular, the metric determines the following.

- The causal structure of spacetime:

  A curve $s \mapsto x(s) = \big(x^0(s), x^1(s), x^2(s), x^3(s)\big)$ is called

  $$\left.\begin{array}{l}\text{spacelike}\\ \text{lightlike}\\ \text{timelike}\end{array}\right\} \iff g_{\mu\nu}\big(x(s)\big)\dot{x}^\mu(s)\dot{x}^\nu(s) \left\{\begin{array}{l} > 0\\ = 0\\ < 0\end{array}\right.$$

  Timelike curves describe motion at subluminal speed and lightlike curves describe motion at the speed of light. Spacelike curves describe motion at superluminal speed which is forbidden for signals.

  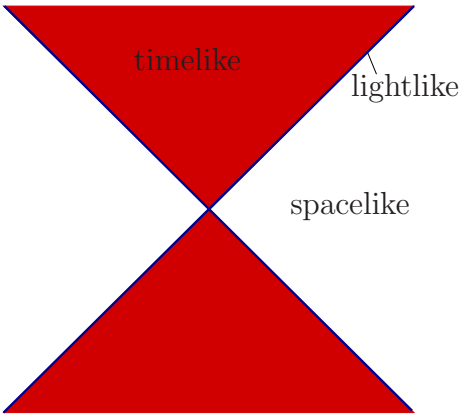

  For timelike curves we can choose the parametrisation such that $g_{\mu\nu}\big(x(\tau)\big)\dot{x}^\mu(\tau)\dot{x}^\mu(\tau) = -c^2$. The parameter τ is then called *proper time*.

  The motion of a material continuum, e.g. of a fluid, can be described by a vector field $U = U^\mu \partial_\mu$ with $g_{\mu\nu} U^\mu U^\nu = -c^2$. The integral curves of U are to be interpreted as the worldlines of the fluid elements.

- The geodesics:

  By definition, the geodesics are the solutions to the Euler-Lagrange equations

  $$\frac{d}{ds}\frac{\partial \mathcal{L}(x, \dot{x})}{\partial \dot{x}^\mu} - \frac{\partial \mathcal{L}(x, \dot{x})}{\partial x^\mu} = 0 \tag{3}$$

of the Lagrangian

$$\mathcal{L}\big(x,\dot{x}\big) \;=\; \frac{1}{2}\, g_{\mu\nu}(x)\dot{x}^\mu\dot{x}^\nu \;. \tag{4}$$

These Euler-Lagrange equations take the form

$$\ddot{x}^\mu \;+\; \Gamma^\mu{}_{\nu\sigma}(x)\dot{x}^\nu\dot{x}^\sigma \;=\; 0 \tag{5}$$

where

$$\Gamma^\mu{}_{\nu\sigma} \;=\; \frac{1}{2}\, g^{\mu\tau}\left(\,\partial_\nu g_{\tau\sigma} \;+\; \partial_\sigma g_{\tau\nu} \;-\; \partial_\tau g_{\nu\sigma}\,\right) \tag{6}$$

are the socalled Christoffel symbols.

The Lagrangian $\mathcal{L}(x,\dot{x})$ is constant along a geodesic (see Worksheet 1), so we can speak of timelike, lightlike and spacelike geodesics. Timelike geodesics ($\mathcal{L}<0$) are to be interpreted as the worldlines of freely falling particles, and lightlike geodesics ($\mathcal{L}=0$) are to be interpreted as light rays.

The Christoffel symbols define a *covariant derivative* that takes tensor fields into tensor fields, e.g.

$$\nabla_\nu U^\mu \;=\; \partial_\nu U^\mu \;+\; \Gamma^\mu{}_{\nu\tau}U^\tau \;, \tag{7}$$

$$\nabla_\nu A_\mu \;=\; \partial_\nu A_\mu \;-\; \Gamma^\rho{}_{\nu\mu}A_\rho \;. \tag{8}$$

- The curvature.

  The Riemannian curvature tensor is defined, in coordinate notation, by

$$R_{\mu\nu\sigma}{}^\tau \;=\; \partial_\mu\Gamma^\tau{}_{\nu\sigma} \;-\; \partial_\nu\Gamma^\tau{}_{\mu\sigma} \;+\; \Gamma^\tau{}_{\mu\rho}\Gamma^\rho{}_{\nu\sigma} \;-\; \Gamma^\tau{}_{\nu\rho}\Gamma^\rho{}_{\mu\sigma}\,. \tag{9}$$

  The curvature tensor determines the relative motion of neighbouring geodesics: If $X = X^\mu\partial_\mu$ is a vector field whose integral curves are geodesics, and if $J = J^\nu\partial_\nu$ connects neighbouring integral curves of X (i.e., if the Lie bracket between X and J vanishes), then the *equation of geodesic deviation* or *Jacobi equation* holds:

$$\big(X^\mu\nabla_\mu\big)\big(X^\nu\nabla_\nu\big)J^\sigma \;=\; R_{\mu\nu\rho}{}^\sigma X^\mu J^\nu X^\rho \;. \tag{10}$$

  If the integral curves of X are timelike, they can be interpreted as worldlines of freely falling particles. In this case the curvature term in the Jacobi equation gives the *tidal force* produced by the gravitational field.

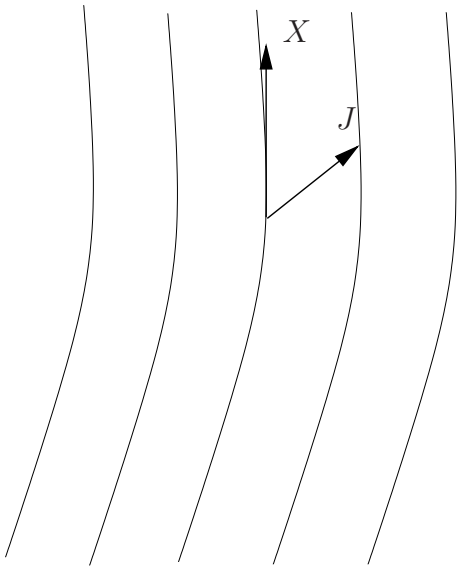

  From the Riemannian curvature tensor one forms the Ricci tensor

$$R_{\nu\sigma} = R_{\mu\nu\sigma}{}^\mu \tag{11}$$

  and the scalar curvature

$$R = R_{\mu\nu}g^{\mu\nu} \;. \tag{12}$$

The spacetime metric is determined, in terms of its sources, by *Einstein's field equation*

$$R_{\mu\nu} \, - \, \frac{R}{2} \, g_{\mu\nu} \, + \, \Lambda \, g_{\mu\nu} \, = \, \kappa \, T_{\mu\nu} \, . \tag{13}$$

The curvature quantity

$$G_{\mu\nu} \, = \, R_{\mu\nu} \, - \, \frac{R}{2} \, g_{\mu\nu} \tag{14}$$

is called the *Einstein tensor field*, Λ is called the *cosmological constant*, and κ is called *Einstein's gravitational constant*.

Based on cosmological observations we believe that we live in a universe with a positive cosmological constant that is of the order of $\Lambda \approx 10^{-52}\mathrm{m}^{-2}$ so that it can be neglected on non-cosmological scales.

Einstein's gravitational constant is related to Newton's gravitational constant G according to $\kappa = 8\pi G/c^4$ as follows from the Newtonian limit of Einstein's theory.

Transvecting Einstein's field equation with $g^{\mu\nu}$ yields

$$- \, R \, + \, 4 \, \Lambda \, g_{\mu\nu} \, = \, \kappa \, T_{\mu\nu} g^{\mu\nu} \, . \tag{15}$$

Re-inserting this expression into Einstein's field equation demonstrates that the latter can be equivalently rewritten as

$$R_{\mu\nu} = \Lambda \, g_{\mu\nu} \, + \, \kappa \left(T_{\mu\nu} - \frac{1}{2} \, T_{\rho\sigma} g^{\rho\sigma} g_{\mu\nu} \right) . \tag{16}$$

The energy-momentum tensor $T_{\mu\nu}$ depends on the matter model that is used for the source of the gravitational field. The most important cases are the following.

- Vacuum: $T_{\mu\nu} = 0$
  Then the field equation simplifies to $R_{\mu\nu} = \Lambda g_{\mu\nu}$. The cosmological constant is relevant only on cosmological scales, otherwise the vacuum field equation can be simplified to $R_{\mu\nu} = 0$. The vacuum field equation looks simple but it is a system of ten scalar second-order coupled non-linear partial differential equations for the ten independent metric coefficients $g_{\mu\nu}$. In this course we will discuss the Schwarzschild metric (the unique spherically symmetric solution of the equation $R_{\mu\nu} = 0$), the Kottler metric (generalisation of the Schwarzschild metric to the case $\Lambda \neq 0$) and the Kerr metric (solution of $R_{\mu\nu} = 0$ that describes a rotating black hole).

- Perfect fluid: $T_{\mu\nu} = \left(\varepsilon \, + \, p \right) \dfrac{U_\mu U_\nu}{c^2} \, + \, p \, g_{\mu\nu}$

  Here U^μ is the four-velocity field of the fluid, normalised according to $g_{\mu\nu} U^\mu U^\nu = -c^2$, which means that the integral curves of U^μ are parametrised by proper time; ε is the energy density in the rest system of the fluid and p is the pressure. For solving Einstein's field equation with a perfect-fluid source, one has to specify an equation of state linking the pressure p to the density ε. The simplest equation of state is that for a "dust", $p = 0$. In this case ε/c^2 is just the rest-mass density. Once an equation of state has been specified, Einstein's equation together with the Euler equation gives a system of partial differential equations for the $g_{\mu\nu}$, the four-velocity U^ρ and the density ε. In this course we will consider, among other things, a spherically symmetric collapsing ball of dust.

- Electrovacuum: $T_{\mu\nu} = F_{\mu\alpha}F_{\nu}{}^{\alpha} - \frac{1}{4}g_{\mu\nu}F_{\alpha\beta}F^{\alpha\beta}$

  Here $F_{\mu\nu}$ is the electromagnetic field strength, $F_{\mu\nu} = -F_{\nu\mu}$. In this case Einstein's field equation together with Maxwell's equations gives a system of partial differential equations for the $g_{\mu\nu}$ and the $F_{\mu\nu}$. The best-known electrovacuum solution without a cosmological constant is the Reissner-Nordström solution (field outside of a charged spherically symmetric static object) which will be treated later in this course.

3 Schwarzschild black holes

3.1 The Schwarzschild metric in Schwarzschild coordinates

The Schwarzschild metric, found by Karl Schwarzschild and independently by J. Droste in 1916, is the unique spherically symmetric solution to Einstein's vacuum field equation without a cosmological constant, $R_{\mu\nu} = 0$. The derivation is a subject for a first course on General Relativity and will not be repeated here. The metric reads

$$g_{\mu\nu}dx^{\mu}dx^{\nu} = -\left(1 - \frac{r_S}{r}\right)c^2\,dt^2 + \frac{dr^2}{\left(1 - \frac{r_S}{r}\right)} + r^2\left(d\vartheta^2 + \sin^2\vartheta\,d\varphi^2\right). \tag{17}$$

It depends on a parameter r_S, called the Schwarzschild radius, with the dimension of a length. For a celestial body of radius $r_\star(t)$ the metric is valid in the exterior region where we have vacuum, i.e., the range of the coordinates is

$$t \in \mathbb{R}\,, \quad r \in \left]\, r_*(t), \infty \,\right[\,, \quad (\vartheta, \varphi) \in S^2\,. \tag{18}$$

The meaning of the parameter r_S follows from comparison with the Newtonian limit:

$$r_S = \frac{2GM}{c^2} \tag{19}$$

where G is Newton's gravitational constant, c is the vacuum speed of light and M is the mass of the central body. On often uses the mass parameter

$$m = GM/c^2 \tag{20}$$

which has the dimension of a length. Then $r_S = 2m$.

For $M = M_\odot$ we have $r_S \approx 3\,\mathrm{km}$. As a consequence, for all stars and all planets we have $r_S < r_*(t)$ so that in these cases there is no problem with the zero in the denominator of g_{rr} at $r = r_S$. The idea of a body with radius smaller than r_S leads to the notion of a Schwarzschild black hole as will be discussed in detail below.

We list some properties of the Schwarzschild metric.

- The Schwarzschild metric is *asymptotically flat*, i.e., it approaches the Minkowski metric for $r \to \infty$. Indeed, if r_S/r is negligibly small in comparison to 1, the Schwarzschild metric is

  $$g_{\mu\nu}dx^{\mu}dx^{\nu} \approx -c^2\,dt^2 + dr^2 + r^2\left(d\vartheta^2 + \sin^2\vartheta\,d\varphi^2\right). \tag{21}$$

  which is the Minkowski metric in spherical polar coordinates.

- The Schwarzschild metric is static (in the domain $r > r_S$), i.e., it admits a timelike Killing vector field that is hypersurface-orthogonal. Indeed, the vector field ∂_t (which is timelike in the domain $r > r_S$) is (i) a Killing vector field, $\partial_t g_{\mu\nu} = 0$, and (ii) orthogonal to the hypersurfaces $t =$ constant, $g_{tr} = g_{t\vartheta} = g_{t\varphi} = 0$. The fact that a spherically symmetric solution to Einstein's vacuum field equation is necessarily static was proven by J. T. Jebsen in 1921 and independently by G. Birkhoff in 1923; we refer to it as to the *Jebsen-Birkhoff theorem*. (Schwarzschild and Droste had *assumed* staticity in their derivations.)

- The r coordinate has the following geometric meaning. For a circle C in the equatorial plane

$$t = t_0\,, \quad r = r_0\,, \quad \vartheta = \pi/2\,, \quad 0 < \varphi < 2\pi \tag{22}$$

the circumference can be read from the metric,

$$\ell_{r_0} = \int_C \sqrt{g_{\mu\nu}\,\frac{dx^\mu}{ds}\,\frac{dx^\nu}{ds}}\,ds = \int_C \sqrt{g_{\varphi\varphi}\left(\frac{d\varphi}{ds}\right)^2}\,ds$$

$$= \int_C \sqrt{r_0^2\left(\frac{d\varphi}{ds}\right)^2}\,ds = \int_0^{2\pi} r_0\,d\varphi = 2\,\pi\,r_0\,. \tag{23}$$

Hence, the length of a rope laid out along this circle is given by the formula for the circumference of a circle that is familiar from Euclidean geometry. Similarly, one finds that the area of a sphere $t = t_0$, $r = r_0$ equals $4\pi r_0^2$ which is again the usual Euclidean formula. For this reason, r is sometimes called the *area coordinate*. – By contrast, for a radial line segment S

$$t = t_0\,, \quad r_1 < r < r_2\,, \quad \vartheta = \vartheta_0\,, \quad \varphi = \varphi_0 \tag{24}$$

the length is

$$\ell_{r_1 r_2} = \int_S \sqrt{g_{\mu\nu}\,\frac{dx^\mu}{ds}\,\frac{dx^\nu}{ds}}\,ds = \int_S \sqrt{g_{rr}\left(\frac{dr}{ds}\right)^2}\,ds$$

$$= \int_{r_1}^{r_2} \sqrt{g_{rr}}\,dr = \int_{r_1}^{r_2} \frac{dr}{\sqrt{1 - \dfrac{r_s}{r}}} \neq r_2 - r_1\,. \tag{25}$$

This demonstrates that r cannot be interpreted as a distance from a centre.

For a hypothetical star with a radius smaller than r_S, the metric in the exterior has a "singularity" at $r = r_S$. The correct interpretation of this singularity was an unsolved problem until the late 1950s. It is the metric coefficient $g_{rr} = g(\partial_r, \partial_r)$ that diverges to infinity at $r = r_S$. This does not necessarily indicate a pathology of the metric; it could very well be that the metric is perfectly regular at $r = r_S$, and that it is the coordinate basis vector field ∂_r that causes the divergence. Then we would only have a "coordinate singularity" at $r = r_S$ that could be removed by a coordinate transformation.

As the Schwarzschild metric is a vacuum solution, $R_{\mu\nu} = 0$, the curvature invariants $R = R_{\mu\nu}g^{\mu\nu}$ and $R_{\mu\nu}R^{\mu\nu}$ vanish identically and give no information. So the simplest curvature

invariant that does give some information is the socalled *Kretschmann scalar* $R_{\mu\nu\rho\sigma}R^{\mu\nu\rho\sigma}$. For the Schwarzschild metric one finds

$$R_{\mu\nu\rho\sigma}R^{\mu\nu\rho\sigma} \;=\; \frac{4\,r_S^2}{r^6}\;. \tag{26}$$

This demonstrates that there is a curvature singularity at $r = 0$ (if we extend the vacuum Schwarzschild solution that far), but it gives us some hope that at $r = r_S$ we might have only a coordinate singularity. This is indeed true. We will discuss below four coordinate systems (Eddington-Finkelstein, Kruskal-Szekeres, Painlevé-Gullstrand and Lemaître) in which the metric is regular at $r = r_S$. We will then see that a spherically symmetric star with radius $r_*(t) < r_S$ necessarily forms a black hole.

3.2 The Schwarzschild metric in other coordinates

(a) Isotropic coordinates

Starting from Schwarzschild coordinates, we define a coordinate transformation that changes only the radial coordinate, $(t, r, \vartheta, \varphi) \mapsto (t, \tilde{r}, \vartheta, \varphi)$, where

$$\tilde{r} \;=\; \frac{1}{2}\Big(\,\sqrt{r^2 - r_S r}\;+\;r\;-\;\frac{r_S}{2}\,\Big)\,. \tag{27}$$

Solving (27) for r yields

$$r \;=\; \frac{\Big(\,\tilde{r}\;+\;\dfrac{r_S}{4}\,\Big)^2}{\tilde{r}}\,, \tag{28}$$

hence

$$dr \;=\; \Big(\,\tilde{r}\;+\;\frac{r_S}{4}\,\Big)\Big(\,\tilde{r}\;-\;\frac{r_S}{4}\,\Big)\,\frac{d\tilde{r}}{\tilde{r}^2} \tag{29}$$

and substituting for r and dr in the Schwarzschild metric yields

$$\begin{aligned} g_{\mu\nu}dx^\mu dx^\nu \;&=\; -\left(\,1\;-\;\frac{r_S\tilde{r}}{\big(\tilde{r}+\frac{r_S}{4}\big)^2}\,\right)c^2dt^2\;+\;\frac{\Big(\,\tilde{r}\;+\;\dfrac{r_S}{4}\,\Big)^2\Big(\,\tilde{r}\;-\;\dfrac{r_S}{4}\,\Big)^2 d\tilde{r}^2}{\left(1-\dfrac{r_S\tilde{r}}{\Big(\tilde{r}+\dfrac{r_S}{4}\Big)^2}\right)\tilde{r}^4} \\ &\qquad +\frac{\Big(\tilde{r}+\dfrac{r_S}{4}\Big)^4}{\tilde{r}^2}\,\Big(\,d\vartheta^2\;+\;\sin^2\vartheta\,d\varphi^2\,\Big) \\ &=\; -\frac{\Big(\,\tilde{r}\;-\;\dfrac{r_S}{4}\,\Big)^2}{\Big(\,\tilde{r}\;+\;\dfrac{r_S}{4}\,\Big)^2}\,c^2dt^2\;+\;\frac{\Big(\,\tilde{r}\;+\;\dfrac{r_S}{4}\,\Big)^4}{\tilde{r}^4}\Big(d\tilde{r}^2+\tilde{r}^2\big(\,d\vartheta^2\;+\;\sin^2\vartheta\,d\varphi^2\,\big)\Big)\,. \end{aligned} \tag{30}$$

The interesting property of isotropic coordinates is that now the spatial part of the metric is conformal to the 3-dimensional Euclidean metric $d\tilde{r}^2+\tilde{r}^2\big(d\vartheta^2+\sin^2\vartheta\,d\varphi^2\big)$. As a conformal factor

does not change angles, the angles between spatial curves represented in isotropic coordinates correspond to the physical angles (i.e., to the ones as measured with the physically correct metric).

Isotropic coordinates are often used for practical caluclations, e.g. in the parametrized post-Newtonian (pPN) approximation formalism.

The pathological value $r = r_S$ corresponds to $\tilde{r} = r_S/4$. At this point, there is no zero in the denominator but the metric coefficient g_{tt} vanishes, so the matrix $\big(g_{\mu\nu}\big)$ becomes degenerate which means that the inverse metric coefficients $g^{\mu\nu}$ don't exist. Thus, in isotropic coordinates the pathological value of the radius coordinate is just shifted to another coordinate position but nothing is gained in view of extending the metric.

(b) Tortoise coordinates

Again we start from Schwarzschild coordinates and transform only the radial coordinate into a new radial coordinate, $(t, r, \vartheta, \varphi) \mapsto (t, \hat{r}, \vartheta, \varphi)$, where

$$\hat{r} \;=\; r \,+\, r_S \ln\Big|\, \frac{r}{r_S} \,-\, 1 \,\Big|\,, \tag{31}$$

$$d\hat{r} \;=\; \frac{r\, dr}{r - r_S}\,. \tag{32}$$

This gives a transcendental equation for r as a function of $\hat{r}$, i.e., the inverse transformation cannot be written in terms of elementary functions, but it is well defined: There is a bijective relation between r running from r_S to ∞ and $\hat{r}$ running from $-\infty$ to ∞.

$\hat{r}$ was called the "tortoise coordinate" by John Wheeler, alluding to Zeno's paradox of Achilles' race against the tortoise. Just as (according to Zeno's argument) Achilles never reaches the tortoise, the coordinate $\hat{r}$ never reaches the point where $r = r_S$ (because it is shifted to $-\infty$).

The tortoise coordinate is important, among other things, for solving wave equations on the Schwarzschild background. Just as the isotropic radius coordinate, it does not help extending the metric beyond $r = r_S$.

(c) Eddington-Finkelstein coordinates

As before, we start out from Schwarzschild coordinates, but this time we transform the time coordinate, $(t, r, \vartheta, \varphi) \mapsto (t', r, \vartheta, \varphi)$ where t' depends on t and r. We will do this in such a way that ingoing radial lightlike geodesics are mapped onto straight lines in the new coordinates. We will see that in these new coordinates the metric coefficients are regular in the whole domain $0 < r < \infty$.

A radial lightlike curve has to satisfy the equations

$$g_{\mu\nu}\, \frac{dx^\mu}{ds}\, \frac{dx^\nu}{ds} \;=\; 0\,, \qquad \frac{d\vartheta}{ds} \;=\; \frac{d\varphi}{ds} \;=\; 0\,. \tag{33}$$

Owing to the symmetry, any such curve must be a geodesic (if the parameter s is chosen appropriately), i.e., the worldline of a classical photon. If we insert the $g_{\mu\nu}$ of the Schwarzschild metric, we get

$$0 \;=\; -\,c^2\left(1\,-\,\frac{r_S}{r}\right)\left(\frac{dt}{ds}\right)^2 \,+\, \frac{1}{\left(1\,-\,\frac{r_S}{r}\right)}\left(\frac{dr}{ds}\right)^2 ,$$

$$\left(\frac{dr}{ds}\frac{ds}{dt}\right)^2 \;=\; c^2\left(1\,-\,\frac{r_S}{r}\right)^2 ,$$

$$\frac{dr}{dt} \;=\; \pm\, c\left(1\,-\,\frac{r_S}{r}\right) , \tag{34}$$

Here the upper sign holds for outgoing photons and the lower sign holds for ingoing photons. Integrating (34) results in

$$\begin{aligned} \pm\, c \int dt \;&=\; \int \frac{dr}{\left(1\,-\,\frac{r_S}{r}\right)} \;=\; \int \frac{\left(r\,-\,r_S\,+\,r_S\right) dr}{r\,-\,r_S} \\ &=\; \int dr \,+\, r_S \int \frac{dr}{r\,-\,r_S} , \end{aligned} \tag{35}$$

hence

$$\pm\, c\, t \;=\; r \,+\, r_S \ln\!\left|r - r_S\right| \,+\, C\,. \tag{36}$$

It is convenient to write the integration constant in the form

$$C \;=\; -\,r_S \ln(r_S) \,+\, c\, t_0\,. \tag{37}$$

Then the equations for radial lightlike geodesics read

$$\pm\, c\, t \;=\; r \,+\, r_S \ln\!\left|\,\frac{r}{r_S}\,-\,1\,\right| \,+\, c\, t_0 \tag{38}$$

where we recognise the tortoise coordinate on the right-hand side. The equations for radial lightlike geodesics hold on the domain $r_S < r < \infty$ and on the domain $0 < r < r_S$ (if we assume that there is vacuum). If we approach r_S from above, we have $t \to -\infty$ along outgoing and $t \to \infty$ along ingoing lightlike geodesics.

The diagram shows ingoing and outgoing radial lightlike geodesics in the exterior region $r_S < r < \infty$ and in the interior region $0 < r < r_S$. In either region the Schwarzschild metric is regular. However, the two regions are separated by the surface $r = r_S$ which shows a singular behaviour in the Schwarzschild coordinates. None of our lightlike geodesics reaches this surface at a finite coordinate time. As the angular coordinates are not shown, any point in this diagram represents a sphere.

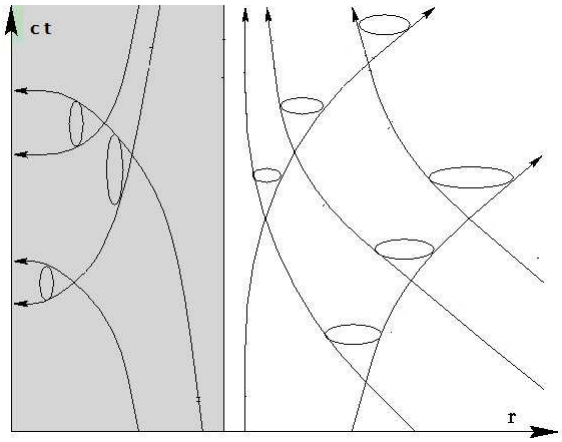

In the interior region r and t have interchanged their causal character: r is a time coordinate, $g_{rr} < 0$, and t is a space coordinate, $g_{tt} > 0$. While in the exterior region t cannot stand still along an observer's worldline, in the interior region r cannot stand still along an observer's worldline. As the Killing vector field ∂_t is not timelike in the interior, in this region the Schwarzschild metric is not static.

	$0 < r < r_S$	$r_S < r < \infty$
∂_r	timelike	spacelike
∂_t	spacelike	timelike

We now transform from Schwarzschild coordinates $(t, r, \vartheta, \varphi)$ to *ingoing Eddington-Finkelstein coordinates* $(t', r, \vartheta, \varphi)$,

$$c\,t' \;=\; c\,t \;+\; r_S \ln\Big|\,\frac{r}{r_S} \;-\; 1\,\Big|\;, \qquad (39)$$

$$c\,dt' \;=\; c\,dt \;+\; \frac{r_S\,dr}{r \;-\; r_S}\;. \qquad (40)$$

This transformation maps ingoing radial lightlike geodesics onto straight lines,

$$-\,c\,t' \;=\; r \;+\; c\,t_0\;. \qquad (41)$$

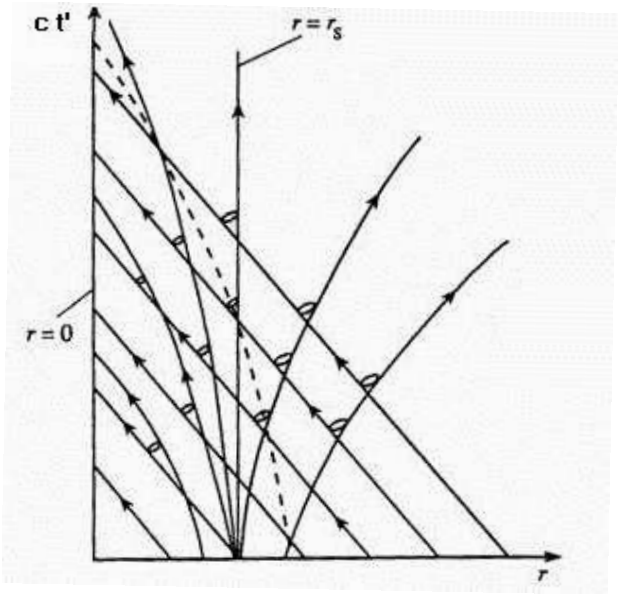

By contrast, the outgoing radial lightlike geodesics are now given by the equation

$$c\,t' \;=\; r \;+\; 2\,r_S \ln\Big|\,\frac{r}{r_S} \;-\; 1\,\Big| \;+\; c\,t_0\;. \qquad (42)$$

We will demonstrate now that in the ingoing Eddington-Finkelstein coordinates the metric coefficients are regular for all values $0 < r < \infty$. We have thus found an analytical extension of the Schwarzschild spacetime across the surface $r = r_S$. The spacetime diagram above shows the radial lightlike geodesics in this extended spacetime.

We calculate the Schwarzschild metric in the new coordinates $(t', r, \vartheta, \varphi)$.

$$g_{\mu\nu}dx^\mu dx^\nu \;=\; -\left(1 \;-\; \frac{r_S}{r}\right)c^2dt^2 \;+\; \frac{dr^2}{1 \;-\; \dfrac{r_S}{r}} \;+\; r^2\Big(d\vartheta^2 + \sin^2\vartheta\,d\varphi^2\Big)$$

$$= \;-\,\frac{r \;-\; r_S}{r}\left(c\,dt' \;-\; \frac{r_S\,dr}{r \;-\; r_S}\right)^2 \;+\; \frac{dr^2}{1 \;-\; \dfrac{r_S}{r}} \;+\; r^2\left(d\vartheta^2 + \sin^2\vartheta\,d\varphi^2\right)$$

$$= \;-\,\frac{r \;-\; r_S}{r}\,c^2\,dt'^2 + \frac{2\,c\,r_S\,\cancel{(r \;-\; r_S)}\,dt'\,dr}{r\,\cancel{(r \;-\; r_S)}} - \frac{r_S^2\,\cancel{(r \;-\; r_S)}\,dr^2}{r\,(r \;-\; r_S)^{\cancel{2}}} + \frac{r\,dr^2}{r \;-\; r_S} + r^2\Big(d\vartheta^2 + \sin^2\vartheta\,d\varphi^2\Big)$$

$$= -\left(1-\frac{r_S}{r}\right)c^2\,dt'^2 + 2\,\frac{c\,r_S}{r}\,dt'\,dr + \frac{\left(1+\frac{r_S}{r}\right)\cancel{\left(1-\frac{r_S}{r}\right)}\,dr^2}{\cancel{\left(1-\frac{r_S}{r}\right)}} + r^2\Big(d\vartheta^2+\sin^2\vartheta\,d\varphi^2\Big)\,. \quad (43)$$

In the new coordinates the Schwarzschild metric is, indeed, regular on the whole domain $0 < r < \infty$. Also the inverse metric exists on this whole domain, as

$$\det\big(g_{\mu\nu}\big) \;=\; \det\begin{pmatrix} -\left(1-\frac{r_S}{r}\right) & \frac{r_S}{r} & 0 & 0 \\ \frac{r_S}{r} & \left(1+\frac{r_S}{r}\right) & 0 & 0 \\ 0 & 0 & r^2 & 0 \\ 0 & 0 & 0 & r^2\sin^2\vartheta \end{pmatrix}$$

$$= \left\{-\left(1-\frac{r_S}{r}\right)\left(1+\frac{r_S}{r}\right) - \frac{r_S^2}{r^2}\right\} r^4\sin^2\vartheta \;=\; -\,r^4\sin^2\vartheta \quad (44)$$

is non-zero for all $r > 0$, apart from the familiar coordinate singularity on the axis, where $\sin\vartheta = 0$.

Eddington-Finkelstein coordinates were introduced by Arthur Eddington already in 1924. However, he did not use them for investigating the behaviour of the Schwarzschild metric at $r = r_S$ but rather for comparing Einstein's general relativity to an alternative gravity theory of Whitehead. The same coordinates were independently rediscovered by David Finkelstein in 1958 who clarified, with their help, the nature of the surface $r = r_S$.

We discuss now the properties of the extended Schwarzschild spacetime that is covered by the ingoing Eddington-Finkelstein coordinates.

- The metric is regular on the whole domain $0 < r < \infty$. It is clear that the spacetime cannot be extended into the domain of negative r-values, as $r = 0$ is a curvature singularity. We have already noticed that the curvature invariant $R_{\mu\nu\sigma\tau}R^{\mu\nu\sigma\tau}$ goes to infinity for $r \to 0$. As the curvature tensor determines the relative acceleration of neighbouring geodesics (recall the geodesic deviation equation), this means that near $r = 0$ any material body will be torn apart by infinitely strong tidal forces. It is widely believed that a true understanding of what is going on near $r = 0$ requires a (not yet existing) quantum theory of gravity.

- At $r = r_S$ the spacetime is perfectly regular. The tidal forces are finite there. By local experiments near $r = r_S$, an observer would not notice anything unusual. However, the hypersurface $r = r_S$ plays a particular role in view of the global structure of the spacetime: From the $r - ct'-$diagram one can read that it is an *event horizon* for all observers in the domain $r > r_S$, i.e., that no signal from the domain $r < r_S$ can reach an observer at $r > r_S$. In particular, photons cannot travel from the domain $r < r_S$ to the domain $r > r_S$. For this reason, the region $r < r_S$ is called a *black hole* whereas the region $r > r_S$ is called the *domain of outer communication*.

- As the angular coordinates ϑ and φ are suppressed, each point in our spacetime diagram on p.12 represents a sphere. Correspondingly, in the diagram each light signal represents an ingoing or outgoing spherical wave front. In the domain $r > r_S$ the radius coordinate is increasing for outgoing spheres and decreasing for ingoing spheres, as it should be in accordance with our geometric intuition. In the domain $0 < r < r_S$, however, we read from the diagram that r is decreasing for ingoing and for outgoing spheres. As $4\pi r^2$ gives the area of a sphere, as measured with the metric, this means that both the ingoing and the outgoing spherical wave fronts have decreasing area. In a terminology introduced by Roger Penrose, they are called *closed trapped surfaces*. The existence of closed trapped surfaces is an important indicator for a black hole and plays a major role in the Hawking-Penrose singularity theorems. Quite generally, the boundary of the region where closed trapped surfaces exist is called the *apparent horizon*. In the Schwarzschild spacetime, the apparent horizon coincides with the event horizon. In more general spacetimes this is not the case.

- Along any future-oriented timelike curve in the domain $r < r_S$, the r-coordinate decreases monotonically, as can be read from the $r - ct'-$diagram. If an observer was foolhardy enough to enter into the region $0 < r < r_S$, he will end up in the singularity at $r = 0$. In the next section we will calculate the proper time that elapses between crossing the horizon and arriving at the singularity. We will see that this time is maximal for a freely falling observer that is dropped from rest at the horizon; in any case, it is finite.

- We have emphasised several times that the Schwarzschild metric applies only to the *exterior region* of a spherically symmetric celestial body, $r > r_*(t)$, because only there is the vacuum field equation satisfied. We may consider a star whose radius $r_*(t)$ is bigger than r_S at the beginning and then shrinks beyond r_S. As soon as the radius is smaller than r_S, the star is doomed. It will collapse to a point in a finite time. The diagram shows this phenomenon, which is known as *gravitational collapse*, in ingoing Eddington-Finkelstein coordinates. The dashed line marks the surface of the star.

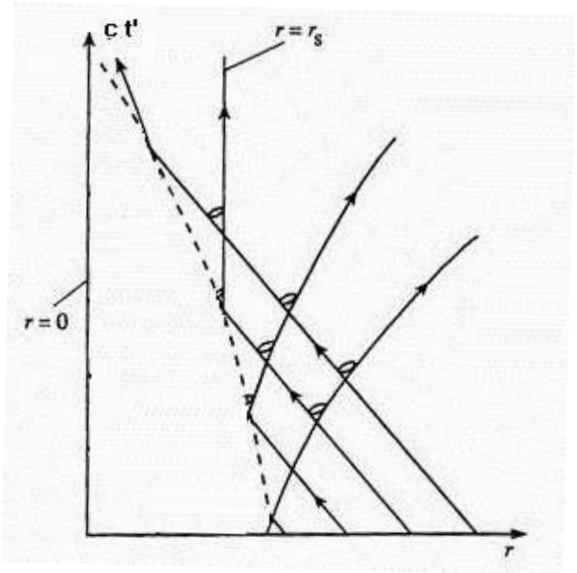

We will discuss later in detail the gravitational collapse of a star that is modelled as a ball of dust. In particular, we will discuss how a distant observer sees the surface of the star approaching the horizon, becoming more and more redshifted.

Instead of ingoing Eddington-Finkelstein coordinates, we could introduce the outgoing Eddington-Finkelstein coordinates $(t'', r, \vartheta, \varphi)$, where

$$c\,t'' \;=\; c\,t \;-\; r_S \ln\left|\frac{r}{r_S} \;-\; 1\right|\,, \qquad\qquad c\,dt'' \;=\; c\,dt \;-\; \frac{r_S\,dr}{r \;-\; r_S}\;. \tag{45}$$

In these coordinates the outgoing radial lightlike geodesics are mapped onto straight lines. In complete analogy to the ingoing Eddington-Finkelstein coordinates, also in these coordinates the metric becomes regular on the whole domain $0 < r < r_S$. In this way we get another analytic extension of the Schwarzschild metric from the domain $r_S < r < \infty$ to the domain $0 < r < \infty$. By construction, it is obvious that it is just the image under time-reflection of the extension we got from the ingoing Eddington-Finkelstein coordinates. Now the hypersurface $r = r_S$ is an event horizon for observers in the region $r < r_S$: Signals can cross this hypersurface only from the inside to the outside, but not from the outside to the inside. For this reason one calls the region $r < r_S$ a *white hole* whereas the region $r > r_S$ is again called the *domain of outer communication*. Up to now, there is no indication for the existence of white holes in Nature.

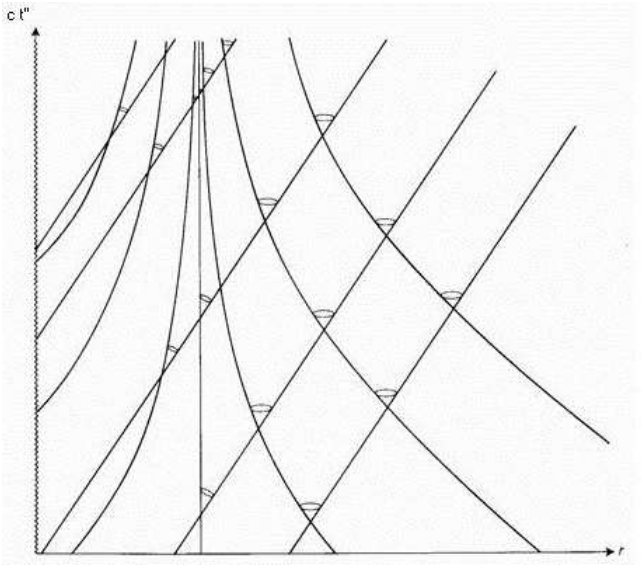

(d) Kruskal-Szekeres coordinates

The *maximal* analytic extension of the Schwarzschild metric was found independently by Martin Kruskal and by György Szekeres in the late 1950s (and also, with different mathematical techniques, by Christian Frønsdal). This maximal analytic extension, which is probably only of mathematical interest, can be found if one transforms on the domain $r_S < r < \infty$, $-\infty < t < \infty$ from Schwarzschild coordinates $(t, r, \vartheta, \varphi)$ to Kruskal-Szekeres coordinates $(u, v, \vartheta, \varphi)$ via

$$u = \sqrt{\frac{r}{r_S} - 1}\; e^{r/(2r_S)} \cosh\frac{c\,t}{2\,r_S}\,, \qquad v = \sqrt{\frac{r}{r_S} - 1}\; e^{r/(2r_S)} \sinh\frac{c\,t}{2\,r_S}\,. \tag{46}$$

These equations cannot be solved for r in terms of elementary functions, but they implicitly determine r and t as functions of u and v.

Differentiating (46) yields

$$du = e^{r/(2r_S)} \left(\left(\cosh\frac{c\,t}{2\,r_S}\right) \frac{r\,dr}{2\,r_S^2\sqrt{\frac{r}{r_S} - 1}} + \left(\sinh\frac{c\,t}{2\,r_S}\right) \sqrt{\frac{r}{r_S} - 1}\; \frac{c\,dt}{2\,r_S} \right), \tag{47}$$

$$dv = e^{r/(2r_S)} \left(\left(\sinh\frac{c\,t}{2\,r_S}\right) \frac{r\,dr}{2\,r_S^2\sqrt{\frac{r}{r_S} - 1}} + \left(\cosh\frac{c\,t}{2\,r_S}\right) \sqrt{\frac{r}{r_S} - 1}\; \frac{c\,dt}{2\,r_S} \right). \tag{48}$$

Hence

$$du^2 - dv^2 \;=\; e^{r/r_S}\left(\frac{r^2\,dr^2}{4\,r_S^3\,(r-r_S)} - \frac{(r-r_S)\,c^2dt^2}{4\,r_S^3}\right) \;=\; e^{r/r_S}\frac{r}{4\,r_S^3}\left(\frac{dr^2}{1-\dfrac{r_S}{r}} - \Big(1-\frac{r_S}{r}\Big)\,c^2dt^2\right) \tag{49}$$

This puts the Schwarzschild metric into the following form:

$$g \;=\; \frac{4\,r_S^3}{r}\,e^{-r/r_S}\big(du^2-dv^2\big) + r^2\Big(d\vartheta^2+\sin^2\vartheta\,d\varphi^2\Big)\,, \tag{50}$$

where r is to be viewed as a function of u and v, implicitly given by (46).

The metric (50) is singular only at $r=0$. As the transformation (46) implies

$$u^2-v^2 = \Big(\frac{r}{r_S}-1\Big)e^{r/r_S}\,, \tag{51}$$

this singularity is located at $v^2-u^2=1$ which is the equation of two hyperbolae, $v=\pm\sqrt{u^2+1}$. The metric is regular on the entire domain bounded by these hyperbolae, i.e., on the entire domain where $v^2-u^2<1$. With the help of the coordinate transformation (46), which was originally considered only on the exterior region $r_S<r<\infty$, $-\infty<t<\infty$, we have now found an analytical extension which is well-defined on a bigger domain. It is actually the maximal analytical extension of the Schwarzschild spacetime. It covers two copies I und I' of the exterior region $r_S<r<\infty$, a black hole interior region II and a white hole interior region II', see the diagram below. In the lettering it is $m=GM/c^2$, hence $r_S=2m$.

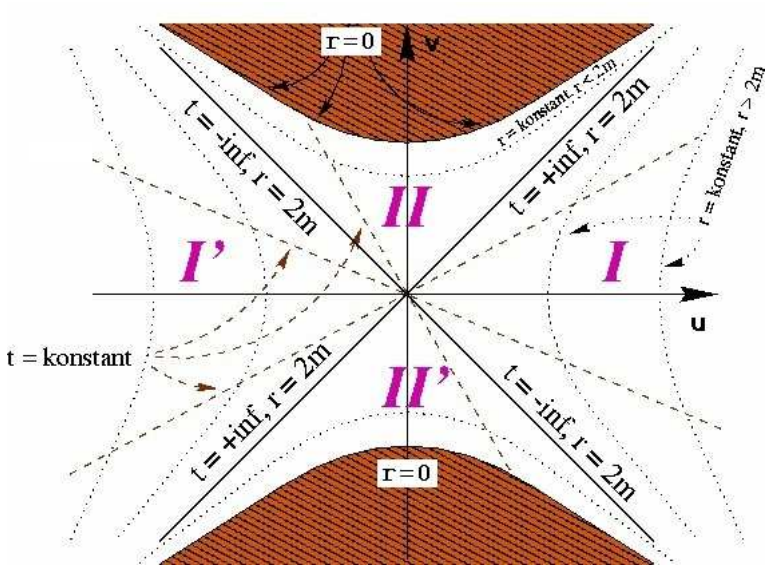

The two exterior regions I and I' meet at the point at the centre of the diagram (which is actually a sphere). In Worksheet 3 we will investigate the geometry of the surfaces ($t=$ constant, $\vartheta=\pi/2$) in the domain $r_S<r<\infty$ which are known as the *Flamm paraboloids*. At the centre of the diagram the Flamm paraboloids of region I are glued together with the Flamm paraboloids of the region I' to form the socalled *Einstein-Rosen bridge*. This is a *wormhole*, but it is non-traversible in the sense that an observer cannot travel at subluminal velocity from region I into region I' or vice versa, as can be read from the diagram.

Whereas in the Eddington-Finkelstein coordinates either the ingoing or the outgoing radial light signals were mapped onto straight lines under 45^o, in the $u-v-$diagram (Kruskal-Szekeres diagram) this is true for both: Indeed, both $\partial_v + \partial_u$ and $\partial_v - \partial_u$ are lightlike as can be read from (50). If a light signal enters into the black-hole interior region II by crossing one of the horizons, it will end up in the singularity at $r = 0$. In the white-hole interior region II' all light signals start at the singularity. They leave this region over one of the horizons.

The Kruskal-Szekeres diagram can be modified by mapping the entire maximally extended spacetime into a compact domain. This can be achieved in such a way that light rays are still under 45^o with respect to the vertical direction. To that end we have to transform each of the two lightlike coordinates $u + v$ and $u - v$ with the help of a funtion that maps the entire real line onto a finite interval. Usually one chooses the arctan function, i.e.

$$U = \arctan(v + u)\,, \quad V = \arctan(v - u)\,. \tag{52}$$

The resulting diagram is known as a *Carter-Penrose diagram* of the maximally extended Schwarzschild spacetime.

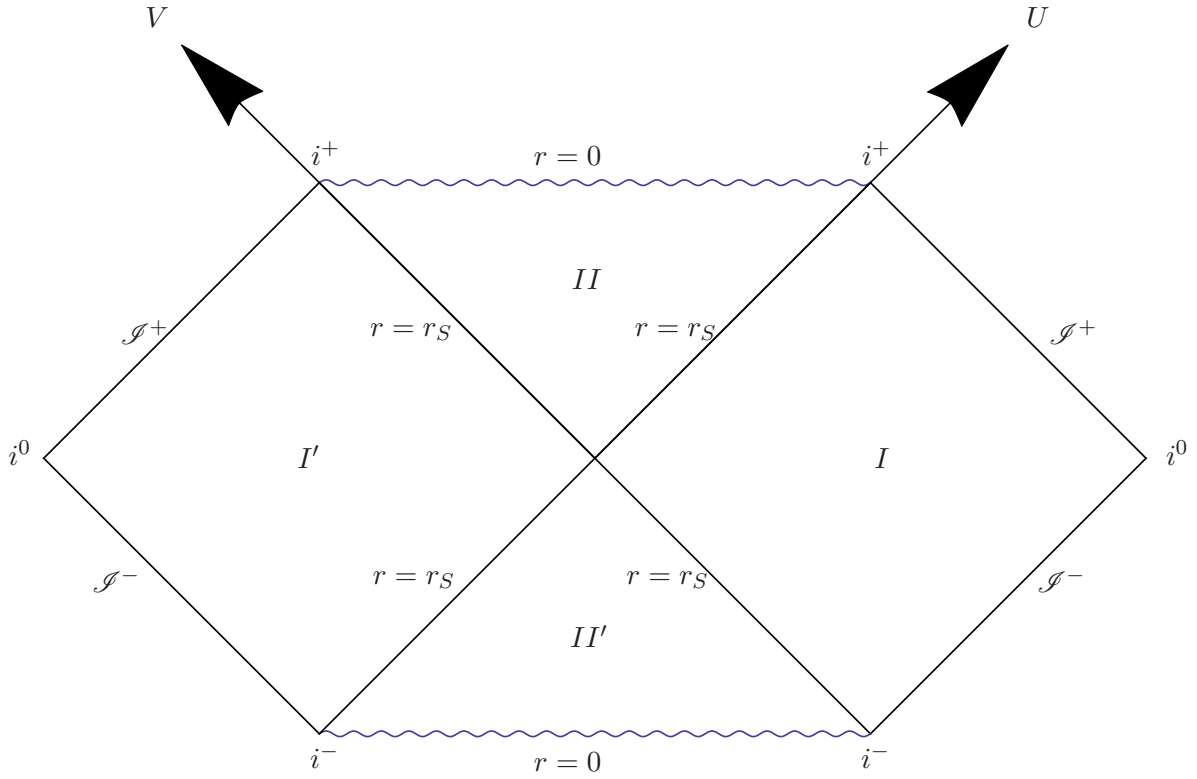

In this diagram we identify the same four regions I, II, I' and II' as in the Kruskal-Szekeres diagram, now each mapped onto a finite domain. The boundary of the spacetime consists of (i) the white-hole singularity at the bottom of the figure, (ii) the black-hole singularity at the top of the figure, (iii) future lightlike infinity $\mathscr{I}^+$ (pronounced "scri plus") where future-oriented lightlike geodesics terminate, (iv) past lightlike infinity $\mathscr{I}^-$ where past-oriented lightlike geodesics terminate, (v) spacelike infinity i^0 where spacelike geodesics terminate, (vi) future timelike infinity i^+ where future-oriented timelike geodesics terminate and (vii) past timelike infinity i^- where past-oriented timelike geodesics terminate.

(e) Painlevé-Gullstrand coordinates

Recall that in isotropic coordinates the spatial part of the metric becomes conformally flat. We will now discuss a coordinate transformation from standard Schwarzschild coordinates to new coordinates, $(t, r, \vartheta, \varphi) \mapsto (\overline{t}, r, \vartheta, \varphi)$ with $\overline{t}$ depending on t and r, such that the hypersurfaces $\overline{t} =$ constant become not only conformally flat but even flat.

We try the ansatz

$$\overline{t} = t + f(r)\,, \quad d\overline{t} = dt + f'(r)\,dr\,. \tag{53}$$

Then the Schwarzschild metric reads

$$\begin{aligned} g_{\mu\nu}dx^\mu dx^\nu \;&=\; -\Big(1-\frac{r_S}{r}\Big)c^2dt^2 \;+\; \frac{dr^2}{1-\dfrac{r_S}{r}} + r^2\Big(d\vartheta^2+\sin^2\vartheta\,d\varphi^2\Big) \\ &=\; -\Big(1-\frac{r_S}{r}\Big)c^2\big(d\overline{t}-f'(r)dr\big)^2 \;+\; \frac{dr^2}{1-\dfrac{r_S}{r}} + r^2\Big(d\vartheta^2+\sin^2\vartheta\,d\varphi^2\Big) \\ &=\; -\Big(1-\frac{r_S}{r}\Big)c^2d\overline{t}^{\,2} + 2f'(r)\Big(1-\frac{r_S}{r}\Big)c^2d\overline{t}\,dr \\ &\quad + \left\{\frac{1}{1-\dfrac{r_S}{r}} - \Big(1-\frac{r_S}{r}\Big)c^2f'(r)^2\right\}dr^2 + r^2\Big(d\vartheta^2+\sin^2\vartheta\,d\varphi^2\Big)\,. \end{aligned} \tag{54}$$

We have achieved our goal if we choose $f(r)$ such that the curly bracket equals unity,

$$\frac{1}{1-\dfrac{r_S}{r}} - \Big(1-\frac{r_S}{r}\Big)c^2f'(r)^2 \;=\; 1\,, \qquad \cancel{1} - \Big(1-\frac{r_S}{r}\Big)^2c^2f'(r)^2 \;=\; \cancel{1} - \frac{r_S}{r}\,, \tag{55}$$

$$f'(r) = \frac{\pm\,1}{c\Big(1-\dfrac{r_S}{r}\Big)}\sqrt{\frac{r_S}{r}}\,. \tag{56}$$

We choose the upper sign. Then

$$d\overline{t} \;=\; dt \;+\; \sqrt{\frac{r_S}{r}}\,\frac{dr}{c\Big(1-\dfrac{r_S}{r}\Big)} \tag{57}$$

and, upon integration,

$$\overline{t} \;=\; t \;+\; \frac{2}{c}\sqrt{r_S r} \;-\; \frac{r_S}{c}\ln\left|\frac{\sqrt{r}\;+\;\sqrt{r_S}}{\sqrt{r}\;-\;\sqrt{r_S}}\right|. \tag{58}$$

In the new coordinates the metric reads

$$g_{\mu\nu}dx^\mu dx^\nu \;=\; -\Big(1-\frac{r_S}{r}\Big)c^2d\overline{t}^{\,2} + 2\,c\,\sqrt{\frac{r_S}{r}}\,d\overline{t}\,dr + dr^2 + r^2\big(d\vartheta^2+\sin^2\vartheta\,d\varphi^2\big)\,. \tag{59}$$

This solution to the vacuum field equation was found independently by Paul Painlevé (1921) and Allvar Gullstrand (1922). Neither of them realised that it was just the Schwarzschild metric in new coordinates.

In Painlevé-Gullstrand coordinates the Schwarzschild metric is regular on the whole domain where $r > 0$. Indeed, it is obvious that the $g_{\mu\nu}$ are finite at $r = r_S$, and the following calculation shows that also the inverse metric exists everywhere on the domain where $r > 0$:

$$\det\bigl(g_{\mu\nu}\bigr) \,=\, \det\begin{pmatrix} -\Bigl(1-\dfrac{r_S}{r}\Bigr) & \sqrt{\dfrac{r_S}{r}} & 0 & 0 \\ \sqrt{\dfrac{r_S}{r}} & 1 & 0 & 0 \\ 0 & 0 & r^2 & 0 \\ 0 & 0 & 0 & r^2\sin^2\vartheta \end{pmatrix} \,=\, r^4\sin^2\vartheta\Bigl(-1+\frac{r_S}{r}-\frac{r_S}{r}\Bigr) \,=\, -\,r^4\sin^2\vartheta\,. \tag{60}$$

The Painlevé-Gullstrand coordinates cover the same black-hole spacetime as the ingoing Eddington-Finkelstein coordinates. By construction, the 3-dimensional hypersurfaces $\overline{t}$ = constant are flat. We will now discuss the family of observers for whom these hypersurfaces are the rest spaces. We will demonstrate that they are ingoing freely falling particles. (Had we chosen the lower sign for $f'(r)$ above, the $d\overline{t}\,dr$ term in the metric would have a minus sign. Then we would have a white-hole metric, as with the outgoing Eddington-Finkelstein coordinates, and the associated observers would be outgoing.)

To that end we recall that the worldlines of freely falling particles are timelike geodesics $x(\tau)$ parametrised by proper time τ. Such curves satisfy

$$g_{\mu\nu}(x)\dot{x}^\mu\dot{x}^\nu \,=\, -\,c^2 \tag{61}$$

where the overdot means derivative with respect to τ, and

$$0 \,=\, \frac{d}{d\tau}\frac{\partial\mathcal{L}(x,\dot{x})}{\partial\dot{x}^\mu} \,-\, \frac{\partial\mathcal{L}(x,\dot{x})}{\partial x^\mu} \tag{62}$$

where

$$\mathcal{L}(x,\dot{x}) \,=\, \frac{1}{2}\,g_{\mu\nu}(x)\dot{x}^\mu\dot{x}^\nu\,. \tag{63}$$

We consider radial motion (i.e., $\dot{\vartheta} \,=\, \dot{\varphi} \,=\, 0$) in the Schwarzschild spacetime in Painlevé-Gullstrand coordinates. Then we get the two equations

$$-\,\Bigl(1-\frac{r_S}{r}\Bigr)c^2\,\dot{\overline{t}}^{\,2} + 2\,c\,\sqrt{\frac{r_S}{r}}\,\dot{\overline{t}}\,\dot{r} + \dot{r}^2 \,=\, -c^2 \tag{64}$$

and

$$0 \,=\, \frac{d}{d\tau}\frac{\partial\mathcal{L}(x,\dot{x})}{\partial\dot{\overline{t}}} \,-\, \frac{\partial\mathcal{L}(x,\dot{x})}{\partial\overline{t}} \,=\, \frac{d}{d\tau}\biggl\{-\,\Bigl(1-\frac{r_S}{r}\Bigr)c^2\,\dot{\overline{t}} \,+\, c\,\sqrt{\frac{r_S}{r}}\,\dot{r}\biggr\} \tag{65}$$

where we have written only the $\overline{t}$-component of the Euler-Lagrange equation (62). We divide (64) by $-c^2$, and we denote by E the constant of motion which is given by (65):

$$\Bigl(1-\frac{r_S}{r}\Bigr)\dot{\overline{t}}^{\,2} - \,2\,\sqrt{\frac{r_S}{r}}\,\dot{\overline{t}}\,\frac{\dot{r}}{c} - \frac{\dot{r}^2}{c^2} \,=\, 1 \tag{66}$$

$$E \,=\, \Bigl(1-\frac{r_S}{r}\Bigr)c^2\,\dot{\overline{t}} \,-\, c\sqrt{\frac{r_S}{r}}\,\dot{r}\,. \tag{67}$$

We want to consider particles that "are dropped from rest at infinity", i.e., with

$$\dot{r}\big|_{r=\infty} \,=\, 0\,. \tag{68}$$

Then from (66) we find that

$$\dot{\overline{t}}\big|_{r=\infty} \,=\, \pm\,1 \tag{69}$$

where we choose the upper sign to have τ and $\overline{t}$ both running in the future direction, and with that we find from (67) that

$$E \,=\, c^2\,\dot{\overline{t}}\big|_{r=\infty} \,=\, c^2\,. \tag{70}$$

With E determined this way, (66) and (67) can be rewritten as

$$1 \,=\, \dot{\overline{t}}^{\,2} \,-\, \left(\sqrt{\frac{r_S}{r}}\,\dot{\overline{t}} \,+\, \frac{\dot{r}}{c}\right)^2\,, \tag{71}$$

$$1 \,=\, \dot{\overline{t}} \,-\, \sqrt{\frac{r_S}{r}}\left(\sqrt{\frac{r_S}{r}}\,\dot{\overline{t}} \,+\, \frac{\dot{r}}{c}\right). \tag{72}$$

Equation (71) is equivalent to

$$\left(\sqrt{\frac{r_S}{r}}\,\dot{\overline{t}} \,+\, \frac{\dot{r}}{c}\right)^2 \,=\, \Big(\dot{\overline{t}}\,-1\Big)\Big(\dot{\overline{t}}\,+1\Big)\,. \tag{73}$$

With (72) inserted on the right-hand side, we get

$$\left(\sqrt{\frac{r_S}{r}}\,\dot{\overline{t}} \,+\, \frac{\dot{r}}{c}\right)^2 \,=\, \sqrt{\frac{r_S}{r}}\left(\sqrt{\frac{r_S}{r}}\,\dot{\overline{t}} \,+\, \frac{\dot{r}}{c}\right)\Big(\dot{\overline{t}}\,+1\Big) \tag{74}$$

and, after rearringing terms,

$$\left(\sqrt{\frac{r_S}{r}}\,\dot{\overline{t}} \,+\, \frac{\dot{r}}{c}\right)\left\{\cancel{\sqrt{\frac{r_S}{r}}\,\dot{\overline{t}}} \,+\, \frac{\dot{r}}{c} \,-\, \cancel{\sqrt{\frac{r_S}{r}}\,\dot{\overline{t}}} \,-\, \sqrt{\frac{r_S}{r}}\right\} \,=\, 0\,. \tag{75}$$

As our particles come in from infinity, $\dot{r}$ is negative, so the curly bracket cannot be zero. Hence, the round bracket must be zero, i.e.

$$\sqrt{\frac{r_S}{r}}\,\dot{\overline{t}} \,=\, -\,\frac{\dot{r}}{c}\,. \tag{76}$$

If we reinsert this result into (72) we find that our freely falling particles must satisfy

$$\dot{\overline{t}} \,=\, 1\,, \quad \frac{\dot{r}}{c} \,=\, -\sqrt{\frac{r_S}{r}}\,. \tag{77}$$

The first equation says that along the worldlines of our freely falling particles the coordinate $\overline{t}$ coincides with proper time. The equation for $\dot{r}$ can be integrated:

$$\frac{dr}{d\overline{t}} \,=\, -\,c\sqrt{\frac{r_S}{r}}\,, \qquad c\,d\overline{t} \,=\, \frac{-\sqrt{r}\,dr}{\sqrt{r_S}}\,, \qquad c\,\overline{t} \,=\, -\,\frac{2}{3}\sqrt{\frac{r^3}{r_S}} \,+\, \text{constant}\,. \tag{78}$$

These curves, which are called the worldlines of the *Painlevé-Gullstrand observers*, are plotted in the figure below.

The 4-velocity of the Painlevé-Gullstrand observers is

$$U \,=\, \dot{\overline{t}}\,\partial_{\overline{t}} + \dot{r}\,\partial_r \,=\, \partial_{\overline{t}} - \,c\,\sqrt{\frac{r_S}{r}}\,\partial_r\,, \tag{79}$$

hence

$$g\big(U,\partial_r\big) \,=\, g\left(\partial_{\overline{t}} - c\sqrt{\frac{r_S}{r}}\partial_r,\,\partial_r\right) \,=\, g_{\overline{t}r} \,-\, c\,\sqrt{\frac{r_S}{r}}\,g_{rr} \,=\, c\,\sqrt{\frac{r_S}{r}} \,-\, c\,\sqrt{\frac{r_S}{r}} \,=\, 0\,. \tag{80}$$

This demonstrates that the hypersurfaces $\overline{t}\,=$ constant are indeed orthogonal to the worldlines of the Painlevé-Gullstrand observers, i.e., that they are what these observers consider as simultaneous. The figure on the right shows the hypersurfaces $\overline{t}\,=$ constant and the worldlines of the Painlevé-Gullstrand observers which become vertical for $r \to \infty$ and horizontal for $r \to 0$. Nothing particular happens with these worldlines at $r = r_S$.

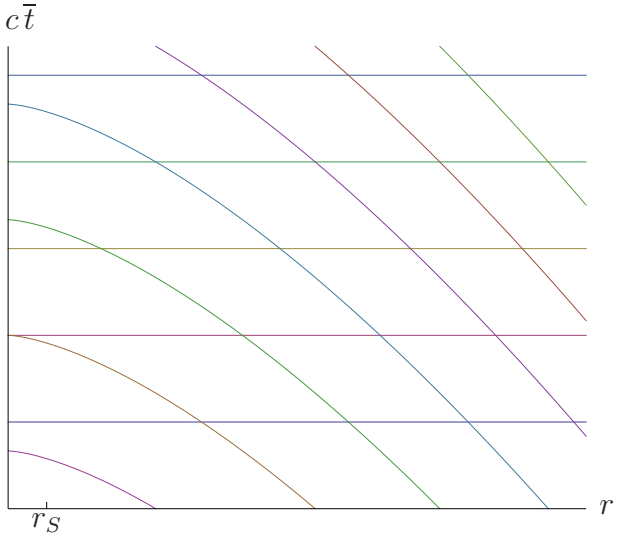

(f) Lemaître coordinates

Starting from the Painlevé-Gullstrand coordinates we perform a transformation $(\overline{t}, r, \vartheta, \varphi) \mapsto (\overline{t}, \overline{r}, \vartheta, \varphi)$ with $\overline{r}$ being a function of $\overline{t}$ and r. We want to choose this function such that $\overline{r}$ is constant along the worldline of each Painlevé-Gullstrand observer. With the equation for these worldlines as given in (78), we see that this is achieved by

$$\overline{r} \,=\, c\,\overline{t} \,+\, \frac{2}{3}\,\sqrt{\frac{r^3}{r_S}}\,. \tag{81}$$

Then the Schwarzschild metric reads

$$g \,=\, -\,c^2\,d\overline{t}^{\,2} \,+\, \frac{r_S}{r}\,d\overline{r}^{\,2} \,+\, r^2\Big(d\vartheta^2 + \sin^2\!\vartheta\,d\varphi^2\Big) \tag{82}$$

where r is to be viewed as a function of $\overline{t}$ and $\overline{r}$,

$$r \,=\, \left(\frac{3}{2}\,\sqrt{r_S}\,\big(\,\overline{r} - c\,\overline{t}\,\big)\right)^{2/3}\,. \tag{83}$$

This form of the Schwarzschild metric was found by George Lemaître in 1933. He clearly saw that, as in these coordinates the metric is regular at $r = r_S$, the "singularity" in the

Schwarzschild coordinates at $r = r_S$ is a mere coordinate singularity. However, he did not understand the character of $r = r_S$ as a horizon.

In Lemaître coordinates the singularity at $r = 0$ is represented as a diagonal line, $c\overline{t} = \overline{r}$. The horizon at $r = r_S$ is represented as a parallel diagonal line, $c\overline{t} = \overline{r} - 2r_S/3$.

The disadvantage of the Lemaître coordinates is in the fact that now the metric is no longer manifestly static. The hypersurfaces $\overline{t} =$ constant now carry the 3-metric

$$g^{(3)} = \frac{r_S}{r}\, d\overline{r}^{\,2} \,+\, r^2\big(d\vartheta^2 + \sin^2\!\vartheta\, d\varphi^2\big)$$

which is time-dependent because r depends not only on $\overline{r}$ but also on $\overline{t}$.

The figure on the right shows the singularity at $r = 0$ (thick line) and the horizon at $r = r_S$ (dashed line) in Lemaître coordinates. The vertical lines are the worldlines of the Painlevé-Gullstrand observers. The horizontal lines are the hypersurfaces $\overline{t} =$ constant (with the angle coordinates not shown).

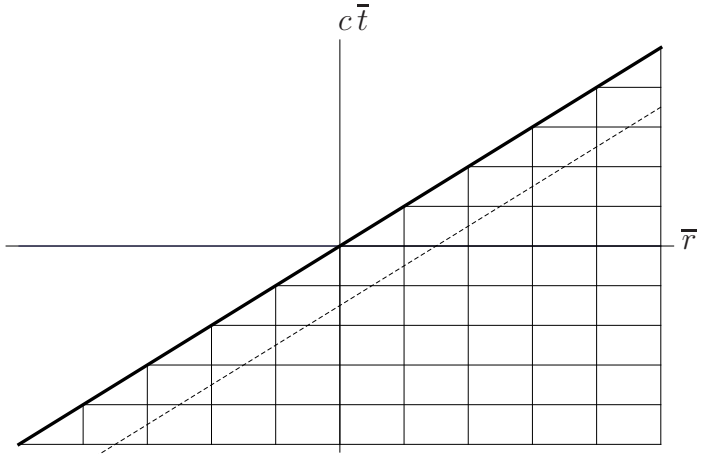

3.3 Timelike geodesics in the Schwarzschild spacetime

Recall that timelike geodesics, if parametrised by proper time, satisfy the equations

$$0 \,=\, \frac{d}{d\tau}\Big(\frac{\partial\mathcal{L}(x,\dot{x}}{\partial\dot{x}^\mu}\Big) \,-\, \frac{\partial\mathcal{L}\big(x,\dot{x}}{\partial x^\mu}\big)\,, \tag{84}$$

where $\mathcal{L}(x,\dot{x}) \,=\, \dfrac{1}{2}\, g_{\mu\nu}(x)\,\dot{x}^\mu\,\dot{x}^\nu$, and

$$g_{\mu\nu}(x)\,\dot{x}^\mu\,\dot{x}^\nu \,=\, -\,c^2\,. \tag{85}$$

For the Schwarzschild metric, which is spherically symmetric, we can specify without loss of generality to the case that the motion is in the equatorial plane, $\vartheta = \pi/2$, $\dot{\vartheta} = 0$. Then

$$\mathcal{L}(x,\dot{x}) \,=\, \frac{1}{2}\left(\,-\,\Big(1-\frac{r_S}{r}\Big)c^2\dot{t}^2 + \frac{\dot{r}^2}{1-\dfrac{r_s}{r}} + r^2\dot{\varphi}^2\right). \tag{86}$$

The t and φ components of the Euler-Lagrange equation give us two constants of motion,

$$\frac{d}{d\tau}\left(\Big(1-\frac{r_s}{r}\Big)c^2\dot{t}\right) \,-\, 0 \,=\, 0\,, \qquad E \,=\, \Big(1-\frac{r_s}{r}\Big)c^2\dot{t} \,=\, \text{constant}\,, \tag{87}$$

$$\frac{d}{d\tau}\Big(r^2\,\dot{\varphi}\Big) \,-\, 0 \,=\, 0\,, \qquad L \,=\, r^2\,\dot{\varphi} \,=\, \text{constant}\,, \tag{88}$$

and the definition of proper time requires

$$-\Big(1-\frac{r_S}{r}\Big)c^2\dot{t}^2 \,+\, \frac{\dot{r}^2}{1-\dfrac{r_S}{r}} \,+\, r^2\dot{\varphi}^2 \,=\, -\,c^2\,. \tag{89}$$

The three equations (87), (88) and (89) determine the trajectories of freely falling particles completely, because one can check that the r component of the Euler-Lagrange equation is a consequence of these three equations. We solve the three equations for the velocities,

$$\dot{t} \,=\, \frac{E}{c^2\Big(1-\dfrac{r_S}{r}\Big)}\,, \tag{90}$$

$$\dot{\varphi} \,=\, \frac{L}{r^2}\,, \tag{91}$$

$$\dot{r}^2 \,=\, \Big(1-\frac{r_S}{r}\Big)\left(\frac{\Big(1-\dfrac{r_S}{r}\Big)c^2E^2}{c^4\Big(1-\dfrac{r_S}{r}\Big)^2} \,-\, \frac{r^2L^2}{r^4} \,-\, c^2\right) \,=\, \frac{E^2}{c^2} \,-\, \Big(1-\frac{r_S}{r}\Big)\Big(\frac{L^2}{r^2}\,+\,c^2\Big)\,. \tag{92}$$

(a) Radial motion

For radial motion we must have $\dot{\varphi}=0$, hence $L=0$. Then we only have to deal with the equations (90) and (92),

$$\dot{t} \,=\, \frac{E}{c^2\left(1-\dfrac{r_S}{r}\right)}\,, \tag{93}$$

$$\dot{r}^2 \,=\, \frac{E^2}{c^2} \,-\, \left(1-\frac{r_S}{r}\right)c^2\,. \tag{94}$$

E is determined if we fix an initial condition. We want to assume that the particle is dropped from rest at a radius r_0, i.e.

$$\dot{r}\Big|_{r=r_0} \,=\, 0\,, \tag{95}$$

Then (94) requires

$$0 \,=\, \frac{E^2}{c^2} \,-\, \Big(1-\frac{r_S}{r_0}\Big)\,c^2\,, \qquad \text{hence} \quad E^2 \,=\, c^4\Big(1-\frac{r_S}{r_0}\Big)\,. \tag{96}$$

Clearly, this equation can hold only if $r_0 > r_S$. This is in agreement with our earlier observation that beyond the horizon the t coordinate is spacelike, so motion at subluminal speed cannot have $\dot{r}=0$ there. With E determined this way, (94) reads

$$\dot{r}^2 \,=\, \left(1-\frac{r_S}{r_0}\right)c^2 \,-\, \left(1-\frac{r_S}{r}\right)c^2 \,=\, c^2\left(\frac{r_S}{r} \,-\, \frac{r_S}{r_0}\right)\,. \tag{97}$$

In Worksheet 5 we will integrate this equation for the limiting case that the particle is dropped from the horizon, $r_0 \to r_S$. We will calculate the lifetime of such a particle, before it ends up in the singularity at $r = 0$, in terms of its proper time. We will find that this is the *maximal* time a particle, or an observer, can spend in the region $0 < r < r_S$, i.e., using a rocket engine, firing in any direction, makes the lifetime *shorter*.

(b) Non-radial motion

Non-radial orbits have $\dot{\varphi} \neq 0$ *everywhere*, because L is a constant of motion. We can thus divide (92) by $\dot{\varphi}^2$ and insert (90) and (91) on the right-hand side,

$$\left(\frac{dr}{d\varphi}\right)^2 = \frac{\dot{r}^2}{\dot{\varphi}^2} = \frac{r^4}{L^2}\left(\frac{E^2}{c^2} - \frac{L^2}{r^2} + \frac{r_S L^2}{r^3} - c^2 + \frac{c^2 r_S}{r}\right)$$

$$= \frac{(E^2 - c^4)}{c^2 L^2}\, r^4 + \frac{c^2 r_S}{L^2}\, r^3 - r^2 + r_S r =: -2\, V_{E,L}(r) \tag{98}$$

which gives us an expression for $dr/d\varphi$, i.e., for the shape of the orbit. For most applications this is what we are interested in; the parametrisation by t or τ is also interesting for some applications, but often we are just satisfied with knowing the shape of the orbit. In (98) we have introduced the *effective potential* $V_{E,L}$ in such a way that a kind of "energy conservation law" holds,

$$\frac{1}{2}\left(\frac{dr}{d\varphi}\right)^2 + V_{E,L}(r) = 0\,. \tag{99}$$

An orbit with constants of motion E and L must be confined to the region where $V_{E,L}(r) \leq 0$; the boundary points, where $V_{E,L}(r) = 0$, are turning points of the orbit where $dr/d\varphi = 0$. So, with the help of the effective potential we can determine for which values of (E, L) bound orbits exist. Similarly, we can determine for which values of (E, L) there are stable or unstable circular orbits.

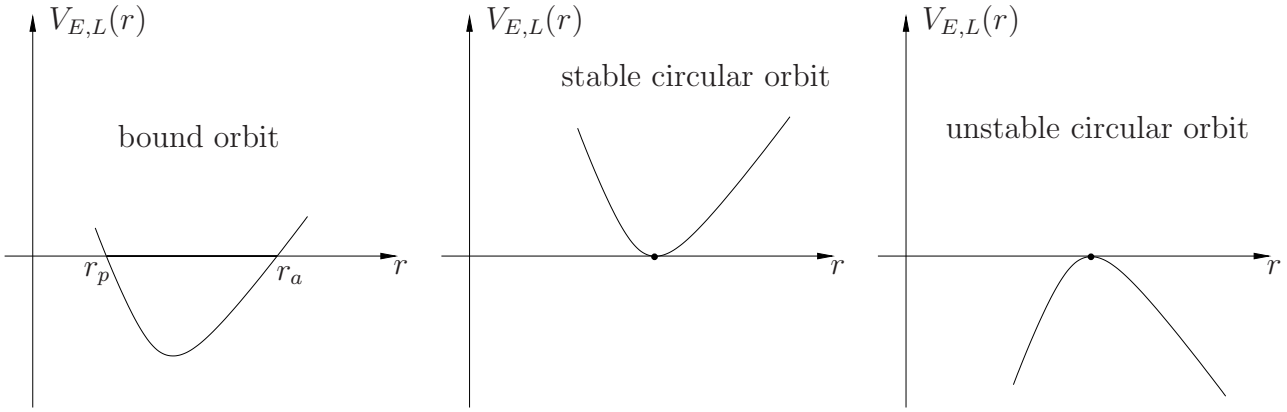

It is our goal to characterise the totality of bound orbits in the Schwarzschild spacetime. As an important step for achieving this goal, we first discuss circular orbits which are also of interest by themselves.

From (99) we find, by differentiating with respect to φ,

$$\frac{d^2r}{d\varphi^2} + V'_{E,L}(r) = 0\,. \tag{100}$$

Here we have divided by $dr/d\varphi$ but note that, by continuity, (100) is valid also in the case that $dr/d\varphi = 0$. For circular orbits we must have

$$dr/d\varphi = 0 \quad \text{and} \quad d^2r/d\varphi^2 = 0\,. \tag{101}$$

These two equations require $V_{E,L}(r) = 0$ and $V'_{E,L}(r) = 0$, i. e.

$$0 \;=\; V_{E,L}(r) \;=\; \frac{(c^4 - E^2)}{2c^2L^2}\,r^4 \;-\; \frac{c^2 r_S}{2L^2}\,r^3 \;+\; \frac{1}{2}\,r^2 \;-\; \frac{r_S}{2}\,r\,, \tag{102}$$

$$0 \;=\; V'_{E,L}(r) \;=\; \frac{2(c^4 - E^2)}{c^2L^2}\,r^3 \;-\; \frac{3c^2 r_S}{2L^2}\,r^2 \;+\; r \;-\; \frac{r_S}{2}\,. \tag{103}$$

Multiplying (102) with $4/r$ and subtracting (103) results in

$$0 \;=\; -\,\frac{c^2 r_S}{2L^2}\,r^3 \;+\; r^2 \;-\; \frac{3\,r_S}{2}\,r\,. \tag{104}$$

Solving for L^2 yields

$$L^2 \;=\; \frac{c^2 r_S r^2}{2r - 3r_S}\,. \tag{105}$$

Upon inserting this result into the equation (103) we find

$$E^2 \;=\; \frac{2\,c^4(r - r_S)^2}{r\,(2r - 3r_S)}\,. \tag{106}$$

As L^2 and E^2 cannot be negative, circular orbits exist only for those r-values that satisfy the inequality

$$r \;>\; \frac{3}{2}\,r_S\,. \tag{107}$$

We will see in the next subsection that at the limiting radius $r = 3r_s/2$ there is a circular *lightlike* geodesic. For $r < 3r_S/2$ the circular orbital velocity is bigger than the velocity of light which means that a circular orbit cannot be realised at such a radius, neither by a freely falling massive particle nor by a photon. Note, however, that such circular orbits can be very well realised by timelike curves that are non-geodesic, i.e., by observers with a rocket engine. Non-geodesic timelike circular motion is possible down to $r = r_S$ where, however, the necessary acceleration (i.e., the necessary amount of petrol) goes to infinity for $r \to r_S$.

We now check stability of the circular geodesic orbits at $r > 3r_S/2$. For stability we must have

$$V''_{E,L}(r) > 0\,. \tag{108}$$

From differentiating the effective potential we find

$$c^2L^2V''_{E,L}(r) \;=\; 6(c^4-E^2)\,r^2 \;-\; 3c^4r_S\,r \;+\; c^2L^2$$

$$=\; 3c^4r(2r-r_S) + \frac{c^4\big(r_Sr^2 - 12r(r-r_S)^2\big)}{2r-3r_S}$$

$$=\; \frac{c^4r\big(3(2r-r_S)(2r-3r_S) + r_Sr - 12(r-r_S)^2\big)}{2r-3r_S}$$

$$=\; \frac{c^4r\Big(3\big(\cancel{4r^2} - \cancel{8r_Sr} + 3r_S^2\big) + r_Sr - 12\big(\cancel{r^2} - \cancel{2r_Sr} + r_S^2\big)\Big)}{2r-3r_S}$$

$$=\; \frac{c^4r_Sr\big(r-3r_S\big)}{2r-3r_S}\,. \tag{109}$$

The stability condition $V''_{E,L}(r) > 0$ is, thus, satisfied for $r > 3r_S$. In the radius interval $3r_S/2 < r < 3r_S$ circular orbits do exist; however, they are unstable which means that practically they cannot be realised, as any small deviation from the initial condition would lead either to an escape orbit (towards infinity) or to a plunge orbit (towards the singularity). The limiting case $r = 3r_S$ is known as the *Innermost Stable Circular Orbit* (ISCO). A massive particle cannot be on a stable orbit around a Schwarzschild black hole at a radius value smaller than $3r_S$. Keep in mind that we are talking about *geodesic* motion. With a rocket engine one can orbit a Schwarzschild black hole at any radius bigger than r_S, see Worksheet 3.

We summarise our results on circular timelike geodesics in the following table:

$r_S < r < 3r_S/2$	circular timelike geodesics do not exist
$3r_S/2 < r < 3r_S$	circular timelike geodesics do exist, but they are unstable
$3r_S < r < \infty$	circular timelike geodesics do exist and are stable

Recall that in the Newtonian theory, i.e., for a particle moving in the Kepler potential, circular stable orbits exist at all radius values $0 < r < \infty$.

We now turn to (non-circular) bound orbits. It is clear that bound orbits can exist only in the domain $r_S < r < \infty$, because in the domain $0 < r < r_S$ of a Schwarzschild black-hole spacetime the radius coordinate is monotonically decreasing along any particle worldline.

For a bound orbit it is necessary that the potential $V_{E,L}(r)$ has in the interval $r_S < r < \infty$ two successive zeros with a local minimum in between, see the figure on p. 24. As $V_{E,L}(r)$ is a fourth order polynomial with the properties that $V_{E,L}(0) = 0$ and $V'_{E,L}(0) = -r_s/2 < 0$, this is possible only if $V_{E,L}(r)$ has exactly three positive zeros, $0 < r_0 < r_p < r_a$, see the figure on the right. The bound motion takes place between the pericentre at r_p and the apocentre at r_a. (The general words are *pericentre* and *apocentre* or *periapsis* and *apapsis*. If the central body is the Sun, one speaks of *perihelion* and *aphelion*; if it is the Earth one says *perigee* and *apogee*. For a black hole the names *peribothron* and *apobothron* have been suggested, but they have not really caught on. In greek "bothros" literally means "pit"; in a mythological context the word has been used for a pit with a fire in it people were dancing around.) For the same values of E and L there is also a "plunge orbit" of a particle that reaches its maximum radius at r_0 and falls into the black hole. For the particle on the bound orbit, r_0 has no geometric meaning.

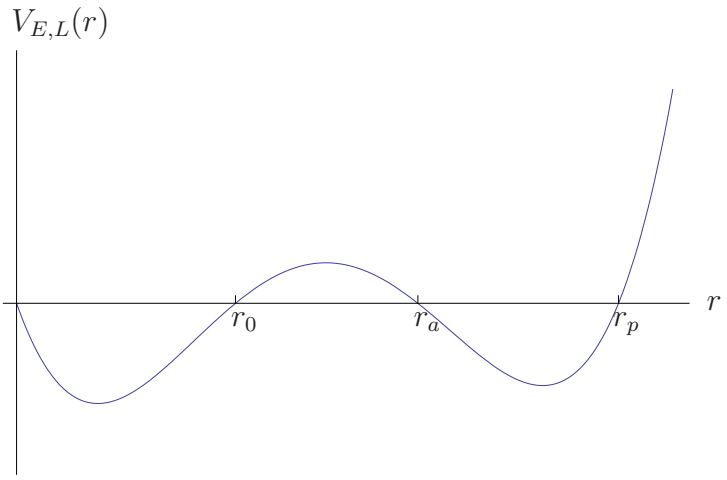

For any values of E and L where the potential $V_{E,L}$ has exactly three positive zeros, $0 < r_0 < r_p < r_a$, there is a bound orbit. The limiting cases are reached if r_p coincides with r_a or with r_0. We will discuss these limiting cases in a minute.

We will first demonstrate that, instead of E and L, we can use r_p and r_a for labeling the potential. This is useful because r_p and r_a have a direct geometric meaning associated with the (bound) orbit we want to characterise. It is even more convenient to use, instead of the pericentral radius r_p and the apocentral radius r_a, the socalled *semi-latus rectum* p and the *eccentricity* e which are defined by

$$r_p = \frac{p}{1+e}\,, \qquad r_a = \frac{p}{1-e}\,. \tag{110}$$

These quantities are familiar from the case of an elliptical orbit but note that they are well-defined for *any* bound orbit. We will now demonstrate that r_0, E and L can be expressed in terms of p and e. To that end we compare the equation by which the effective potential was introduced,

$$V_{E,L}(r) \;=\; \frac{(c^4 - E^2)}{2c^2L^2}\, r^4 \;-\; \frac{c^2 r_S}{2L^2}\, r^3 \;+\; \frac{1}{2}\, r^2 \;-\; \frac{r_S}{2}\, r\,, \tag{111}$$

with the representation in terms of its zeros,

$$V_{E,L}(r) \;=\; \frac{(c^4 - E^2)}{2c^2L^2}\, r \left(r - \frac{p}{1-e}\right)\left(r - \frac{p}{1+e}\right)(r - r_0)\,. \tag{112}$$

Comparing coefficients of r^3, r^2 and r yields three equations,

$$\frac{c^2 r_S}{\not{2}\,\not{L}^2} = \frac{(c^4 - E^2)}{\not{2}\,c^2\,\not{L}^2}\,\frac{\big(r_0(1-e^2)+2p\big)}{(1-e^2)}\,, \tag{113}$$

$$\frac{1}{\not{2}} = \frac{(c^4 - E^2)}{\not{2}\,c^2\,L^2}\,\frac{\big(p^2+2pr_0\big)}{(1-e^2)}\,, \tag{114}$$

$$\frac{r_S}{\not{2}} = \frac{(c^4 - E^2)}{\not{2}c^2 L^2}\,\frac{r_0 p^2}{(1-e^2)}\,, \tag{115}$$

which can be solved for r_0, E and L. From (114) and (115) we find

$$r_0 = \frac{r_S p}{p - 2r_s} \tag{116}$$

which manifestly implies that $r_S < r_0$. Inserting (116) into (114) and (115) yields

$$E^2 = \frac{c^4\Big(2r_S^2(1-e^2)+2p(p-2r_S)\Big)}{p\big(2p-3r_S-r_S e^2\big)}\,, \qquad L^2 = \frac{c^2 r_S p^2}{2p-3r_S-r_S e^2}\,. \tag{117}$$

With (116) and (117) we can reexpress our potential (112) in terms of p and e,

$$\begin{aligned} V_{E,L}(r) = \tilde{V}_{p,e}(r) &= \frac{(p-2r_S)}{2p^3}\,(1-e^2)\,r\left(r-\frac{p}{1-e}\right)\left(r-\frac{p}{1+e}\right)\left(r-\frac{r_S p}{p-2r_S}\right) \\ &= \frac{1}{2p^3}\,r\Big(r\big(1-e\big)-p\Big)\Big(r\big(1+e\big)-p\Big)\Big(r\big(p-2r_S\big)-r_S p\Big)\,. \end{aligned} \tag{118}$$

It is preferable to use p and e for characterising the orbit rather than E and L because the former directly give us some information about the geometry of the orbit.

We will now discuss for which values of p and e bound orbits do exist. For the sake of comparison, note that in the Newtonian case (i.e., for Kepler ellipses) all values $0 < p < \infty$ and $0 \le e < 1$ are possible. For finding the allowed values in the case of Schwarzschild geodesics, we recall that for a bound orbit we need three positive zeros of the potential $V_{E,L}(r) = \tilde{V}_{p,e}(r)$, see the plot on p. 28. Clearly, the limiting values of p and e correspond to the limiting cases where two of these three zeros coincide, i.e., if either $r_a = r_p$ or $r_p = r_0$.

The first case is easily understood. If $r_p = r_a$ we have a stable circular orbit at this radius value, see figure on the right. For the same values of E and L we also have a plunge orbit between r_0 and the singularity at $r = 0$, but this is irrelevant for the discussion of bound orbits. From the calculation above we know that a stable circular orbit, and thus the situation depicted in the plot, is possible for all values $r_p = r_a > 3r_S$.

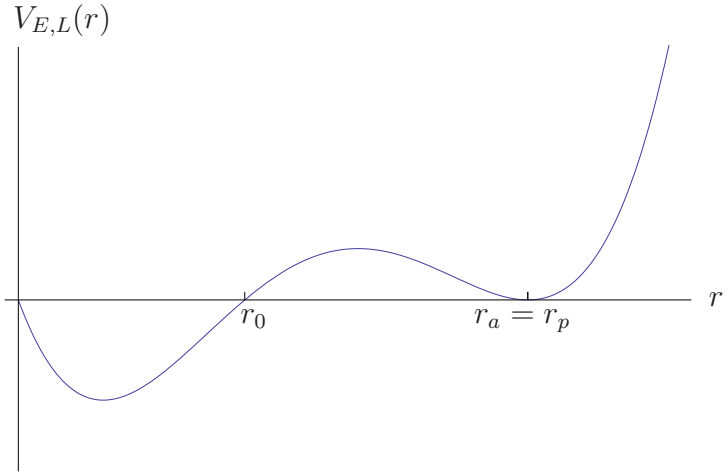

The second limiting case of bound orbits is more intriguing. If $r_0 = r_p$, there is an unstable circular orbit at this radius coordinate, see figure on the right. For the same values of E and L, there are two additional orbits that approach $r_0 = r_p$ asymptotically. One is an orbit that spirals away from $r_0 = r_p$ in the direction of decreasing r and ends up in the singularity. This has nothing to do with bound orbits. The other one is an orbit that spirals away from $r_0 = r_p$ in the direction of increasing r, reaches a maximum radius at r_a and then spirals back towards $r_0 = r_p$. Such an orbit is called *homoclinic*. (Quite generally, in the theory of dynamical systems an orbit that asymptotically starts and ends at the *same* equilibrium point is called homoclinic, while it is called *heteroclinic* if it connects two different equilibrium points. In the Schwarzschild spacetime there are no heteroclinic orbits. Heteroclinic orbits occur, e.g., in the Kottler spacetime, i.e., in the Schwarzschild spacetime with a cosmological constant, as we will briefly discuss later.) A homoclinic orbit makes infinitely many turns around the centre while asymptotically approaching the limiting circle at $r_0 = r_p$.

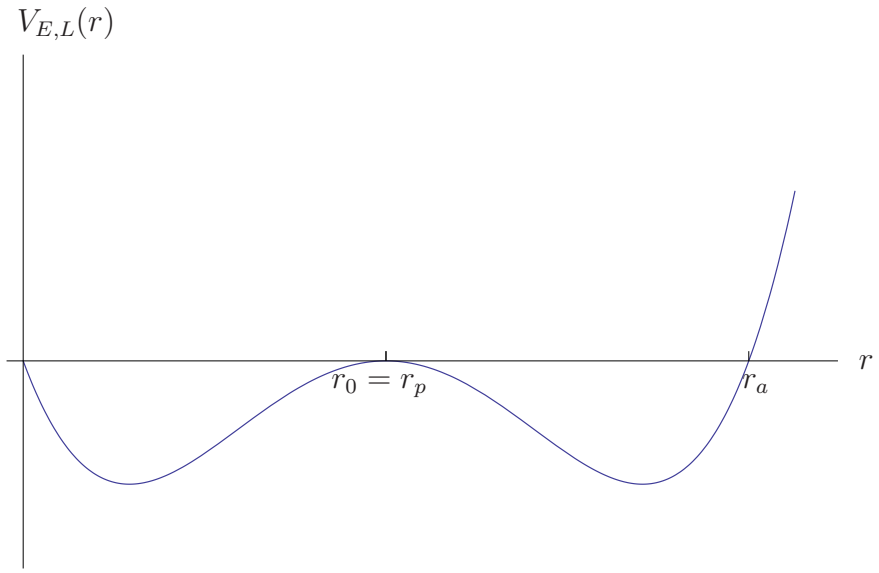

The homoclinic orbits give us a boundary line in the (p, e)-plane for bound orbits. The equation for this boundary line is given by

$$r_0 = r_p\,, \qquad \frac{r_S\, p}{p - 2r_S} = \frac{p}{1+e}\,, \qquad r_S \cancel{p}(1+e) \;=\; \cancel{p}(p - 2r_S)\,, \tag{119}$$

$$p - 3r_S - r_S e = 0\,. \tag{120}$$

This gives us the region of bound orbits in the (p, e)-plane which is shown in the figure on the next page. It is bounded from above by the line $e = 1$ and bounded from below by the stable circular orbits, $e = 0$ and $3r_S < p < \infty$. It is bounded on the left by the homoclinic orbits, $p - 3r_S - r_S e = 0$. This boundary line is often called the *separatrix*. The separatrix is a straight line connecting the points $(p, e) = (3r_s, 0)$ and $(p, e) = (4r_S, 1)$. The former is the ISCO, the latter is an orbit which asymptotically spirals from $r_p = 2r_S$ to $r_a = \infty$. Along the separatrix, the radius coordinate $r_0 = r_p$ of the unstable limit curve varies monotonically from $3r_S$ to $2r_S$. We see that only the unstable circular orbits in this radius interval can serve as limit curves for homoclinic orbits; the ones between $r = 3r_S/2$ and $r = 2r_S$ are limit curves for orbits that spiral out to infinity. Every homoclinic orbit has the same constants of motion E and L as the unstable circular orbit which it approaches asymptotically. The circular orbit at $r = 2r_S$ is (somewhat misleadingly) called the "marginally bound" orbit.

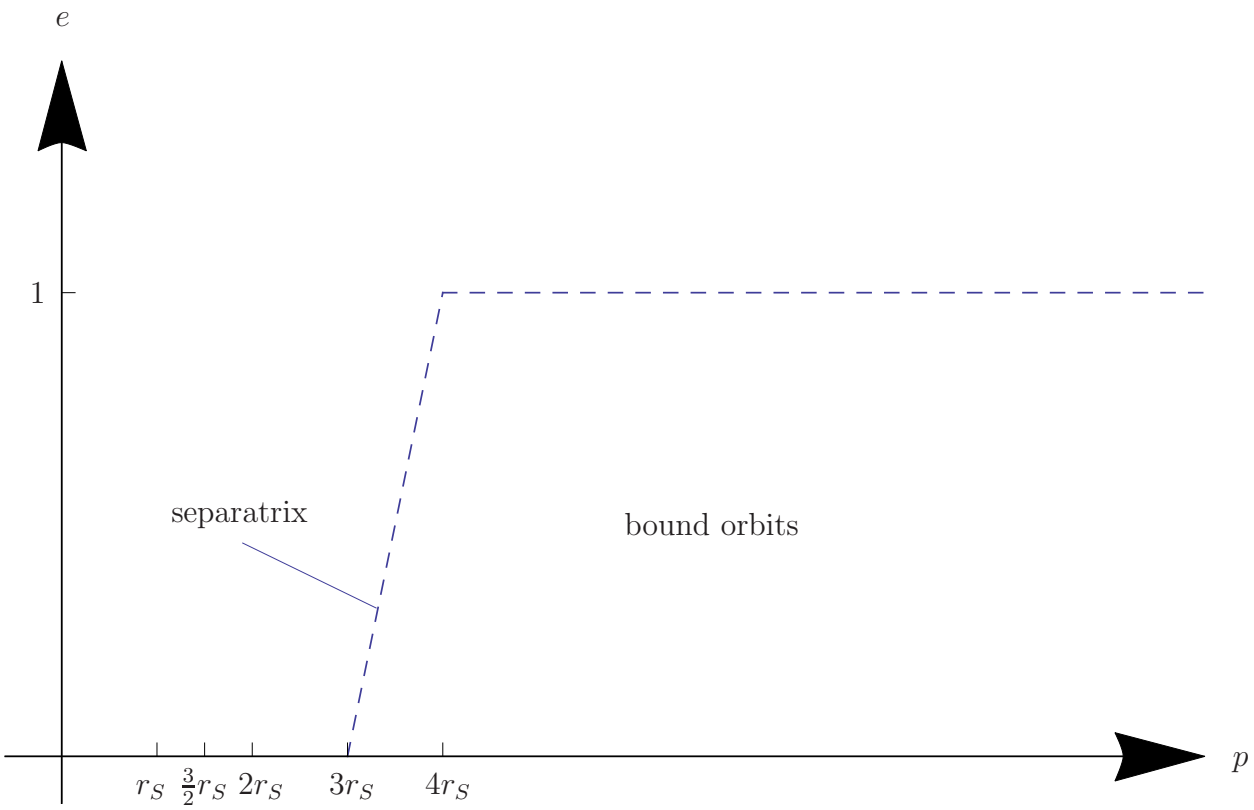

Bound orbits near the separatrix are known as *zoom-whirl* orbits. Such an orbit periodically "zooms" out to its apocentre, which can be arbitrarily far away because e can be arbitrarily close to 1. In between, it makes a large number of "whirls" near its pericentre r_p which lies close to a limit curve of a homoclinic orbit, i.e., between $2r_S$ and $3r_S$.

The picture on the right shows the potential $V_{E,L}(r)$ for a choice of E and L where such a zoom-whirl orbit occurs between r_p and r_a. For the same values of E and L there is also a plunge orbit with many whirls near r_0. If a body orbits a black hole, it follows approximately a geodesic as long as its mass is much smaller than the mass of the black hole. If such a body would be on a zoom-whirl orbit, it would produce a characteristic gravitational-wave signal.

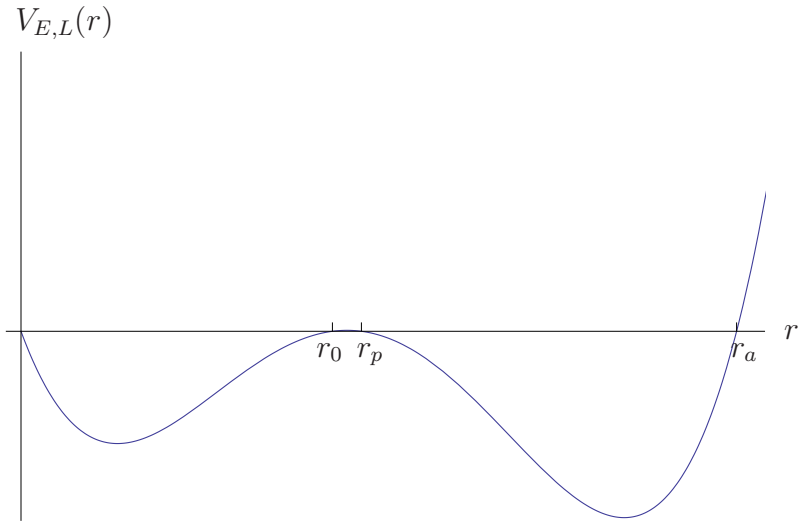

From the equations we have derived so far we can easily find an exact expression for the precession of the pericentre of a bound orbit. Recall that in the Newtonian theory, for motion in the Kepler potential, the bound orbits are ellipses, i.e., they come back to the same point in space after one revolution. This is different for bound orbits in the Schwarzschild spacetime.

If we write the orbit equation (99) in the form

$$d\varphi = \frac{\pm\, dr}{\sqrt{-2V_{E,L}(r)}}\,, \tag{121}$$

integration over one revolution, from one passage through the pericentre to the next, results in

$$2\pi + \Delta = \left(\int_{r_p}^{r_a} - \int_{r_a}^{r_p}\right) \frac{dr}{\sqrt{-2V_{E,L}(r)}}\,. \tag{122}$$

Here we have chosen the signs according to the fact that on the leg from r_p to r_a the radius coordinate is increasing whereas on the leg from r_a to r_p it is decreasing. Δ gives the precession of the pericentre during one revolution. Using p and e for characterising the orbit, (122) can be rewritten as

$$\Delta = 2\int_{p/(1+e)}^{p/(1-e)} \frac{dr}{\sqrt{-2\tilde{V}_{p,e}(r)}} - 2\pi \tag{123}$$

where $\tilde{V}_{p,e}(r)$ is given by (118). One usually gives the quantity Δ/T where T is the coordinate time that has elapsed between the two successive passages through the pericentre. For the planets in our Solar system, Δ/T is tiny: For Mercury it is 43 "/cy (arcseconds per century), for Venus 8.6 "/cy, for Earth 3.8 "/cy, for Mars 1.4 "/cy and for the other planets practically unmeasurable. The perihelion precession of Mercury is long known: In 1859 Le Verrier realised that the observed precession cannot be fully explained by the perturbation of the other planets. He even suggested the existence of an additional planet, called *Vulcan*, that was supposed to be closer to the Sun as Mercury. Now we know that Vulcan does not exist and that the anomalous perihelion precession is precisely explained by general relativity. Einstein gave this explanation before Schwarzschild (and Droste) found the exact spherical vacuum solution for the field equation. He used the linearised theory which is applicable if r_p (and thus also r_a and p) are big in comparison to r_S. From the exact expression (123) we can reproduce Einstein's result: After a bit of algebra, Taylor expansion yields

$$\Delta = \frac{3\pi r_S}{p} + O\Big(\big(r_S/p\big)^2\Big)\,. \tag{124}$$

If one introduces the semi-major axis a,

$$a = \frac{1}{2}\left(r_p + r_a\right) = \frac{1}{2}\Big(\frac{p}{1+e} + \frac{p}{1-e}\Big) = \frac{p}{1-e^2}\,, \tag{125}$$

one finds the familiar expression,

$$\Delta = \frac{3\pi r_S}{a(1-e^2)} + O\Big(\big(r_S/a\big)^2\Big) = \frac{6\pi G^2 M}{c^2 a(1-e^2)} + O\Big(\big(r_S/a\big)^2\Big)\,. \tag{126}$$

If a (or equivalently p) is big in comparison to r_S, the $O\Big(\big(r_s/a\big)^2\Big)$ term can be neglected and one gets the linearised approximation formula for the precession of the pericentre. If an orbit comes close to the centre, which is possible in particular for black holes, the linearised formula is of course not applicable and the precession of the pericentre may be quite big. Note that both the exact and the linearised formula give a non-zero Δ even in the limit $e \to 0$. Of course, an exactly circular orbit does not have a pericentre, so one cannot see the precession in this limit.

3.4 Lightlike geodesics in the Schwarzschild spacetime

For a discussion of the lightlike geodesics in the Schwarzschild spacetime we proceed in a similar fashion as for the timelike ones. Again, we restrict to the equatorial plane and consider the Euler-Lagrange equation

$$0 \,=\, \frac{d}{ds}\Big(\frac{\partial \mathcal{L}(x,\dot{x}}{\partial \dot{x}^\mu}\Big) \,-\, \frac{\partial \mathcal{L}(x,\dot{x})}{\partial x^\mu} \tag{127}$$

with the Lagrangian

$$\mathcal{L}(x,\dot{x}) \,=\, \frac{1}{2}\left(\,-\, \Big(1-\frac{r_S}{r}\Big)c^2\dot{t}^2 + \frac{\dot{r}^2}{1-\dfrac{r_s}{r}} + r^2\dot{\varphi}^2 \right), \tag{128}$$

but now the dot denotes derivative with respect to an affine parameter s and $\mathcal{L}(x,\dot{x}) = 0$.

The t and φ components of the Euler-Lagrange equation are the same as before,

$$\frac{d}{d\tau}\left(\Big(1-\frac{r_s}{r}\Big)c^2\dot{t}\right) \,-\, 0 \,=\, 0\,, \qquad E \,=\, \Big(1-\frac{r_s}{r}\Big)c^2\dot{t} \,=\, \text{constant}\,, \tag{129}$$

$$\frac{d}{d\tau}\Big(r^2\,\dot{\varphi}\Big) \,-\, 0 \,=\, 0\,, \qquad L \,=\, r^2\,\dot{\varphi} \,=\, \text{constant}\,, \tag{130}$$

while the third equation now reads

$$-\Big(1-\frac{r_S}{r}\Big)c^2\dot{t}^2 \,+\, \frac{\dot{r}^2}{1-\dfrac{r_S}{r}} \,+\, r^2\dot{\varphi}^2 \,=\, 0\,. \tag{131}$$

The three equations (129), (130) and (131) completely determine the lightlike geodesics, because one can check that the r component of the Euler-Lagrange equation is a consequence of these three equations. We solve these three equations for the velocities,

$$\dot{t} \,=\, \frac{E}{c^2\Big(1-\dfrac{r_S}{r}\Big)}\,, \tag{132}$$

$$\dot{\varphi} \,=\, \frac{L}{r^2}\,, \tag{133}$$

$$\dot{r}^2 \,=\, \Big(1-\frac{r_S}{r}\Big)\left(\frac{\Big(1-\dfrac{r_S}{r}\Big)c^2E^2}{c^4\Big(1-\dfrac{r_S}{r}\Big)^2} \,-\, \frac{r^2L^2}{r^4}\right) \,=\, \frac{E^2}{c^2} \,-\, \Big(1-\frac{r_S}{r}\Big)\,\frac{L^2}{r^2}\,. \tag{134}$$

As we have discussed the radial light rays already above, when introducing Eddington-Finkelstein coordinates, we consider now only non-radial ones. Then we can use φ as the curve parameter.

From (132), (133) and (134) we find the *orbit equation* for light rays

$$\Big(\frac{dr}{d\varphi}\Big)^2 \,=\, \frac{\dot{r}^2}{\dot{\varphi}^2} \,=\, \frac{r^4}{L^2}\left(\frac{E^2}{c^2} \,-\, \frac{L^2}{r^2} \,+\, \frac{r_SL^2}{r^3}\right) \,=\, \frac{E^2}{c^2L^2}\,r^4 \,-\, r^2 \,+\, r_Sr\,. \tag{135}$$

(a) Circular light rays

We will first inquire if there are circular lightlike geodesics. To that end we consider the orbit equation (135) and its derivative with respect to φ,

$$2\,\frac{\cancel{dr}}{\cancel{d\varphi}}\,\frac{d^2r}{d\varphi} \;=\; \Big(\,\frac{4\,E^2r^3}{c^2L^2} \;-\; 2\,r \;+\; r_S\,\Big)\,\frac{\cancel{dr}}{\cancel{d\varphi}}\;. \tag{136}$$

As in the timelike case, dividing by $dr/d\varphi$ is legitimate, by continuity, even if $dr/d\varphi = 0$. For a circular lightlike geodesic we must have $\dfrac{dr}{d\varphi} = 0$ and $\dfrac{d^2r}{d\varphi^2} = 0$, which gives us the following two equations:

$$0 \;=\; \frac{E^2r^4}{c^2L^2} \;-\; r^2 \;+\; r_S\,r\;, \tag{137}$$

$$0 \;=\; \frac{4\,E^2r^3}{c^2L^2} \;-\; 2\,r \;+\; r_S\,. \tag{138}$$

To eliminate E^2/L^2, we multiply the first equation with $4/r$ and subtract the second equation. This results in

$$0 \;=\; -\,2\,r \;+\; 3\,r_S \qquad\Longleftrightarrow\qquad r \;=\; \frac{3}{2}\,r_S \;=\; \frac{3GM}{c^2}\;. \tag{139}$$

We have thus shown that there is a circular lightlike geodesic (or *photon circle*) at the radius value $3GM/c^2$. For the sake of illustration, one may assume that there is a tunnel built around such a circular lightlike geodesic; then by looking into this tunnel one would have the visual impression that the tunnel is perfectly straight and at the end of the tunnel one would see the back of one's own head.

As we can choose *any* plane through the origin as our equatorial plane $\vartheta = \pi/2$, there is actually a *photon sphere* at this radius value in the sense that every great circle on this sphere is a lightlike geodesic. The photon sphere at $r = 3r_S/2$ does, of course, not exist for stars whose physical radius r_* is bigger than $3r_S/2$. It is relevant only for black holes and for (hypothetical) *ultracompact stars* where $r_S < r_* < 3r_S/2$.

We will show in the 4th worksheet that the photon circles at $r = 3r_S/2$ are unstable in the following sense: A lightlike geodesic in the equatorial plane with an initial condition that deviates slightly from that of a photon circle at $r = 3r_S/2$ will spiral away from $r = 3r_S/2$ and either go to infinity or to the horizon.

For later convenience, we also calculate the value of the constant of motion L^2/E^2 that corresponds to a photon circle: If we insert the value $r = 3r_S/2$ into the equation

$$0 \;=\; \frac{E^2r^3}{c^2L^2} \;-\; r \;+\; r_S \tag{140}$$

we find

$$\frac{E^2}{c^2L^2} \;=\; \frac{\dfrac{3}{2}\,r_S - r_S}{\dfrac{27}{8}\,r_S^3} \;=\; \frac{4}{27\,r_S^2}\;. \tag{141}$$

(b) Exact deflection angle

From the orbit equation of light rays we can derive an exact formula for the deflection angle. We want to consider a light ray that comes in from infinity, goes through a minimum radius value at $r = r_m$ and then escapes back to infinity. We want to express the deflection angle δ in terms of r_m and the mass of the central body.

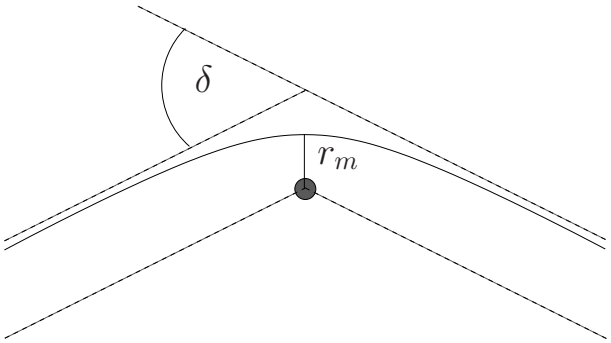

We start out from the orbit equation (135). E^2/L^2 is determined by the condition that

$$0 \;=\; \Big(\frac{dr}{d\varphi}\Big)^2\Big|_{r=r_m} \;=\; \frac{E^2}{c^2L^2}\,r_m^4 \;-\; r_m^2 \;+\; r_S\,r_m$$

$$\Longrightarrow \qquad \frac{E^2}{c^2L^2} \;=\; \frac{1}{r_m^2} \;-\; \frac{r_S}{r_m^3}\,. \tag{142}$$

We can, thus, rewrite the orbit equation (135) as

$$d\varphi \;=\; \frac{\pm dr}{\sqrt{\Big(\dfrac{1}{r_m^2} \;-\; \dfrac{r_S}{r_m^3}\Big)\,r^4 \;-\; r^2 \;+\; r_S\,r}}\,. \tag{143}$$

Integration over the light ray results in

$$\int_{\varphi_0}^{\varphi_0+\pi+\delta} d\varphi \;=\; \Big(\;-\int_{\infty}^{r_m} \;+\; \int_{r_m}^{\infty}\Big)\,\frac{dr}{\sqrt{\Big(\dfrac{1}{r_m^2} \;-\; \dfrac{r_S}{r_m^3}\Big)\,r^4 \;-\; r^2 \;+\; r_S\,r}} \tag{144}$$

where the signs of the two integrals on the right-hand side had to be chosen in agreement with the fact that φ is always increasing. We have thus found an exact formula,

$$\pi \;+\; \delta \;=\; 2\int_{r_m}^{\infty} \frac{r_m\,dr}{\sqrt{\Big(1 \;-\; \dfrac{r_S}{r_m}\Big)\,r^4 \;-\; r_m^2\,r^2 \;+\; r_m^2\,r_S\,r}}\,, \tag{145}$$

for the deflection angle δ in terms of an elliptic integral. r_m labels the light ray. It is clear that only values $r_m > r_S$ are possible because a light ray cannot come back if it has crossed the horizon. We will soon see that, actually, r_m cannot be arbitrarily close to r_S.

From the derivation it is clear that the integrand has a singularity at the lower bound $r = r_m$, so the evaluation of the integral needs some care. A more detailed analysis shows that the integral is finite for all values of r_m that are bigger than $3r_S/2$. If we consider a sequence of light rays with r_m approaching $3r_S/2$ from above, the deflection angle δ becomes bigger and bigger which means that the light rays make more and more turns around the centre. In the limit $r_m \to 3r_S/2$ the integral goes to infinity and the limiting light ray spirals asymptotically towards a circle at $r = 3r_S/2$. This is a general feature of lightlike geodesics in spherically symmetric and static spacetimes: If an unstable photon circle is approached, the deflection angle goes to infinity.

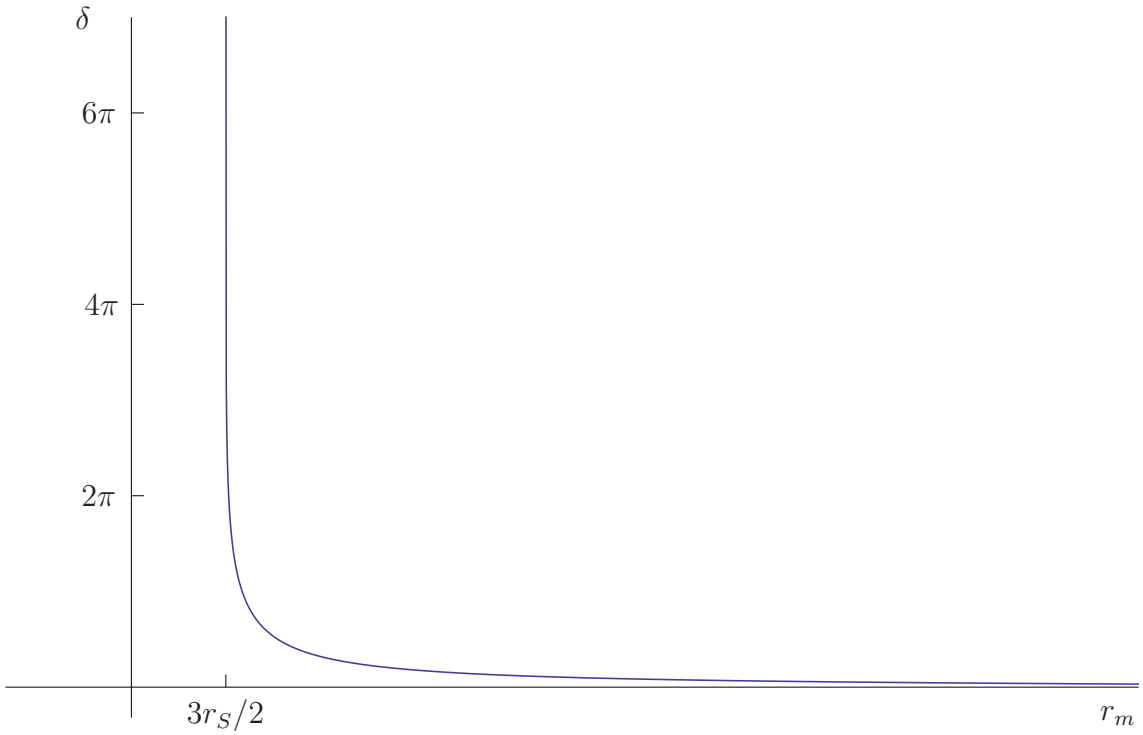

Plot of the bending angle δ against the minimum radius r_m.

(c) Shadow of a Schwarzschild black hole

We fix an observer at radius r_O and consider all light rays that go from the position of this observer into the past. (To put this another way, we consider all light rays that *arrive* at the position of the observer.) They fall into two categories: Category I consists of light rays that go out to infinity, category II consists of light rays that go to the horizon at $r = r_S$. The borderline case that separates the two categories is given by light rays that asymptotically spiral towards the light sphere at $r = 3r_S/2$.

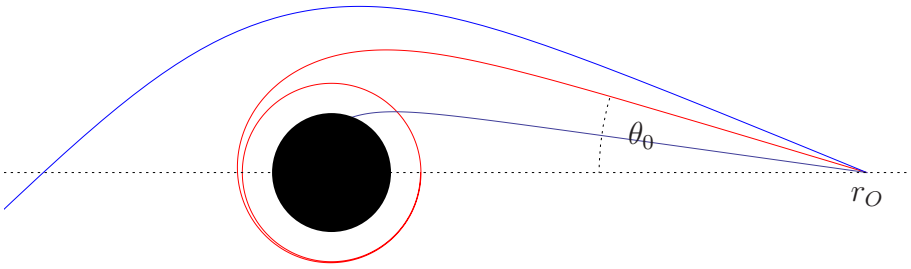

Now assume that there are light sources distributed everywhere in the spacetime but not between the observer and the black hole. Then the initial directions of light rays of category I correspond to points at the observer's sky that are bright, and the initial directions of light rays of category II correspond to points at the observer's sky that are dark, known as the *shadow* of the black hole. The boundary of the shadow corresponds to light rays that spiral towards $r = 3r_S/2$. It is our goal to calculate the angular radius θ_0 of the shadow, in dependence of r_S and r_O.

For any light ray, the initial direction makes an angle θ with respect to the axis that is given, according to the picture, by

$$\tan\theta \;=\; \lim_{\Delta x\to 0}\frac{\Delta y}{\Delta x}\,.$$

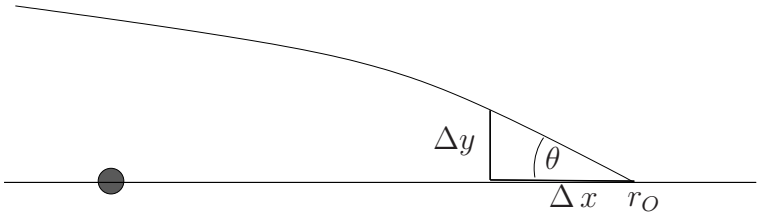

From the Schwarzschild metric in the equatorial plane,

$$g \;=\; -\Big(1-\frac{r_S}{r}\Big)c^2dt^2 \;+\; \frac{dr^2}{1-\dfrac{r_S}{r}} \;+\; r^2d\varphi^2\,, \tag{146}$$

we can read the length Δx and Δy in the desired limit,

$$\tan\theta \;=\; \frac{r\,d\varphi}{\Big(1-\dfrac{r_S}{r}\Big)^{-1/2}dr}\bigg|_{r=r_O}\,. \tag{147}$$

$dr/d\varphi$ can be expressed with the help of the orbit equation (135), hence

$$\tan^2\theta \;=\; \frac{r_O^2\Big(1-\dfrac{r_S}{r_O}\Big)}{\dfrac{E^2r_O^4}{c^2L^2}-r_O^2+r_Sr_O} \;=\; \frac{r_O-r_S}{\dfrac{E^2r_O^3}{c^2L^2}-r_O+r_S}\,. \tag{148}$$

By elementary trigonometry,

$$\frac{1}{\tan^2\theta} = \frac{E^2 r_O^3}{c^2 L^2 \big(r_O - r_S\big)} - 1\,,$$

$$\frac{\sin^2\theta}{\sin^2\theta} + \frac{\cos^2\theta}{\sin^2\theta} = \frac{E^2 r_O^3}{c^2 L^2 \big(r_O - r_S\big)}\,,$$

$$\sin^2\theta = \frac{c^2 L^2 \big(r_O - r_S\big)}{E^2 r_O^3}\,. \tag{149}$$

The angular radius θ_0 of the shadow is given by the angle θ for a light ray that spirals towards $r = 3r_S/2$. This light ray must have the same constants of motion E and L as a circular light ray at $r = 3r_S/2$ (because the tangent vectors of these two light rays come arbitrarily close to each other),

$$\frac{c^2 L^2}{E^2} \;=\; \frac{27}{4} r_S^2 \tag{150}$$

as we have calculated in (141).

This gives us θ_0 in dependence of $r_S = 2GM/c^2$ and r_O,

$$\sin^2\theta_0 \;=\; \frac{27\, r_S^2 (r_O - r_S)}{4\, r_O^3}\,. \tag{151}$$

This formula was found by J. Synge [Mon. Not. Roy. Astron. Soc. **131**, 463 (1966)] and independently by Y. Zeldovich and I. Novikov [Sov. Phys. Usp. 8, 522 (1966)]. Neither of them used the word "shadow" which was introduced only in 2000 by Heino Falcke. If the observer is far away from the black hole, $r_O - r_S \approx r_O$, (151) can be approximated by

$$\tan\theta_0 \;\approx\; \sin\theta_0 \;\approx\; \sqrt{3} \times \frac{3\, r_S}{2\, r_O}\,.$$

Up to a factor of $\sqrt{3}$, θ_0 is then the angular radius under which a sphere of radius $3r_S/2$ is seen from a distance r_O according to Euclidean geometry. This means that a naive Euclidean estimate correctly gives the order of magnitude of the diameter of the shadow if the observer is far away.

Note that

$r_O \to \infty$: $\theta_0 \to 0$ (i.e., the shadow vanishes).

$r_O = 3r_S/2$: $\theta_0 = \pi/2$ (i.e., the shadow covers half of the sky).

$r_O \to r_S$: $\theta_0 \to \pi$ (i.e., the shadow covers the whole sky).

The following picture shows, for various observer positions, in red the part of the sky that is bright. Note that our calculation applies to a static observer at the corresponding position. For a moving observer the aberration formula has to be applied. As the aberration formula maps circles onto circles, the shadow of a Schwarzschild black hole is *always* seen circular, independent of the state of motion of the observer. For an observer moving towards the black hole the shadow is smaller than for a static observer, for an obsever moving away from the black hole it is bigger.

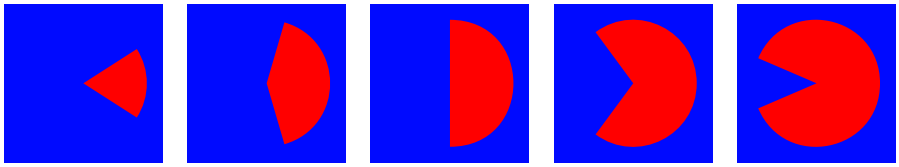

$r_O = 1.05\, r_S$ $r_O = 1.3\, r_S$ $r_O = 3\, r_S/2$ $r_O = 2.5\, r_S$ $r_O = 6\, r_S$

We have good evidence that there is a supermassive black hole at the centre of our Galaxy, associated with the radio source Sgr A*. For the shadow of this black hole ($M \approx 4 \times 10^6\, M_\odot$, $r_O \approx 8.5\,\mathrm{kpc}$) Synge's formula gives an angular diameter of $2\theta_0 \approx 54\,\mu\mathrm{as}$. This corresponds to the angle under which a grapefruit on the Moon is seen from Earth. Another promising candidate is the black hole at the centre of the galaxy M87 in the constellation Virgo. In this case ($M \approx 6 \times 10^9\, M_\odot$, $r_O \approx 16\,\mathrm{Mpc}$) one finds $2\theta_0 \approx 38\,\mu\mathrm{as}$. For all other known black-hole candidates the predicted angular diameter of the shadow is considerably smaller. A picture of the shadow of the object at the centre of M87 was actually made public in April 2019, and of the object of the centre of our Galaxy in May 2022, see below.

Note that the shadow would exist not only for a black hole, but in exactly the same way also for an ultracompact star ($r_S < r_* < 3r_S/2$), provided the star is dark. It is the light sphere at $r = 3r_S/2$ and not the horizon at $r = r_S$ that is relevant for the formation of the shadow. The existence of ultracompact stars is highly speculative. Also, a wormhole would cast a shadow if there is no light coming out of its mouth. However, again, the existence of wormholes is highly speculative.

Our calculation was based on the Schwarzschild metric, so it does not apply to a *rotating* black hole. The latter is to be described by the Kerr metric; we will show later that then the shadow turns out to be non-circular. In any case, our calculation with the Schwarzschild metric gives the correct order of magnitude for the size of the shadow.

For observing the shadow we need light sources which provide a bright backdrop against which the shadow can be seen. We need to know how many images each light source produces. To that end we fix a static observer at radius r_O and a static light source at radius r_L. We exclude the case that observer and light source are exactly aligned (i.e., that they are on a straight line through the origin of the coordinate system) which would give rise to Einstein rings instead of point images. If one thinks of each lightlike geodesic as being surrounded by a thin bundle that is focussed onto the observer's retina (or onto a photographic plate) with a lens, every lightlike geodesic from the light source to the observer gives rise to an image.

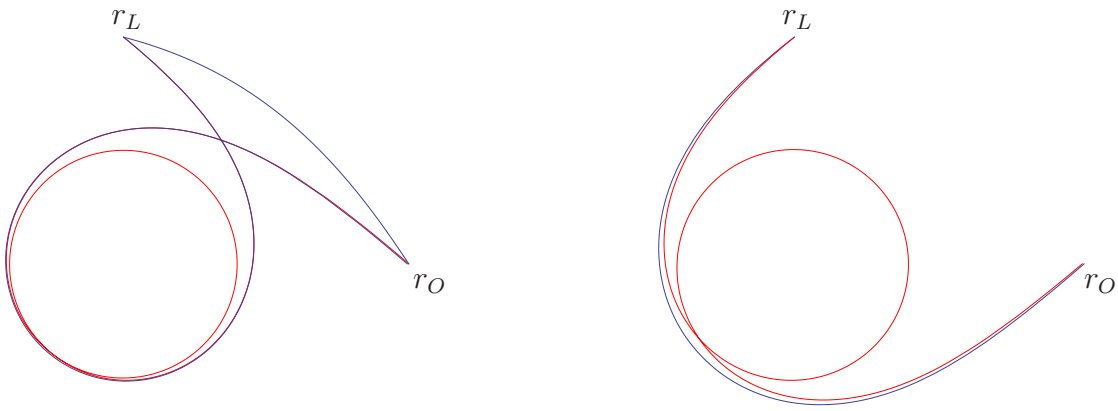

The qualitative imaging features follow from the fact that the bending angle grows monotonically to infinity for light rays that approach the photon sphere at $r = 3r_S/2$. As a consequence, for any integer $n = 0, 1, 2, 3, \ldots$ there is a light ray from the light source to the observer that makes n full turns in the clockwise sense, and another light ray from the light source to the observer that makes n full turns in the counter-clockwise sense. Hence, there are two infinite sequences of light rays from the light source to the observer, one in the clockwise sense (left picture) and one in the counter-clockwise sense (right picture). Either sequence has as its limit curve a light ray that spirals asymptotically towards $r = 3r_S/2$. The pictures are not just qualitatively correct; they show numerically integrated lightlike geodesics in the Schwarzschild spacetime. One sees that for each sequence the light rays with $n = 1, 2, 3, \ldots$ lie practically on top of each other. Correspondingly, the observer sees infinitely many images on either side of the centre. Each sequence rapidly approaches the boundary of the shadow.

In the picture on the right, which is again the result of a calculation, the shadow is shown as a black disc. On either side only the outermost image ($n = 0$) can be isolated, all the other ones clump together and they are very close to the boundary of the shadow. If there are many light sources, their higher-order images form a bright ring around the shadow.

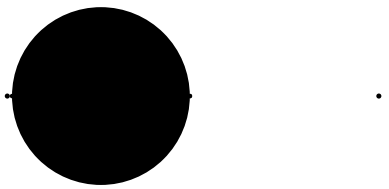

It can be shown that the outermost images are brighter than all the other ones combined. Of the two outermost images, the brighter one is called the *primary image* and the other one is called the *secondary image*. All the remaining ones, which correspond to light rays that make at least one full turn around the centre, are known as *higher-order images*.

The first computer simulation of the visual appearance of a Schwarzschild black hole was produced by J.-P. Luminet in 1979. Here it is assumed that the light comes from a rotating accretion disc. Part of the disc is in front of the black hole, so it covers part of the shadow. The rear part of the disc appears bent upwards because of the light bending. One side of the disc is approaching the observer; because of time-reversed aberration, it appears brighter than the receding side. Time-reversed aberration is sometimes called *beaming*. The higher-order images form a thin bright ring around the shadow.

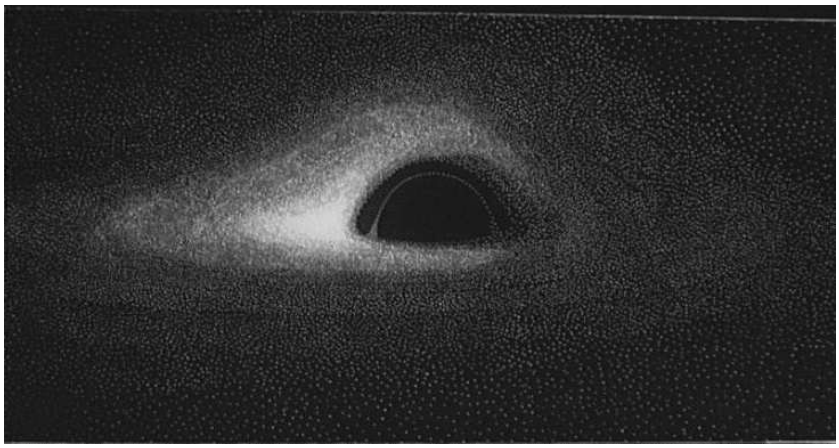

From J.-P. Luminet, Astron. Astrophys. 75, 228 (1979)

A similar simulation was shown in the movie "Interstellar". Here the viewing angle is smaller, i.e., the accretion disc is seen almost exactly edge-on. For this reason one sees both the upper side and the lower side of the rear part of the disc.

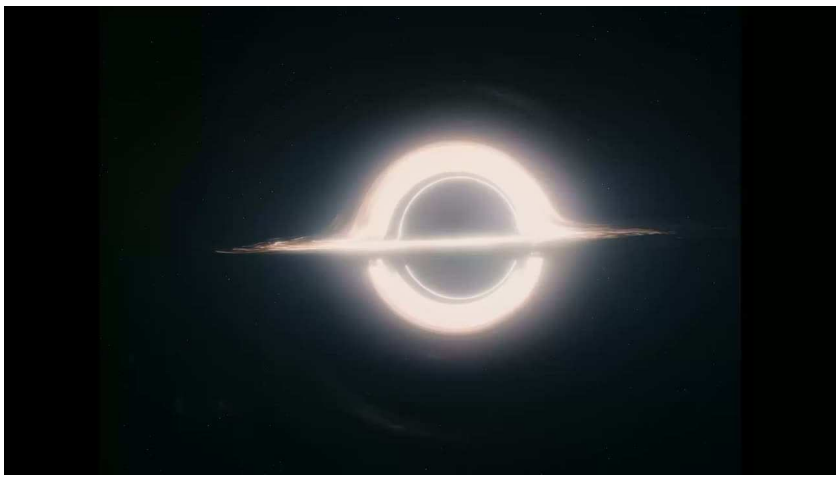

From the movie "Interstellar"

Finally, on 10 April 2019 the first "real picture" of a black hole was presented to the public. The data were taken in April 2017, so the evaluation took two years. The picture was produced by a collaboration of approximately 350 scientists with the so-called *Event Horizon Telescope*. In contrast to what the name suggests, this is not one telescope but it consists of many (radio) telescopes distributed over one hemisphere of the Earth. Each of these telescopes measures the intensity and the phase of the incoming radiation. From these data the Fourier transform of the image can be calculated, from which then a real image is produced. This method is known as *aperture synthesis*. It was invented in the 1950s by Martin Ryle which earned him the physics Nobel Prize in 1974. When used with telescopes on different continents one speaks of *Very Long Baseline Interferometry* (VLBI).

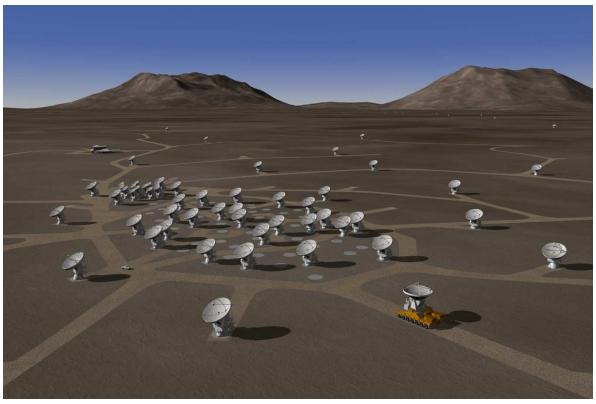

ALMA

In 2017, when the successful observations took place, the Event Horizon Telescope included the *Atacama Large Millimeter Array* (ALMA) and the *ALMA Pathfinder Experiment* (APEX) in Chile, the *South Pole Telescope* (SPT), the *Large Millimeter Telescope* (LMT) in Mexico, the *James Clerk Maxwell Telescope* (JCMT) and the *Submillimeter Array* (SMA) on Hawaii, the *Submillimeter Telescope Observatory* (SMT) in Arizona, USA, and the *Pico Veleta Telescope* (PV) in Spain. As scattering would wash out the image at larger wave lengths, the observations were made at a wave length of 1.3 mm which corresponds to a frequency of 230 GHz. At such a small wave length, VLBI is possible only since a few years. As radiation at 1.3 mm is partially blocked by the water vapour in our atmosphere, only telescopes at a high altitude can be used. Although our Sun is not very bright at 1.3 mm, the observations were done during the night time because then the atmosphere is more stable. At four nights in April 2017, the weather conditions were excellent so that observations were possible at all stations. Both Sgr A* and M87 were observed. However, the environment of Sgr A* turned out to change so rapidly that it took approximately five years to produce a picture. In the case of M87 the central black hole is a thousand times heavier, so the orbital periods of particles revolving around the black hole are of the order of days, rather than minutes as for Sgr A*. This is the reason why a surprisingly good picture of this object could be produced, see next page

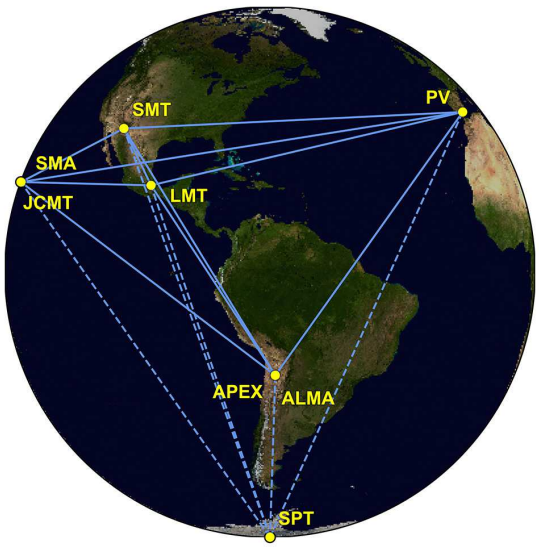

Event Horizon Telescope

One clearly sees a black disc in the centre and a bright ring around it. The bright ring is interpreted as radiation coming from an accretion disc. The fact that one side of the ring is considerably brighter than the other indicates that this side is moving towards us. Comparison with simulations indicate that the spin vector of the accretion disc points into the page and a bit to the left. (In the pictures North is up and West is right.) All observations are in agreement with the assumption that the spin of the black hole is aligned with the spin of the accretion disc. The fact that the shadow is practically circular does not mean that the black hole is non-rotating: As we look onto the system almost from the bottom, even for a fast rotating black hole the shadow would be seen as almost circular. The thin ring of higher-order images around the shadow is not visible; this is in agreement with simulations which show that it is too faint.

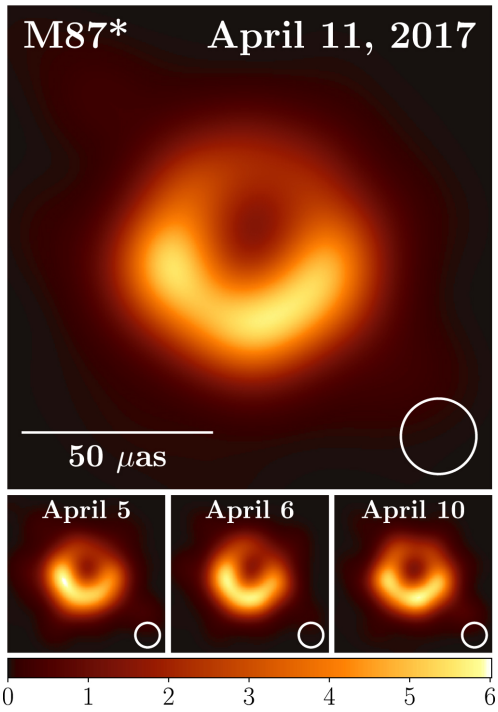

M87* – From The Event Horizon Telescope Collaboration, Astrophys. J. Lett. 875, L1 (2019)

In the case of the centre of our Galaxy pictures were released only in May 2022, more than five years after the data were taken. Somewhat surprisingly, also in this case the pictures suggest that we look approximately from the top or from the bottom onto the black hole. Many scientists had expected that the view would be more edge-on, such as in the Luminet and the Interstellar pictures. If we are really looking from the top or from the bottom on the black hole, this would mean that the spin axis is approximately tangent to the galactic disc and, very coincidentally, pointing approximately towards us (or away from us).

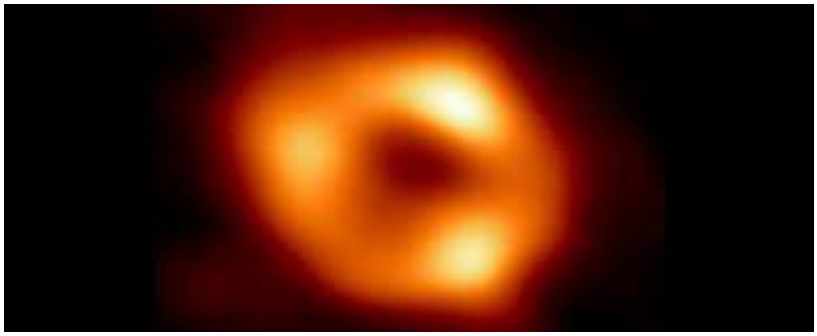

Sgr A* – From The Event Horizon Telescope Collaboration, Astrophys. J. Lett. 930, L12 (2022)

4 4. Spherically symmetric gravitational collapse

Stars are stable as long as the pressure balances the gravitational attraction. If the nuclear fuel at the core of a star is used up, the star becomes unstable, possibly blows away some of its mass in a nova or supernova explosion and then collapses. According to present knowledge, there are three possible end states of a star.

- A star could end up as a *white dwarf*, where the electrons form a degenerate Fermi gas. The *electron degeneracy pressure* can balance the gravitational attraction. White dwarfs have a radius of about 5000 km, i.e., they are similar in size to the Earth. It was shown by S. Chandrasekhar in the early 1930s that a white dwarf must have a mass $M \lessapprox 1.4\, M_\odot$. This work won him the physics Nobel prize in 1983.

- Another possible end state is a *neutron star*. Neutron stars are much more difficult to understand than white dwarfs. Roughly speaking, they consist of extremely densely packed neutrons. It is the *neutron degeneracy pressure* that balances gravity so that a stable object results. Typically, a neutron star has a radius between 10 and 20 km. Similarly to the Chandrasekhar limit for white dwarfs, there is an upper limit for the mass of a neutron star, but it is not yet precisely known. The most massive neutron star that has been found so far has a little bit more than 2 Solar masses. Most experts believe that the maximal mass of a neutron star is less than 3 Solar masses.

- A star that is so massive that it cannot end up as a white dwarf or a neutron star is believed to undergo *gravitational collapse* and to form a *black hole* at the end of its life. If the star is spherically symmetric (i.e., in particular non-rotating), then the domain outside of the star is always given by the Schwarzschild metric, owing to the Jebsen-Birkhoff theorem. If the star that has fallen through its Schwarzschild radius, it is doomed. Then the entire interior of the star must end up in a singularity at $r = 0$ in a finite time. This follows from the consideration in the preceding section, because a mass element on the surface of the star must move on a timelike curve in the ambient vacuum Schwarzschild spacetime.

In this chapter we want to discuss the dynamical process of the collapse. In analytical terms, this is possible only for the simple case of a spherically symmetric ball of dust. In a sense, this is a trivial situation, because it is clear that in the case of perfect spherical symmetry the entire star must collapse into a singularity under the influence of its own gravity if there is no pressure. However, it is remarkable that the metric inside the star can be determined fully analytically as an exact solution to Einstein's field equation (with a dust source), and that an exact analytical formula can be given for the radius of the star as a function of time.

The following calculation follows J. R. Oppenheimer and H. Snyder [Phys. Rev. **56**, 455 (1939)]. It is based on the exact solution of Einstein's field equation for a spherically symmetric dust which had been found by R. Tolman [Proc. Nat. Acad. Sci. **20**, 169 (1934)] already a few years earlier.

It is shown in a first course on general relativity that any spherically symmetric metric can be written, in spherical polar coordinates $(t, \rho, \vartheta, \varphi)$, as

$$g \;=\; -\,c^2 e^{\nu(t,\rho)} dt^2 \;+\; e^{\lambda(t,\rho)} d\rho^2 \;+\; Y(t,\rho)^2 \big(d\vartheta^2 + \sin^2\vartheta\, d\varphi^2\big)\,. \tag{152}$$

We want to solve Einstein's field equation

$$R_{\beta\gamma} - \frac{R}{2} g_{\beta\gamma} = \kappa T_{\beta\gamma} \tag{153}$$

with the energy-momentum tensor of a dust,

$$T^{\beta\gamma} = \mu U^\beta U^\gamma \tag{154}$$

where μ is the mass density, depending on t and ρ, and

$$U \;=\; U^\beta \, \frac{\partial}{\partial x^\beta} \tag{155}$$

is the four-velocity field of the dust. We will choose the coordinates such that the dust particles move on t-lines,

$$U^\beta \;=\; \alpha \, \delta^\beta_t \, . \tag{156}$$

The factor α is determined by the normalisation condition

$$-\, c^2 \;=\; g_{\beta\gamma} U^\beta U^\gamma \;=\; -\, c^2 \alpha^2 e^{\nu(t,\rho)} \, , \tag{157}$$

$$\alpha \;=\; e^{-\nu(t,\rho)/2} \, , \tag{158}$$

hence

$$U \;=\; e^{-\nu(t,\rho)/2} \, \frac{\partial}{\partial t} \, . \tag{159}$$

From the field equation it follows that $\nabla_\beta T^{\beta\gamma} = 0$ which implies that the dust particles move on geodesics,

$$\nabla_U U = 0 \, . \tag{160}$$

Again, we assume that this result is known from a first course in general relativity.

Claim: $\nabla_U U = 0$ implies that the metric function ν is independent of ρ.

Proof: From $\nabla_U U = 0$ we have

$$0 \;=\; g\big(\nabla_U U, \partial/\partial\rho\big) \;=\; U\, g\big(U, \partial/\partial\rho\big) - g\big(U, \nabla_U \partial/\partial\rho\big)$$

$$= e^{-\nu/2} \frac{\partial}{\partial t} \Big(e^{-\nu/2} \underbrace{g\big(\partial/\partial t, \partial/\partial\rho\big)}_{=g_{t\rho}=0} \Big) - e^{-\nu} g\big(\partial/\partial t, \nabla_{\partial/\partial t} \partial/\partial\rho\big)$$

$$= \; - \, e^{-\nu} \, g\big(\partial/\partial t, \nabla_{\partial/\partial\rho} \partial/\partial t\big) \;=\; - \, e^{-\nu} \, \frac{1}{2} \, \frac{\partial}{\partial\rho} g\big(\partial/\partial t, \partial/\partial t\big) \;=\; - \, e^{-\nu} \, \frac{1}{2} \, \frac{\partial}{\partial\rho} \, g_{tt}$$

$$= \; e^{-\nu} \, \frac{c^2}{2} \, \frac{\partial}{\partial\rho} \, e^\nu \;=\; e^{-\nu} \, \frac{c^2}{2} \, e^\nu \, \frac{\partial\nu}{\partial\rho} \;=\; \frac{c^2}{2} \, \frac{\partial\nu}{\partial\rho} \, , \tag{161}$$

hence $\partial\nu/\partial\rho = 0$. □

We can thus introduce a new time coordinate τ by

$$d\tau = e^{\nu(t)/2} dt\,, \qquad \tau = \int_{t_0}^{t} e^{\nu(\tilde{t})/2} d\tilde{t}\,. \tag{162}$$

In the coordinates $(\tau, \rho, \vartheta, \varphi)$, the metric reads

$$g = -c^2 d\tau^2 + e^{\tilde{\lambda}(\tau,\rho)} d\rho^2 + \tilde{Y}(\tau,\rho)^2 \big(d\vartheta^2 + \sin^2\vartheta\, d\varphi^2\big) \tag{163}$$

with transformed functions $\tilde{\lambda}$ and $\tilde{Y}$. In the following we will drop the tildes.

As the metric is not regular (in the chosen coordinates) at any point where $Y = 0$, we may assume that $Y > 0$ without loss of generality.

The four-velocity of the dust is

$$U \;=\; c\,\frac{\partial}{\partial\tau} \tag{164}$$

and the energy-momentum tensor is

$$T_{\beta\gamma} = \mu \delta^\tau_\beta \delta^\tau_\gamma\,. \tag{165}$$

From these expressions we read that τ is proper time of the dust particles. This form of the metric is known as a spherically symmetric dust in *comoving coordinates*.

We will now evaluate the field equation

$$R_{\beta\gamma} - \frac{R}{2} g_{\beta\gamma} = \kappa T_{\beta\gamma}\,. \tag{166}$$

This requires calculating the Christoffel symbols and, thereupon, the components of the Ricci tensor of the metric (163) which can be quickly done, e.g., with Mathematica. One finds that there are four non-trivial equations.

The $\tau\tau-$component:

$$-\frac{c^2 e^{-\lambda}}{Y}\left(2\,\frac{\partial^2 Y}{\partial\rho^2} - \frac{\partial\lambda}{\partial\rho}\frac{\partial Y}{\partial\rho}\right) - \frac{c^2 e^{-\lambda}}{Y^2}\left(\frac{\partial Y}{\partial\rho}\right)^2 + \frac{c^2}{Y^2} + \frac{1}{Y^2}\left(\frac{\partial Y}{\partial\tau}\right)^2 + \frac{1}{Y}\,\frac{\partial\lambda}{\partial\tau}\,\frac{\partial Y}{\partial\tau} = \kappa\, c^4 \mu\,. \tag{167}$$

The $\rho\rho-$component:

$$\frac{e^{\lambda}}{\cancel{Y}^2}\left\{e^{-\lambda}\Big(\frac{\partial Y}{\partial\rho}\Big)^2 - \frac{2Y}{c^2}\,\frac{\partial^2 Y}{\partial\tau^2} - \frac{1}{c^2}\left(\frac{\partial Y}{\partial\tau}\right)^2 - 1\right\} = 0\,. \tag{168}$$

The $\vartheta\vartheta-$component:

$$\frac{\cancel{Y}}{2}\left\{e^{-\lambda}\left(2\,\frac{\partial^2 Y}{\partial\rho^2} - \frac{\partial\lambda}{\partial\rho}\frac{\partial Y}{\partial\rho}\right) - \frac{1}{c^2}\,\frac{\partial Y}{\partial\tau}\frac{\partial\lambda}{\partial\tau} - \frac{2}{c^2}\,\frac{\partial^2 Y}{\partial\tau^2} - \frac{Y}{2\,c^2}\left(\frac{\partial\lambda}{\partial\tau}\right)^2 - \frac{Y}{c^2}\,\frac{\partial^2\lambda}{\partial\tau^2}\right\} = 0\,. \tag{169}$$

The $\tau\rho-$component:

$$\frac{1}{\cancel{Y}}\left\{\frac{\partial Y}{\partial\rho}\frac{\partial\lambda}{\partial\tau} - 2\,\frac{\partial^2 Y}{\partial\tau\partial\rho}\right\} = 0\,. \tag{170}$$

The $\varphi\varphi-$components gives the same equation as the $\vartheta\vartheta-$components and all other components reduce to the identity $0 = 0$.

To solve this system of differential equations, we begin with (170).

$$\frac{\partial\lambda}{\partial\tau} \;=\; \frac{2\dfrac{\partial^2 Y}{\partial\tau\partial\rho}\dfrac{\partial Y}{\partial\rho}}{\Big(\dfrac{\partial Y}{\partial\rho}\Big)^2} \;=\; \frac{\dfrac{\partial}{\partial\tau}\Big(\dfrac{\partial Y}{\partial\rho}\Big)^2}{\Big(\dfrac{\partial Y}{\partial\rho}\Big)^2} \;=\; \frac{\partial}{\partial\tau}\ln\Big(\frac{\partial Y}{\partial\rho}\Big)^2 . \tag{171}$$

Hence

$$\frac{\partial}{\partial\tau}\left(-\lambda + \ln\Big(\frac{\partial Y}{\partial\rho}\Big)^2 \right) \;=\; 0\,,$$

which gives, upon integration,

$$-\lambda + \ln\Big(\frac{\partial Y}{\partial\rho}\Big)^2 \;=\; H(\rho) \tag{172}$$

with some function $H(\rho)$. Exponentiating (172) yields

$$e^{-\lambda}\left(\frac{\partial Y}{\partial\rho}\right)^2 = e^{H(\rho)}\,. \tag{173}$$

With the help of this expression, its ρ derivative

$$e^{-\lambda}\left(2\,\frac{\partial Y}{\partial\rho}\,\frac{\partial^2 Y}{\partial\rho^2} - \frac{\partial\lambda}{\partial\rho}\left(\frac{\partial Y}{\partial\rho}\right)^2\right) = e^{H(\rho)}\,H'(\rho) \tag{174}$$

and (170) we can eliminate λ and its derivatives from the remaining three components of the field equation (167), (168) and (167).

The $\tau\tau-$component:

$$-\frac{c^2}{Y}\Big(\frac{\partial Y}{\partial\rho}\Big)^{-1} e^{H(\rho)}H'(\rho) - \frac{c^2}{Y^2}\,e^{H(\rho)} + \frac{c^2}{Y^2} + \frac{1}{Y^2}\left(\frac{\partial Y}{\partial\tau}\right)^2 + \frac{2}{Y}\,\frac{\partial Y}{\partial\tau}\Big(\frac{\partial Y}{\partial\rho}\Big)^{-1}\frac{\partial^2 Y}{\partial\tau\partial\rho} = \kappa\,c^4\mu\,. \tag{175}$$

The $\rho\rho-$component:

$$e^{H(\rho)} - \frac{2Y}{c^2}\,\frac{\partial^2 Y}{\partial\tau^2} - \frac{1}{c^2}\left(\frac{\partial Y}{\partial\tau}\right)^2 - 1 = 0\,. \tag{176}$$

The $\vartheta\vartheta-$component:

$$\Big(\frac{\partial Y}{\partial\rho}\Big)^{-1}\left\{e^{H(\rho)}H'(\rho) - \frac{2}{c^2}\,\frac{\partial Y}{\partial\tau}\,\frac{\partial^2 Y}{\partial\rho\partial\tau} - \frac{2}{c^2}\,\frac{\partial Y}{\partial\rho}\,\frac{\partial^2 Y}{\partial\tau^2} - \frac{2\,Y}{c^2}\,\frac{\partial^3 Y}{\partial\tau^2\partial\rho}\right\} = 0\,. \tag{177}$$

We see that we only have to solve (176). Then (175) determines the mass density μ and (177) is also satisfied because the curly bracket in (177) is just the ρ derivative of the left-hand side of (176).

As (176) involves no ρ derivatives, we may fix an arbitrary value of ρ and then view (176) as an *ordinary* differential equation for Y as a function of τ.

$$\frac{2Y}{c^2}\frac{d^2 Y}{d\tau^2} + \frac{1}{c^2}\Big(\frac{dY}{d\tau}\Big)^2 = G \tag{178}$$

where

$$G = e^{H(\rho)} - 1 \tag{179}$$

with the chosen value of ρ. We substitute

$$u \,=\, \frac{1}{c^2}\Big(\frac{dY}{d\tau}\Big)^2 . \tag{180}$$

This implies

$$\frac{d}{dY}\big(uY\big) \,=\, u \,+\, Y\frac{du}{dY} \,=\, \frac{1}{c^2}\Big(\frac{dY}{d\tau}\Big)^2 \,+\, \frac{2Y}{c^2}\,\frac{\cancel{dY}}{\cancel{d\tau}}\,\frac{d^2Y}{d\tau^2}\,\frac{\cancel{d\tau}}{\cancel{dY}} \,=\, G\,,$$

$$uY = GY + F \tag{181}$$

with another integration constant F (which depends on the chosen value of ρ, just as G does). Upon resubstituting for u we find

$$\frac{1}{c^2}\Big(\frac{dY}{d\tau}\Big)^2 \,= G \,+\, \frac{F}{Y}\,. \tag{182}$$

This ordinary differential equation for Y as a function of τ can be integrated. We have to do the integration separately for the cases that G is positive, negative or zero. To that end we write

$$G \,=\, -\,\varepsilon\, f^2 \tag{183}$$

where ε takes the value $+1$, -1 or 0, and f is a postive constant (dependent on the chosen value of ρ). Then (182) reads

$$\frac{1}{c^2}\Big(\frac{dY_\varepsilon}{d\tau}\Big)^2 \,= -\varepsilon\, f^2 \,+\, \frac{F}{Y_\varepsilon}\,. \tag{184}$$

We first solve this for the case $\varepsilon = 0$,

$$\frac{1}{c^2}\Big(\frac{dY_0}{d\tau}\Big)^2 \,=\, \frac{F}{Y_0}\,. \tag{185}$$

As Y_0 is positive, this equation requires F to be non-negative,

$$\sqrt{Y_0}\,dY_0 \,=\, \pm\, c\,\sqrt{F}\,d\tau\,, \tag{186}$$

$$\frac{2}{3}\,Y_0^{3/2} \,=\, \pm\, c\,\sqrt{F}\,\big(\tau - \tau_0\big) \tag{187}$$

with another integration constant τ_0 (which may depend on ρ), hence

$$Y_0 \,=\, \Big(\frac{9c^2}{4}\,F\,\big(\tau - \tau_0\big)^2\Big)^{1/3}\,. \tag{188}$$

We next solve (184) for $\varepsilon = \pm 1$. To that end we transform the time coordinate, $\tau \mapsto \eta_\varepsilon$, by

$$d\eta_\varepsilon \,=\, \frac{f}{Y_\varepsilon}\,c\,d\tau\,. \tag{189}$$

Then

$$\frac{1}{c^2}\Big(\frac{dY_\varepsilon}{d\eta_\varepsilon}\frac{d\eta_\varepsilon}{d\tau}\Big)^2 \;=\; -\,\varepsilon\,f^2 \;+\; \frac{F}{Y_\varepsilon}\,,$$

$$\frac{1}{\cancel{c^2}}\Big(\frac{dY_\varepsilon}{d\eta_\varepsilon}\Big)^2\frac{f^2\cancel{c^2}}{Y_\varepsilon^2} \;=\; -\,\varepsilon\,f^2 \;+\; \frac{F}{Y_\varepsilon}\,,$$

$$\Big(\frac{dY_\varepsilon}{d\eta_\varepsilon}\Big)^2 \;=\; -\,\varepsilon\,Y_\varepsilon^2 \;+\; \frac{FY_\varepsilon}{f^2}\,,$$

$$\frac{dY_\varepsilon}{\sqrt{\dfrac{FY_\varepsilon}{f^2} - \,\varepsilon\,Y_\varepsilon^2}} \;=\; \pm\,d\eta_\varepsilon\,. \tag{190}$$

This is an elementary integral that can be found in an integration table. The result is

$$2\arctan\left(\frac{\sqrt{Y_1}}{\sqrt{\frac{F}{f^2}-Y_1}}\right) = \pm\big(\eta_1-\eta_{1,0}\big) \tag{191}$$

for $\varepsilon = 1$ and

$$2\,\mathrm{arctanh}\left(\frac{\sqrt{Y_{-1}}}{\sqrt{\frac{F}{f^2}+Y_{-1}}}\right) = \pm\big(\eta_{-1}-\eta_{-1,0}\big) \tag{192}$$

for $\varepsilon = -1$. As (189) determines η_ε only up to an additive constant, we may choose the integration constants $\eta_{1,0} = 0$ and $\eta_{-1,0} = 0$ without loss of generality. Then we find for $\varepsilon = 1$

$$\frac{\sqrt{Y_1}}{\sqrt{\frac{F}{f^2}-Y_1}} = \pm\tan\Big(\frac{\eta_1}{2}\Big)\,,$$

$$Y_1\left(1+\tan^2\Big(\frac{\eta_1}{2}\Big)\right) \;=\; \frac{F}{f^2}\tan^2\Big(\frac{\eta_1}{2}\Big)\,,$$

$$Y_1 \;=\; \frac{F}{f^2}\sin^2\Big(\frac{\eta_1}{2}\Big) \;=\; \frac{F}{2\,f^2}\,\big(1-\cos\eta_1\big)\,. \tag{193}$$

Resubstituting this result into (189) gives the relation between η_1 and τ,

$$\big(1-\cos\eta_1\big)\,d\eta_1 \;=\; \frac{2\,f^3c\,d\tau}{F}\,,$$

$$\eta_1-\sin\eta_1 \;=\; \frac{2\,f^3c}{F}\,\big(\tau-\tau_0\big)\,, \tag{194}$$

again with an integration constant τ_0 (that may depend on ρ). Inserting (194), which determines η as a transcendental function of τ, into (193) gives us Y_1 as a function of τ. By a completely analogous calculation we find for $\varepsilon = -1$:

$$Y_{-1} \;=\; \frac{F}{f^2}\sinh^2\Big(\frac{\eta_{-1}}{2}\Big) \;=\; \frac{F}{2\,f^2}\,\big(\cosh\eta_{-1}-1\big)\,, \tag{195}$$

$$\sinh\eta_{-1} - \eta_{-1} \;=\; \frac{2\,f^3 c}{F}\,\big(\tau - \tau_0\big)\,. \tag{196}$$

Now making the dependence of ρ explicit again, we summarise our findings in the following way. By (182) and (183), the three solutions $Y = Y_\varepsilon$ satisfy

$$\frac{1}{c^2}\Big(\frac{\partial Y_\varepsilon(\tau,\rho)}{\partial\tau}\Big)^2 \;= -\varepsilon f(\rho)^2 \;+\; \frac{F(\rho)}{Y_\varepsilon(\tau,\rho)}\,. \tag{197}$$

They are explicitly given as

$$Y_0(\tau,\rho) \;=\; \Big(\frac{9c^2}{4}\,F(\rho)\,\big(\tau-\tau_0(\rho)\big)^2\Big)^{1/3} \tag{198}$$

$$Y_1(\tau,\rho) \;=\; \frac{F(\rho)}{2\,f(\rho)^2}\,\big(1-\cos\eta_1\big)\,,\quad \eta_1 - \sin\eta_1 \;=\; \frac{2\,f(\rho)^3 c}{F(\rho)}\,\big(\tau-\tau_0(\rho)\big)\,, \tag{199}$$

$$Y_{-1}(\tau,\rho) \;=\; \frac{F(\rho)}{2\,f(\rho)^2}\,\big(\cosh\eta_{-1}-1\big)\,,\quad \sinh\eta_{-1} - \eta_{-1} \;=\; \frac{2\,f(\rho)^3 c}{F(\rho)}\,\big(\tau-\tau_0(\rho)\big)\,. \tag{200}$$

Here $f(\rho)$, $F(\rho)$ and $\tau_0(\rho)$ are arbitrary functions. For each of the three cases, the corresponding function λ is determined by (173) with $e^{H(\rho)} = 1 + G(\rho) = 1 - \varepsilon\,f(\rho)^2$, i.e.

$$e^{-\lambda_\varepsilon(\tau,\rho)}\,\Big(\frac{\partial Y_\varepsilon(\tau,\rho)}{\partial\rho}\Big)^2 = 1 - \varepsilon\,f(\rho)^2\,. \tag{201}$$

Inserting (197) into (175) gives the mass density,

$$\frac{3\,F'(\rho)}{\dfrac{\partial Y_\varepsilon(\tau,\rho)^3}{\partial\rho}} = \kappa\,c^2\,\mu_\varepsilon(\tau,\rho)\,. \tag{202}$$

By (201), the metric reads

$$g \;=\; -c^2 d\tau^2 \;+\; \Big(\frac{\partial Y_\varepsilon(\tau,\rho)}{\partial\rho}\Big)^2\frac{d\rho^2}{\big(1-\varepsilon f(\rho)^2\big)} + Y_\varepsilon(\tau,\rho)^2\Big(d\vartheta^2 + \sin^2\vartheta\,d\varphi^2\Big)\,. \tag{203}$$

This is the general spherically symmetric solution to Einstein's field equation with a dust source. It was found by Lemaître in 1933 and independently by Tolman in 1934. As it was further discussed by Bondi in 1947, it is known as the Lemaître-Tolman-Bondi (LTB) solution. It involves a parameter ε that can take the values 0, +1 or −1, and three arbitrary functions $f(\rho)$, $F(\rho)$ and $\tau_0(\rho)$. As the metric (203) preserves its form under a transformation of the ρ coordinate, there are actually only two arbitrary functions with a physical meaning involved. They can be chosen, e.g., to be the initial density and the initial radial velocity.

If we choose $F(\rho)$ to be a constant, the mass density vanishes by (202), so in this case the LTB solution gives a spherically symmetric vacuum solution. By the Jebsen-Birkhoff theorem, this must be equal to the Schwarzschild solution, for any choice of ε, $f(\rho)$ and $\tau_0(\rho)$. This gives another family of coordinate representations of the Schwarzschild metric.

Oppenheimer and Snyder took the LTB solution from the Tolman paper. They matched this solution at a certain radius ρ_0 to the exterior vacuum Schwarzschild solution, thereby getting

a general-relativistic model for a collapsing ball of dust. Here we will not do this for a general LTB solution. We will rather specialise to the case that the mass density is independent of ρ, i.e., to the case of a homogeneous ball of dust. For this case we will then explicitly determine the surface of the star and the event horizon inside the star as functions of the time coordinate τ. To that end we now specialise the LTB solution to the case of a spatially constant density, $\partial\mu_\varepsilon/\partial\rho = 0$, and then do the matching afterwards.

Claim: If $\mu_\varepsilon > 0$ and $\partial\mu_\varepsilon/\partial\rho = 0$, the coordinates can be chosen such that the metric reads

$$g = -c^2 d\tau^2 + K_\varepsilon(\tau)^2 \Big\{ \frac{d\rho^2}{1-\varepsilon\rho^2} + \rho^2 \big(d\vartheta^2 + \sin^2\vartheta \, d\varphi^2 \big) \Big\} \tag{204}$$

with $\varepsilon = 0, 1, -1$. Here

$$K_0(\tau) = \Big(\frac{9}{4} \, c^2 A \Big)^{1/3} \tau^{2/3} \,, \tag{205}$$

$$K_1(\tau) = \frac{A}{2} \big(1 - \cos\eta_1 \big) \,, \quad \eta_1 - \sin\eta_1 = \frac{2}{A} \, c\,\tau \,, \tag{206}$$

$$K_{-1}(\tau) = \frac{A}{2} \big(\cosh\eta_{-1} - 1 \big) \,, \quad \sin\eta_{-1} - \eta_{-1} = \frac{2}{A} \, c\,\tau \,, \tag{207}$$

with a constant $A > 0$. The mass density is

$$\mu_\varepsilon(\tau) = \frac{3\,A}{\kappa\, c^2 K_\varepsilon(\tau)^3} \,. \tag{208}$$

Proof: If the mass density is strictly positive, (202) requires that $F'(\rho) > 0$. It is, thus, possible to make a coordinate transformation $\big(\tau, \rho, \vartheta, \varphi\big) \mapsto \big(\tau, \tilde\rho, \vartheta, \varphi\big)$ such that

$$F(\rho) = A\,\tilde\rho^3 \,, \quad \frac{d\tilde\rho}{d\rho} = \frac{F(\rho)^{-2/3} F'(\rho)}{3\,A^{1/3}} \tag{209}$$

with a constant $A > 0$. We perform such a coordinate trransformation and then drop the tilde. This fixes the radial coordinate up to a multiplicative constant (as long as we leave A unspecified). We define

$$K_\varepsilon(\tau, \rho) := \frac{1}{\rho} \, Y_\varepsilon(\tau, \rho) \,. \tag{210}$$

It is our goal to show that, actually, K_ε depends only on τ and not on ρ. With (210) the differential equation (202) reads

$$\kappa\, c^2 \mu_\varepsilon(\tau) \, \frac{\partial}{\partial\rho} \Big(\rho^3 K_\varepsilon(\tau, \rho)^3 \Big) = 3 \, \frac{d}{d\rho} \Big(A\rho^3 \Big) \,.$$

Based on our assumption that μ_ε is independent of ρ, integration results in

$$\kappa\, c^2 \mu_\varepsilon(\tau) \, \rho^3 K_\varepsilon(\tau, \rho)^3 - 3\,A\rho^3 = \tilde S(\tau)$$

with some function $\tilde S(\tau)$, hence

$$K_\varepsilon(\tau, \rho)^3 = Q(\tau) + \frac{S(\tau)}{\rho^3} \tag{211}$$

with

$$Q(\tau) = \frac{3\,A}{\kappa\, c^2 \mu_\varepsilon(\tau)}\,, \quad S(\tau) = \frac{\tilde{S}(\tau)}{\kappa\, c^2 \mu_\varepsilon(\tau)}\,. \tag{212}$$

On the other hand, (197) requires

$$\frac{\rho^2}{c^2}\Big(\frac{\partial K_\varepsilon(\tau,\rho)}{\partial \tau}\Big)^2 = -\varepsilon\, f(\rho)^2 + \frac{A\rho^2}{K_\varepsilon(\tau,\rho)}\,,$$

$$\frac{\rho^2}{c^2}\left(\frac{\partial}{\partial\tau}\Big(Q(\tau)+\frac{S(\tau)}{\rho^3}\Big)^{1/3}\right)^2 = -\varepsilon\, f(\rho)^2 + A\,\rho^2\left(Q(\tau)+\frac{S(\tau)}{\rho^3}\right)^{-1/3},$$

$$\frac{\rho^2}{c^2}\left(\frac{1}{3}\Big(Q(\tau)+\frac{S(\tau)}{\rho^3}\Big)^{-2/3}\Big(\dot{Q}(\tau)+\frac{\dot{S}(\tau)}{\rho^3}\Big)\right)^2 = -\varepsilon\, f(\rho)^2 + A\,\rho^2\left(Q(\tau)+\frac{S(\tau)}{\rho^3}\right)^{-1/3},$$

$$\Big(Q(\tau)+\frac{S(\tau)}{\rho^3}\Big)^{-4/3}\Big(\dot{Q}(\tau)+\frac{\dot{S}(\tau)}{\rho^3}\Big)^2 = -9\,c^2\,\frac{\varepsilon\, f(\rho)^2}{\rho^2} + 9\,A\,c^2\Big(Q(\tau)+\frac{S(\tau)}{\rho^3}\Big)^{-1/3}. \tag{213}$$

Differentiation with respect to τ yields

$$\Big(Q(\tau)+\frac{S(\tau)}{\rho^3}\Big)^{-4/3} 2\left(\dot{Q}(\tau)+\frac{\dot{S}(\tau)}{\rho^3}\right)\left(\ddot{Q}(\tau)+\frac{\ddot{S}(\tau)}{\rho^3}\right) - \frac{4}{3}\left(Q(\tau)+\frac{S(\tau)}{\rho^3}\right)^{-7/3}\Big(\dot{Q}(\tau)+\frac{\dot{S}(\tau)}{\rho^3}\Big)^3$$

$$= -3\,A\,c^2\Big(Q(\tau)+\frac{S(\tau)}{\rho^3}\Big)^{-4/3}\Big(\dot{Q}(\tau)+\frac{\dot{S}(\tau)}{\rho^3}\Big)\,. \tag{214}$$

Note that $\Big(Q(\tau)+S(\tau)/\rho^3\Big) \neq 0$ because otherwise the metric would be degenerate. Moreover, $\Big(\dot{Q}(\tau)+\dot{S}(\tau)/\rho^3\Big)$ must be non-zero as well: If this expression were zero, this would mean that K_ε and thus Y_ε are independent of τ. In the cases $\varepsilon = 1$ and $\varepsilon = -1$ this can be true, by (199) and (200), respectively, only if $f(\rho) = 0$. But then (197) implies for all three cases that $F(\rho)$ is zero, in contradiction to our assumption that $F(\rho) = A\rho^3$. So we can multiply both sides of (214) with $\Big(Q(\tau)+S(\tau)/\rho^3\Big)^{7/3}\Big(\dot{Q}(\tau)+\dot{S}(\tau)/\rho^3\Big)^{-1}$ which results in

$$2\left(\ddot{Q}(\tau)+\frac{\ddot{S}(\tau)}{\rho^3}\right)\Big(Q(\tau)+\frac{S(\tau)}{\rho^3}\Big) - \frac{4}{3}\left(\dot{Q}(\tau)+\frac{\dot{S}(\tau)}{\rho^3}\right)^2 = -3\,A\,c^2\Big(Q(\tau)+\frac{S(\tau)}{\rho^3}\Big)\,. \tag{215}$$

Comparing coefficients of ρ^{-3} gives us three equations:

$$2Q\,\ddot{Q} - \frac{4}{3}\dot{Q}^2 = -3Ac^2Q\,, \tag{216}$$

$$2Q\ddot{S} + 2\ddot{Q}S - \frac{8}{3}\dot{Q}\,\dot{S} = -3Ac^2S\,, \tag{217}$$

$$2S\ddot{S} - \frac{4}{3}\dot{S}^2 = 0\,. \tag{218}$$

(218) can be integrated: As

$$3\big(S^{1/3}\big)^{\cdot\cdot} = \big(S^{-2/3}\dot{S}\big)^{\cdot} = -\frac{2}{3}S^{-5/3}\dot{S}^2 + S^{-2/3}\ddot{S} = S^{-5/3}\Big(-\frac{2}{3}\dot{S}^2 + S\ddot{S}\Big)\,, \tag{219}$$

(218) says that $S^{1/3}$ is a linear function of τ,

$$S(\tau) = \big(\alpha\,\tau + \beta\big)^3\,. \tag{220}$$

On the other hand, if we multiply (216) with $-3S^2/4$, (217) with $3QS/4$ and (218) with $-3Q^2/4$ and add the resulting three equations together, we get

$$\dot{Q}^2S^2 - 2\dot{Q}\dot{S}QS + \dot{S}^2Q^2 = 0\,. \tag{221}$$

Q is different from zero by (212). If also S is different from zero, we may divide by S^2Q^2 and get

$$\Big(\frac{\dot{Q}}{Q} - \frac{\dot{S}}{S}\Big)^2 = 0\,. \tag{222}$$

We will demonstrate that this leads to a contradiction, i.e., that S must be equal to zero. To that end we rewrite (222) as

$$\Big(\ln\frac{Q}{S}\Big)^{\cdot} = 0 \tag{223}$$

which implies

$$\ln\frac{Q(\tau)}{S(\tau)} = k\,, \quad Q(\tau) = e^k\,S(\tau) \tag{224}$$

with a constant k. By (220),

$$Q(\tau) = e^k\big(\alpha\,\tau + \beta\big)^3\,. \tag{225}$$

But then the left-hand side of (216) is zero whereas, by (212), the right-hand side is not. This is the desired contradiction. We have therefore proven that $S(\tau)$ must be equal to zero. Hence, K_ε is a function of τ only,

$$Y_\varepsilon(\tau,\rho) = \rho\,K_\varepsilon(\tau)\,, \tag{226}$$

and (213) simplifies to

$$Q(\tau)^{-4/3}\dot{Q}(\tau)^2 - 9\,A\,c^2\,Q(\tau)^{-1/3} = -\,9\,c^2\varepsilon\,\frac{f(\rho)^2}{\rho^2}\,. \tag{227}$$

As the left-hand side is independent of ρ and the right-hand side is independent of τ, the expression on either side must be a constant. This is, of course, a non-trivial result only in the case $\varepsilon \neq 0$ where it implies that $f(\rho^2) = q\,\rho^2$ with a constant $q > 0$. We now insert the expressions $F(\rho) = A\rho^3$ and $f(\rho)^2 = q\,\rho^2$ into (198), (199) and (200) and absorb the constant q into the constant A. Then comparing with (226) shows that in each of the three cases $\tau_0(\rho)$ must be a constant. By a coordinate transformation $(\tau,\rho,\vartheta,\varphi) \mapsto (\tau + \text{const.},\rho,\vartheta,\varphi)$ we can make this constant equal to zero. With (198), (199) and (200) specified in this way, the metric (203) takes, indeed the form of (204) with K_ε given by (205, (206) and (207). The formula (208) for the mass density follows from (211) and (212) with $S(\tau) = 0$. □

Note that in (204) the expression in the curly brackets is the metric of a three-dimensional Riemannian space with constant curvature, i.e. is flat space for $\varepsilon = 0$, the 3-sphere for $\varepsilon = 1$ and hyperbolic 3-space for $\varepsilon = -1$. Also note that the transformed radius coordinate ρ is dimensionless. If ρ ranges over its maximal domain, (204) gives a cosmological dust solution of the field equation known as *Friedmann solution*. Here, however, we are interested in the case that this metric is valid only for $0 < \rho < \rho_0$, where ρ_0 is the radius coordinate of the surface of a ball of dust, and that the metric is joined at $\rho = \rho_0$ to an exterior Schwarzschild vacuum.

A particle on the surface of the star must have as its worldline a radial timelike geodesic of the ambient Schwarzschild metric. We know that then along this worldline the Schwarzschild area coordinate r has to satisfy equation (94),

$$\frac{1}{c^2}\Big(\frac{dr}{d\tau}\Big)^2 \;=\; \text{const.} + \frac{r_S}{r}\,. \tag{228}$$

Inside the star, the area radius coordinate is given by

$$r = \rho K_\varepsilon(\tau)\,, \tag{229}$$

as we read from (204). This implies that the area radius coordinate at the surface of the star is

$$r_0(\tau) = \rho_0 K_\varepsilon(\tau)\,. \tag{230}$$

for all τ. The function K_ε was determined by solving the differential equation

$$\frac{1}{c^2}\left(\frac{\partial}{\partial\tau}\Big(\rho\, K_\varepsilon(\tau)\Big)\right)^2 \;=\; -\varepsilon\,\rho^2 + \frac{A\,\rho^2}{K_\varepsilon(\tau)}\,. \tag{231}$$

With (229), comparison of (228) and (231) at the surface of the star yields

$$A\,\rho_0^3 = r_S\,. \tag{232}$$

The density (208) is thus given by

$$\kappa\, c^2 \mu_\varepsilon(\tau) \;=\; \frac{3\, r_S}{\rho_0^3 K_\varepsilon(\tau)^3}\,. \tag{233}$$

With $\kappa = 8\pi G/c^4$ and $r_S = 2GM/c^2$ this can be rewritten as

$$\mu_\varepsilon(\tau) \;=\; \frac{6M}{\rho_0^3 K_\varepsilon(\tau)^3 8\pi} \;=\; \frac{M}{\frac{4}{3}\pi r_0(\tau)^3}\,. \tag{234}$$

So $\mu_\varepsilon(\tau)$ is given by the usual Euclidean formula for the density of a mass M distributed homogeneously over a sphere of radius $r_0(\tau) = \rho_0 K_\varepsilon(\tau)$. As M was defined asymptotically by comparison with the Newtonian theory, and as the spatial geometry is non-flat (unless $\varepsilon = 0$), this result was not to be expected and can be considered only as a concidence.

We plot the surface of the star in an $r - c\tau-$diagram. The surface is given by (230) with K_ε from (205), (206) and (207). The plots are shown in the picture on the next page for the three cases $\varepsilon = 0$, 1 and -1.

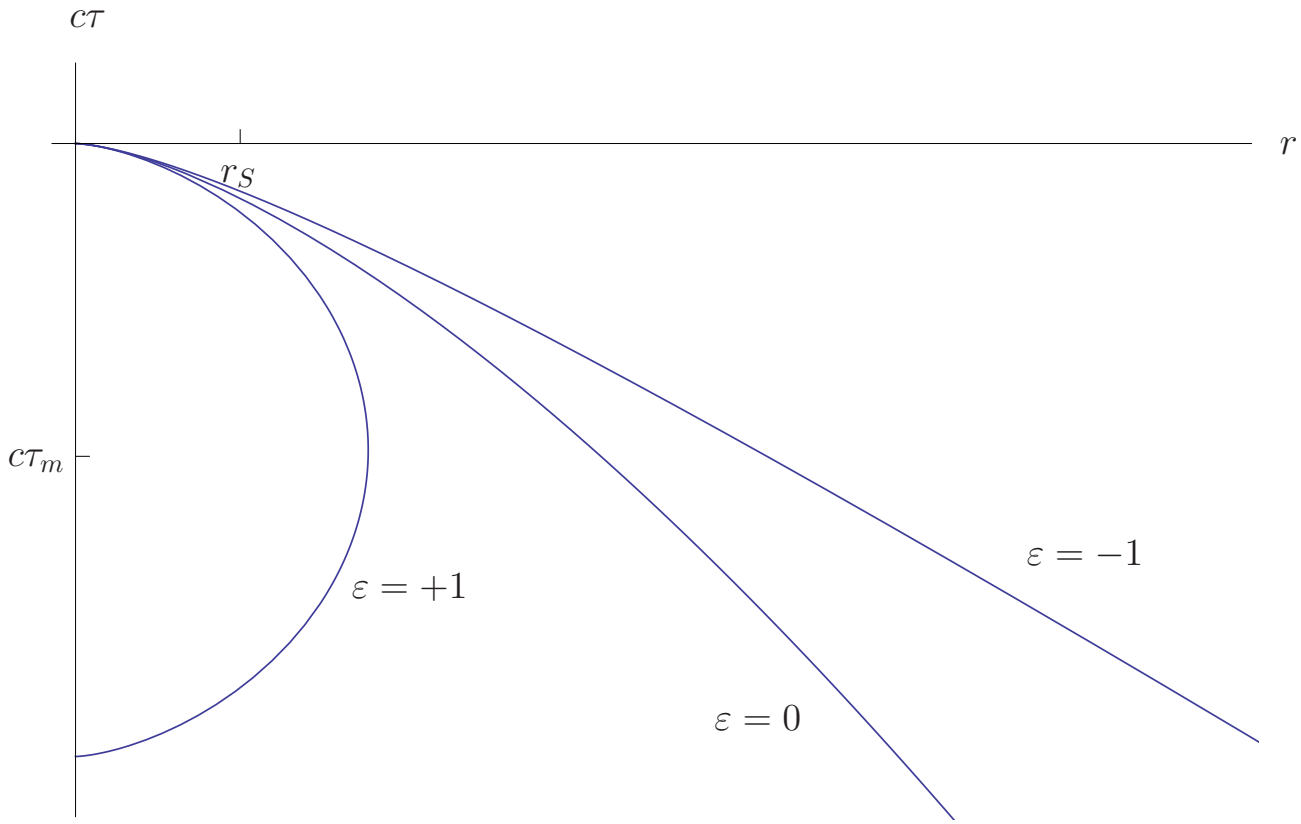

In all three cases the star collapses in a finite time. We have chosen the τ coordinate such that the collapse is finished at $\tau = 0$. For $\tau < 0$, the centre $r = 0$ is regular (i.e., the singularity in spherical polar coordinates at $r = 0$ is a mere coordinate singularity, just as in Minkowski spacetime). For $\tau > 0$ the centre at $r = 0$ features the curvature singularity we know from the vacuum Schwarzschild spacetime. From the diagram above one might be tempted to interpret it now as the worldline of a point particle, with the entire mass of the collapsed star concentrated on this worldline. This interpretation, however, is utterly wrong: From the Carter-Penrose diagram on p.17 we read that the singularity is *spacelike*. It may be associated with an infinite mass density, but it is not a (timelike) worldline.

In the final stage of the collapse, near $\tau = 0$, the three cases $\varepsilon = 0$, 1 and -1 are similar. They differ by their initial conditions. For $\varepsilon = 0$ the surface of the star coincides with worldlines of Painlevé-Gullstrand observers, i.e., it describes free fall from rest at infinity. For $\varepsilon = -1$ the star falls from infinity with an inwards directed asymptotic initial velocity. The physically most relevant case is the case $\varepsilon = +1$. This describes free fall from rest with a finite initial radius if we choose the initial hypersurface at $\tau = \tau_m$. As indicated in the diagram, τ_m is the time where $K_1(\tau)$ reaches its maximum which corresponds to $\eta_1 = -\pi/2$. We may match this solution at $\tau = \tau_m$ to a star which for $-\infty < \tau < \tau_m$ has constant radius $r_* = \rho_0 K_1(\tau_m) = r_S/(2\rho_0^2)$. The combined solution then describes a star that is static up to some time and then suddenly collapses like a ball of dust. We concentrate on this case in the following and determine the radial lightlike geodesics inside the star, to see how the horizon is formed. If we want to identify the lightlike geodesics with real light rays we have, of course, to assume that the star is transparent.

From the metric (204) we read that the radial lightlike geodesics inside the star are given by

$$0 \;=\; -\,c^2 d\tau^2 + K_1(\tau)^2 \frac{d\rho^2}{1-\rho^2}\,, \tag{235}$$

$$\pm\, c\,\frac{d\tau}{d\eta_1}\,d\eta_1 \;=\; K_1(\tau)\,\frac{d\rho}{\sqrt{1-\rho^2}} \tag{236}$$

where the upper sign is for outgoing and the lower sign for ingoing light rays. With $d\tau/d\eta_1$ and $K_1(\tau)$ from (206):

$$\pm\, c\,\frac{A}{2}\big(1-\cos\eta_1\big)\,d\eta_1 \;=\; c\,\frac{A}{2}\big(1-\cos\eta_1\big)\,\frac{d\rho}{\sqrt{1-\rho^2}}\,,$$

$$\pm\, d\eta_1 \;=\; \frac{d\rho}{\sqrt{1-\rho^2}}$$

$$\pm\, d\eta_1 \;=\; d\big(\arcsin\rho\big)\,,$$

$$\eta_{1,i} \pm \eta_1 \;=\; \arcsin\rho\,,$$

$$\rho \;=\; \sin\big(\eta_{1,i} \pm\, \eta_1\big) \tag{237}$$

with an integration constant $\eta_{1,i}$ that labels the geodesics. The area radius coordinate is

$$r = \rho\, K_1(\tau) = \frac{A}{2}\big(1-\cos\eta_1\big)\rho$$

$$= \;\frac{r_S}{2\rho_0^3}(1-\cos\eta_1)\sin\big(\eta_{1,i} \pm\, \eta_1\big)\,. \tag{238}$$

Together with the equation

$$\tau = \frac{r_S}{2c\rho_0^3}\,\big(\eta_1 - \sin\eta_1\big)$$

this gives the radial lightlike geodesics in parametrised form, $\big(r(\eta_1), \tau(\eta_1)\big)$.

The diagram on the next page shows outgoing radial lightlike geodesics (i.e., with the + sign) for three different values of $\eta_{1,i}$ as dashed curves. As the angle coordinates are not shown, each of these curves represents a sphere's worth of lightlike geodesics. A radial lightlike geodesic starting at the centre of the star can do one of two things after crossing the surface of the star: Either it goes to infinity (lower dashed curve) or it goes to the singularity at $r = 0$ (upper dashed curve). The borderline case is formed by geodesics that continue on the surface $r = r_S$ after leaving the star (middle dashed curve). It can be read from the picture that this middle dashed curve gives the event horizon for the total spacetime, consisting of the collapsing star and the vacuum exterior: It is impossible to send a signal at subluminal speed from inside the horizon to an observer outside. The horizon comes into existence at the centre of the star, expands until it reaches the (collapsing) surface at $r = r_S$ and then continues in the vacuum region at this fixed r value.

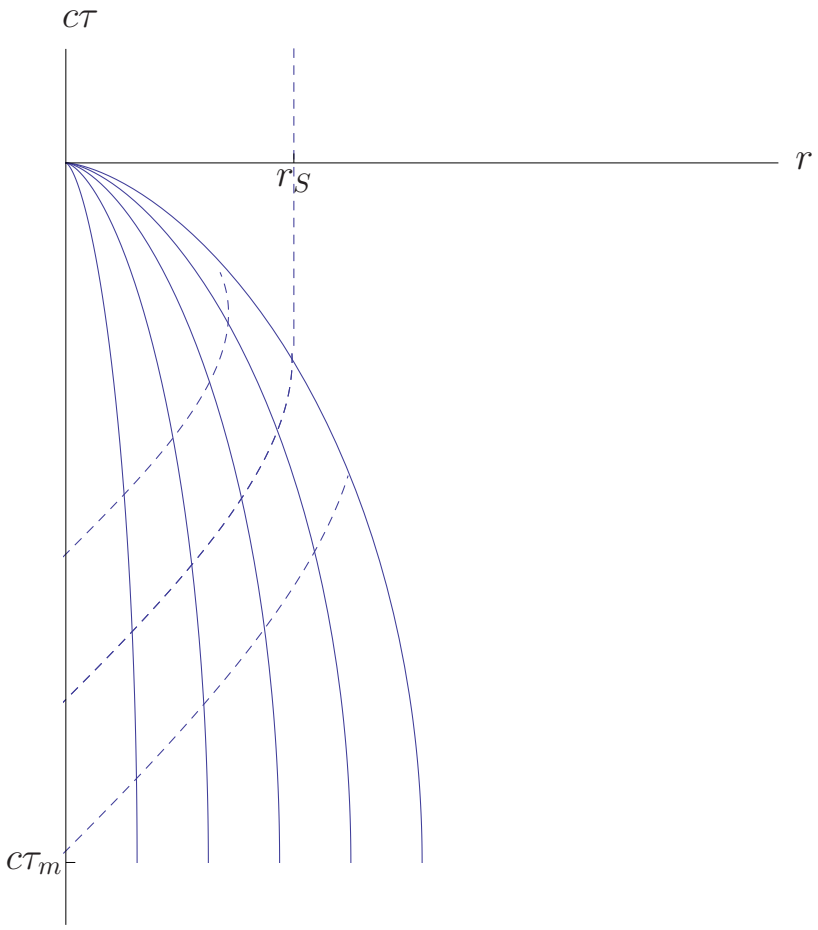

Recall that the *apparent horizon* is defined as the boundary of the region where closed trapped surfaces exist, i.e., where both the ingoing and the outgoing radial lightlike geodesics go into the direction of decreasing area coordinate r. From the picture we read that, also in the interior of the star, closed trapped surfaces exist only inside the event horizon. This is a general feature: The apparent horizon is never outside of the event horizon. In the vacuum Schwarzschild spacetime it coincides with the event horizon. This is not the case within the collapsing star: As the upper dashed curve in the diagram goes for the most part into the direction of increasing r coordinate, although lying beyond the event horizon, the apparent horizon does *not* coincide with the event horizon.

5 Other spherically symmetric and static black holes

In this chapter we will briefly discuss a few spherically symmetric and static black-hole metrics other than Schwarzschild, i.e., metrics that do not solve the vacuum field equation without a cosmological constant. We will summarise only a few main features without going too much into detail because these metrics are usually thought to be of less astrophysical relevance.

5.1 Kottler black holes

The Kottler metric is the unique spherically symmetric solution to Einstein's vacuum field equation with a cosmological constant, $R_{\mu\nu} = \Lambda\, g_{\mu\nu}$. The derivation is completely analogous to the Schwarzschild metric and will not be given here. In particular, the Jebsen-Birkhoff theorem is valid also in the case with a non-vanishing cosmological constant, i.e., the solution is necessarily static. It depends, of course, on the value of the cosmological constant and, just as the Schwarzschild metric, on an integration constant with the dimension of a length which we denote again r_S. The metric reads

$$g \;=\; -\,f(r)\,c^2dt^2 \;+\; \frac{dr^2}{f(r)} \;+\; r^2\big(d\vartheta^2 + \sin^2\vartheta d\varphi^2\big) \tag{239}$$

where

$$f(r) = 1 - \frac{r_S}{r} - \frac{\Lambda}{3}\,r^2\,. \tag{240}$$

This solution was found by F. Kottler in 1918 (and almost simultaneously by H. Weyl). For $\Lambda = 0$, it reduces of course to the Schwarzschild metric. For $r_S = 0$, it reduces to the *de Sitter solution* if $\Lambda > 0$ and to the *anti-de Sitter solution* if $\Lambda < 0$. For this reason, the Kottler metric is also known as the Schwarzschild-de Sitter metric in the case $\Lambda > 0$ and as the Schwarzschild-anti-de Sitter metric in the case $\Lambda < 0$. The name "Schwarzschild metric with a cosmological constant" is also used occasionally.

The most important difference in comparison to the Schwarzschild solution is in the fact that the metric is *not* asymptotically flat, i.e., it does *not* approach the Minkowski metric for $r \to \infty$. Therefore, r_S cannot be determined by considering the region $r \gg r_S$ and comparing with the Newtonian approximation. However, if $|\Lambda|$ is small, there is a region where $r \gg r_S$ and still $r^2 \ll |\Lambda|^{-1}$. In this domain, the comparison with the Newtonian theory is possible and the identification $r_S = 2GM/c^2$ is justified.

The physical relevance of the Kottler metric has to be discussed with care. It is true that we believe to live in a universe with a small but non-zero positive cosmological constant, $\Lambda \approx 10^{-55}\,\mathrm{km}^{-2}$. However, for this value of Λ, the term $\Lambda r^2/3$ is negligibly small in comparison to r_S/r unless $r^3 \gtrsim r_S \times 3 \times 10^{55}\,\mathrm{km}^2$. For planets, stars and stellar or supermassive black holes this means that the Λ term becomes relevant only at very large distances where the approximation of the gravitational field as being spherically symmetric is not really valid because of the presence of neighbouring masses. Only if these neighbouring masses are thought of as being homogeneously smeared out can this approximation be maintained. For this reason the Kottler spacetime is not of very high astrophysical relevance, but it has several features which are interesting from a conceptual point of view.

As the contribution from the cosmological constant vanishes for $r \to 0$, the Kottler metric has a curvature singularity at $r = 0$, just as the Schwarzschild metric. This implies that the metric cannot be extended from the domain $r > 0$ into the domain $r < 0$. One may consider the domain $r < 0$ as a spacetime in its own right. The Kottler metric with a constant $r_S > 0$ on the domain $r < 0$ is the same as the Kottler metric with a constant $r_S < 0$ on the domain $r > 0$, as is obvious from a coordinate transformation $r \to -r$. We will not consider this possibility here and rather restrict to the domain $r > 0$ assuming that $r_S > 0$, as suggested by our identification $r_S = 2GM/c^2$.

Keeping a positive value for r_S fixed, we want to investigate the structure of the spacetime in dependence of Λ which is allowed to take any value between $-\infty$ and ∞. The metric has a zero in the denominator where $f(r) = 0$. Based on our experience with the Schwarzschild metric we expect that such a zero indicates a horizon and that by transforming to coordinates of the Eddington-Finkelstein type the metric becomes regular there. We first investigate how these zeros change in dependence of Λ. On the domain $0 < r < \infty$ the function f has the same zeros as the third-order polynomial

$$P(r) \;=\; -\,r\,f(r) = \frac{\Lambda}{3}\,r^3 \;-\; r \;+\; r_S \tag{241}$$

whose derivative is

$$P'(r) = \Lambda\,r^2 \;-\; 1\,. \tag{242}$$

For any value of Λ, the function $P(r)$ starts at $r = 0$ with a positive value, $P(0) = r_S$, and a negative derivative, $P'(0) = -1$, see the plot below.

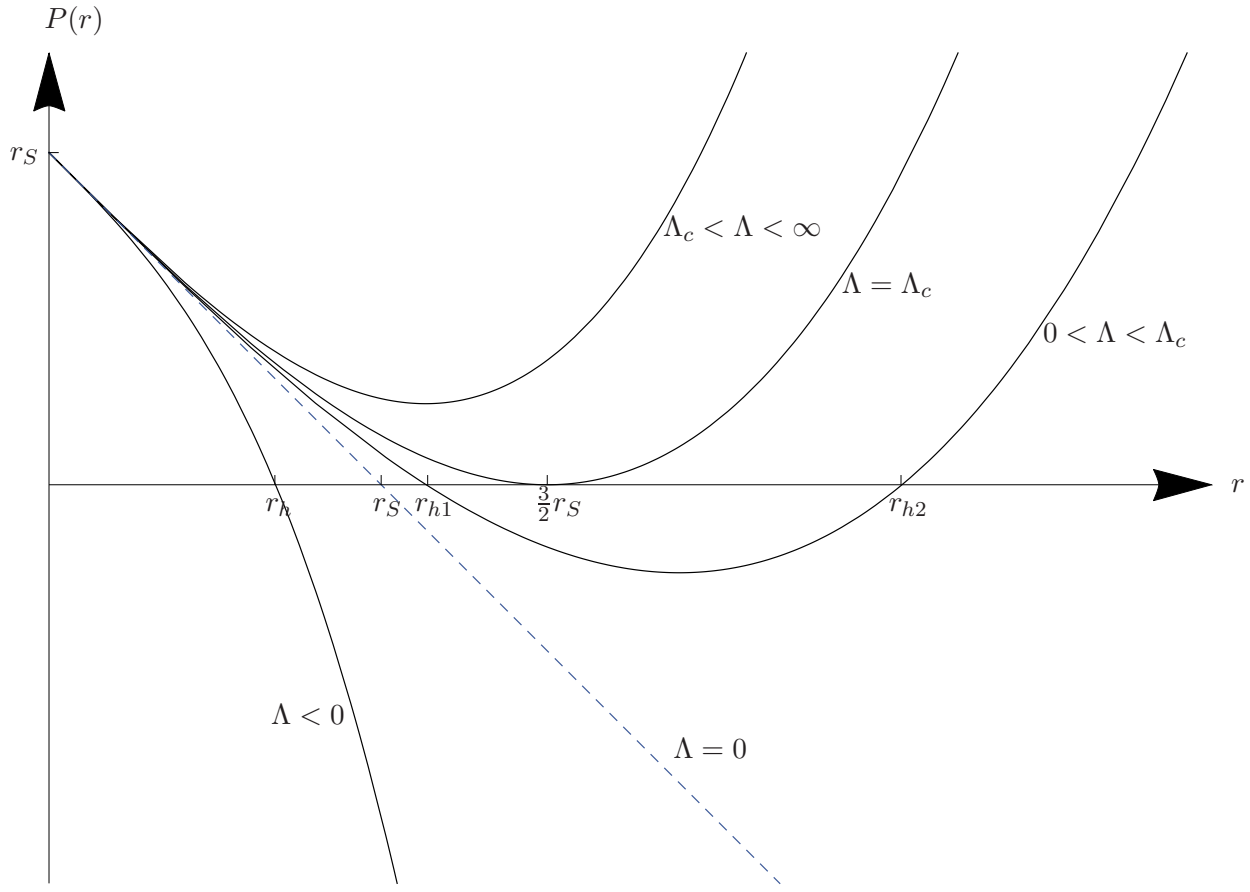

For $\Lambda < 0$ we have $P'(r) < 0$, so $P(r)$ has precisely one real positive zero, $P(r_h) = 0$. Hence, there is precisely one horizon. r_h is situated between 0 and r_S. We have $r_h \to 0$ for $\Lambda \to -\infty$ and, of course, $r_h \to r_S$ for $\Lambda \to 0$

For $\Lambda > 0$, we have $P(r) \to \infty$ for $r \to \infty$. Together with the fact that $P'(0) < 0$ this implies that $P(r)$ must have a minimum at some radius value between 0 and ∞. As $P(r)$ is a third-order polynomial, it can have only one minimum. At this minimum value, $P(r)$ may be positive, zero or negative. In the first case $P(r)$ has no positive real zeros, in the second case it has a double zero, and in the third case it has two different positive real zeros. The critical value Λ_c where a double zero occurs is found by setting $P(r)$ and $P'(r)$ equal to zero,

$$0 \,=\, \frac{\Lambda_c}{3}\, r^3 \,-\, r \,+\, r_S\,, \qquad 0 = \Lambda_c\, r^2 \,-\, 1\,.$$

Solving for Λ_c yields

$$\Lambda_c \,=\, \frac{4}{9 r_S^2} \tag{243}$$

and reinserting this result into $P'(r) = 0$ shows that the double zero occurs at $r = 3r_S/2$. For $0 < \Lambda < \Lambda_c$ there are two positive real zeros r_{h1} and r_{h2} where $r_S < r_{h1} < r_{h2}$; for $\Lambda = \Lambda_c$ there is a double zero at $r = 3r_S/2$ which indicates a degenerate horizon; for $\Lambda_c < \Lambda < \infty$ there is no zero and, thus, no horizon, see the plots on the previous page.

To demonstrate that the zeros of $f(r)$ can be removed by a coordinate transformation and have, indeed, the character of a horizon, we proceed as for the Schwarzschild metric. Radial lightlike geodesics in the Kottler spacetime are given by

$$0 \,=\, -\, f(r)\, c^2 dt^2 + \frac{dr^2}{f(r)}\,, \quad \pm\, c\, dt \,=\, \frac{dr}{f(r)} \tag{244}$$

where the upper sign is for outgoing and the lower sign for ingoing radial lightlike geodesics. We transform to (generalised) ingoing Eddington-Finkelstein coordinates $\big(r, t'\big)$ where

$$c\, t' \,=\, c\, t \,-\, r \,+\, \int \frac{dr}{f(r)} \,=\, c\, t \,-\, r \,-\, \int \frac{r\, dr}{P(r)}\,. \tag{245}$$

In this expression the indefinite integral can be written in terms of the zeros of the third-order polynomial $P(r)$ (and an integration constant that can be chosen at will) but we do not write this out because the solution formulas for cubic equations are rather awkward. In any case, the integral can be easily evaluated numerically, for any value of Λ.

In analogy to the Schwarzschild spacetime, one can check that the Kottler metric becomes regular on the entire domain $0 < r < \infty$ in ingoing Eddington-Finkelstein coordinates. By construction, the ingoing radial light rays are given as straight lines under 45^o in an $r - ct'-$diagram,

$$c\, t' \,=\, -\, r \,+\, \text{constant}\,, \tag{246}$$

whereas the outgoing ones are given as

$$c\, t' \,=\, -\, r \,+\, 2 \int \frac{dr}{f(r)}\,. \tag{247}$$

For $\Lambda < 0$, the spacetime covered by the ingoing Eddington-Finkelstein coordinates describes a black hole with an event horizon at a radius $r_h \in \,]\, 0, r_S \,[$. The qualitative features are quite similar to the Schwarzschild case $\Lambda = 0$. The plots below show the radial light rays in Schwarzschild coordinates (r, t) and in ingoing Eddington-Finkelstein coordinates (r, t'), where the little ellipses indicate the future light-cones. If we use outgoing rather than ingoing Eddington-Finkelstein coordinates, we get of course a white-hole spacetime which is just the time reversed version of the black-hole spacetime.

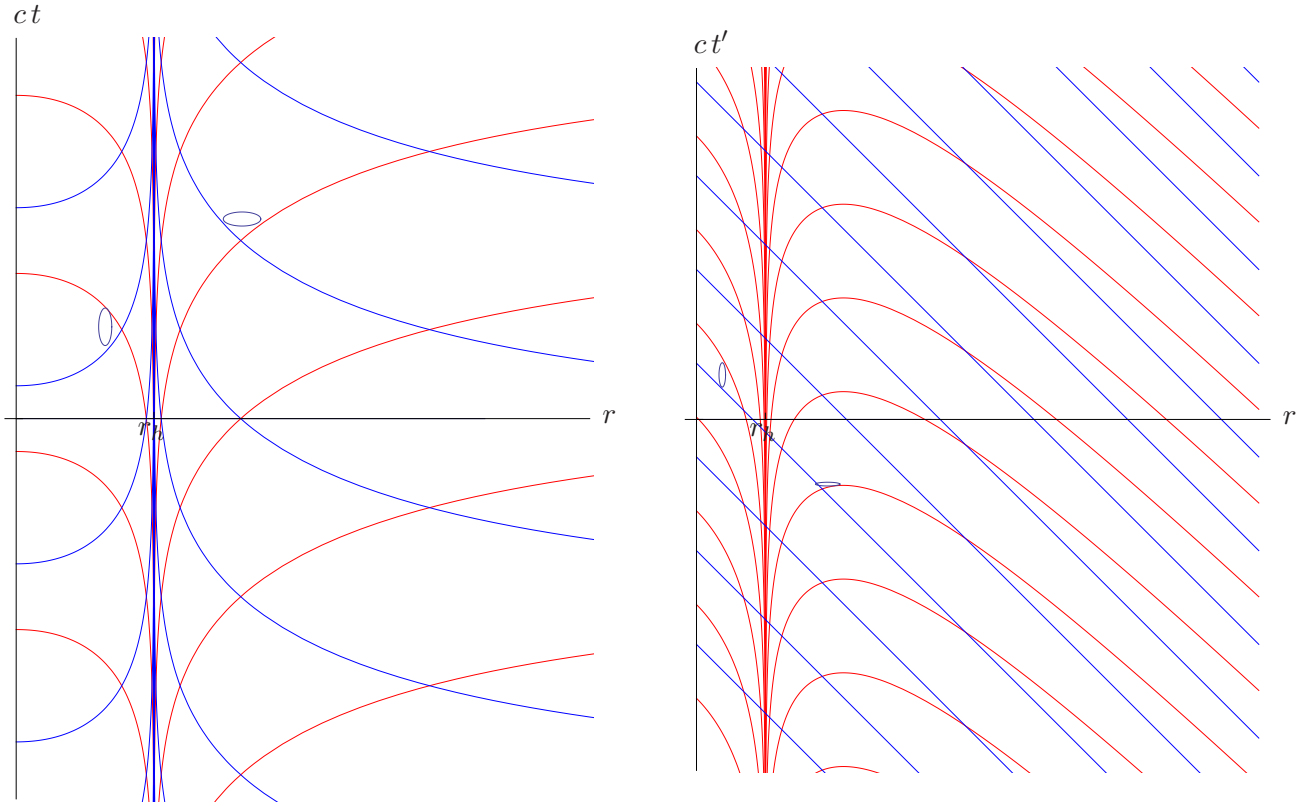

We can construct the maximal analytical extension of the Kottler spacetime with $\Lambda < 0$ in the same way as for the Schwarzschild spacetime by introducing (generalised) Kruskal-Szekeres coordinates

$$u \;=\; h(r)\cosh\frac{c\,t}{2\,r_S}\;, \qquad v \;=\; h(r)\sinh\frac{c\,t}{2\,r_S}\;, \tag{248}$$

where now

$$h(r) = \exp\left(\frac{1}{2r_S}\int_0^r \frac{d\tilde{r}}{f(\tilde{r})}\right). \tag{249}$$

Just as in the Schwarzschild case, this transformation, applied to the region $r_h < r < \infty$, $-\infty < t < \infty$ maps both the ingoing and the outgoing radial light rays onto straight lines under 45^o. The expression $u^2 - v^2 = h(r)^2$ approaches zero for $r \to r_h$ and becomes negative if analytically extended beyond the horizon. Mapping the maximal analytical extension into a compact domain by introducing the lightlike coordinates

$$U = \arctan(v + u)\,, \quad V = \arctan(v - u) \tag{250}$$

gives us the Carter-Penrose diagram of the maximally extended Kottler spacetime with $\Lambda < 0$, see next page.

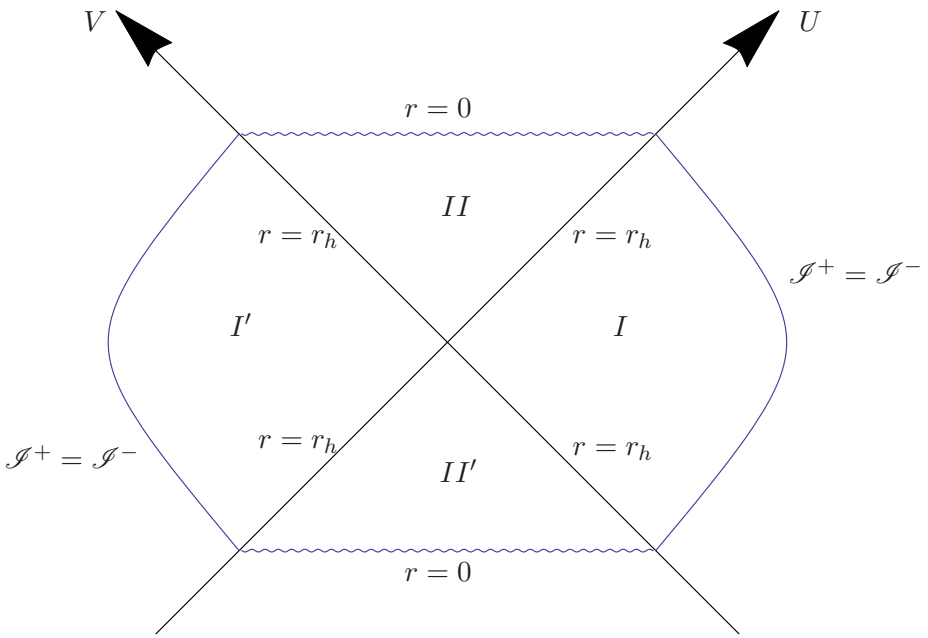

The region I is the region outside of the horizon, where the transformation was originally applied. The ingoing Eddington-Finkelstein coordinates cover regions I and II, whereas the outgoing Eddington-Finkelstein coordinates cover regions I and II'. The only difference to the Carter-Penrose diagram of the Schwarzschild spacetime is in the fact that $\mathscr{I}^+$ (defined as the set of all points at $r = \infty$ where future-oriented lightlike geodesics terminate) and $\mathscr{I}^-$ (the same for past-oriented lightlike geodesics) now have a different structure: In the Schwarzschild case $\mathscr{I}^+$ and $\mathscr{I}^-$ were disjoint and lightlike, now $\mathscr{I}^+$ coincides with $\mathscr{I}^-$ and is timelike.

We now turn to the case $0 < \Lambda < \Lambda_c$. Again, the plots below show the radial light rays in Schwarzschild and in ingoing Eddington-Finkelstein coordinates with the little ellipses indicating the future light-cones.

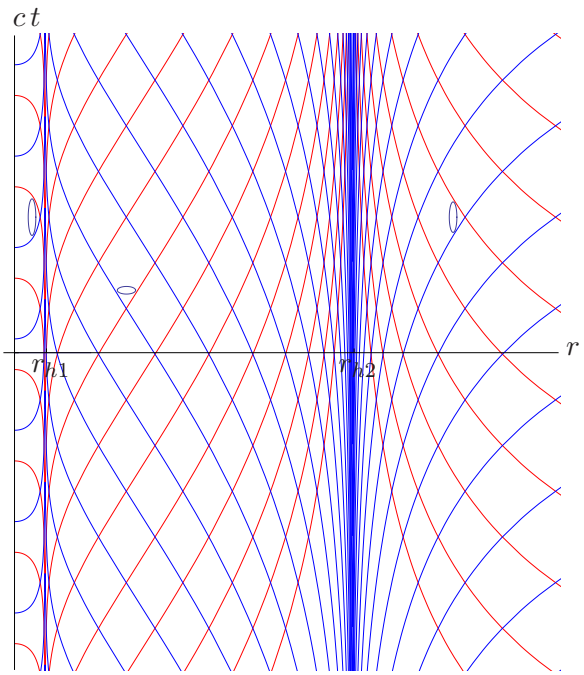

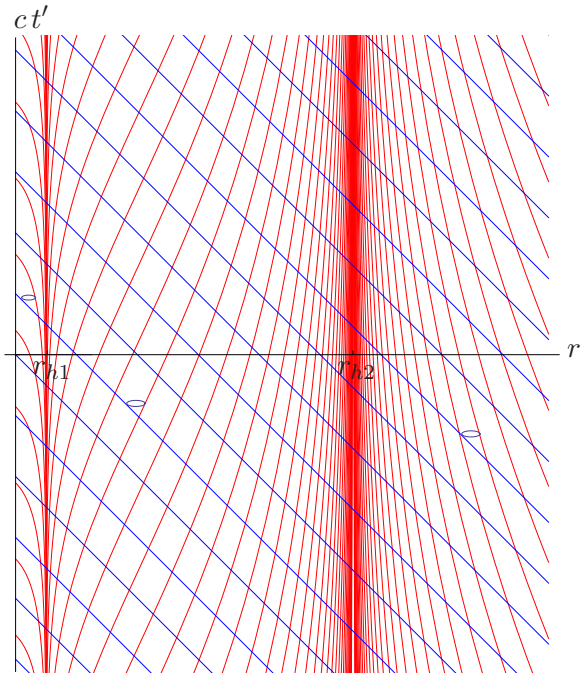

In this case we have two horizons. The inner one at $r = r_{h1}$ is known as the black-hole horizon while the outer one at $r = r_{h2}$ is known as the cosmological horizon. It is $r_S < r_{h1} < r_{h2}$. The vector field $\partial/\partial t$ is timelike between the two horizons, i.e., in this region the spacetime is static and an observer is free to move in the direction of increasing or decreasing r. In the other two regions $\partial/\partial t$ is spacelike. An observer is forced to move in the direction of decreasing r. From the static region, an observer can send signals to the interior non-static region $0 < r < r_{h1}$ but he cannot receive signals from there. By contrast, he can receive signals from the exterior non-static region $r_{h2} < r < \infty$ but he cannot send signals to this region. Again, an analogous construction with outgoing Eddington-Finkelstein coordinates gives a white hole.

For constructing the Carter-Penrose diagram we introduce again the (generalised) Kruskal-Szekeres coordinates (248), this time on the domain $r_{h1} < r < r_{h2}$, $-\infty < t < \infty$, extend analytically and then compactify with the help of the transformation (250).

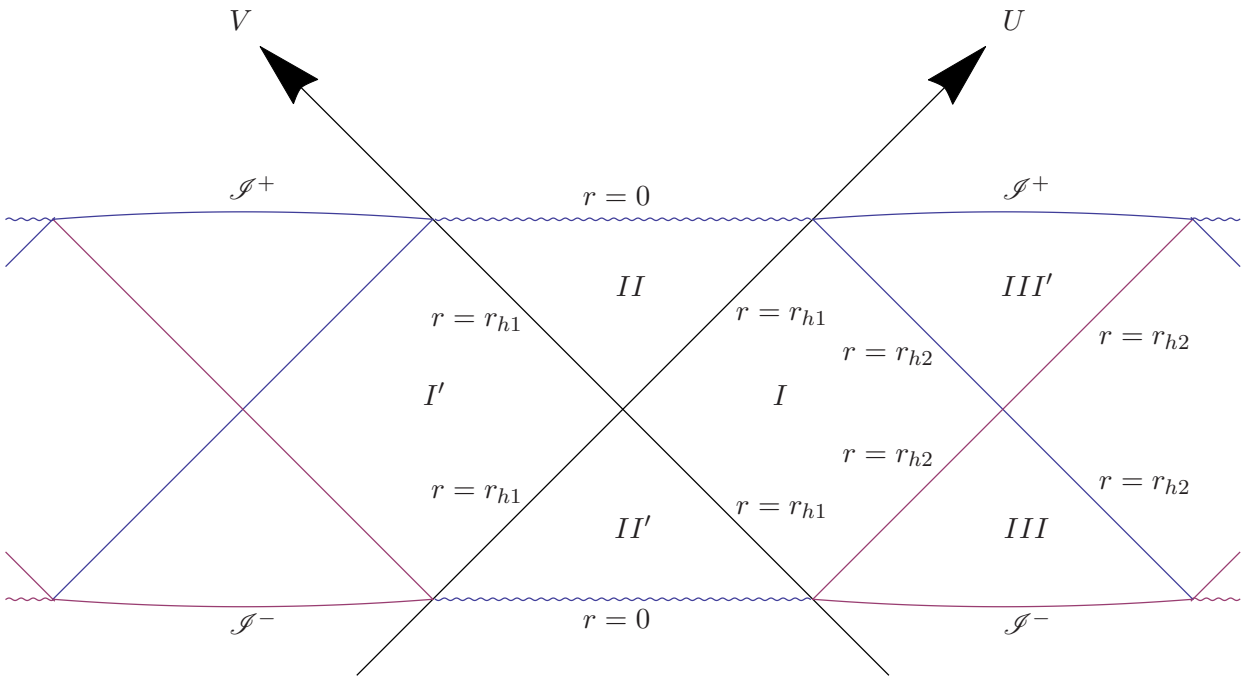

The ingoing Eddington-Finkelstein coordinates cover the regions II, I and III whereas the outgoing Eddington-Finkelstein coordinates cover the regions III', I and II'. In this case $\mathscr{I}^+$ and $\mathscr{I}^-$ are spacelike. The diagram is infinitely extended to the right and to the left.

Finally, we consider the case $\Lambda_c < \Lambda < \infty$. Then there is no horizon. $\partial/\partial t$ is everywhere spacelike, i.e., the spacetime is non-static. The metric is regular on the entire domain $0 < r < \infty$ in Schwarzschild coordinates; so there is no particular advantage in introducing Eddington-Finkelstein coordinates. If the timelike vector field ∂/∂_r is interpreted as future-pointing, the curvature singularity at $r = 0$ sucks in all signals and material bodies, but it is not a black hole because there is no horizon. A singularity that is not hidden behind a horizon is called "naked". Note, however that in the case at hand the singularity is not visible to any observer until he really arrives there. If the timelike vector field ∂/∂_r is interpreted as past-pointing, all signals and material bodies move away from the singularity, so the singularity is visible to an observer anywhere in the spacetime.

The plot on the right shows the radial light rays in Schwarzschild coordinates. If the little ellipses indicate the future light cones, the singularity is attractive and not visible until one arrives there. If one changes the time-orientation (i.e., if one interprets the little ellipses as indicating the past light cones), the singularity is repellent and can be seen from anywhere in the spacetime.

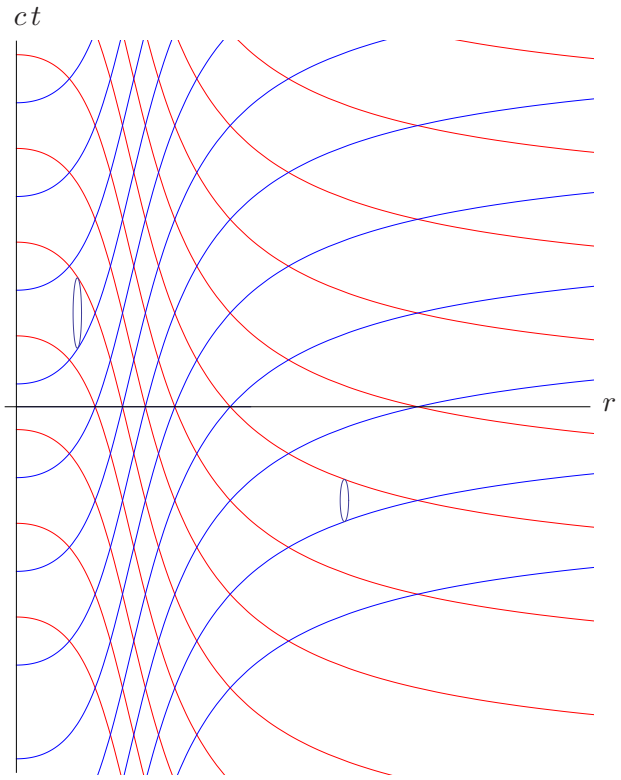

As there are no horizons, the spacetime cannot be analytically extended. The Carter-Penrose diagram, which is constructed again with the transformations (248) and (250), is shown below for the case that the vector field $\partial/\partial r$ is interpreted as future-pointing. In this case $\mathscr{I}^+$ is the empty set because all future-pointing lightlike (or timelike) curves terminate at the singularity.

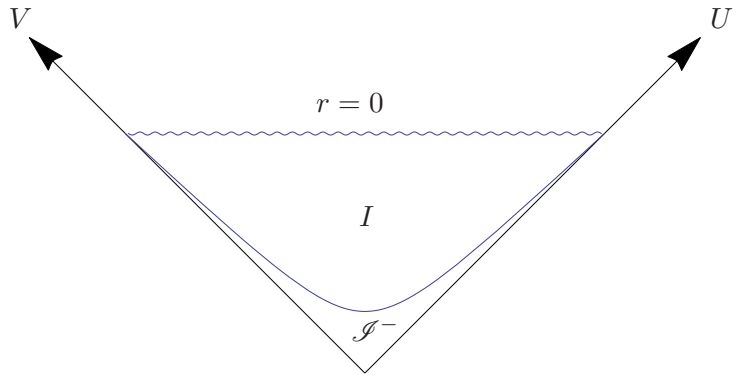

We will now discuss the lightlike and timelike geodesics in the Kottler spacetime. Just as in the Schwarzschild case we may restrict, without loss of generality, to the equatorial plane. Then the geodesics are to be derived from the Lagrangian

$$\mathcal{L}(x,\dot{x}) \;=\; \frac{1}{2}\left(\;-\;f(r)\,c^2\dot{t}^2+\frac{\dot{r}^2}{f(r)}+r^2\dot{\varphi}^2\right). \tag{251}$$

The t and φ components of the Euler-Lagrange equation give us two constants of motion,

$$E \;=\; f(r)\,c^2\dot{t}\,, \qquad L \;=\; r^2\,\dot{\varphi}\,. \tag{252}$$

Moreover, we must have

$$-\,f(r)\,c^2\dot{t}^2+\frac{\dot{r}^2}{f(r)}+r^2\dot{\varphi}^2 \;=\; -\,\varepsilon\,c^2 \tag{253}$$

where $\varepsilon = 1$ for timelike and $\varepsilon = 0$ for lightlike geodesics.

We will discuss the lightlike geodesics in Worksheet 8. We will demonstrate that they satisfy the second-order differential equation

$$\frac{d^2r}{d\varphi^2} - \frac{2}{r}\Big(\frac{dr}{d\varphi}\Big)^2 = r - \frac{3}{2}r_S\,. \tag{254}$$

which determines, for given initial values $r(0)$ and $dr/d\varphi(0)$, a unique solution. We see that the cosmological constant has completely dropped out. Hence, the lightlike geodesics in the Kottler spacetime are given by precisely the same curves in the coordinate picture as without Λ term. From (254) we read, in particular, that circular light rays can exist only at $r = 3r_S/2$ which is again independent of Λ. It was pointed out by M. Ishak and W. Rindler [Phys. Rev. D 76, 043006 (2007)] that, nonetheless, lensing observations are influenced by Λ. In particular, the angular radius θ_0 of the shadow of a Kottler black hole does depend on Λ,

$$\sin^2\theta_0 = \frac{1-\dfrac{r_S}{r_O}-\dfrac{\Lambda}{3}r_O^2}{\Big(\dfrac{4}{27r_S^2}-\dfrac{\Lambda}{3}\Big)r_O^2} = \frac{1-\dfrac{r_S}{r_O}-\dfrac{\Lambda}{3}r_O^2}{\Big(\dfrac{\Lambda_c}{3}-\dfrac{\Lambda}{3}\Big)r_O^2} \tag{255}$$

as we will demonstrate in Worksheet 8. Here it is assumed that the observer is static at radius coordinate r_O (which is possible only if r_O is in the domain where $f(r) > 0$.

Now we turn to timelike geodesics. To that end we have to consider equations (252) and (253) with $\varepsilon = 1$. These imply

$$\dot r^2 = f(r)\Big(f(r)\,c^2\dot t^2 - r^2\dot\varphi^2 - c^2\Big)\,,$$

$$\dot r^2 = f(r)^2\,c^2\,\frac{E^2}{f(r)^2\,c^4} - f(r)\Big(r^2\,\frac{L^2}{r^4}+c^2\Big)\,,$$

$$\dot r^2 = \frac{E^2}{c^2} - f(r)\Big(\frac{L^2}{r^2}+c^2\Big)\,. \tag{256}$$

By writing the function $f(r)$ explicitly,

$$\dot r^2 = \frac{E^2}{c^2} - L^2\Big(\frac{1}{r^2}-\frac{r_S}{r^3}-\frac{\Lambda}{3}\Big) - c^2\Big(1-\frac{r_S}{r}-\frac{\Lambda}{3}r^2\Big)\,,$$

and differentiating with respect to the proper time parameter τ we find

$$2\,\dot r\,\ddot r = \bigg(-L^2\Big(-\frac{2}{r^3}+\frac{3\,r_S}{r^4}\Big) - c^2\Big(\frac{r_S}{r^2}-\frac{2\,\Lambda}{3}\,r\Big)\bigg)\dot r\,,$$

$$\ddot r = L^2\Big(\frac{1}{r^3}-\frac{3\,r_S}{2\,r^4}\Big) - c^2\Big(\frac{r_S}{2\,r^2}-\frac{\Lambda}{3}\,r\Big)\,. \tag{257}$$

Although we have divided by $\dot r$, (257) is true also at points where $\dot r = 0$, because of continuity.

We first investigate if there are equilibrium points. If we choose initial conditions $\dot r(\tau_0) = 0$ and $\dot\varphi(\tau_0) = 0$, (256) and (257) require, respectively,

$$0 = \frac{E^2}{c^2} - f\big(r(\tau_0)\big)c^2\,, \tag{258}$$

$$\ddot{r}(\tau_0) = -c^2\Big(\frac{r_S}{2\,r(\tau_0)^2} - \frac{\Lambda}{3}\,r(\tau_0)\Big)\,. \tag{259}$$

The first equation (258) says that our initial conditions can be realised only if $f\big(r(\tau_0)\big) > 0$. This is clear from what was said before, because the t-lines are timelike only in the domain where $f(r) > 0$. As such a domain doesn't exist for $\Lambda_c < \Lambda$, we have to consider only the two cases $\Lambda < 0$ and $0 < \Lambda < \Lambda_c$. (The case $\Lambda = 0$ is the Schwarzschild case which is already known to us, and the case $\Lambda = \Lambda_c$ can be treated by a limit procedure.)

For $\Lambda < 0$, (259) says that $\ddot{r}(\tau_0)$ is always negative. If we place a particle with initial velocity zero anywhere in the domain where $f(r) > 0$, it will start moving towards the centre. So a negative cosmological constant doesn't change the attractive character of gravitation.

For $0 < \Lambda < \Lambda_c = 4/(9r_S^2)$, (259) says that $\ddot{r}(\tau_0)$ is negative only on part of the domain where $f(r) > 0$, namely:

$$\begin{aligned}
\ddot{r}(\tau_0) < 0 &\iff r < r_{\rm eq}\,,\\
\ddot{r}(\tau_0) = 0 &\iff r = r_{\rm eq}\,,\\
\ddot{r}(\tau_0) > 0 &\iff r > r_{\rm eq}\,,
\end{aligned} \tag{260}$$

where

$$r_{\rm eq} = \Big(\frac{3r_S}{2\Lambda}\Big)^{1/3}. \tag{261}$$

This reflects the fact that a positive cosmological constant has a *repellent* effect: For $r > r_{\rm eq}$ this repulsion dominates over the attractive effect produced by the r^{-1} term in the function $f(r)$, for $r < r_{\rm eq}$ it is vice versa. At $r_{\rm eq}$ there is a balance between repulsion and attraction, so a particle that is placed at this radius coordinate will stay put. Note that $r_{\rm eq}$ is, indeed, in the domain where $f(r)$ is positive, because

$$\begin{aligned}
f(r_{\rm eq}) &= 1 - \frac{r_S}{r_{\rm eq}} - \frac{\Lambda}{3}\,{r_{\rm eq}}^2 = 1 - r_S\left(\frac{2\Lambda}{3r_S}\right)^{1/3} - \frac{\Lambda}{3}\left(\frac{3r_S}{2\Lambda}\right)^{2/3}\\
&= 1 - \big(\Lambda\,r_S^2\big)^{1/3}\left(\Big(\frac{2}{3}\Big)^{1/3} + \Big(\frac{1}{3\times 4}\Big)^{1/3}\right)\\
&= 1 - \Big(\Lambda\frac{9r_S^2}{4}\Big)^{1/3}\left(\Big(\frac{8}{27}\Big)^{1/3} + \Big(\frac{1}{27}\Big)^{1/3}\right)\\
&= 1 - \Big(\frac{\Lambda}{\Lambda_c}\Big)^{1/3}\Big(\frac{2}{3} + \frac{1}{3}\Big) = 1 - \Big(\frac{\Lambda}{\Lambda_c}\Big)^{1/3} > 0\,.
\end{aligned} \tag{262}$$

From (260) we read that the equilibrium at $r_{\rm eq}$ is unstable: If we place a particle at rest at a slightly bigger radius value than $r_{\rm eq}$ it will be accelerated in the direction of increasing r, and if we do it at a slightly smaller value it will be accelerated in the direction of decreasing r. In any case, it will start moving away from the equilibrium position.

We now turn to circular timelike geodesics. To that end we write (256) in the form of an energy conservation law,

$$\frac{1}{2}\,\dot{r}^2 + V_{E,L}(r) = 0 \tag{263}$$

with

$$V_{E,L}(r) = \frac{f(r)}{2}\Big(\frac{L^2}{r^2} + c^2\Big) - \frac{E^2}{2c^2}\,. \tag{264}$$

Note that this is not exactly the same effective potential we have used for the Schwarzschild spacetime, because here the kinetic energy term is formed with $\dot{r} = dr/d\tau$ whereas in the Schwarzschild case it was formed with $dr/d\varphi$. However, we can use this effective potential in exactly the same way for determining the circular timelike geodesics: They are given by the equations $V_{E,L}(r) = 0$ and $V'_{E,L}(r) = 0$ and stability is determined by the sign of $V''_{E,L}(r)$. The condition

$$V_{E,L}(r) = \frac{1}{2}\Big(1 - \frac{r_S}{r} - \frac{\Lambda}{3}r^2\Big)\Big(\frac{L^2}{r^2} + c^2\Big) - \frac{E^2}{2c^2} = 0 \tag{265}$$

requires that $f(r) = 1 - r_S/r^2 - (\Lambda/3)r^2 > 0$ and thus $\Lambda < \Lambda_c$. Again, this reflects the fact that timelike curves can stay at a constant r value only in a region where ∂_t is timelike. At all r values where this is the case, (265) determines E as a function of L and r. By differentiating (265) we find

$$V'_{E,L}(r) = \frac{L^2}{2}\Big(-\frac{2}{r^3} + \frac{3r_S}{r^4}\Big) + \frac{c^2}{2}\Big(\frac{r_S}{r^2} - \frac{2\Lambda}{3}r\Big)\,. \tag{266}$$

Then the condition $V'_{E,L}(r) = 0$ determines L,

$$L^2 \;=\; \frac{c^2\, r_S\, r^2\Big(1 - \dfrac{2\Lambda r^3}{3r_S}\Big)}{2\Big(r - \dfrac{3}{2}\,r_S\Big)}\,. \tag{267}$$

To assure $L^2 > 0$, we must have either

$$1 - \frac{2\Lambda r^3}{3r_S} < 0 \quad \text{and} \quad r < \frac{3}{2}r_S \tag{268}$$

or

$$1 - \frac{2\Lambda r^3}{3r_S} > 0 \quad \text{and} \quad r > \frac{3}{2}r_S\,. \tag{269}$$

The first pair of conditions implies

$$\Lambda > \frac{3r_S}{2r^3} > \frac{3r_S}{2}\left(\frac{2}{3r_S}\right)^3 = \frac{4}{9r_S^2} = \Lambda_c \tag{270}$$

which is in contradiction to the fact that a region where $f(r) > 0$ doesn't exist for $\Lambda > \Lambda_c$. So the second pair of conditions must be satisfied. For $\Lambda < 0$, it reduces to

$$\frac{3}{2}r_S < r < \infty\,. \tag{271}$$

This means that in this case circular timelike geodesics exist for exactly the same radius values as in the Schwarzschild spacetime. For $0 < \Lambda < \Lambda_c$, it can be rewritten as

$$\frac{3}{2} r_S < r < r_{\text{eq}} \tag{272}$$

with r_{eq} from (261). These two limiting values for circular timelike geodesics are easily understood: For $r \to 3r_S/2$ the orbital velocity of a circular timelike geodesic approaches the velocity of light, while for $r \to r_{\text{eq}}$ it approaches zero.

To investigate stability of the circular orbits we have to determine the sign of $V''_{E,L}(r)$. To that end it is convenient to rewrite (266) as

$$r^4 V'_{E,L}(r) = L^2\Big(-r + \frac{3r_S}{2}\Big) + \frac{c^2}{2}\Big(r_S r^2 - \frac{2\Lambda}{3} r^5\Big) . \tag{273}$$

By differentiating this expression with respect to r and using $V'_{E,L}(r) = 0$ we find

$$r^4 V''_{E,L}(r) = L^2(-1) + c^2\Big(r_S r - \frac{5\Lambda}{3} r^4\Big) . \tag{274}$$

Inserting (267) results in

$$\begin{aligned} r^4 V''_{E,L}(r) &= -\frac{c^2 r^2\Big(r_S - \frac{2\Lambda}{3} r^3\Big)}{2r - 3r_S} + c^2 r\Big(r_S - \frac{5\Lambda}{3} r^3\Big) \\ &= \frac{c^2 r}{2r - 3r_S}\Big(-\cancel{r_S r} + \frac{2\Lambda}{\cancel{3}} r^4 + \cancel{2} r_S r - \frac{\cancel{10}^{\,8}\Lambda}{3} r^4 - 3r_S^2 + 5\Lambda r_S r^3\Big) \\ &= \frac{c^2 r}{2r - 3r_S}\left(r_s(r - 3r_S) - \frac{\Lambda r^3}{3}\big(8r - 15 r_S\big)\right) \\ &= \frac{c^2 r^4 (8r - 15 r_S)}{3(2r - 3r_S)}\left(\frac{3r_S(r - 3r_S)}{r^3(8r - 15 r_S)} - \Lambda\right) \end{aligned} \tag{275}$$

i.e.,

$$V''_{E,L}(r) = \frac{c^2(8r - 15 r_S)}{3(2r - 3r_S)}\Big(F(r) - \Lambda\Big) \tag{276}$$

with

$$F(r) = \frac{3\, r_S\big(r - 3r_S\big)}{r^3\big(8\, r - 15\, r_S\big)} . \tag{277}$$

The diagram on the next page shows a plot of the function $F(r)$ restricted to the interval $15r_S/8 < r < \infty$. If r approaches $15r_S/8$ from above, this function diverges towards $-\infty$. From (276) we read that stable circular orbits exist in the region below the graph of this function; this follows from the fact that there the pre-factor in (276) is positive, $8\, r - 15\, r_S > 0$ and $2\, r - 3\, r_S > 0$, so the sign of $\ddot{r}$ is indeed determined by the sign of $\Lambda - F(r)$. In the diagram the dotted line marks the circular lightlike orbit at $r = 3r_S/2$ whereas the dashed line marks the equilibrium radius $r = r_{\text{eq}}$; i.e., circular timelike orbits exist between the dashed and the dotted line. On the interval $3r_S/2 < r < 15r_S/8$ the graph of the function $\Lambda = F(r)$ lies above the dashed line (not shown), i.e., no circular orbits can exist at radius values in this interval.

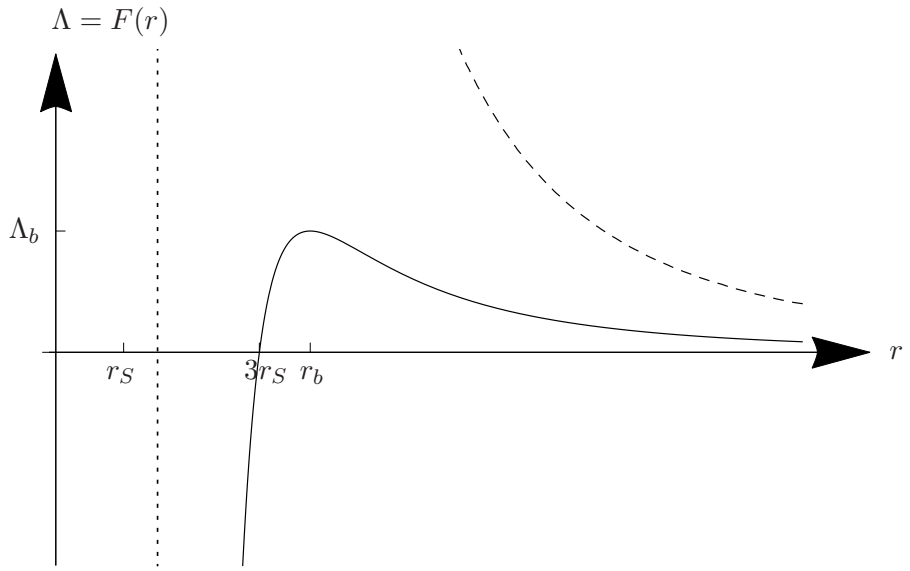

We observe that the function $F(r)$ takes a maximum at a radius value r_b. From the plot of the function $\Lambda = F(r)$ we read: For $0 < \Lambda < \Lambda_b$ stable circular orbits exist between an ISCO (Innermost Stable Circular Orbit) and an OSCO (Outermost Stable Citrcular Orbit). For $\Lambda < 0$ they exist between an ISCO and infinity. For $\Lambda > \Lambda_b$, there are no stable circular orbits. To find the radius value r_b where $F(r)$ takes its maximum value we evaluate the equation $F'(r_b) = 0$:

$$\frac{\cancel{3r_S}r_b^3(8r_b - 15r_S) - \cancel{3r_S}(r_b - 3r_S)(32r_b^3 - 45r_b^2 r_S)}{r_b^6(8r_b - 15r_S)^2} \;=\; 0\,,$$

$$8r_b^4 - 15r_S r_b^3 - 32r_b^4 + 45r_S r_b^3 + 96r_S r_b^3 - 135r_S^2 r_b^2 \;=\; 0\,,$$

$$-24r_b^2 + 126r_S r_b - 135r_S^2 \;=\; 0\,, \quad \frac{r_b^2}{r_S^2} - \frac{21}{4}\frac{r_S}{r_b} + \frac{45}{8} \;=\; 0\,,$$

$$\frac{r_b}{r_S} \;=\; \frac{21}{8} \pm \sqrt{\frac{21\times 21}{64} - \frac{8\times 45}{64}} \;=\; \frac{21 \pm 9}{8}\,.$$

We have to choose the plus sign because $r_b > 3r_S$,

$$r_b \;=\; \frac{15}{4} r_S\,. \tag{278}$$

At $r = r_b$, the function $F(r)$ takes the value

$$\Lambda_b \;=\; F(r_b) \;=\; \frac{3r_S\Big(\frac{15}{4}r_S - 3r_S\Big)}{\frac{15^3}{4^3}r_S^3\Big(\frac{8\times 15}{4}r_S - 15r_S\Big)} \;=\; \frac{16}{15^2\times 5^2\, r_S^2} \;=\; \frac{16}{5625\, r_S^2}\,. \tag{279}$$

Note that Λ_b is much smaller than the critical value $\Lambda_c = 4/(9r_S^2)$ where the horizons vanish. For $\Lambda_b < \Lambda < \Lambda_c$ we still have circular timelike geodesics, but all of them are unstable.

We mention in passing that in the Kottler spacetime with $0 < \Lambda < \Lambda_b$ socalled *heteroclinic* orbits occur, i.e. orbits, which asymptotically connect two different unstable circular orbits. Recall from p.29 that in the Schwarzschild spacetime there are only *homoclinic* orbits, i.e., timelike geodesics that spiral for $\tau \to -\infty$ and for $\tau \to \infty$ towards the *same* unstable circular orbit. The occurrence of heteroclinic orbits is characteristic of situations where one has competing attractive and repulsive forces which may balance each other.

5.2 Reissner-Nordström black holes

The Reissner-Nordström metric is the unique spherically symmetric and asymptotically flat solution to the Einstein equation (without a cosmological constant) with the energy-momentum tensor of a Maxwell field. It is a static metric that describes the spacetime around a spherically symmetric charged object. Just as in the Schwarzschild case, the field is static even for a pulsating source. We do not give a derivation of the Reissner-Nordström metric which requires solving the coupled system of the Einstein and the Maxwell equations under the assumption of spherical symmetry and then adding the condition of asymptotic flatness. Without the latter condition, there is also the socalled Bertotti-Robinson spacetime. As an alternative to requiring asymptotic flatness, it can also be excluded by the assumption that the area function r, defined by the property that the group orbits (spheres parametrised by ϑ and φ) have area $4\pi r^2$, is a "good coordinate", i.e., that dr has no zeros. In the Bertotti-Robinson spacetime dr is identically zero, i.e., r cannot be used as a coordinate.

The Reissner-Nordström metric reads

$$g \;=\; -\,c^2 f(r) dt^2 + \frac{dr^2}{f(r)} + r^2\big(d\vartheta^2 + \sin^2\vartheta\, d\varphi^2\big) \tag{280}$$

where

$$f(r) = 1 - \frac{r_S}{r} + \frac{r_Q^2}{r^2}\,. \tag{281}$$

It was found independently by H. Reissner (1916), H. Weyl (1917) and G. Nordström (1918). It contains two integration constants r_S and r_Q with the dimension of a length. Comparison with the Newtonian theory for large r shows that, as in the Schwarzschild metric,

$$r_S = \frac{2GM}{c^2} \tag{282}$$

where M is the mass of the central object. The interpretation of r_Q can be read from the electric field that is associated with the metric:

$$r_Q^2 = \frac{GQ^2}{4\pi\varepsilon_0 c^4} \tag{283}$$

where Q is the electric charge. (Here we assume that the central object carries an *electric* charge. If one believes in the existence of magnetic monopoles, one could also consider a *magnetic* charge.)

We can match the Reissner-Nordström solution at some appropriate radius value to an interior solution, e.g. to a charged perfect fluid, to get a model for a spherically symmetric charged star. Here we are interested in Reissner-Nordström black holes, so we will assume that the electro-vacuum Reissner-Nordström metric is valid all the way down to $r = 0$.

Just as the Schwarzschild metric, the Reissner-Nordström metric has a curvature singularity at $r = 0$. This can be verified by calculating the Kretschmann scalar which diverges at $r = 0$ We will now investigate if this singularity is hidden behind a horizon. From the metric we read that a coordinate singularity of the same kind as the one at $r = r_S$ in the Schwarzschild case occurs at those real and positive r values where the function $f(r)$ given in (281) has a zero. This gives a quadratic equation for r,

$$r^2 - r_S r + r_Q^2 = 0\,. \tag{284}$$

Any real and positive solution of this equation gives a horizon, as we will demonstrate immediately with the help of (generalised) Eddington-Finkelstein coordinates. Solving the quadratic equation yields

$$r_\pm \,=\, \frac{1}{2}\left(r_S \pm \sqrt{r_S^2 - 4r_Q^2}\right). \tag{285}$$

We have

(a) two horizons if $0 < 4r_Q^2 < r_S^2$ (black hole),

(b) one degenerate horizon at $r_- = r_+ = r_S/2$ if $4r_Q^2 = r_S^2$ (extremal black hole), and

(c) no horizon if $4r_Q^2 > r_S^2$ (naked singularity).

In the limit $r_Q \to 0$ we recover of course the Schwarzschild case. In this limit $r_- \to 0$ and $r_+ \to r_S$.

We consider case (a) in some detail and treat the other two cases only briefly later. So let us assume that $0 < 4r_Q^2 < r_S^2$ which implies that (285) gives us two real radius values, $0 < r_- < r_+$. As the metric (280) has the same general structure as the Kottler (and in particular the Schwarzschild) metric, just with a different function $f(r)$ now given by (281), we can construct (generalised) Eddington-Finkelstein and Kruskal coordinates by the same method as before. To that end we first write down the equation for radial lightlike geodesics,

$$\pm c\,dt = \frac{dr}{f(r)} = \frac{r^2\,dr}{(r-r_-)(r-r_+)} \tag{286}$$

which can be integrated,

$$\pm c\,(t-t_0) = \frac{r_+^2}{r_+ - r_-}\ln\bigl(|r-r_+|\bigr) \,-\, \frac{r_-^2}{r_+ - r_-}\ln\bigl(|r-r_-|\bigr)\,. \tag{287}$$

The transformation to ingoing Eddington-Finkelstein coordinates $\bigl(r, t', \vartheta, \varphi\bigr)$ is then given by

$$c\,dt' \,=\, c\,dt \,-\, dr \,+\, \frac{dr}{f(r)} \tag{288}$$

which yields, upon integration,

$$c\,t' \,=\, c\,t \,-\, r \,+\, \frac{r_+^2}{r_+ - r_-}\ln\bigl(|r-r_+|\bigr) \,-\, \frac{r_-^2}{r_+ - r_-}\ln\bigl(|r-r_-|\bigr)\,. \tag{289}$$

In these coordinates the ingoing radial light rays are given by

$$c\,(t' - t_0) = -\,r \tag{290}$$

and the outgoing ones by

$$c\,(t' - t_0) = -\,r \;+\; \frac{r_+^2}{r_+ - r_-}\ln\big(|r - r_+|\big) \;-\; \frac{r_-^2}{r_+ - r_-}\ln\big(|r - r_-|\big)\,. \tag{291}$$

The two plots on the right show the radial light rays in the Reissner-Nordström black-hole spacetime, first in the Schwarzschild-like coordinates and then in ingoing Eddington-Finkelstein coordinates. The region I is similar to the exterior part of the Schwarzschild spacetime. Here ∂_t is timelike and an observer can move in the direction of decreasing or increasing r. No signal from the other side of the horizon at $r = r_+$ can reach an observer in region I, so it is indeed justified to speak of a black hole. The region II is non-static. Just as in the interior part of the Schwarzschild spacetime, an observer must move in the direction of decreasing r. However, in contrast to the Schwarzschild spacetime this region does not extend to the singularity at $r = 0$. There is another static region III between $r = 0$ and $r = r_-$. In this region an observer is again free to move in the direction of decreasing or increasing r. As indicated by the future light cones, there are timelike curves that end in the singularity, but there are also timelike curves that escape from the singularity. We will show that, in particular, timelike *geodesics* never reach the singularity. On part of region III the hypersurfes $t' = \text{const.}$ are non-spacelike.

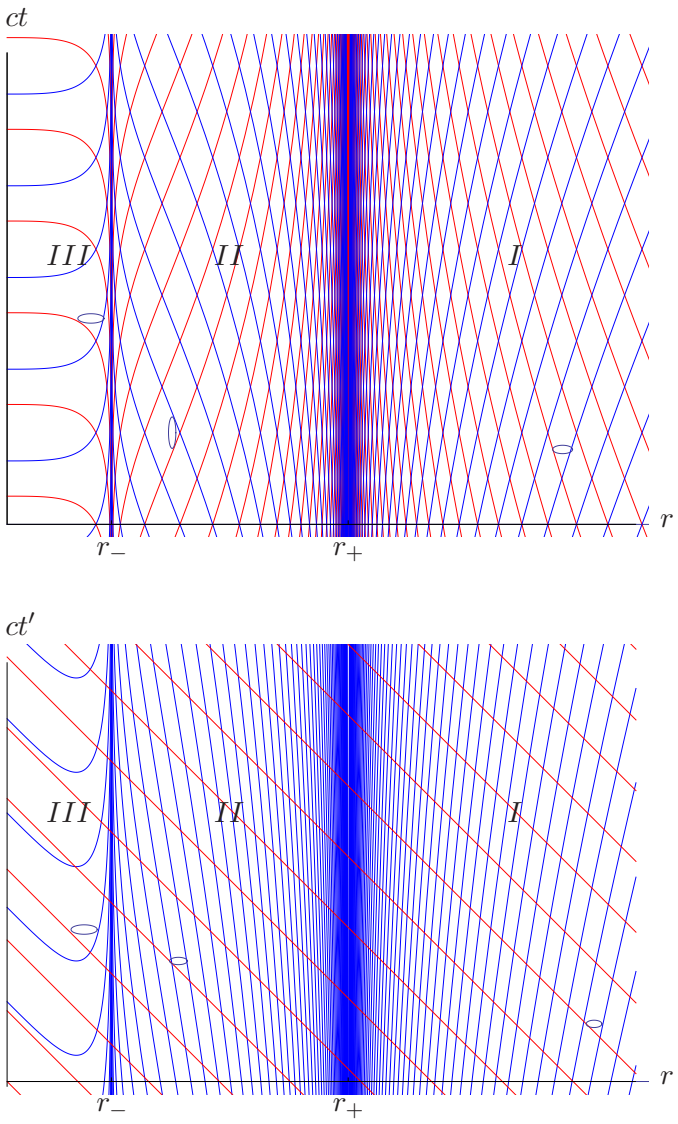

Note the differences between the Reissner-Nordström spacetime and the Kottler spacetime: The cosmological constant modifies the Schwarzschild metric at big radii, while the charge modifies the Schwarzschild spacetime at small radii. In cases where there are two horizons, in the Kottler spacetime we have a static region between two non-static regions, while in the Reissner-Nordström spacetime we have a non-static region between two static regions.

We will now demonstrate that in the Reissner-Nordström spacetime a timelike geodesic cannot reach the singularity. As always in spherically symmetric spacetimes, we need only consider timelike geodesics in the equatorial plane.

We use the constants of motion

$$E = -\frac{\partial \mathcal{L}(x,\dot{x})}{\partial \dot{t}} = c^2\, f(r)\, \dot{t} \tag{292}$$

and

$$L = \frac{\partial \mathcal{L}(x,\dot{x})}{\partial \dot{\varphi}} = r^2 \dot{\varphi}\,, \tag{293}$$

and we parametrise the timelike geodesic by proper time,

$$-\,c^2 \;=\; -\,f(r)\,c^2\,\dot{t}^2 \;+\; \frac{\dot{r}^2}{f(r)} \;+\; r^2\dot{\varphi}^2\,. \tag{294}$$

We substitute the constants of motion into the last equation:

$$-\,c^2 \;=\; -\,\frac{E^2}{c^2\, f(r)} \;+\; \frac{\dot{r}^2}{f(r)} \;+\; \frac{L^2}{r^2}\,,$$

and we multiply by $f(r)$,

$$\frac{E^2}{c^2} - \; c^2\, f(r) = \dot{r}^2 \;+\; \frac{L^2}{r^2}\, f(r)\,. \tag{295}$$

We consider a timelike geodesic in region III, i.e., in the domain where $0 < r < r_-$. Then the function $f(r)$ is positive, so (295) implies that

$$\frac{E^2}{c^2} - \; c^2\, f(r) \geq 0\,,$$

$$\frac{E^2}{c^2} \geq \; c^2 \left(1 - \frac{r_S}{r} + \frac{r_Q^2}{r^2}\right). \tag{296}$$

For $r \to 0$, the right-hand side goes to $+\infty$ (as we assume $r_Q \neq 0$). On the other hand, (296) requires this expression to be bounded by a finite number E^2/c^2. As a consequence, r must be bounded away from 0. In other words, for every timelike geodesic in the domain $0 < r < r_-$ there is a region $0 < r < r_{\min}$ into which this geodesic cannot enter; in particular, an observer in free fall will never arrive at the singularity at $r = 0$. This may be interpreted as saying that the singularity is repulsive. In Worksheet 9 we will show that a radially infalling observer crosses region III in a finite proper time. So there is the possibility of extending the spacetime from region III to the future. Such a possibility did not exist for the Schwarzschild spacetime (because in the latter case there was no region III). In Worksheet 9 we will also show that for a timelike geodesic in region III the radial acceleration $d^2r/d\tau^2$ is always positive, i.e., the acceleration points outward. This corroborates the observation that in the Reissner-Nordström spacetime the singularity at $r = 0$ is repulsive. Note that here we consider timelike *geodesics*, i.e., freely falling uncharged particles. Charged particles will, of course, feel a Lorentz force which is either repulsive or attractive, depending on whether the charge of the particle has the same sign or the opposite sign of the charge of the black hole. We will not consider the motion of charged particles in the Reissner-Nordström metric in this lecture course.

We will now construct the maximal extension of the Reissner-Nordström black-hole spacetime. We use the same transformation to (generalised) Kruskal-Szekeres coordinates as for the Kottler spacetime, see (248) and (249), but now of course with the function $f(r)$ of the Reissner-Nordström metric which is given in (281). Then we compactify the diagram with the help of the transformations (250).

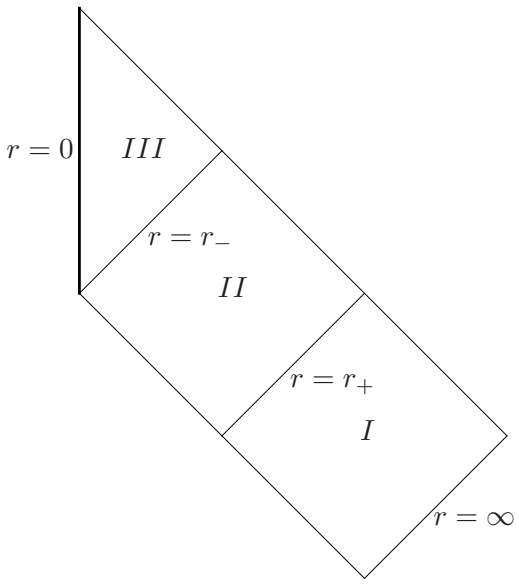

We begin with the domain covered by ingoing Eddington-Finkelstein coordinates, i.e., with regions I, II and III as shown in the spacetime diagrams on p.71. The horizons at r_- and r_+ are generated by radial light rays, so they must make an angle of 45^o with the horizontal. The singularity at $r = 0$ is vertical which reflects the fact that it can be avoided by timelike curves, see picture on the right.

We can glue a region II', which is isometric to region II, to the future of region III, so that observers can escape from region III into this region II'. We can further extend the spacetime by gluing a region I', which is isometric to region I, to the future of region II'. For an observer in region I, the singularity at the centre of region III is hidden behind a horizon, so for this observer it is a black hole. For an observer in region I', however, it is a *white hole*.

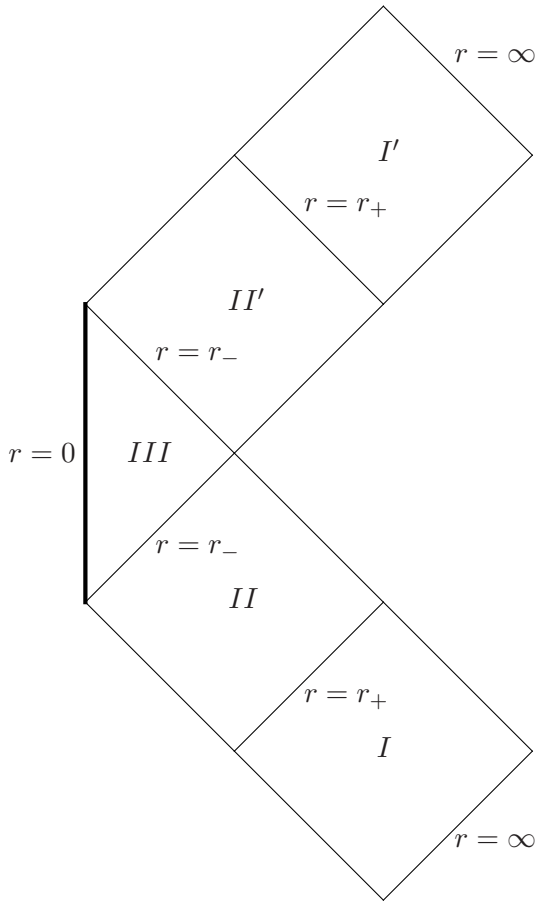

In the middle of the figure we can match another copy of region III, and we can infinitely extend the diagram to the future and to the past, see the picture below. Every singularity is at the centre of a black hole for observers in some asymptotically flat regions and at the centre of a white hole for observers in some other asymptotically flat region. In this sense, every Reissner-Nodström black hole is at the same time a white hole. If we think of a Reissner-Nordström black hole as being the result of gravitational collapse, the past extension of the original spacetime I, II and III has no physical relevance, similarly to the lower left-hand portion of the Kruskal diagram; one would have to replace this part by an interior solution. The future extension, however, would not be cut away by the interior of the collapsing star, so the conclusion that one can escape from region III would still be true.

The presence of the region III and the possibility of extending the spacetime towards the future of this region is a completely new feature which has no analogue in the Schwarzschild or Kottler case. While in the Schwarzschild spacetime any observer that has crossed the horizon will inevitably end up in the singularity, a charged black hole seems to be more benign: Only those observers who deliberately accelerate towards $r = 0$ will hit the singularity; all other observers that have entered into region III, in particular the freely falling ones, will escape from this region through region II' into another asymptotically flat spacetime region I'. At least that's what the mathematical model of the Reissner-Nordström spacetime describes. However, we have to take into account that, according to our present knowledge, all celestial bodies have a net charge that is very small. Therefore, we expect for all black holes that r_- is very close to 0. As the curvature becomes infinite for $r \to 0$, this means that the tidal forces are so strong at r_- that a macroscopic observer will be ripped apart before entering the region III. The situation is different for (elementary) particles. However, even in this case there is a minimum radius beyond which the classical spacetime description is no longer applicable and a (yet-to-be-found) quantum theory of gravity would have to take over.

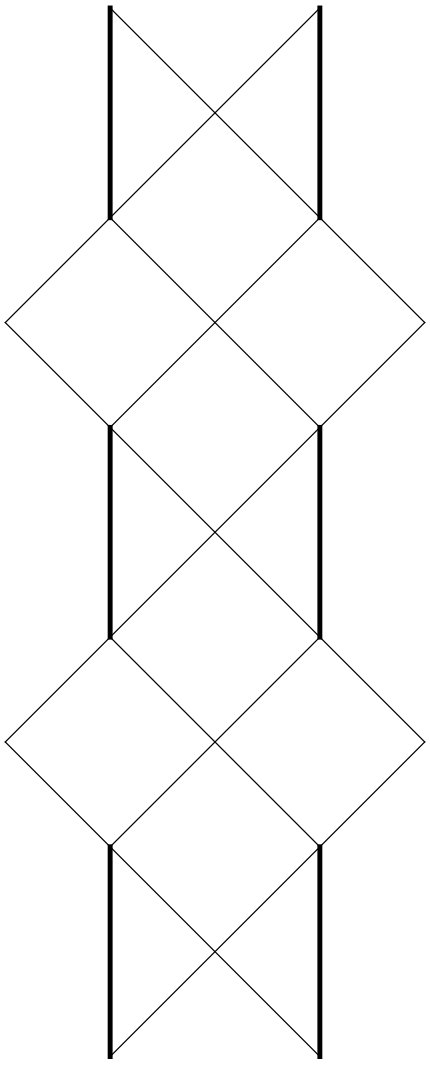

It is believed that this break-down of the classical spacetime theory certainly takes place at a distance from $r = 0$ of the order of the Planck length $\ell_P = \sqrt{\hbar G/c^3} \approx 1.6 \times 10^{-35}\,\mathrm{m}$. Following this line of thought, one may conclude that for (elementary) particles the escape through region III is possible if $r_- \gg \ell_P$. We will discuss a numerical example in Worksheet 9 to investigate if a Reissner-Nordström black hole with $r_- \gg \ell_p$ may be viewed as realistic.

So much for a Reissner-Nordström black hole with $0 < 4r_Q^2 < r_S^2$.

We now briefly consider the case of an extremal Reisner-Nordström black hole, $4r_Q^2 = r_S^2$. Then we have a degenerate horizon at $r_- = r_+ = r_S/2$ and the radial light rays satisfy

$$\pm\, cdt = \frac{dr}{f(r)} = \frac{4\,r^2 dr}{(2r - r_S)^2}\,, \quad (297)$$

$$\pm\, c(t - t_0) = \frac{2r(r - r_S)}{2r - r_S} + r_S \ln\left|2r - r_S\right|\,. \quad (298)$$

Correspondingly, the transformation to ingoing Eddington-Finkelstein coordinates simplifies to

$$c\,dt' \;=\; c\,dt \;-\; dr + \frac{4\,r^2\,dr}{(2\,r - r_S)^2}\,, \quad (299)$$

$$c\,t' \;=\; c\,t \;-\; \frac{r\,r_S}{2\,r - r_S} + r_S \ln\left(\left|2\,r - r_S\right|\right)\,. \quad (300)$$

The two plots on the right show the radial light rays in the extremal Reissner-Nordström black-hole spacetime, first in the Schwarzschild-like coordinates and then in ingoing Eddington-Finkelstein coordinates. Obviously, the only difference with respect to the non-extremal black-hole case is in the fact that now the region II is missing: The static region I is separated from the static region III by the degenerate horizon at $r_- = r_+ = r_S/2$.

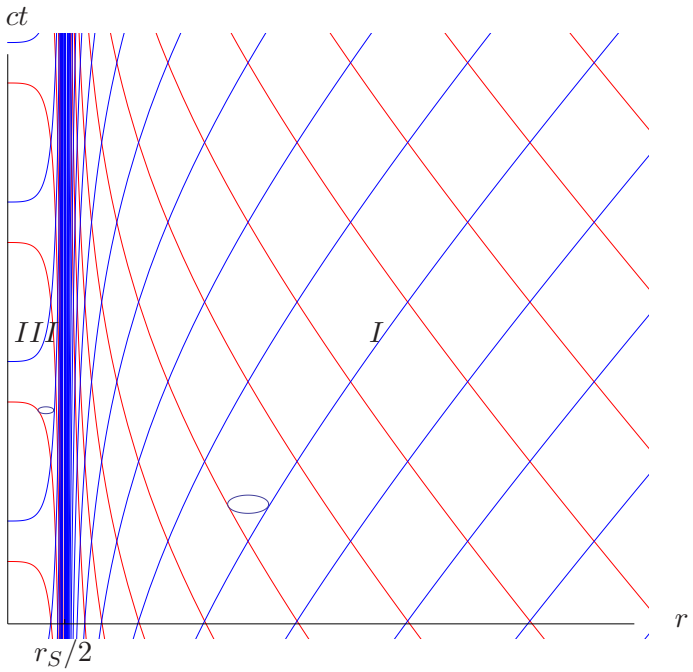

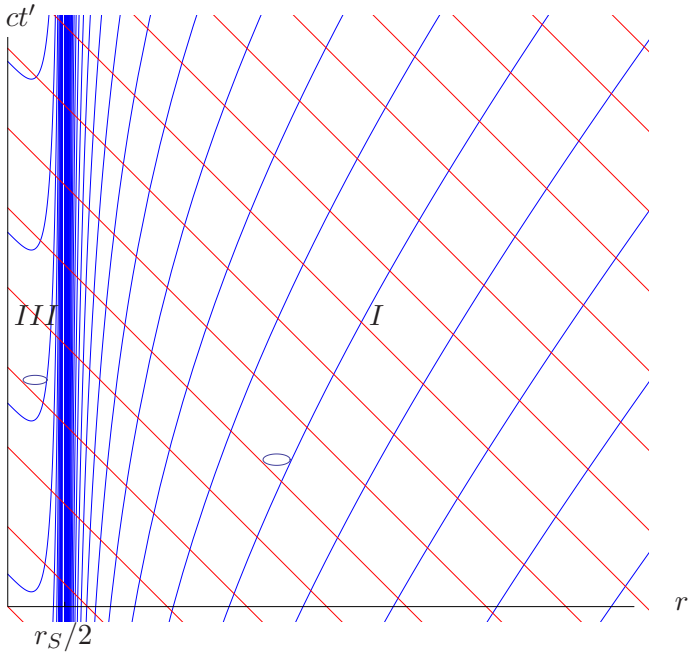

The Carter-Penrose diagram for the extremal Reissner-Nordström black hole can be easily constructed from that of the non-extremal case: We just have to observe that now the region II has shrunk to a point. The resulting Carter-Penrose diagram is shown on the next page. As in the non-extremal black-hole case, the figure extends up and down to infinity.

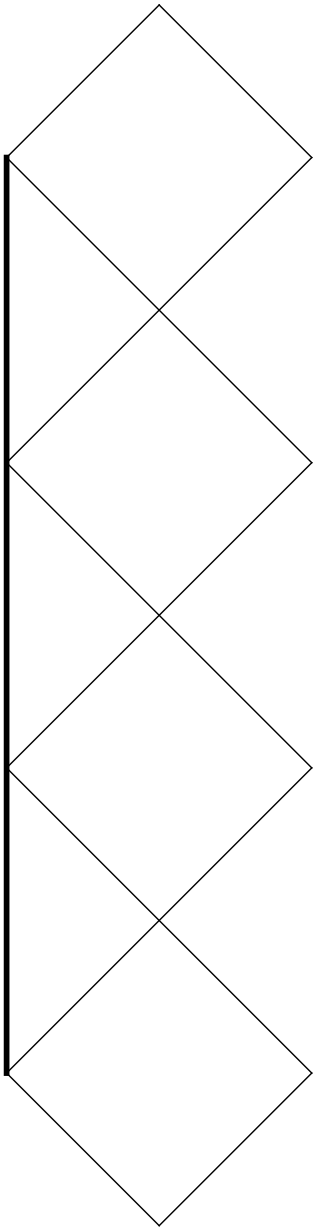

Finally, we look at the case of a naked singularity, $4r_Q^2 > r_S^2$. Then the radial light rays are given by

$$\pm\, c\,(t - t_0) \;=\; \int \frac{dr}{\left(1 - \dfrac{r_S}{r} + \dfrac{r_Q^2}{r^2}\right)}$$

$$= \; r + \frac{r_S}{2}\ln\bigl(|r^2 - r_S r + r_Q^2|\bigr) - \frac{2r_Q^2 - r_S^2}{\sqrt{4r_Q^2 - r_S^2}}\arctan\frac{2r - r_S}{\sqrt{4r_Q^2 - r_S^2}}\,.$$

There are no horizons, so there is no need for introducing other coordinates. A plot of the radial light rays is shown in the following diagram. The spacetime, as shown in this diagram, cannot be extended.

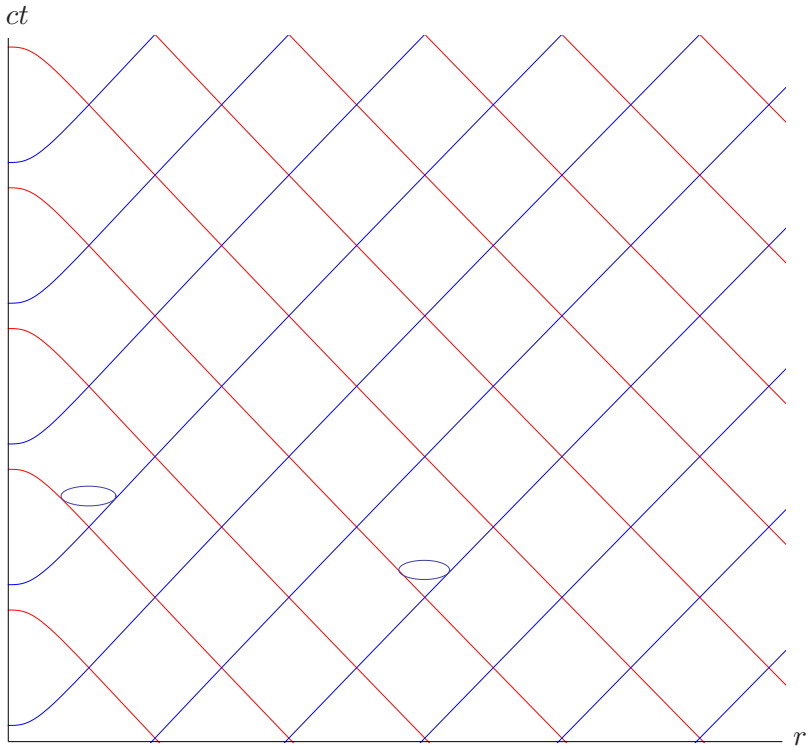

The spacetime is static everywhere. Observers can freely move in the direction of increasing or decreasing r. The singularity at $r = 0$ is exposed to the eyes of observers anywhere in the spacetime. If a singularity is not hidden behind a horizon, one says that it is *naked*.

Already in the late 1960s Roger Penrose formulated the "Cosmic Censorship Hypothesis", saying that under physically reasonable assumptions a naked singularity will never form: If a star or some other massive object undergoes gravitational collapse such that a (true, curvature) singularity is formed, then there will always be a horizon that hides this singularity from the eyes of a distant observer. Until now, this is still a hypothesis. The task is to prove the non-existence of naked singularities under assumptions that are generally accepted as "physically reasonable".

In addition to the Schwarzschild, the Kottler and the Reissner-Nordström metrics many other spherically symmetric and static spacetimes have been investigated. If one goes beyond vacuum and electro-vacuum solutions of Einstein's field equation, either by allowing more complicated energy-momentum tensors or by modifying Einstein's field equation, one can construct spacetimes with quite different properties. Among other things, it was possible to construct *regular black holes*, i.e. spacetimes with a black-hole horizon but no curvature singularity inside the horizon. We will not discuss such spaetimes here.

6 Kerr black holes

All known celestial bodies rotate, so it is very likely that also black holes are rotating. A black hole that rotates at a constant rate is described by a spacetime that is stationary and axisymmetric, i.e., in appropriately chosen coordinates $(t, r, \vartheta, \varphi)$ the metric coefficients are independent of t and φ. If we ignore the cosmological constant, and if we assume that the black hole is uncharged, we have thus to look for a solution to Einstein's vacuum field equation, $R_{\mu\nu} = 0$, that is stationary and axisymmetric.

For spherically symmetric vacuum solutions the situation is quite simple: There is only a one-parameter family of such solutions, given by the Schwarzschild metric. By contrast, the class of stationary and axisymmetric vacuum solutions is vast. The exterior regions around two rotating stars with different interior structure will be completely different from each other and from the region around a rotating black hole. It is far from obvious by which property the region around a rotating black hole is distinguished among all stationary and axisymmetric vacuum solutions.

The vacuum solution that actually describes rotating black holes was found by R. Kerr in 1963, almost half a century after Schwarzschild had discovered the spherically symmetric solution. The way in which Kerr found this solution was very involved and cannot be reviewed here. Actually, the original Kerr paper [Phys. Rev. Lett. 11, 237 (1963)] is less than two pages long and doesn't give much of a derivation at all. After the solution had been found, many people tried to rederive it in a systematic way. In 1965 Newman and Janis [J. Math. Phys. 6, 915 (1965)] showed that the Kerr metric can be found by applying a kind of "complex coordinate transformation" to the Schwarzschild metric. This method became known as the "Newman-Janis trick". A more systematic, but technically very involved path to the Kerr metric was brought forward by F. Ernst [J. Math. Phys. 15, 1409 (1974)] who showed that the stationary and axisymmetric solutions to the vacuum Einstein equation can be expressed in terms of a complex potential, now known as the Ernst potential. The simplest rotating solution to the Ernst equation, i.e., to the differential equation satisfied by the Ernst potential, gives the Kerr metric.

Here we will not give a derivation of the Kerr metric, we will just write it down and then discuss it in detail. We will work with the Kerr metric in a coordinate representation that was found by R. Boyer and R. Lindquist [J. Math. Phys. 8, 265 (1967)]. Kerr had given the metric in a different coordinate system.

In Boyer-Lindquist coordinates the Kerr metric reads

$$g = -\left(1 - \frac{2mr}{\rho^2}\right) c^2 dt^2 + \frac{\rho^2}{\Delta} dr^2 + \rho^2 d\vartheta^2$$

$$+\sin^2\vartheta \left(r^2 + a^2 + \frac{2mra^2\sin^2\vartheta}{\rho^2}\right) d\varphi^2 - \frac{4mra\sin^2\vartheta}{\rho^2}\, c\, dt\, d\varphi \tag{301}$$

where

$$\rho^2 := r^2 + a^2\cos^2\vartheta\,, \quad \Delta := r^2 - 2mr + a^2\,. \tag{302}$$

The Kerr metric depends on two parameters, m and a, both of which have the dimension of a length. We will discuss the physical meaning of m and a in a minute.

The metric (301) satisfies indeed Einstein's vacuum field equation $R_{\mu\nu} = 0$. It is straightforward (though tedious, if you do it by hand) to verify this. As was said before, it is recommendable to write a little computer programme, e.g. with Mathematica, that calculates the inverse metric coefficients, the Christoffels, the curvature tensor and the Ricci tensor from any given covariant metric coefficients. With such a programme it takes a few seconds to verify that (301) gives a vanishing Ricci tensor.

In the following section we discuss some general features of the Kerr metric in Boyer-Lindquist coordinates. Already now, we observe that the metric coefficients are independent of t and φ, i.e., that ∂_t and ∂_φ are Killing vector fields. For sufficiently large r, the metric coefficient g_{tt} is negative, so the Killing vector field ∂_t is timelike. A metric with a timelike Killing vector field is called *stationary*. An observer who lives on an integral curve of such a vector field sees a time-independent metric. The other Killing vector field ∂_φ is spacelike, at least for positive r, because then $g_{\varphi\varphi}$ is positive. This second Killing vector field describes invariance of the spacetime geometry under rotations about the z axis. A metric with such a symmetry is called *axisymmetric*. The Kerr metric has no other linearly independent Killing vector fields, i.e., it has no other symmetries in addition to stationarity and axisymmetry. This is the main difference to the Schwarzschild metric. The latter is invariant also under rotations about the x and the y axes, i.e., it is spherically symmetric. Moreover, the Killing vector field of the Schwarzschild metric was orthogonal to the hypersurfaces t = constant. In the Kerr metric this is not the case because of the non-zero $g_{t\varphi}$. We may consider, in the tangent space at each point of the spacetime, the three-dimensional orthocomplement of ∂_t, i.e., the local rest spaces of the observers who live on t lines. These orthocomplements, however, do not admit three-dimensional integral manifolds; one should think of the integral curves of ∂_t as "twisting" like spaghetti on a fork. One calls a spacetime *static* if it admits a timelike Killing vector field that is orthogonal to hypersurfaces. The Schwarzschild metric is static, whereas the Kerr metric with $a \neq 0$ is stationary but not static. The fact that the Kerr metric is axisymmetric and stationary but not static suggests that it is associated with a stationarily rotating source. Kerr thought that this source would be a spinning point mass. But then Newman and Janis observed that the source is not concentrated in a point but rather in a ring, as we will discuss below. The Kerr metric describes a rotating black hole, at least for a certain range of the parameter a, with a ring singularity at the centre.

6.1 Properties of the Kerr metric

(a) Asymptotic flatness

For $r \to \infty$, the Kerr metric (301) approaches the Minkowski metric in ordinary spherical polar coordinates, i.e., the metric is "asymptotically flat". This observation is crucial for the interpretation of the two parameters m and a on which the Kerr metric depends. At the time when Kerr discovered the metric named after him, no exact solution for a rotating body in general relativity was known. However, one did know an *approximative* solution which holds around a rotating body whose gravitational field is weak. This had been found by the Viennese scientists J. Lense and H. Thirring (with essential contributions by Einstein) already in 1917.

By comparison with this approximative solution it was clear that one had to identify

$$m = \frac{GM}{c^2}\,, \quad a = \frac{J}{Mc} \tag{303}$$

where M is the mass and J is the angular momentum of the source. Keep in mind that both m and a have the dimension of a length. As a should vanish for a source with $J = 0$, the identification $a = J/(Mc)$ can be guessed, up to a possible numerical factor, just by a dimensional analysis.

The Kerr metric includes the following special cases.

- $a = 0$ and $m \neq 0$: This corresponds to sending $J \to 0$ with $M \neq 0$ kept fixed. Then the Kerr metric (301) reduces to the Schwarzschild metric in Schwarzschild coordinates.

- $a \neq 0$ and $m = 0$: This case corresponds to sending $J \to 0$ and $M \to 0$ in such a way that the quotient J/M remains fixed. We get the metric

$$g = -c^2 dt^2 + \frac{\rho^2}{r^2 + a^2} dr^2 + \left(r^2 + a^2\right) \sin^2\vartheta \, d\varphi^2 + \rho^2 d\vartheta^2 \,. \tag{304}$$

  This is the Minkowski metric in spheroidal coordinates. To see this, one has to transform from (r, ϑ, φ) to Cartesian coordinates (x, y, z) by

$$x = \sqrt{r^2 + a^2} \cos\varphi \sin\vartheta \,, \quad y = \sqrt{r^2 + a^2} \sin\varphi \sin\vartheta \,, \quad z = r \cos\,\theta \,. \tag{305}$$

$$dx = \frac{r}{\sqrt{r^2 + a^2}} \cos\varphi \sin\vartheta \, dr - \sqrt{r^2 + a^2} \sin\varphi \sin\vartheta d\varphi + \sqrt{r^2 + a^2} \cos\varphi \cos\vartheta d\vartheta \,,$$

$$dy = \frac{r}{\sqrt{r^2 + a^2}} \sin\varphi \sin\vartheta \, dr + \sqrt{r^2 + a^2} \cos\varphi \sin\vartheta \, d\varphi + \sqrt{r^2 + a^2} \sin\varphi \cos\vartheta \, d\vartheta \,,$$

$$dz = \cos\vartheta \, dr - r \sin\vartheta \, d\vartheta \,. \tag{306}$$

  This transforms the metric (304) to the standard Minkowski metric

$$g = -c^2 dt^2 + dx^2 + dy^2 + dz^2 \,. \tag{307}$$

  The picture on the next page shows the surfaces $r =$ constant which are spheroids (i.e., rotationally symmetric ellipsoids) and the surfaces $\vartheta =$ constant which are hyperboloids. The set

$$r = 0 \quad \text{and} \quad \vartheta = \pi/2 \tag{308}$$

  is the focal ring of the spheroids, given in the (x, y, z) system as the circle

$$x^2 + y^2 = a^2 \quad \text{and} \quad z = 0 \,. \tag{309}$$

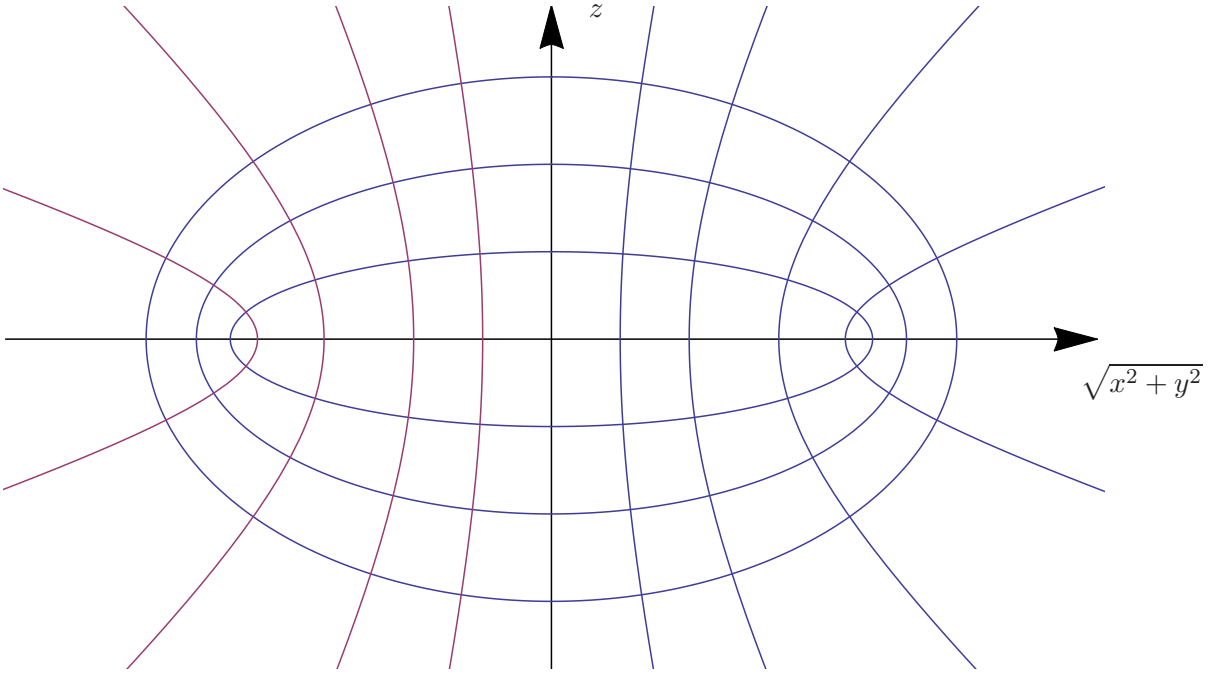

For $m = 0$ and $a = 0$ the Kerr metric (301) reduces to the Minkowski metric in ordinary spherical polar coordinates. This case corresponds to sending $J \to 0$ and $M \to 0$ in such a way that the quotient J/M goes to zero as well. – From now on we will assume $m > 0$ throughout.

(b) The range of the coordinates

The fact that for $a \to 0$ the Kerr metric (301) reduces to the Schwarzschild metric might suggest to have the coordinates running over the same range as in the Schwarzschild case, i.e., to have t running over all of $\mathbb{R}$, ϑ and φ coordinatising the 2-sphere in the usual fashion, and r running from 0 to ∞. However, as to the range of the r coordinate there is actually no reason for this restriction if $a \neq 0$. From the metric we read that $(t = t_0, r = 0)$ is a 2-sphere, parametrised by ϑ and φ, that has a finite area, see Worksheet 10. It is *not* a point, in contrast to what we are used to from the case of spherical polar coordinates on flat space. Of course, one has to make sure that all the metric coefficients are non-singular on this sphere. This is indeed true, unless in the equatorial plane $\vartheta = \pi/2$, see item (c) below. If we remove the ring at $\vartheta = \pi/2$ from the 2-sphere $(t = t_0, r = 0)$, the two remaining hemispheres are perfectly regular with a finite area. This allows extending the spacetime to the domain of negative r values. A convenient way of plotting this situation is by using $e^{r/m}$ for the radial coordinate, see the picture on the next page. Then $r = 0$ is represented as a sphere with the domain of positive r values on the exterior and the domain of negative r values on the interior. The origin corresponds to $r = -\infty$.

In summary, the range of the Boyer-Lindquist coordinates of the Kerr metric with $a^2 > 0$ is $t \in \mathbb{R}$, $r \in \mathbb{R}$, $(\vartheta, \varphi) \in S^2$. For $a = 0$, there is a pointlike singularity at $r = 0$ and the r coordinate is restricted by $0 < r < \infty$. (The domain $-\infty < r < 0$ could be considered as another spacetime which is disconnected from the domain $0 < r < \infty$. The Schwarzschild metric with positive m and r ranging over the negative half-axis is isometric with the Schwarzschild metric with negative m and r ranging over the positive half-axis. As in this spacetime the curvature singularity at $r = 0$ is naked, it is usually believed to be unphysical.)

(c) The ring singularity

The metric coefficient g_{tt} of the Kerr metric becomes singular at $\rho^2 = 0$. In the Schwarzschild limit $a \to 0$ the equation $\rho^2 = 0$ reduces to $r^2 = 0$ which is known to be a curvature singularity. One would therefore expect that $\rho^2 = 0$ is a curvature singularity also in the Kerr metric with $a \neq 0$. This is indeed true as can be verified by calculating e.g. the Kretschmann scalar $R_{\mu\nu\sigma\tau}R^{\mu\nu\sigma\tau}$ which diverges for $\rho^2 \to 0$. The condition $\rho^2 = r^2 + a^2\cos^2\vartheta = 0$ is equivalent to

$$r = 0 \quad \text{and} \quad \vartheta = \frac{\pi}{2} \tag{310}$$

if $a \neq 0$. This is a ring, see picture on the right. We will discuss the geometry of the sphere $r = 0$, which contains the ring singularity, in Worksheet 10.

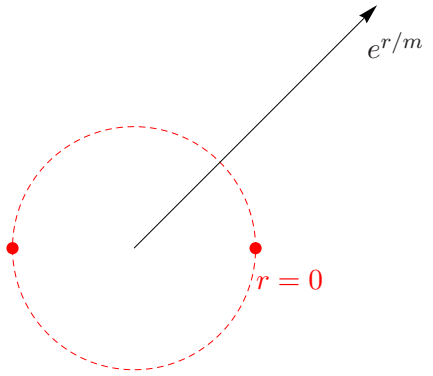

(d) The horizons

The metric coefficient g_{rr} becomes singular if $\Delta = 0$. In the Schwarzschild case (where we restrict to $r > 0$) this corresponds to the coordinate singularity at $r = 2m$. We know that this coodinate singularity in the Schwarzschild metric can be removed by a transformation e.g. to Eddington-Finkelstein coordinates and that in the correspondingly extended spacetime the surface $r = 2m$ plays the role of a horizon. Therefore, it is natural to assume that also in the case $a \neq 0$ the equation $\Delta = 0$ gives a horizon. We will demonstrate this immediately.

The equation

$$0 = \Delta = r^2 - 2mr + a^2 \tag{311}$$

is a quadratic equation for r with the solution

$$r_\pm = m \pm \sqrt{m^2 - a^2}\,. \tag{312}$$

We distinguish three cases:

$0 < a^2 < m^2$: There are two real solutions, $0 < r_- < r_+$, i.e., two horizons. The outer horizon at r_+ is an event horizon that hides its interior with the ring sinularity for an outside observer. So in this case we have a *Kerr black hole*. (Mathematically, one may also consider the time-reversed situation which gives a *Kerr white hole*.)

$0 < a^2 = m^2$: There is a double solution $r_- = r_+ = m$ which is real and positive if $m > 0$, i.e., there is one degenerate horizon. Again, this is an event horizon for an observer in the exterior domain. In this case we speak of an *extreme Kerr black hole*. (Again, one may also consider an *extreme Kerr white hole*.)

$m^2 < a^2$: There are no real solutions and thus no horizons. The ring singularity is exposed to the eyes of any observer, even for an observer at an arbitrarily large distance. In this case we speak of a *Kerr naked singularity*.

In the black-hole case, the region $r > r_+$ is called the *domain of outer communication* because in this region any two observers can communicate with each other without being hindered by a horizon.

For planets, stars or galaxies, $a = J/(Mc)$ is usually *bigger* than $m = GM/c^2$. This seems to suggest that such an object would end up as a naked singularity if it undergoes gravitational collapse. However, this does not take into account that gravitational collapse is believed to be preceded by a kind of explosion. During such an explosion the body can lose not only mass but also angular momentum so that eventually it may end up as a black hole. We have already mentioned that in the late 1960s Roger Penrose formulated the socalled *Cosmic Censorship Hypothesis* according to which any gravitational collapse that starts out from physically realistic initial conditions leads to a black hole and not to a naked singularity. (The name refers to the idea that Nature acts like a censor prohibiting that a distant observer can see a singularities.) Although several partial results have been achieved, the Cosmic Censorship Hypothesis has not been made into a mathematical theorem so far. Of course, the crucial point is to give a mathematically precise formulation of which initial conditions should be considered as physically realistic.

For demonstrating that the Kerr metric for $0 < a^2 < m^2$ describes, indeed, a black hole with two horizons determined by the equation $\Delta = 0$ we have to transform to generalised ingoing Eddington-Finkelstein coordinates. To that end consider the vector fields

$$\ell^\mu_\pm \partial_\mu = \pm\partial_r + \frac{r^2 + a^2}{\Delta\, c}\,\partial_t + \frac{a}{\Delta}\,\partial_\varphi\,. \tag{313}$$

By inserting these vector fields, for the plus sign and for the minus sign, into the Kerr metric (301) one sees that they are lightlike,

$$g(\ell^\mu_\pm \partial_\mu, \ell^\nu_\pm \partial_\nu) = 0\,. \tag{314}$$

We will show in Worksheet 10 that the integral curves of $\ell^\mu_\pm \partial_\mu$ are geodesics, i.e., that these curves are indeed light rays. From the sign in front of ∂_r in (313) we read that the integral curves of $\ell^\mu_+ \partial_\mu$ are outgoing and the integral curves of $\ell^\mu_- \partial_\mu$ are ingoing. As the factor in front of ∂_φ in (313) goes to zero for $r \to 0$, both families of curves become radial for large r. In contrast to spherically symmetric spacetimes, the Kerr spacetime does not admit light rays which are radial everywhere; a light ray that comes in from infinity with a radial initial direction is being "dragged" by the rotating mass. The integral curves of the vector field (313) with the upper sign are known as the *outgoing principal null geodesics*; with the lower sign they are known as the *ingoing principal null geodesics*. Recall that "null" is often used as synonymous with "lightlike".

Along each principal null geodesic, we can use r as the parameter. As we read from (313), t, φ and ϑ are then given as functions of r by the differential equations

$$\frac{dt}{dr} = \pm\,\frac{(r^2 + a^2)}{c\,\Delta}\,, \qquad \frac{d\varphi}{dr} = \pm\,\frac{a}{\Delta}\,, \qquad \frac{d\vartheta}{dr} = 0\,. \tag{315}$$

Here the upper sign refers to the outgoing and the lower sign to the ingoing curves. We see that in the Schwarzschild case $a = 0$ the principal null geodesics satisfy $d\varphi/dr = 0$ and $d\vartheta/dr = 0$, i.e., they reduce to the radial null geodesics. The new feature in the Kerr case is in the fact that now not only the t coordinate must be transformed to remove the singularity of dt/dr at the horizon(s), but also the φ coordinate to remove the singularity of $d\varphi/dr$. The latter expresses the fact that the principal null geodesics approach the horizons in an infinite whirl.

By integrating the first equation in (315) we get the projection to the $r-ct$ plane of the ingoing and outgoing principal null geodesics, see the following picture. The φ and ϑ coordinates are not shown. Whereas φ depends on r, according to the second equation in (315), ϑ is constant along each of the principal null geodesics and both dt/dr and $d\varphi/dr$ are independent of ϑ. As to the ϑ dependence, we just have to keep in mind that in the case of $\vartheta = \pi/2$ the principal null geodesics are blocked at the ring singularity, whereas for all other values of ϑ they pass through one of the throats at $r = 0$. The picture refers to the case $0 < a^2 < m^2$ where we have two horizons.

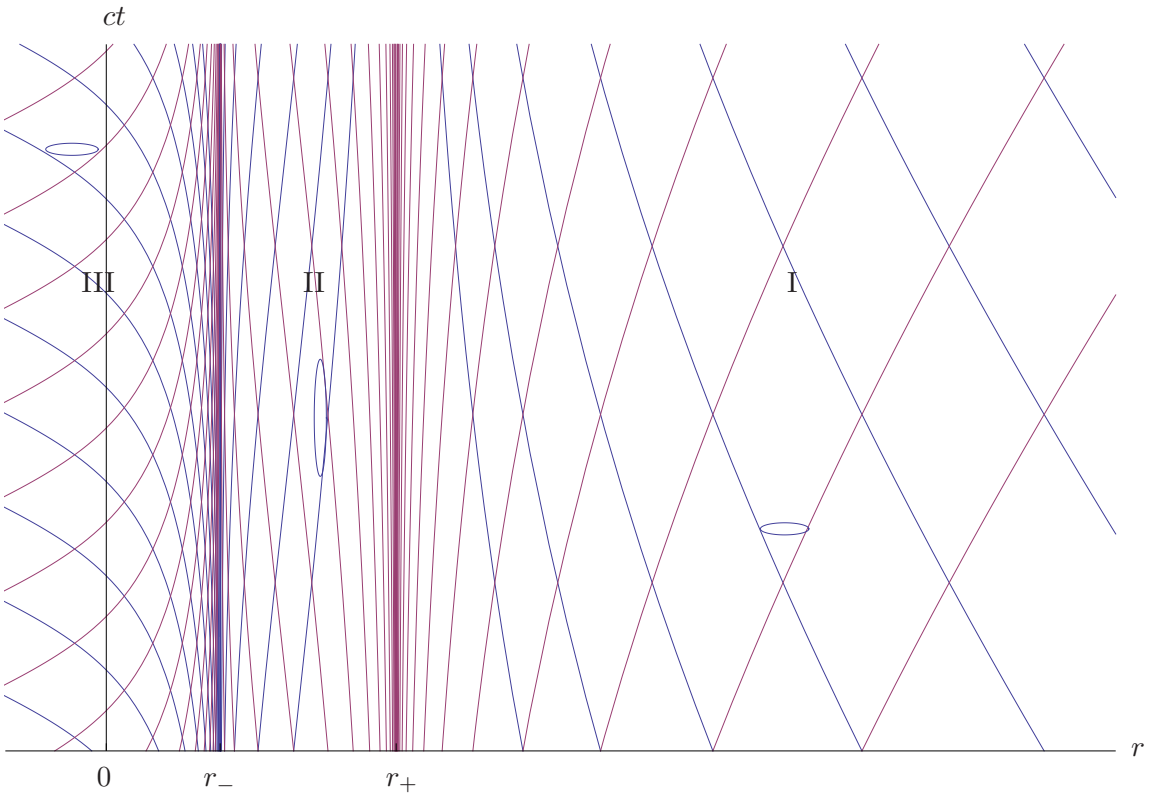

The passage to (generalised) ingoing Eddington-Finkelstein coordinates requires a transformation $(t, r, \vartheta, \varphi) \mapsto (\tilde{t}, \tilde{r}, \tilde{\vartheta}, \tilde{\varphi})$ that maps the ingoing principal null geodesics onto straight lines under 45^o degrees. From (315) we read that this is achieved by setting

$$c\, d\tilde{t} = c\, dt + \frac{2mr}{\Delta}\, dr\,, \quad d\tilde{r} = dr\,, \quad d\tilde{\vartheta} = d\vartheta\,, \quad d\tilde{\varphi} = d\varphi + \frac{a}{\Delta}\, dr\,. \tag{316}$$

Then the ingoing principal null geodesics are indeed given by

$$c\,\frac{d\tilde{t}}{d\tilde{r}} = -1\,, \qquad \frac{d\tilde{\vartheta}}{d\tilde{r}} = 0\,, \qquad \frac{d\tilde{\varphi}}{d\tilde{r}} = 0\,, \tag{317}$$

and the outgoing ones by

$$c\,\frac{d\tilde{t}}{d\tilde{r}} = \frac{r^2 + a^2 + 2mr}{\Delta}\,, \qquad \frac{d\tilde{\vartheta}}{d\tilde{r}} = 0\,, \qquad \frac{d\tilde{\varphi}}{d\tilde{r}} = \frac{2\,a}{\Delta}\,. \tag{318}$$

These curves are plotted below in a $(\tilde{r} = r, c\,\tilde{t})$ diagram. Again, we assume that $0 < a^2 < m^2$. For $a \to 0$ this picture reduces to the plot of the radial and lightlike Schwarzschild geodesics in ingoing Eddington-Finkelstein coordinates, recall the diagram on p.12. The $\tilde{\varphi}$ and $\tilde{\vartheta} = \vartheta$ coordinates are not shown in the diagram. Keep in mind that only the ingoing principal null geodesics have $\tilde{\varphi} =$ constant while the outgoing ones approach the horizons in an infinite whirl.

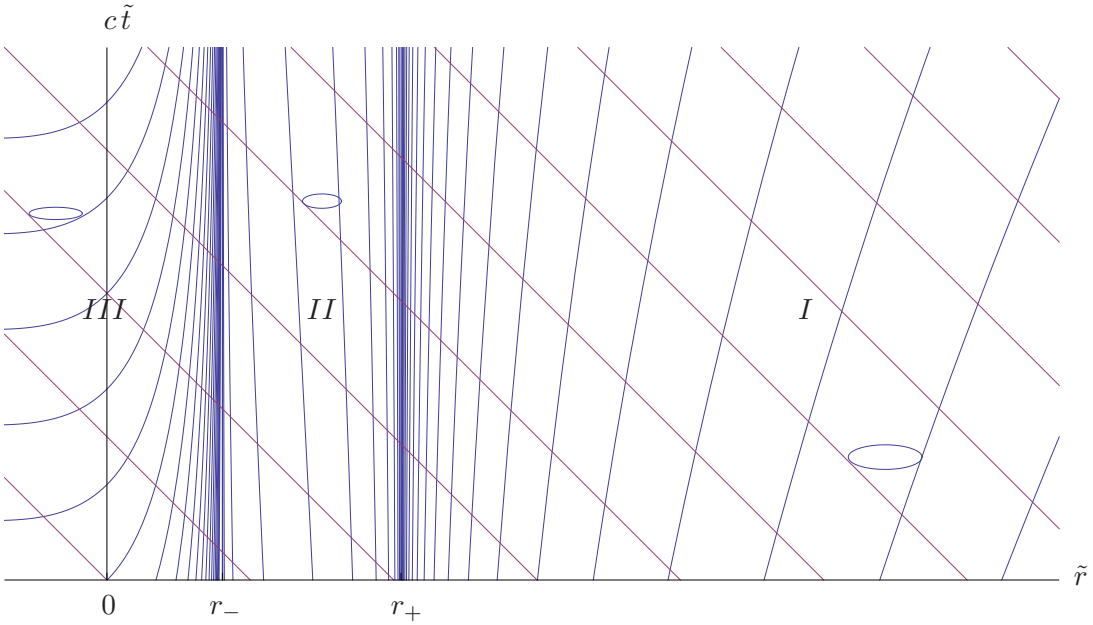

In the case $0 < a^2 = m^2$ the two horizons come together and the region II is gone. In the case $m^2 < a^2$ there are no horizons; in the $r - ct$ plot all principal null geodesics go from $+\infty$ to $-\infty$ or vice versa, except for the ones with $\vartheta = \pi/2$ which are blocked at the ring singularity.

Here we have constructed a black hole by using the (generalised) ingoing Eddington-Finkelstein coordinates. There are of course analogously defined outgoing coordinates which join the regions I, II and III to produce a Kerr white-hole spacetime. The (generalised) ingoing Eddington-Finkelstein coordinates $(\tilde{t}, \tilde{r}, \tilde{\vartheta}, \tilde{\varphi})$ are related to the Kerr coordinates $(\hat{u}, \hat{r}, \hat{\vartheta}, \hat{\varphi})$ which were used by Roy Kerr in his original publication by the simple relations $\hat{u} = c\,\tilde{t} + \tilde{r}$, $\hat{r} = \tilde{r}$, $\hat{\vartheta} = \tilde{\vartheta}$ and $\hat{\varphi} = \tilde{\varphi}$.

As the Kerr spacetime is not spherically symmetric, we cannot draw a Penrose diagram in the strict sense. However, if we restrict to motion along the axis $\vartheta = 0$ (or $\vartheta = \pi$), we can draw a Penrose diagram for this $(1 + 1)$ dimensional spacetime. Note that ingoing and outgoing principal null geodesics that start tangentially to the axis remain tangential everywhere. The figure on the right shows the Penrose diagram for the axis of a Kerr black hole with $0 < a^2 < m^2$. In the extreme case, $a^2 = m^2$, there is no region II. The r-coordinate ranges from $-\infty$ to ∞. As we are on the axis, the ring singularity is not met.

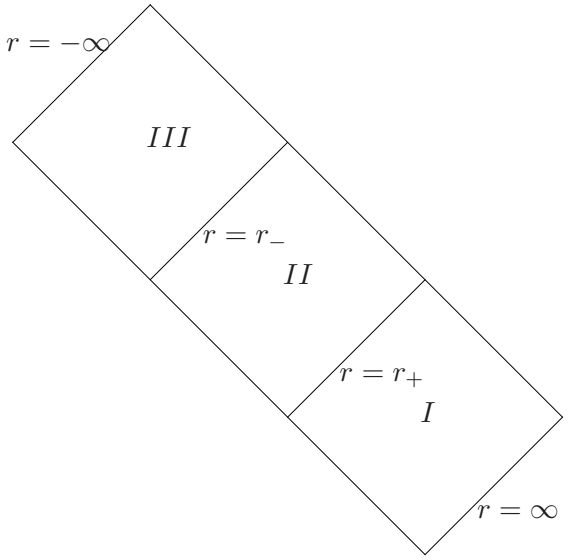

The maximal analytic extension of the Kerr black-hole spacetime restricted to the axis gives a Penrose diagram with infinitely many copies of the regions I, II and III, see below.

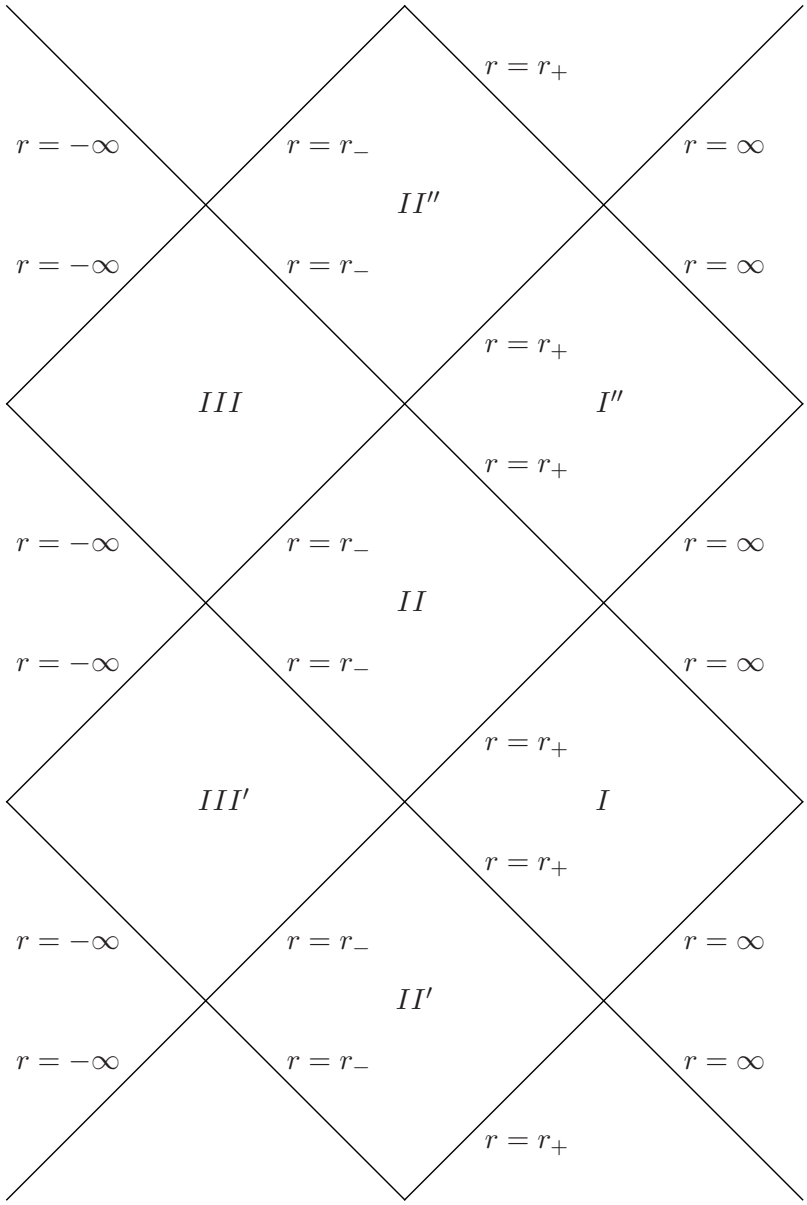

In the extreme case $0 < a^2 = m^2$ the regions II are gone, i.e., there are infinitelky many copies of region I and region III only. In the naked-singularity case $m^2 < a^2$ there is only one block, with $r = \infty$ at the upper right and at the lower right, and $r = -\infty$ at the upper left and at the lower left.

(d) The Killing vector fields ∂_t and ∂_φ

We have already mentioned that the metric coefficients are independent of t and of φ, so the vector fields ∂_t and ∂_φ are Killing vector fields. On a domain where ∂_t is timelike ($g_{tt} < 0$), we may interpret the transformation $t \to t +$ constant as a time translation; invariance under this transformation then means that the metric is *stationary*. Similarly, on a domain where

∂_φ is spacelike ($g_{\varphi\varphi} > 0$), we may interpret the transformation $\varphi \to \varphi +$ constant as a spatial rotation about the z axis; invariance under this transformation then means that the metric is *axisymmetric*. From the fact that the metric approaches the Minkowski metric for $r \to \infty$ it follows that the conditions $g_{tt} < 0$ and $g_{\varphi\varphi} > 0$ are indeed satisfied for large r. In the inner part of the spacetime, however, these conditions are violated. The region where $g_{tt} > 0$ is bounded by two surfaces which are known as the "stationarity limit surfaces". They are determined by

$$0 = g_{tt} = 1 - \frac{2mr}{\rho^2}\,, \qquad 0 = r^2 + a^2\cos^2\vartheta - 2mr\,, \qquad a^2\sin^2\vartheta = \Delta\,. \tag{319}$$

Clearly, these surfaces lie in the region where $\Delta \geq 0$ and equality, $\Delta = 0$, holds exactly at the poles $\sin\vartheta = 0$ if $a \neq 0$. In the black-hole case $0 < a^2 \leq m^2$ one stationarity limit surface lies in the region $r > r_+$ and touches the outer horizon at the poles, while the other stationarity limit surface lies in the region $r < r_-$ and touches the inner horizon at the poles.

The region between the outer stationarity limit surface and the outer horizon is known as the *ergoregion*. This name refers to the fact that energy can be extracted from a Kerr black hole by dropping a particle into the ergoregion, splitting it into two particles there and getting one of them back with a higher energy than the compound had had before. This socalled *Penrose process* will be discussed later when we have the equations for timelike geodesics in the Kerr spacetime at our disposal. In the ergoregion a timelike vector must have a non-vanishing φ component, as can be read from the metric, i.e., "all observers must rotate".

In the Schwarzschild case $a \to 0$ the outer stationarity limit surface merges with the horizon at $r = 2m$ (while the inner one merges with the curvature singularity at $r = 0$), so there is no ergoregion in this case.

The picture on the right shows for a Kerr black hole with $a = 0.9\,m$ the ergoregion (dark shaded) and the rest of the domain where $g_{tt} > 0$ (light shaded). We have indicated the sphere $r = 0$ by a red dashed line, the ring singularity by a red blob and the horizons by solid lines. The picture is rotationally symmetric about the vertical axis.

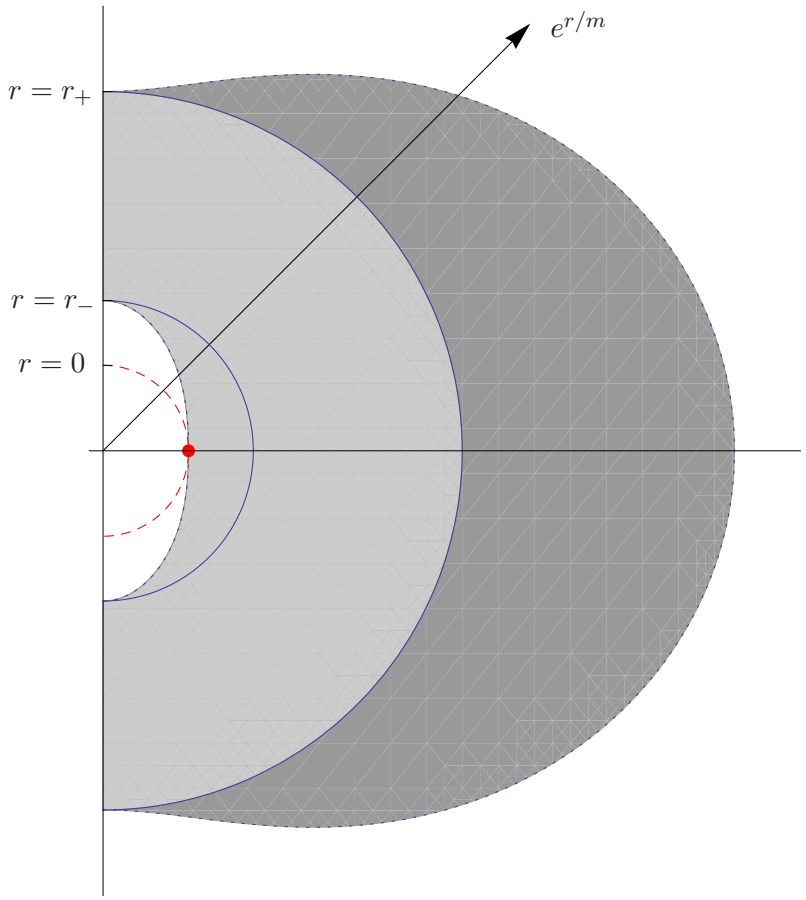

The region where $g_{\varphi\varphi} < 0$, i.e.

$$(r^2 + a^2)\rho^2 + 2mra^2\sin^2\vartheta < 0\,,$$

lies completely in the domain $r < 0$ and touches the ring singularity. It is known as the *causality violating region*. In this region the φ lines, which are circles in the spacetime, are timelike. An observer can move along such a line and thereby return to his or her own past. Closed timelike curves lead to the familiar kind of paradoxa, e.g., to the possibility of killing one's parents before being born. In the case of a Kerr black hole the region with closed timelike curves is accessible only for those observers who actually jump into the black hole; for an observer in the domain of outer comunication it is without relevance.

The plot on the right shows the causality violating region (shaded) for a Kerr black hole with $a = 0.9\,m$. As before, we have marked the sphere $r = 0$ by a red dashed line and the ring singularity by a red blob. On the boundary of the causality violating region the φ lines are lightlike.

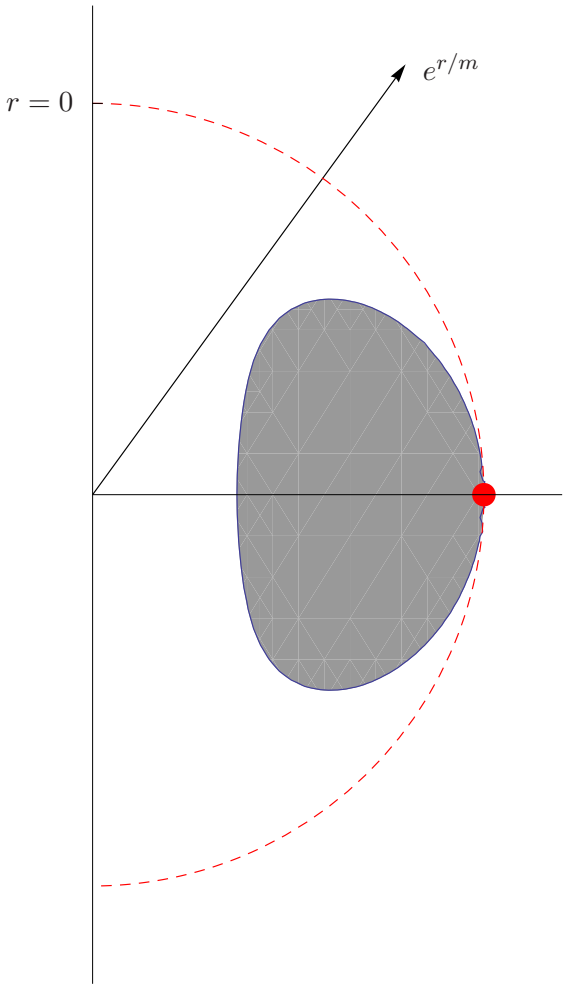

Although we have seen that, in the black-hole case $0 < a^2 \leq m^2$, the vector field ∂_t fails to be timelike inside the ergoregion, it is nonetheless justified to say that the spacetime is stationary on the entire domain of outer communication. The reason is that, near any radius value r_0 with $r_+ < r_0 < \infty$, it is possible to find a constant Ω such that the vector field $\partial_t + \Omega\partial_\varphi$ is timelike near r_0. So there is always a family of observers, defined on a spherical shell $r_0 - \varepsilon < r < r_0 + \varepsilon$, who see a time-independent metric. The vector field ∂_t is distinguished among all vector fields of the form $\partial_t + \Omega\partial_\varphi$ by the fact that it is timelike in the limit $r \to \infty$.

(e) Stationary observers and ZAMOs

Observers whose worldlines are t lines are called *stationary*. They exist only in the domain where $g_{tt} < 0$, i.e. between the outer stationarity limit surface and $r = \infty$ and between the inner stationarity limit surface and $r = -\infty$. In particular, stationary observers do not exist in the ergoregion. We will now investigate on which part of the spacetime the hypersurfaces $t =$ constant are spacelike. In the Schwarzschild case, where the t-lines were orthogonal to the hypersurfaces $t =$ constant, the t-lines were timelike exactly on the same domain where the hypersurfaces $t =$ constant were spacelike, namely on the domain of outer communication where $r > r_S = 2m$. In the Kerr case, where the t-lines are not orthogonal to the hypersurfaces $t =$ constant, this is different.

The Kerr metric (301) induces a 3-dimensional metric on each hypersurface $t =$ constant which is determined by setting dt equal to zero. As the resulting metric is diagonal, it is positive definite if and only if $g_{rr} > 0$, $g_{\vartheta\vartheta} > 0$ and $g_{\varphi\varphi} > 0$, i.e., the hypersurfaces $t =$ constant are spacelike if and only if these three conditions are satisfied. From the metric we read that $g_{rr} > 0$ is equivalent to $\Delta > 0$, i.e., it holds everywhere except between the two horizons. The condition $g_{\vartheta\vartheta} > 0$ is true everywhere and the condition $g_{\varphi\varphi} > 0$ holds everywhere except in the causality violating region. This demonstrates that all three conditions are satisfied, in particular, on the entire domain of outer communication of a Kerr black hole, $0 < a^2 \leq m^2$, i.e., on the entire domain where $r > r_+$. If the hypersurfaces $t =$ constant are spacelike, the worldlines orthogonal to these hypersurfaces are timelike, i.e., they are possible worldlines of observers. These observers are known as *Zero Angular Momentum Observers*, often abbreviated as ZAMOs. In contrast to the stationary observers they exist on the entire domain of outer communication, including the ergoregion. We will now calculate their 4-velocities.

As ∂_r and ∂_ϑ are orthogonal to both ∂_t and ∂_φ the 4-velocity of a ZAMO must be of the form

$$U^\mu \partial_\mu = \alpha\big(\partial_t + \omega\,\partial_\varphi\big) \tag{320}$$

where α and ω are functions of r and ϑ. The condition

$$0 = g\big(U^\mu\partial_\mu, \partial_\varphi\big) = \alpha\big(g_{t\varphi} + \omega\, g_{\varphi\varphi}\big) \tag{321}$$

gives

$$\omega = -\frac{g_{t\varphi}}{g_{\varphi\varphi}} \tag{322}$$

and the condition

$$-c^2 = g\big(U^\mu\partial_\mu, U^\nu\partial_\nu\big) = \alpha^2\big(g_{tt} + 2\omega g_{t\varphi} + \omega^2 g_{\varphi\varphi}\big) \tag{323}$$

gives

$$\alpha = c\,\Big(-g_{tt} + \frac{2\,g_{t\varphi}^2}{g_{\varphi\varphi}} - \frac{g_{t\varphi}^2}{\cancel{g_{\varphi\varphi}^2}}\cancel{g_{\varphi\varphi}}\Big)^{-1/2}, \tag{324}$$

hence

$$U^\mu\partial_\mu = \frac{c\,\big(g_{\varphi\varphi}\,\partial_t - g_{t\varphi}\,\partial_\varphi\big)}{\sqrt{g_{\varphi\varphi}}\sqrt{-g_{tt}g_{\varphi\varphi} + g_{t\varphi}^2}}\,. \tag{325}$$

The qantity under the square-root in the denominator is minus the determinant of the $t-\varphi$ block of the matrix $(g_{\mu\nu})$, which can be calculated:

$$\begin{aligned}
D := g_{tt}g_{\varphi\varphi} - g_{t\varphi}^2 &= -c^2\Big(1 - \frac{2mr}{\rho^2}\Big)\sin^2\vartheta\Big(r^2 + a^2 + \frac{2mra^2\sin^2\vartheta}{\rho^2}\Big) - \frac{4m^2r^2a^2c^2\sin^4\vartheta}{\rho^4} \\
&= \frac{c^2\sin^2\vartheta}{\rho^4}\Big(-\big(\rho^2 - 2mr\big)\Big(\big(r^2+a^2\big)\rho^2 + 2mra^2\sin^2\vartheta\Big) - 4m^2r^2a^2\sin^2\vartheta\Big) \\
&= \frac{c^2\sin^2\vartheta}{\cancel{\rho^4}^2}\Big(-\cancel{\rho^4}^2(r^2+a^2) - \cancel{\rho^2}2mra^2\sin^2\vartheta + 2mr(r^2+a^2)\cancel{\rho^2}\Big) \\
&= \frac{c^2\sin^2\vartheta}{\cancel{\rho^2}}\Big(-\cancel{\rho^2}(r^2+a^2) + 2mr\cancel{(r^2 + a^2\cos^2\vartheta)}\Big) = -c^2\Delta\sin^2\vartheta\,.
\end{aligned} \tag{326}$$

Note that $g_{t\varphi} \to 0$ for $r \to \pm\infty$, i.e., in this limit the stationary observers and the ZAMOs coincide.

6.2 Lightlike and timelike geodesics of the Kerr metric

The geodesics of the Kerr metric have a very rich structure. Even after having worked with them for many years one still discovers features one hadn't known before. Therefore we can give only a few selected results here. In view of physical interpretation, we are interested in lightlike geodesics (light signals or classical photons) and in timelike geodesics (freely falling massive particles).

Recall that for any metric the geodesics are the solutions to the Euler-Lagrange eqations with the Lagrangian

$$\mathcal{L}(x,\dot{x}) = \frac{1}{2} g_{\mu\nu}(x)\dot{x}^\mu \dot{x}^\nu \,. \tag{327}$$

The Lagrangian itself is always a constant of motion

$$g_{\mu\nu}(x)\dot{x}^\mu \dot{x}^\nu = -\varepsilon\, c^2 \tag{328}$$

where $\varepsilon = 0$ for lightlike geodesics and $\varepsilon = 1$ for timelike geodesics parametrised by proper time. In the following we will not discuss spacelike geodesics but they are also covered by our equations if we allow ε to be a negative constant.

For the Kerr metric in Boyer-Lindquist coordinates $x = (t, r, \vartheta, \varphi)$, the metric coefficients are independent of t and of φ. The corresponding components of the Euler-Lagrange equation give us two constants of motion,

$$E = -\frac{\partial \mathcal{L}(x,\dot{x})}{\partial \dot{t}} = -g_{tt}\dot{t} - g_{t\varphi}\dot{\varphi} \qquad \text{and} \qquad L = \frac{\partial \mathcal{L}(x,\dot{x})}{\partial \dot{\varphi}} = g_{t\varphi}\dot{t} + g_{\varphi\varphi}\dot{\varphi}\,. \tag{329}$$

Up to dimensional factors, E is to be interpreted as the energy of the classical photon or the massive particle, while L is to be interpreted as the z component of its angular momentum. (It would be more appropriate to write L_z instead of L, but for the sake of brevity we stick with L.)

The equations for E and L can be solved for $\dot{t}$ and $\dot{\varphi}$,

$$g_{\varphi\varphi}E + g_{t\varphi}L = -(g_{tt}g_{\varphi\varphi} - g_{t\varphi}^2)\dot{t}\,, \tag{330}$$

$$g_{t\varphi}E + g_{tt}L = (g_{tt}g_{\varphi\varphi} - g_{t\varphi}^2)\dot{\varphi}\,. \tag{331}$$

Upon inserting $D = g_{tt}g_{\varphi\varphi} - g_{t\varphi}^2$ from (326) we get

$$\rho^2\,\dot{t} = \frac{\cancel{\sin^2\vartheta}\big((r^2+a^2)\rho^2 + 2mra^2\sin^2\vartheta\big)E - 2mra\cancel{\sin^2\vartheta}\,c\,L}{c^2\Delta\cancel{\sin^2\vartheta}}\,, \tag{332}$$

$$\rho^2\dot{\varphi} = \frac{-\cancel{c}\,2mra\sin^2\vartheta E - \cancel{c^2}\big(\rho^2 - 2mr\big)L}{\cancel{c^2}\Delta\sin^2\vartheta}\,. \tag{333}$$

For any choice of the constants of motion, these two equations determine t and φ as functions of the curve parameter if r and ϑ are known as functions of the curve parameter. However, the third constant of motion $\mathcal{L}(x,\dot{x}) = -\varepsilon c^2/2$ gives us only one equation for the two unknown functions r and ϑ.

In the case of spherical symmetry we could restrict to the equatorial plane, $\vartheta = \pi/2$, without loss of generality. Then we had three constants of motion (E, L and $\mathcal{L}$) for a dynamical system with three degrees of freedom (t, φ and r), and the Euler-Lagrange equations reduced to three first-order equations that could be solved for $\dot{t}$, $\dot{\varphi}$ and $\dot{r}$. The geodesics could then be written in terms of integrals over the metric coefficients and the constants of motion. A dynamical system with n degrees of freedom allows such a reduction to first-order form whenever there are n independent constants of motion with pairwise vanishing Poisson brackets. If this is the case the dynamical system is called "completely integrable" or "integrable in the sense of Liouville". For the Kerr metric, which is only axisymmetric but not spherically symmetric, we cannot restrict to the equatorial plane; the geodesics are not in general contained in a plane. So our dynamical system has four degrees of freedom (t, φ, r and ϑ) while from the symmetries of the spacetime we get only three constants of motion (E, L and $\mathcal{L}$). This seems to indicate that the geodesic equation in the Kerr metric fails to be completely integrable.

Fortunately, this is not the case. It was discovered by Brandon Carter that there is a fourth constant of motion which is not related to any symmetry of the spacetime. Together with the constants of motion E, L and $\mathcal{L}$ the Carter constant K secures complete integrability of the Kerr geodesic equation. It is true that *every* constant of motion is related with a symmetry transformation on the phase space, i.e., on the (co)tangent bundle over spacetime, but not in general to a symmetry of the spacetime. A constant of motion is related to a symmetry of the spacetime, i.e., to a Killing vector field, if and only if it is linear in the velocities $\dot{x}^\mu$ or, equivalently, in the momenta $p_\mu = g_{\mu\nu}\dot{x}^\nu$. The Carter constant is quadratic in the $\dot{x}^\mu$, as we will see.

Carter found the constant of motion that is named after him by working in the Hamiltonian, rather than the Lagrangian, formalism. The Carter constant made its appearance as a separation constant for the Hamilton-Jacobi equation. We will follow this path now in detail.

For the geodesic equation of any spacetime, we can pass from the Lagrangian to the Hamiltonian formalism by introducing the canonical momenta

$$p_\mu = \frac{\partial \mathcal{L}(x,\dot{x})}{\partial \dot{x}^\mu} = g_{\mu\nu}(x)\dot{x}^\nu \,. \tag{334}$$

This equation can be solved for the velocities by multiplying with $g^{\sigma\mu}$,

$$\dot{x}^\sigma = g^{\sigma\mu}(x)p_\mu \,. \tag{335}$$

The Hamiltonian is

$$\begin{aligned}\mathcal{H}(x,p) &= \dot{x}^\mu p_\mu - \mathcal{L}(x,\dot{x}) = \dot{x}^\mu p_\mu - \frac{1}{2}g_{\tau\sigma}(x)\dot{x}^\tau\dot{x}^\sigma \\ &= g^{\mu\nu}(x)p_\nu p_\mu - \frac{1}{2}g_{\tau\sigma}(x)g^{\tau\mu}p_\mu g^{\sigma\nu}p_\nu \\ &= g^{\mu\nu}(x)p_\nu p_\mu - \frac{1}{2}\delta^\mu_\sigma p_\mu g^{\sigma\nu}(x)p_\nu = \frac{1}{2}g^{\mu\nu}(x)p_\nu p_\mu \,. \end{aligned} \tag{336}$$

Note that

$$\mathcal{H}(x,p) = \mathcal{L}(x,\dot{x}) = -\frac{1}{2}\,\varepsilon\,c^2\,, \tag{337}$$

i.e. the Hamiltonian is given by the same quantity as the Lagrangian, just expressed in terms of the momenta instead of the velocities. This is a consequence of the fact that the Lagrangian is a quadratic form in the velocities.

In particular, the Hamiltonian is a constant of motion which is always true if the Hamiltonian does not explicitly depend on the curve parameter. It is then possible to solve the equations of motion with the help of the time-independent Hamilton-Jacobi equation (where "time" refers to the curve parameter),

$$\mathcal{H}\big(x, \partial S/\partial x\big) \;=\; -\,\frac{1}{2}\,\varepsilon\,c^2\,. \tag{338}$$

Here the notation means that in the argument of the Hamiltonian we have to replace p_μ with the partial derivative $\partial S/\partial x^\mu$ of a function $S(x) = S(t,\varphi,r,\vartheta)$ that is to be determined. The goal is to find a *complete integral* of this partial differential equation, i.e., a solution $S(x)$ that involves as many independent constants as the system has degrees of freedom. In our case, we need three constants of motion in addition to $\mathcal{H} = -\varepsilon\,c^2/2$.

The usual first try to find such a solution is with a separation ansatz,

$$S(t,\varphi,r,\vartheta) = S_t(t) + S_\varphi(\varphi) + S_r(r) + S_\vartheta(\vartheta)\,. \tag{339}$$

From classical mechanics we know that it is always possible to separate off a cyclic coordinate, i.e., a coordinate that does not occur in the Hamiltonian. Then the corresponding momentum is a constant of motion and the function S is linear in the cyclic coordinate, with the constant of motion as the pre-factor. As we know that t and φ are cyclic coordinates, with corresponding constants of motion $p_t = -E$ and $p_\varphi = L$, we specify the separation ansatz according to

$$S(t,\varphi,r,\vartheta) = -Et + L\varphi + S_r(r) + S_\vartheta(\vartheta)\,. \tag{340}$$

We have to plug this ansatz into the Hamilton-Jacobi equation. For that purpose we need the contravariant metric coefficients $g^{\mu\nu}$. The matrix of covariant components $g_{\mu\nu}$ of the Kerr metric is of the form

$$\big(g_{\mu\nu}\big) \;=\; \begin{pmatrix} g_{tt} & g_{t\varphi} & 0 & 0 \\ g_{t\varphi} & g_{\varphi\varphi} & 0 & 0 \\ 0 & 0 & g_{rr} & 0 \\ 0 & 0 & 0 & g_{\vartheta\vartheta} \end{pmatrix}\,. \tag{341}$$

With the determinant D from (326) we calculate the inverse matrix:

$$\big(g^{\mu\nu}\big) \;=\; \begin{pmatrix} D^{-1}g_{\varphi\varphi} & -D^{-1}g_{t\varphi} & 0 & 0 \\ -D^{-1}g_{t\varphi} & D^{-1}g_{tt} & 0 & 0 \\ 0 & 0 & g_{rr}^{-1} & 0 \\ 0 & 0 & 0 & g_{\vartheta\vartheta}^{-1} \end{pmatrix} = \begin{pmatrix} g^{tt} & g^{t\varphi} & 0 & 0 \\ g^{t\varphi} & g^{\varphi\varphi} & 0 & 0 \\ 0 & 0 & g^{rr} & 0 \\ 0 & 0 & 0 & g^{\vartheta\vartheta} \end{pmatrix} \tag{342}$$

So the Hamilton-Jacobi equation reads

$$g^{tt}E^2 - 2g^{t\varphi}EL + g^{\varphi\varphi}L^2 + g^{rr}S_r'(r)^2 + g^{\vartheta\vartheta}S_\vartheta'(\vartheta)^2 = -\varepsilon\, c^2\,,$$

$$\frac{g_{\varphi\varphi}E^2}{D} + \frac{2g_{t\varphi}EL}{D} + \frac{g_{tt}L^2}{D} + g_{rr}^{-1}S_r'(r)^2 + g_{\vartheta\vartheta}^{-1}S_\vartheta'(\vartheta)^2 = -\varepsilon\, c^2\,,$$

$$-\frac{\cancel{\sin^2\vartheta}\Big(r^2 + a^2 + \dfrac{2mra^2\sin^2\vartheta}{\rho^2}\Big)E^2}{c^2\Delta\cancel{\sin^2\vartheta}} + \frac{4mra\cancel{\sin^2\vartheta}\,\cancel{c}\,EL}{\rho^2\cancel{c}^2\Delta\cancel{\sin^2\vartheta}} + \frac{\cancel{c^2}\Big(1 - \dfrac{2mr}{\rho^2}\Big)L^2}{\cancel{c^2}\Delta\sin^2\vartheta}$$

$$+\frac{\Delta}{\rho^2}S_r'(r)^2 + \frac{1}{\rho^2}S_\vartheta'(\vartheta)^2 = -\varepsilon\, c^2\,,$$

$$\Big(-(r^2+a^2)(r^2+a^2-a^2\sin^2\vartheta) - 2mra^2\sin^2\vartheta\Big)\frac{E^2}{c^2\Delta} + \frac{4mraEL}{c\Delta}$$

$$+\big(r^2+a^2-a^2\sin^2\vartheta - 2mr\big)\frac{L^2}{\Delta\sin^2\vartheta} + \Delta S_r'(r)^2 + S_\vartheta'(\vartheta)^2 = -\varepsilon\, c^2\rho^2\,,$$

$$-(r^2+a^2)^2\frac{E^2}{c^2\Delta} + \frac{\cancel{\Delta}a^2\sin^2\vartheta E^2}{c^2\cancel{\Delta}} + \frac{4mraEL}{c\,\Delta} + \frac{\cancel{\Delta}L^2}{\cancel{\Delta}\sin^2\vartheta}$$

$$-\frac{a^2\cancel{\sin^2\vartheta}L^2}{\Delta\cancel{\sin^2\vartheta}} + \Delta S_r'(r)^2 + S_\vartheta'(\vartheta)^2 = -\varepsilon\, c^2(r^2 + a^2\cos^2\vartheta)\,,$$

$$-\frac{1}{\Delta}\Big((r^2+a^2)\frac{E}{c} - aL\Big)^2 - \cancel{\frac{2(r^2+a^2)aEL}{\Delta c}} + \Big(\frac{L}{\sin\vartheta} - \frac{a}{c}\sin\vartheta\, E\Big)^2$$

$$+\cancel{\frac{2a\sin\vartheta EL}{c\sin\vartheta}} + \cancel{\frac{4mraEL}{c\Delta}} + \Delta S_r'(r)^2 + S_\vartheta'(\vartheta)^2 \;=\; -\varepsilon r^2 - \varepsilon\, c^2a^2\cos^2\vartheta\,.$$

$$S_\vartheta'(\vartheta)^2 + \Big(\frac{L}{\sin\vartheta} - \frac{a}{c}\sin\vartheta\, E\Big)^2 + \varepsilon\, c^2a^2\cos^2\vartheta$$

$$= -\Delta S_r'(r)^2 + \frac{1}{\Delta}\Big((r^2+a^2)\frac{E}{c} - aL\Big)^2 - \varepsilon\, c^2r^2 \;=:\; K\,. \tag{343}$$

The first expression is independent of r whereas the second expression is independent of ϑ. This implies that K depends neither on r nor on ϑ, so it is a constant of motion. K is the Carter constant.

With $S'_\vartheta(\vartheta) = p_\vartheta$ and $S'_r(r) = p_r$ we have found that

$$p_\vartheta^2 = K - \Big(\frac{L}{\sin\vartheta} - \frac{a}{c}\sin\vartheta\, E\Big)^2 - \varepsilon\, c^2 a^2 \cos^2\vartheta\,, \tag{344}$$

$$\Delta p_r^2 = -K + \frac{1}{\Delta}\Big((r^2+a^2)\frac{E}{c} - aL\Big)^2 - \varepsilon\, c^2 r^2\,. \tag{345}$$

Now we have all four components of the equation of motion in first-order form: The equations (332) and (333) above give us $\dot t$ and $\dot\varphi$,

$$\rho^2\,\dot t = \frac{\Big((r^2+a^2)\rho^2 + 2mra^2\sin^2\vartheta\Big)E - 2mracL}{c^2\Delta}\,, \tag{346}$$

$$\rho^2\dot\varphi = \frac{-2mra\sin^2\vartheta\, E - c\big(\rho^2 - 2mr\big)L}{c\Delta\sin^2\vartheta}\,. \tag{347}$$

The two equations (344) and (345), with $p_\vartheta = g_{\vartheta\vartheta}\dot\vartheta = \rho^2\dot\vartheta$ and $p_r = g_{rr}\dot r = \rho^2\dot r/\Delta$, give us $\dot\vartheta$ and $\dot r$:

$$\rho^4\dot\vartheta^2 = K - \Big(\frac{L}{\sin\vartheta} - \frac{a}{c}\sin\vartheta\, E\Big)^2 - \varepsilon\, c^2 a^2\cos^2\vartheta\,, \tag{348}$$

$$\rho^4\dot r^2 = -K\Delta + \Big((r^2+a^2)\frac{E}{c} - aL\Big)^2 - \varepsilon\, c^2 r^2\Delta\,. \tag{349}$$

(346), (347), (348) and (349) determine the geodesics.

Note that the right-hand side of (348) depends only on ϑ while the right-hand side of (349) depends only on r. So the only coupling of the r motion to the ϑ motion is through the ρ^4 term on the left-hand side. One can completely decouple the two equations by introducing the *(Zakharov-)Mino parameter*, λ, which is related to the affine parameter s we have used for the parametrisation by

$$\frac{ds}{d\lambda} = \rho^2\,. \tag{350}$$

Then we have

$$\rho^2(\,\cdot\,)^{\cdot} = \frac{d}{d\lambda}(\,\cdot\,)\,. \tag{351}$$

If we write the left-hand sides of (346), (347) , (348) and (349) with the derivatives with respect to λ, the r motion is completely decoupled from the ϑ motion. For any choice of the constants of motion (which determine the initial velocities) and any choice of initial conditions $\vartheta(0)$ and $r(0)$ we can solve (348) and (349) to get $\vartheta(\lambda)$ and $r(\lambda)$. This can be done by separation of variables, resulting in elliptic integrals. Upon inserting these results into (346) and (347) we can determine $t(\lambda)$ and $\varphi(\lambda)$ by integrating these equations with initial conditions $t(0)$ and

$\varphi(0)$. Finally, we can express the result $\big(t(\lambda), \varphi(\lambda), \vartheta(\lambda), r(\lambda)\big)$ in terms of the affine parameter s (i.e., proper time in the case of timelike geodesics) instead of the (Zakharov-)Mino parameter λ if we like to do so. In this way we get all the geodesics in the Kerr spacetime. We will see in the following that, actually, for several special classes of geodesics the solution can be found without using the (Zakharov-)Mino parameter.

Of course, one is free to choose any four independent combinations of the constants of motion (ε, E, L, K) for characterising a geodesic. For some applications it is advantageous to use (ε, E, L, Q) where

$$Q = K - (L - aE/c)^2 \,. \tag{352}$$

The name "Carter constant" is frequently used for Q as well. K has a more direct interpretation than Q because in the case of a non-spinning black hole ($a = 0$) it reduces to $\big|\vec{L}\,\big|^2$ where – up to a dimensional factor – $\vec{L}$ is the angular momentum vector. (Keep in mind that, by abuse of notation, we use the letter L for the z component of $\vec{L}$, i.e., $L^2 = \big|\vec{L}\,\big|^2$ only for motion in the equatorial plane.)

We will now study some aspects of lightlike and timelike geodesics separately.

(a) Lightlike geodesics

We will now investigate the *spherical* lightlike geodesics which are crucial for constructing the shadow of a Kerr black hole. Recall that in the Schwarzschild case the boundary curve of the shadow was determined by lightlike geodesics that asymptotically spiral towards the photon sphere at $r = 3r_S/2 = 3m$. As the spherical symmetry is broken in the Kerr spacetime, we cannot expect that there still is a photon sphere. We will see that the photon sphere is replaced by a *photon region* which is filled with lightlike geodesics each of which stays on a sphere $r =$ constant. Such geodesics are called "spherical".

We specify the equations (348) and (349) to the case that we have a lightlike geodesic, i.e., $\varepsilon = 0$:

$$\rho^4 \dot{\vartheta}^2 = K - \Big(\frac{L}{\sin\vartheta} - \frac{a}{c}\sin\vartheta\, E\Big)^2 =: \Theta(\vartheta)\,, \tag{353}$$

$$\rho^4 \dot{r}^2 = -K\Delta + \Big((r^2+a^2)\frac{E}{c} - aL\Big)^2 =: R(r)\,. \tag{354}$$

Spherical lightlike geodesics have to satisfy $\dot{r} = 0$ and $\ddot{r} = 0$, so by (354) the two equations $R(r) = 0$ and $R'(r) = 0$ have to hold. This gives us the following two equations:

$$0 = -K\big(r^2 + a^2 - 2mr\big) + \Big((r^2+a^2)\frac{E}{c} - aL\Big)^2 , \tag{355}$$

$$0 = -K(\cancel{2}r - \cancel{2}m) + \cancel{2}\Big((r^2+a^2)\frac{E}{c} - aL\Big)\frac{2rE}{c}\,. \tag{356}$$

We multiply the first equation with $(r-m)$ and the second with $\Delta = r^2 + a^2 - 2mr$. Then the difference of the two equations yields

$$0 = \cancel{\Big((r^2+a^2)\frac{E}{c} - aL\Big)}\Big\{\Big((r^2+a^2)\frac{E}{c} - aL\Big)(r-m) - \frac{2rE}{c}\big(r^2+a^2-2mr\big)\Big\}\,,$$

$$aL\big(r-m\big) \;=\; \frac{E}{c}\Big(\big(r^2+a^2\big)\big(r-m\big) - 2r\Delta\Big)\,,$$
$$ac\frac{L}{E} \;=\; r^2+a^2 \;-\; \frac{2r\Delta}{r-m}\,. \tag{357}$$

To determine K, we insert (357) into (356) ,

$$0 = -K\big(r-m\big) + \Big(\big(r^2+a^2\big) - ac\frac{L}{E}\Big)\,\frac{2rE^2}{c^2}\,.$$
$$\frac{c^2K}{E^2}\big(r-m\big) \;=\; \Big(\cancel{r^2}+\cancel{a^2}-\cancel{r^2}-\cancel{a^2}+\frac{2\,r\,\Delta}{r-m}\Big)\,2\,r\,,$$
$$\frac{c^2K}{E^2} \;=\; \frac{4\,r^2\,\Delta}{(r-m)^2}\,. \tag{358}$$

(357) and (358) determine the constants of motion for spherical lightlike geodesics at radius coordinate r.

To find out at which r values spherical lightlike geodesics actually exist, we need to evaluate (353). As the left-hand side of this equation is the square of a real quantity, it cannot be negative, hence we must have $\Theta(\vartheta) \geq 0$:

$$K - \Big(\frac{L}{\sin\vartheta} - \frac{a}{c}\sin\vartheta\,E\Big)^2 \;\geq\; 0\,,$$
$$\frac{c^2K}{E^2} - \frac{\Big(\dfrac{acL}{E} - a^2\sin^2\vartheta\Big)^2}{a^2\sin^2\vartheta} \;\geq\; 0\,,$$
$$\frac{4\,r^2\,\Delta}{(r-m)^2} - \frac{\Big(r^2+a^2\;-\;\dfrac{2r\Delta}{r-m} - a^2\sin^2\vartheta\Big)^2}{a^2\sin^2\vartheta} \;\geq\; 0\,,$$
$$4\,r^2\,\Delta\,a^2\sin^2\vartheta \;-\; \big(r-m\big)^2\Big(\rho^2 \;-\; \frac{2r\Delta}{r-m}\Big)^2 \;\geq\; 0\,,$$
$$\Big(\rho^2\big(r-m\big) \;-\; 2r\Delta\Big)^2 \;\leq\; 4\,r^2\,\Delta\,a^2\sin^2\vartheta\,. \tag{359}$$

This inequality determines the photon region. For $a = 0$, the right-hand side vanishes, so the left-hand side must be equal to zero, $0 = r^2(r-m) - 2r(r^2-2mr) = 3r^2m - r^3$. In this case the photon region reduces to the photon sphere, $r = 3m = 3r_S/2$. In the case $a \neq 0$, however, it is not a 2-dimensional surface in space, but rather a 3-dimensional region with a boundary.

Through each point of the photon region there is a spherical lightlike geodesic. Along each of these geodesics, the ϑ coordinate oscillates between a maximal and a minimal value; the turning points of the ϑ motion occur on the boundary of the photon region where $\Theta(\vartheta) = 0$. The φ motion of a spherical lightlike geodesic may be quite complicated; in the ergoregion it may even be non-monotonous.

For $0 < a^2 < m^2$, the photon region consists of three connected components: An exterior photon region in the domain $r > r_+$ and two interior photon regions in the domain $r < r_-$ that are separated from each other by the ring singularity. In the exterior photon region all

spherical lightlike geodesics are unstable with respect to radial perturbations, as can be verified by calculating the sign of $R''(r)$. Therefore, these spherical lightlike geodesics can serve as limit curves for lightlike geodesics that approach them asymptotically. In the interior photon regions there are both stable and unstable spherical lightlike geodesics. For the formation of the shadow, only the exterior photon region is of relevance. The exterior photon region has a crescent-shaped cross section, which becomes bigger and bigger with increasing a. For $a \to 0$ it shrinks to the photon sphere at $r = 3m$ as already mentioned.

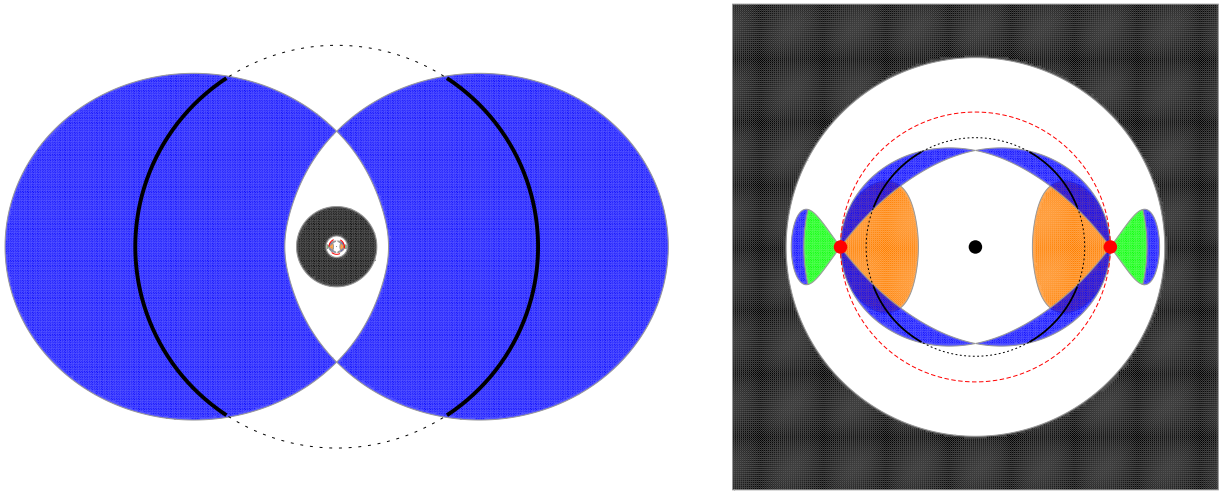

The picture on the left shows the photon regions for a Kerr black hole of $a = 0.75\,m$ in a diagram where $e^{r/m}$ is the radius coordinate, the picture on the right gives an enlarged view of the interior region. Unstable spherical lightlike geodesics exist in the blue region, stable ones in the green region. The domain between the two horizons is shown in black. The ring singularity is indicated by red blobs and the throats at $(r = 0, \cos\vartheta \neq 0)$ by red dashed half-circles. The causality violating region, where $g_{\varphi\varphi} < 0$, is marked in orange, cf. p. 88. In each of the two pictures a black line shows the projection of one particular spherical lightlike geodesic. In Worksheet 11 we will discuss the special case of *circular* lightlike geodesics. In a Kerr spacetime with $a \neq 0$, there are exactly five of them, three in the equatorial plane and two off the equatorial plane. In the domain of outer communication, $r > r_+$, there are two circular lightlike geodesics which are situated at the intersection of the boundary of the photon region with the equatorial plane; the outer one is counter-rotating and the inner one is co-rotating with the black hole.

To construct the shadow of a Kerr black hole, we fix an observer in the domain of outer communication, i.e., at Boyer-Lindquist coordinates (r_O, ϑ_O) with $r_O > r_+$. Clearly, the shape of the shadow at the observer's celestial sphere will depend on the observer's state of motion. We do the calculation for one particular observer; for any other observer that passes through the same event with a different 4-velocity the shadow is then determined by the aberration formula. In the Schwarzschild case, we have assumed that the observer is static, i.e., that his worldline is a t line. In the Kerr spacetime we will not choose an observer moving on a t line because this would exclude the ergoregion.

We find it more convenenient to choose instead an observer associated with the tetrad

$$e_0 \;=\; \frac{(r^2+a^2)\partial_t + ac\partial_\varphi}{c\,\rho\sqrt{\Delta}}\Big|_{(r_O,\vartheta_O)}\,, \qquad e_1 \;=\; \frac{\partial_\vartheta}{\rho}\Big|_{(r_O,\vartheta_O)}\,,$$

$$e_2 \;=\; \frac{-\,c\,\partial_\varphi - a\sin^2\vartheta\,\partial_t}{c\,\rho\sin\vartheta}\Big|_{(r_O,\vartheta_O)}\,, \qquad e_3 \;=\; \frac{-\,\sqrt{\Delta}\,\partial_r}{\rho}\Big|_{(r_O,\vartheta_O)}\,. \tag{360}$$

It is readily verified that this tetrad is pseudo-orthonormal, $g(e_\mu, e_\nu) = \eta_{\mu\nu}$. We interpret e_0 as the 4-velocity of our observer; then e_1, e_2 and e_3 form an orthonormal basis in the rest space of the observer.

Note that the observer's 4-velocity is chosen such that e_0 is in the plane spanned by the ingoing and outgoing principal null directions. This follows immediately from the representation of principal null geodesics given in (315).

For the construction of the shadow we have to consider past-oriented lightlike geodesics issuing from the position of the observer. If such a geodesic is given as a curve $\big(t(s), \varphi(s), \vartheta(s), r(s)\big)$ parametrised by an affine parameter s, its tangent vector k at the observation event is

$$k \;=\; \dot t\partial_t + \dot\varphi\partial_\varphi + \dot\vartheta\partial_\vartheta + \dot r\partial_r\,. \tag{361}$$

On the other hand, as k is lightlike and past-pointing, it can be written as

$$k = N\big(-\,e_0 + \cos\psi\sin\theta\,e_1 + \sin\psi\sin\theta\,e_2 + \cos\theta\,e_3\big) \tag{362}$$

with some positive factor N. This equation determines the celestial coordinates (ψ, θ) associated with the direction of the light ray. According to our choice of the tetrad, $\theta = 0$ corresponds to the direction towards the black hole.

We now calculate succesively $g(k, e_0)$, $g(k, e_1)$, $g(k, e_2)$ and $g(k, e_3)$ from (362) and insert (361). This results in the following four equations.

$$N \;=\; g(k,e_0) \;=\; g\Big(\dot t\partial_t + \dot\varphi\partial_\varphi, \frac{(r^2+a^2)\partial_t + ac\partial_\varphi}{c\,\rho\,\sqrt{\Delta}}\Big)$$

$$= \frac{(r^2+a^2)\big(\dot t\,g_{tt} + \dot\varphi\,g_{t\varphi}\big)}{c\,\rho\sqrt{\Delta}} + \frac{a\big(\dot t\,g_{t\varphi} + \dot\varphi\,g_{\varphi\varphi}\big)}{\rho\,\sqrt{\Delta}} \;=\; \frac{-(r^2+a^2)E}{c\,\rho\sqrt{\Delta}} + \frac{aL}{\rho\,\sqrt{\Delta}}\,, \tag{363}$$

$$N\cos\psi\sin\theta \;=\; g(k,e_1) \;=\; g\Big(\dot\vartheta\partial_\vartheta, \frac{\partial_\vartheta}{\rho}\Big) \;=\; \frac{\dot\vartheta\,g_{\vartheta\vartheta}}{\rho} \;=\; \dot\vartheta\,\rho\,, \tag{364}$$

$$N\sin\psi\sin\theta \;=\; g(k,e_2) \;=\; g\Big(\dot t\partial_t + \dot\varphi\partial_\varphi, \frac{-\,c\,\partial_\varphi - a\sin^2\vartheta\,\partial_t}{c\,\rho\sin\vartheta}\Big)$$

$$= -\,\frac{\dot t g_{t\varphi} + \dot\varphi g_{\varphi\varphi}}{\rho\sin\vartheta} - \frac{a\sin\vartheta\big(\dot t g_{tt} + \dot\varphi g_{t\varphi}\big)}{c\,\rho} \;=\; -\,\frac{L}{\rho\sin\vartheta} + \frac{a\sin\vartheta\,E}{c\,\rho}\,, \tag{365}$$

$$N\cos\theta \;=\; g(k,e_3) \;=\; -\,g\Big(\dot r\partial_r, \frac{\sqrt{\Delta}}{\rho}\,\partial_r\Big) \;=\; -\,\frac{\dot r\,\sqrt{\Delta}\,g_{rr}}{\rho} \;=\; -\,\frac{\dot r\,\rho}{\sqrt{\Delta}}\,. \tag{366}$$

Here all metric functions have to be evaluated at the position of the observer. (364) and (365) imply

$$\frac{\sin\psi}{\cos\psi} \;=\; \frac{-\,\dfrac{L}{\rho\sin\vartheta} \;+\; \dfrac{a\sin\vartheta\,E}{c\,\rho}}{\dot\vartheta\,\rho}\,,$$

$$\rho^4\,\dot\vartheta^2\,\frac{\sin^2\psi}{\cos^2\psi} \;=\; \Big(\frac{L}{\sin\vartheta} - \frac{a\sin\vartheta\,E}{c}\Big)^2\,,$$

$$\rho^4\,\dot\vartheta^2\sin^2\psi \;=\; \Big(\frac{L}{\sin\vartheta} - \frac{a\sin\vartheta\,E}{c}\Big)^2\big(1-\sin^2\psi\big)\,,$$

$$\Big\{\rho^4\,\dot\vartheta^2 \;+\; \Big(\frac{L}{\sin\vartheta} - \frac{a\sin\vartheta\,E}{c}\Big)^2\Big\}\sin^2\psi \;=\; \Big(\frac{L}{\sin\vartheta} - \frac{a\sin\vartheta\,E}{c}\Big)^2\,, \tag{367}$$

and with (353)

$$K\sin^2\psi \;=\; \frac{E^2}{c^2\,a^2\sin^2\vartheta}\Big(\frac{caL}{E} - \,a^2\sin^2\vartheta\Big)^2\,,$$

$$\sin^2\psi \;=\; \left.\frac{\Big(\dfrac{caL}{E} - \,a^2\sin^2\vartheta\Big)^2}{\dfrac{c^2\,K}{E^2}\,a^2\sin^2\vartheta}\right|_{\vartheta=\vartheta_O} \tag{368}$$

where in the last line we have made explicit that the metric functions have to be evaluated at the position of the observer.

Similarly, (363) and (366) imply

$$\cos\theta \;=\; \frac{\dfrac{-\,\dot r\,\rho}{\sqrt{\Delta}}}{\dfrac{-(r^2+a^2)E}{c\,\rho\sqrt{\Delta}} \;+\; \dfrac{aL}{\rho\,\sqrt{\Delta}}} \;=\; \frac{\dot r\,\rho^2}{\dfrac{(r^2+a^2)E}{c} \;-\; aL}\,,$$

$$\big(1 \;-\; \sin^2\theta\big)\Big(\frac{(r^2+a^2)E}{c} \;-\; aL\Big)^2 \;=\; \rho^4\dot r^2\,,$$

$$-\rho^4\dot r^2 + \Big(\frac{(r^2+a^2)E}{c} \;-\; aL\Big)^2 \;=\; \Big(\frac{(r^2+a^2)E}{c} \;-\; aL\Big)^2\sin^2\theta\,. \tag{369}$$

With (354) this results in

$$\Delta\,K \;=\; \frac{E^2}{c^2}\Big(r^2+a^2 \;-\; \frac{caL}{E}\Big)^2\sin^2\theta\,,$$

$$\sin^2\theta \;=\; \left.\frac{\Delta\,\dfrac{c^2K}{E^2}}{\Big(r^2+a^2 \;-\; \dfrac{caL}{E}\Big)^2}\right|_{r=r_O} \tag{370}$$

where, again, in the last line we have made explicit that the metric funtions have to be evaluated at the position of the observer. (368) and (370) determine for each lightlike geodesic with known constants of motion L/E and K/E^2 the celestial coordinates (ψ,θ).

Now recall from our discussion of the Schwarzschild metric how the shadow of a black hole is defined: We assume that there are light sources distributed everywhere but not between the black hole and the observer. We divide into two classes the light rays issuing from the observer into the past: The geodesics in one class go out to infinity after being deflected by the black hole, so they can reach a light source. The geodesics of the other class go towards the horizon, so they do not reach one of the light sources. In the Schwarzschild case, the borderline between the two classes corresponded to light rays that spiraled towards the photon sphere at $r = 3r_S/2 = 3m$. In the Kerr case, the circular orbits at the photon sphere are replaced by the spherical orbits in the photon region. In other words, for determining the boundary curve of the shadow we have to determine those lightlike geodesics that asymptotically approach a spherical lightlike geodesic.

If two geodesics become asymptotically tangent to each other, they must have the same constants of motion. This follows from the fact that the constants of motion are determined by the tangent of the geodesic at any one point. So the lightlike geodesics that correspond to the boundary curve of the shadow must have the constants of motion given by (357) and (358), where r ranges over the radius values allowed by the inequality (359) for the photon region. Having determined the constants of motion as a function of the parameter r in this way, we plug the corresponding expressions into the right-hand sides of (368) and (370). This gives us the boundary of the shadow as a curve parametrised by r on the celestial sphere of the observer, $\big(\psi(r), \theta(r)\big)$. This is a fully analytic representation of the boundary curve. For each choice of a with $0 < a^2 \leq m^2$ and of the observer position (r_O, ϑ_O) the result can be easily plotted, where we have to represent the celestial sphere of the observer in an appropriate way. It is convenient to use stereographic projection with the direction towards the black hole, $\theta = 0$, as the origin.

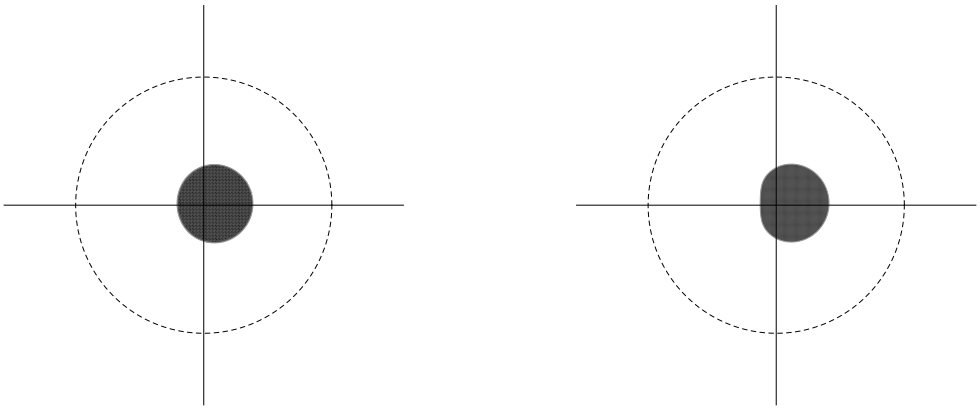

The two images show the shadow for an observer at $(r_O = 6m, \vartheta_O = \pi/2)$ in stereographic projection. The dashed line marks the celestial equator $\theta = \pi/2$. On the left, the spin is chosen to be $a = 0.7\,m$; in this case, the deviation of the shadow from a circular shape is not easily visible to the naked eye. (Note that an observer wouldn't see in the sky the cross-hairs that indicate the direction towards the black hole!) On the right, the black hole is extreme, $a = m$. In this case the deviation from the circular shape is conspicuous. The asymmetry is easily understood from the fact that a rotating black hole "drags" the light rays. As we have chosen positive a values, the spin vector is pointing up in the pictures. In the case that the spin vector points down the shadow is flattened on the right.

The pictures below show the shadow of an extreme black hole, $a = m$, as seen by observers at $r_O = 5m$ and different inclination angles. For $\vartheta_O = \pi/2$ (observer in the equatorial plane), the asymmetry is obvious; for $\vartheta_O = 0$, or $\vartheta_O = \pi$, (observer on the axis) the shadow is again circular, which is clear from the rotational symmetry about the axis. So if we look approximately from the top or from the bottom onto a black hole, the shadow doesn't tell us whether or not the black hole is spinning. This seems to be the case for the shadow of M87*, and, surprisingly, also for the shadow of Sgr A^*, recall p. 42.

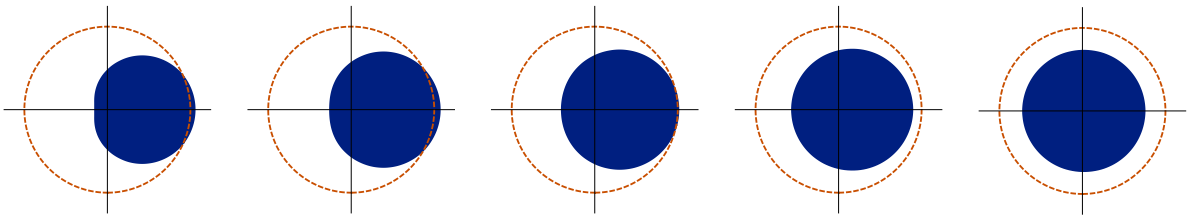

$\vartheta_O = \pi/2$ $\vartheta_O = 3\pi/8$ $\vartheta_O = \pi/4$ $\vartheta_O = \pi/8$ $\vartheta_O = 0$

From (368) and (370) we read that (ψ, θ) is on the boundary curve of the shadow if and only if $(\pi - \psi, \theta)$ is on the boundary curve of the shadow. This implies that the shadow is always symmetrical with respect to a horizontal axis, even for an observer off the equatorial plane, $\vartheta_O \neq \pi/2$. This is a remarkable result which was not to be expected from the symmetry of the spacetime.

From the analytical formula for the boundary curve of the shadow one finds an expression for the *vertical* angular radius, θ_v, of the shadow. We give it here only for the case that the observer is in the equatorial plane, $\vartheta_O = \pi/2$:

$$\sin^2\theta_v = \frac{27m^2r_O^2\big(a^2 + r_O(r_O - 2m)\big)}{r_O^6 + 6a^2r_O^4 + 3a^2(4a^2 - 9m^2)r_O^2 + 8a^6} = \frac{27m^2}{r_O^2}\Big(1 + O(m/r_O)\Big) \tag{371}$$

We see that, up to terms of order $O(m/r_O)$, Synge's formula (151) is still correct for the vertical radius of the shadow. So, if interpreted appropriately, our numerical estimates for the shadows of the black holes at the centres of our Galaxy and of M87 are valid for rotating black holes as well, see p. 38. The surprisingly simple formula (371) was found only recently. It was given by Arne Grenzebach in his PhD Thesis, see A. Grenzebach [The Shadow of Black Holes, Springer Briefs in Physics (2016)].

(b) Timelike geodesics

We concentrate on two aspects of timelike geodesics. Firstly we investigate circular timelike orbits in the equatorial plane. Secondly, we discuss some general features of the ϑ motion.

We consider a Kerr black hole with $0 < a^2 < m^2$, viewing $a = 0$ and $a^2 = m^2$ as limiting cases. We want to determine the circular timelike geodesics in the domain of outer communication, $r > r_+$. We start out from equations (348) and (349). For timelike geodesics ($\varepsilon = 1$) in the equatorial plane ($\vartheta = \pi/2$, $\dot\vartheta = 0$) these equations simplify to

$$0 = K - \Big(L - \frac{aE}{c}\Big)^2\,, \tag{372}$$

$$\rho^4\dot r^2 = -K\,\Delta + \Big(\big(r^2 + a^2\big)\frac{E}{c} - aL\Big)^2 - c^2r^2\Delta\,. \tag{373}$$

Inserting (372) into (373) yields

$$\rho^4\dot{r}^2 = -\Big(L - \frac{aE}{c}\Big)^2\,\Delta + \Big(\big(r^2+a^2\big)\frac{E}{c} - aL\Big)^2 - c^2r^2\Delta =: -2V_{E,L}(r)\,. \tag{374}$$

Circular orbits have to satisfy $\dot{r} = 0$ and $\ddot{r} = 0$, hence $V_{E,L}(r) = 0$ and $V'_{E,L}(r) = 0$. This system of two equations can be solved for the constants of motion E and L. The calculation is elementary, but rather tedious, so that we prefer letting MATHEMATICA do it for us. The result is

$$\frac{cL}{E} = \frac{\pm\sqrt{mr^3}\,(r^2+a^2-2mr) - a^3m - amr(3r-4m)}{r(r-2m)^2 - a^2m}\,, \tag{375}$$

$$\frac{E^2}{c^4} = \frac{r^3(r-3m)(r-2m)^2 - a^2mr^2(3r-5m) \pm 2am\sqrt{mr^3}\,(r^2+a^2-2mr)}{\big(r(r-2m)^2 - a^2m\big)^2}\,, \tag{376}$$

where the upper sign holds for co-rotating and the lower sign for counter-rotating geodesics.

As we consider the domain of outer communication where r is positive, $\sqrt{mr^3}$ is real. Therefore, the only restriction on the r values comes from the condition that $E^2/c^4 \geq 0$. This condition is plotted on the right. Counter-rotating circular timelike geodesics exist at radius values above the solid line, co-rotating ones above the dashed line. The limiting values are the radii of lightlike circular orbits in the equatorial plane, see Worksheet 11. In the Schwarzschild limit, circular timelike geodesics exist for $r > 3m$, as we already know. For the extreme Kerr black hole, $a^2 = m^2$, counter-rotating circular timelike geodesics exist for $r > 4m$ while co-rotating ones exist for $r > m$. As in the extreme case $r_+ = m$, this means that in this limiting case the co-rorating orbits cover the entire range of r values up to the horizon.

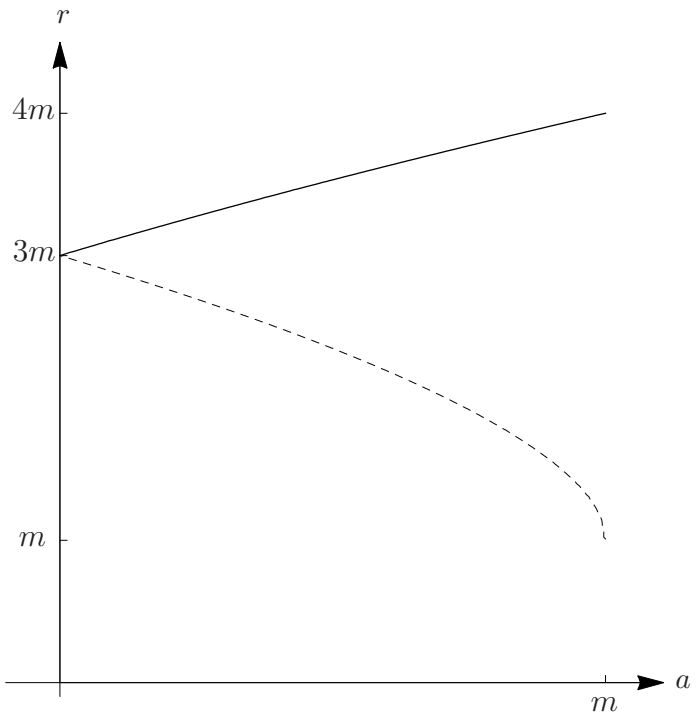

We are now going to investigate for which radius values the timelike circular geodesics are stable. The condition for stability is

$$V''_{E,L}(r) > 0 \tag{377}$$

where we have to insert for E and L the values for circular geodesics. This condition is plotted on the next page.

Counter-rotating orbits are stable at r values above the solid line, while co-rotating ones are stabe above the dashed line. In the Schwarzschild limit, the innermost stable circular orbit (ISCO) is at $r = 6m$, as we know. The counter-rotating ISCO is at a bigger radius, with a maximum at $r = 9m$ for the extreme case. The co-rotating ISCO is at a smaller value than in the Schwarzschild case and approaches $r = m$, i.e., the radius coordinate of the horizon, in the extreme case. This gives rise to the fact that objects on a co-rotating stable orbit around a Kerr black hole can suffer much stroger gravitational time dilation effects than on a stable orbit around a Schwarzschild black hole.

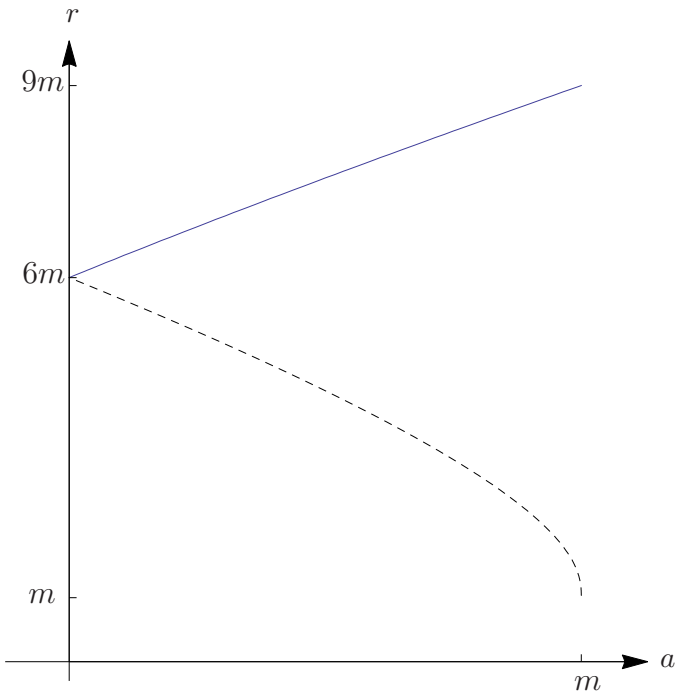

Actually, the limit $a^2 \to m^2$ is rather subtle. The Boyer-Lindquist coordinates show a particularly pathological behaviour near the (degenerate) horizon in this case. The fact that the co-rotating ISCO approaches the same value of the r coordinate as the horizon does not mean that the two things coincide in the limit. In contrast to what the Boyer-Lindquist coordinates suggest, there is still a finite distance between them. In the extreme Kerr spacetime, the distance (as measured with the metric along an r line) of the horizon from *any* point in the domain of outer communication is actually infinite, as we will see in Worksheet 11.

We now turn to a discussion of some general features of the ϑ motion of timelike geodesics. We use the Mino parameter λ for the parametrisation, recall (350).

Then, according to equation (348), the ϑ motion of timelike ($\varepsilon = 1$) geodesics satisfies

$$\left(\frac{d\vartheta}{d\lambda}\right)^2 = K - \left(\frac{L}{\sin\vartheta} - \frac{a\,E}{c}\sin\vartheta\right)^2 - c^2a^2\cos^2\vartheta\,. \tag{378}$$

For the following it will be convenient to use the constant of motion

$$Q = K - \left(L - \frac{a\,E}{c}\right)^2 \tag{379}$$

instead of K. It was already mentioned that the name "Carter constant" is used both for K and for Q. In terms of Q, (378) reads

$$\left(\frac{d\vartheta}{d\lambda}\right)^2 = Q + \left(L - \frac{a\,E}{c}\right)^2 - \left(\frac{L}{\sin\vartheta} - \frac{a\,E}{c}\sin\vartheta\right)^2 - c^2a^2\cos^2\vartheta$$

$$= Q + L^2 - \cancel{2\,L\frac{a\,E}{c}} + \frac{a^2E^2}{c^2} - \frac{L^2}{\sin^2\vartheta} + \cancel{2\,L\frac{a\,E}{c}} - \frac{a^2E^2}{c^2}\sin^2\vartheta - c^2a^2\cos^2\vartheta$$

$$= Q - \frac{L^2\big(1-\sin^2\vartheta\big)}{\sin^2\vartheta} + \frac{a^2E^2}{c^2}\big(1-\sin^2\vartheta\big) - c^2a^2\cos^2\vartheta$$

$$= Q - \frac{L^2\cos^2}{\sin^2\vartheta} + \Big(\frac{a^2E^2}{c^2} - c^2a^2\Big)\cos^2\vartheta\,. \tag{380}$$

For analysing the possible ϑ motions, we write

$$u := \cos^2\vartheta\,, \qquad \frac{du}{d\lambda} = -2\cos\vartheta\sin\vartheta\,\frac{d\vartheta}{d\lambda}\,. \tag{381}$$

Then

$$\Big(\frac{du}{d\lambda}\Big)^2 = 4\cos^2\vartheta\sin^2\vartheta\,\Big(\frac{d\vartheta}{d\lambda}\Big)^2$$

$$= 4\cos^2\vartheta\sin^2\vartheta\,\Big\{Q - \frac{L^2\cos^2}{\sin^2\vartheta} + \Big(\frac{a^2E^2}{c^2} - c^2a^2\Big)\cos^2\vartheta\Big\}$$

$$= 4\,u\,\big(1-u\big)\,\Big\{Q - \frac{L^2}{1-u} + \Big(\frac{a^2E^2}{c^2} - c^2a^2\Big)\,u.\Big\}$$

$$= 4\,u\,\Big\{Q\big(1-u\big) - L^2u + \Big(\frac{a^2E^2}{c^2} - c^2a^2\Big)\,u\,\big(1-u\big)\Big\}\,.$$

With the abbreviation

$$T(u) := Q\big(1-u\big) - L^2u + \Big(\frac{a^2E^2}{c^2} - c^2a^2\Big)\,u\,\big(1-u\big) \tag{382}$$

this allows us to write

$$\sin^2\vartheta\,\Big(\frac{d\vartheta}{d\lambda}\Big)^2 = \frac{1}{4\cos^2\vartheta}\,\Big(\frac{du}{d\lambda}\Big)^2 = T(u)\,. \tag{383}$$

This last equation tells us that all values of $u = \cos^2\vartheta$ where $T(u) < 0$ are forbidden whereas values where $T(u) \geq 0$ are allowed. Turning points ($d\vartheta/d\lambda = 0$) occur at those values of $u = \cos^2\vartheta$ where $T(u) = 0$ and where we are not on the axis, $u \neq 1$. As $u = \cos^2\vartheta$, the function $T(u)$ is defined on the interval $0 \leq u \leq 1$. For $a \neq 0$, it is a second-order polynomial, depending on the constants of motion Q, L and E. The graph of $T(u)$ is a parabola, connecting the end points $T(0) = Q$ and $T(1) = -L^2$.

On the basis of these observations, we can now analyse the possible ϑ motions. We distinguish the cases $Q > 0$, $Q = 0$ and $Q < 0$.

Case A: $Q > 0$:

In the picture on the next page we have fixed a value $Q > 0$ and a value $L \neq 0$ which still allows to vary E. We have plotted the function $T(u)$ for a value of E such that $a^2E^2/c^2 - c^2a^2 < -Q - L^2$ (dotted) and for a value of E such that $a^2E^2/c^2 - c^2a^2 > -Q - L^2$ (dashed). In any case, only an interval $0 \leq u \leq u_0 = \cos^2\vartheta_0$ with $0 < \vartheta_0 < \pi/2$ is allowed. The motion oscillates about the equatorial plane ($u = 0$), with turning points at $\pi - \vartheta_0$ and ϑ_0.

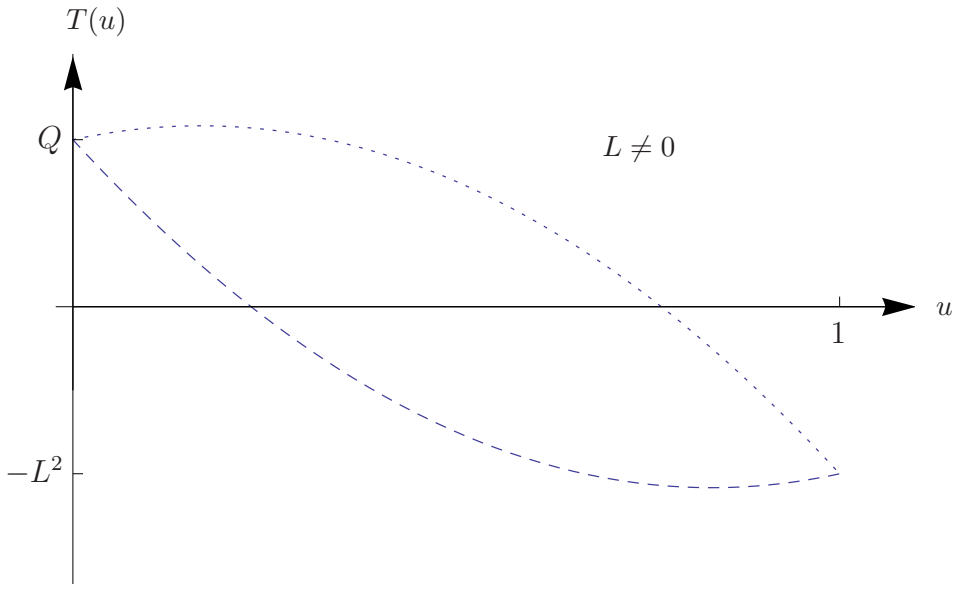

An oscillatory behaviour of the ϑ motion between a value ϑ_0 and a value $\pi - \vartheta_0$ is what we know from bound orbits in the Schwarzschild spacetime (or from the Kepler ellipses in Newtonian theory, for that matter).

The case $L = 0$ is special insofar as now the zero of the function $T(u)$ is at $u = 1$, i.e., on the axis, see the picture below. If $a^2E^2/c^2 - c^2a^2 < -Q$ (dotted), the entire interval $0 \leq u \leq 1$ is allowed. There are no turning points, the motion goes through the axis. If $a^2E^2/c^2 - c^2a^2 > -Q$ (dashed), only an interval $0 \leq u \leq u_0 = \cos^2\vartheta_0$ with $0 < \vartheta_0 < \pi/2$ is allowed. The motion oscillates about the equatorial plane, with turning points at $\pi - \vartheta_0$ and ϑ_0. In the borderline case $a^2E^2/c^2 - c^2a^2 = -Q$ (solid) the motion asymptotically approaches the axis in the future and in the past.

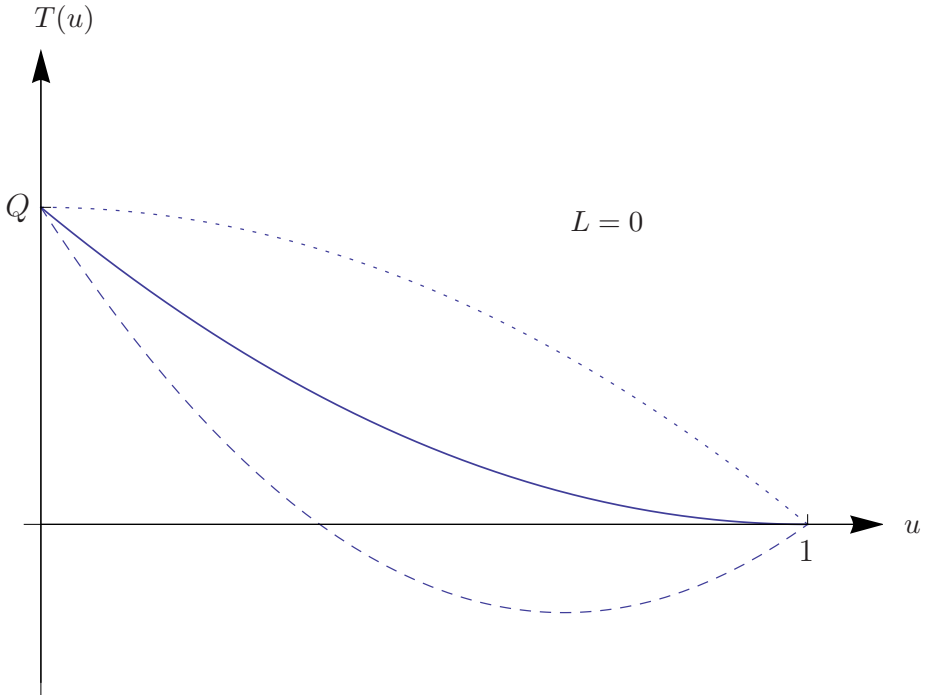

Case B: $Q = 0$

Also in this case we first fix a value $L \neq 0$. If $a^2E^2/c^2 - c^2a^2 > L^2$ (dotted), an interval $0 \leq u \leq u_0 = \cos^2\vartheta_0$ is allowed. As $T(u) \to 0$ for $u \to 0$, the equatorial plane is asymptotically approached. If $a^2E^2/c^2 - c^2a^2 < L^2$ (dashed), the motion is confined to the equatorial plane. The same is true in the borderline case $a^2E^2/c^2 - c^2a^2 = L^2$ (solid).

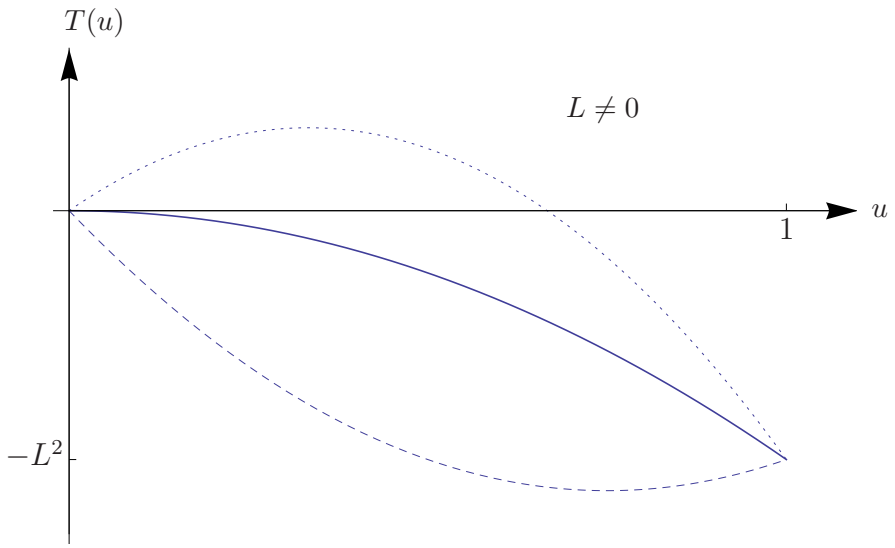

Again, the case $L = 0$ is special. If $a^2E^2/c^2 - c^2a^2 > 0$ (dotted), the entire interval $0 \leq u \leq 1$ is allowed. There are no turning points. The motion goes through the axis. As $T(u) \to 0$ for $u \to 0$, the equatorial plane is asymptotically approached. If $a^2E^2/c^2 - c^2a^2 < 0$ (dashed), the motion must be confined to the equatorial plane or to the axis. In the borderline case $a^2E^2/c^2 - c^2a^2 = 0$ (solid) the motion is confined to a cone $\vartheta =$ constant. Again, this includes as special cases motion in the equatorial plane and in the axis.

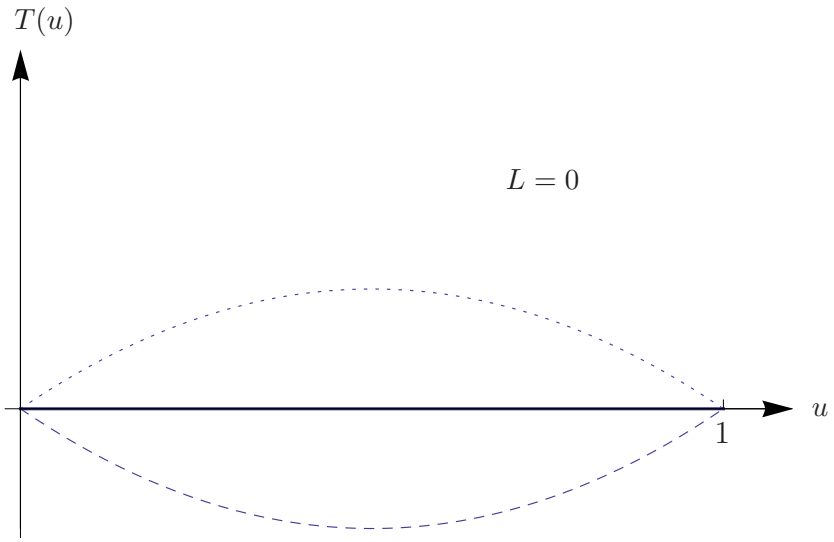

Note that motion in the equatorial plane *must* have $Q = 0$.

Case C: $Q < 0$

If $a^2E^2/c^2 - c^2a^2 < -Q - L^2$ (dotted), an interval $u_1 = \cos^2\vartheta_1 \le u \le u_2 = \cos^2\vartheta_2$ with $0 < \vartheta_2 < \vartheta_1 < \pi/2$ is allowed. The motion stays either in the northern hemisphere, oscillating between ϑ_1 and ϑ_2, or in the southern hemisphere, oscillating between $\pi - \vartheta_1$ and $\pi - \vartheta_2$. If $a^2E^2/c^2 - c^2a^2 > -Q - L^2$ (dashed), no motion is allowed. In the borderline case $a^2E^2/c^2 - c^2a^2 = -Q - L^2$ (solid), the motion stays on a cone.

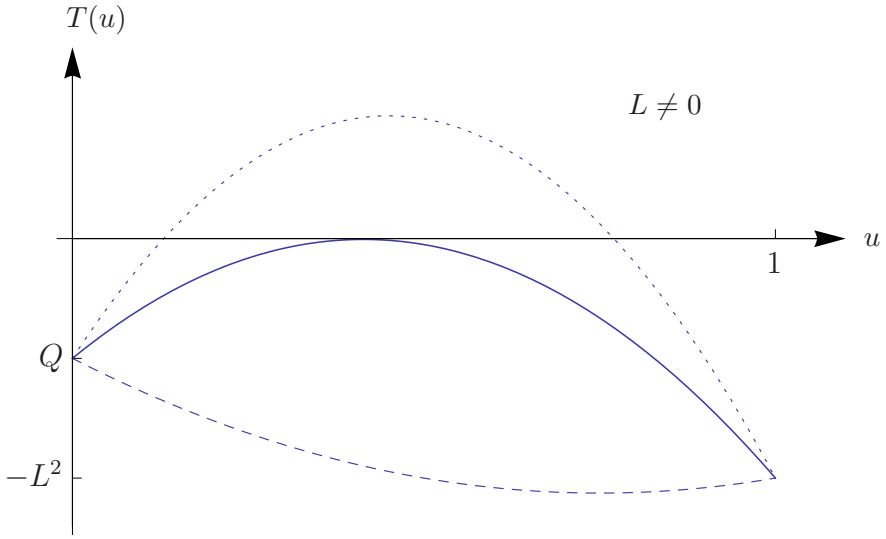

Orbits oscillating between two cones, or staying on a cone, are called *vortical*. They do not occur in the Schwarzschild spacetime except for the case of radial geodesics that stay, indeed, on a cone.

The special case $L = 0$ is plotted below. If $a^2E^2/c^2 - c^2a^2 < -Q$ (dotted), an interval $u_0 = \cos^2\vartheta_0 \le u \le 1$ with $0 < \vartheta_0 < \pi/2$ is allowed. The motion goes through the axis. It stays either in the northern hemisphere, with turning points at ϑ_0, or in the southern hemisphere, with turning points at $\pi - \vartheta_0$. If $a^2E^2/c^2 - c^2a^2 > -Q$ (dashed) or $a^2E^2/c^2 - c^2a^2 = -Q$ (solid), the motion is confined to the axis.

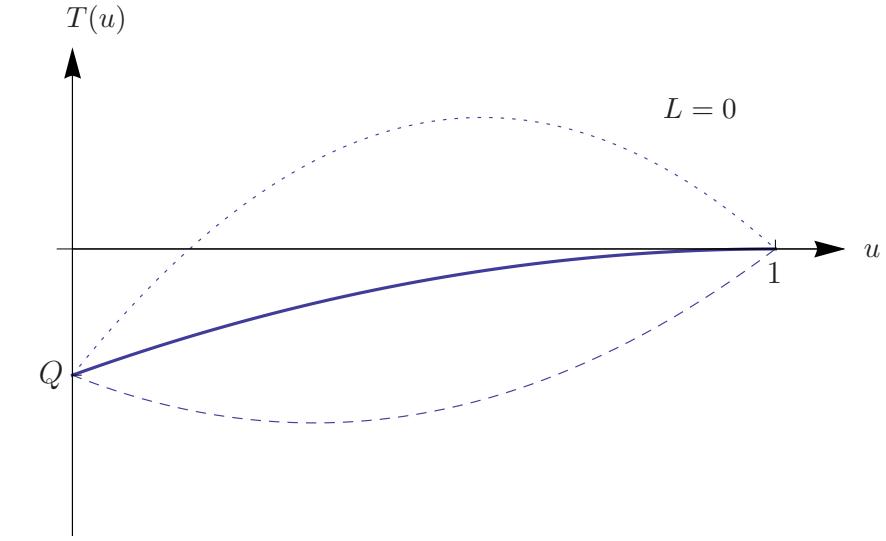

6.3 Ergoregion and Penrose process

For an observer in the domain of outer communication (i.e., outside of the outer horizon) of a Kerr black hole, the most important new feature in comparison to a Schwarzschild black hole is the presence of the ergoregion. In particular, this gives rise to the possibility of extracting energy from the black hole via the socalled Penrose process. We will now discuss this possibility in some detail.

We consider a Kerr black hole with $0 < a \leq m$. (The restriction to positive values of a is no loss of generality because we are free to transform the azimuthal coordinate, $\varphi \mapsto -\varphi$.) In this section we consider only the domain of outer communication which we denote, as before, as region I, i.e.

$$I \,:\, r > r_+ = m + \sqrt{m^2 - a^2}\,. \tag{384}$$

The ergoregion is that part of region I where the Killing vector field ∂_t is spacelike. We decompose the region I into the part outside the ergoregion,

$$I_a \,:\, r > r_+ \text{ and } g_{tt} = -c^2\Big(1 - \frac{2mr}{\rho^2}\Big) < 0\,, \tag{385}$$

and the ergoregion

$$I_b \,:\, r > r_+ \text{ and } g_{tt} = -c^2\Big(1 - \frac{2mr}{\rho^2}\Big) > 0\,. \tag{386}$$

The interface between I_a and I_b, where $g_{tt} = 0$, is the stationarity limit surface. In the picture on p. 87 the ergoregion I_b is the dark shaded region.

We have aleady mentioned that inside the ergoregion the hypersurfaces $\varphi =$ constant are spacelike, i.e., the worldline of an observer or a light signal cannot be tangent to such a hypersurface. This is another effect of the "dragging" by a rotating black hole: Every observer that is close to the black hole (inside the ergoregion) must have a velocity with a non-vanishing φ component, i.e., the observer is forced to rotate about the black hole whatever propulsion might be used. As a preparation for discussing the Penrose process, we want to quantify the allowed angular velocities for observers. To that end, we consider an observer on a φ line (i.e., on a circle about the axis of the black hole) with constant angular velocity Ω. Such an observer is, of course, not in general freely falling, i.e., he needs a rocket engine or some other kind of propulsion. The 4-velocity is

$$U \;=\; \frac{c\,\big(\partial_t + \Omega\,\partial_\varphi\big)}{\sqrt{-\big(g_{tt} + 2g_{t\varphi}\Omega + g_{\varphi\varphi}\Omega^2\big)}}\,. \tag{387}$$

We want to determine the allowed values for the constant angular velocity Ω, depending on the r and ϑ coordinate where the observer is circling. These allowed values are determined by the condition of $\partial_t + \Omega\partial_\varphi$ being timelike, $g_{tt} + 2g_{t\varphi}\Omega + g_{\varphi\varphi}\Omega^2 \,<\, 0$. This is true for $\Omega_- < \Omega < \Omega_+$ where $\Omega_\pm$ are the solutions of the quadratic equation

$$\frac{g_{tt}}{g_{\varphi\varphi}} + 2\frac{g_{t\varphi}}{g_{\varphi\varphi}}\Omega + \Omega^2 \;=\; 0\,, \tag{388}$$

hence

$$\Omega_\pm \;=\; \frac{-\,g_{t\varphi} \pm \sqrt{g_{t\varphi}^2 - g_{tt}g_{\varphi\varphi}}}{g_{\varphi\varphi}}\,. \tag{389}$$

We will now determine the signs of Ω_- and Ω_+. First of all, observe that

$$g_{\varphi\varphi} = \sin^2\vartheta\Big(r^2 + a^2 + \frac{2mra^2\sin^2\vartheta}{\rho^2}\Big) > 0 \tag{390}$$

everywhere in region I except on the axis which is to be excluded because there our circular orbit degenerates into a point. Also, as we have chosen $a > 0$,

$$g_{t\varphi} \;=\; -\,\frac{2mrac}{\rho^2}\sin^2\vartheta < 0 \tag{391}$$

everywhere in region I except on the axis.

In region I_a (i.e., outside the ergoregion) we have $g_{tt} < 0$ and thus $\sqrt{g_{t\varphi}^2 - g_{tt}g_{\varphi\varphi}} > -g_{t\varphi}$. This implies that in this region $\Omega_- < 0$ and $\Omega_+ > 0$, i.e., there is allowed motion in the positive and in the negative φ direction, as we are used to.

By contrast, in the ergoregion I_b we have $g_{tt} > 0$ and thus $\sqrt{g_{t\varphi}^2 - g_{tt}g_{\varphi\varphi}} < -g_{t\varphi}$. This implies that in this region both Ω_- and Ω_+ are positive, i.e., only motion in the positive φ direction is allowed.

We will now demonstrate that the values Ω_- and Ω_+ tend to the same limit Ω_H if the horizon is approached. To that end, we recall that we have calculated already in (326) that

$$g_{t\varphi}^2 - g_{tt}g_{\varphi\varphi} \;=\; c^2\Delta\sin^2\vartheta\,. \tag{392}$$

This allows to rewrite $\Omega_\pm$ as

$$\Omega_\pm \;=\; \frac{\dfrac{2\,cmra\sin^2\vartheta}{\rho^2} \pm c\sqrt{\Delta}\sin\vartheta\,.}{\sin^2\vartheta\Big(r^2 + a^2 + \dfrac{2mra^2\sin^2\vartheta}{\rho^2}\Big)} \tag{393}$$

If the horizon is approached, $r \to r_+$, we have $\Delta \to 0$ and thus

$$\begin{aligned}\lim_{r\to r_+}\Omega_\pm \;&=\; \frac{2\,cmr_+a\,\cancel{\sin^2\vartheta}}{\cancel{\sin^2\vartheta}\,\Big(\big(r_+^2 + a^2\big)\big(r_+^2 + a^2\cos^2\vartheta\big) + 2mr_+a^2\sin^2\vartheta\Big)} \\ &=\; \frac{2\,cmr_+a}{2mr_+\big(r_+^2 + a^2\cos^2\vartheta\big) + 2mr_+a^2\sin^2\vartheta} \;=\; \frac{c\,a}{r_+^2 + a^2} \;=:\; \Omega_H\,.\end{aligned} \tag{394}$$

Ω_H is known as the "angular velocity of the horizon". Note that Ω_H is independent of ϑ which may be interpreted as saying that the horizon rotates rigidly. The vector field $\partial_t + \Omega_H\partial_\varphi$ is timelike and non-geodesic everywhere inside the ergoregion. On the horizon $r = r_+$ it becomes tangent to the outgoing principal null geodesics, as can be verified by comparison with (315), so it becomes lightlike and geodesic.

After these preparations we will now consider the motion of freely falling particles (i.e., of timelike geodesics) in the region I. Recall that, for a timelike geodesic $\gamma(\tau) = \big(t(\tau), \varphi(\tau), \vartheta(\tau), r(\tau)\big)$ with tangent vector $\dot\gamma = \dot t\partial_t + \dot\varphi\partial_\varphi + \dot\vartheta\partial_\vartheta + \dot r\partial_r$ we have two constants of motion:

The energy E and the z component L of the angular momentum,

$$E = -\frac{\partial \mathcal{L}}{\partial \dot{t}} = -g_{tt}\dot{t} - g_{t\varphi}\dot{\varphi} = -g\big(\dot{\gamma}, \partial_t\big)\,, \tag{395}$$

$$L = \frac{\partial \mathcal{L}}{\partial \dot{\varphi}} = g_{\varphi\varphi}\dot{\varphi} + g_{\varphi t}\dot{t} = g\big(\dot{\gamma}, \partial_\varphi\big)\,. \tag{396}$$

$\dot{\gamma}$ must be timelike and future-pointing everywhere. Outside of the ergoregion, ∂_t is also timelike and future-pointing, hence

$$E = -g\big(\dot{\gamma}, \partial_t\big) > 0\,. \tag{397}$$

Inside the ergoregion, however, ∂_t is spacelike. Then the scalar product $g(\dot{\gamma}, \partial_t)$ may be positive, negative or zero, i.e., inside the ergoregion there exist freely falling particles with negative energies. Of course, as E is a constant of motion, such a particle cannot move into the region I_a; it can leave the region I_b only over the horizon at r_+.

As $\partial_t + \Omega_H \partial_\varphi$ is timelike and future-pointing inside the ergoregion, we have

$$0 > g\big(\partial_t + \Omega_H \partial_\varphi, \dot{\gamma}\big) = -E + \Omega_H L\,. \tag{398}$$

As $\Omega_H > 0$, this implies

$$L < \frac{E}{\Omega_H} \tag{399}$$

which demonstrates that particles with negative E must also have negative L.

We are now ready for a discussion of the Penrose process. Assume that a freely falling particle is released outside the ergoregion. This particle must have an energy $E > 0$. Let this particle enter the ergoregion and decay into two particles there, one with an energy $E_1 > 0$ and another one with an energy $E_2 < 0$. Of course, we assume energy conservation, $E = E_1 + E_2$, hence $E_1 > E$. The decaying process may be arranged in a way that the particle with positive energy E_1 returns to the region I_a while the particle with the negative energy E_2 is swallowed by the black hole. Then we have the following energy balance:

	black hole	outside particle
initial energy	E_0	E
final energy	$E_0 + E_2 < E_0$	$E_1 > E$

We see that it is possible to extract energy from a rotating black hole by this process. Obviously, the process can be repeated only until all energy of the black hole has been used up. Actually, the process terminates earlier: As we have seen that particles with negative E have negative L, the black hole loses not only energy but also angular momentum when swallowing the infalling particle. The Penrose process can be repeated only until the black hole has lost all its angular momentum; then it is a Schwarzschild black hole which has no ergoregion. – If the black hole is surrounded by a magnetic field, it is possible to extract rotational energy from the black hole in a much more efficient way. This modified Penrose process is known as the Blandford-Znajek process and it is believed to provide the necessary energy for the powerful jets that are observed with Active Galactic Nuclei.

7 Black holes in astrophysics

In this chapter we give a brief overview of the black-hole candidates that are actually observed in the sky and we discuss why we are quite optimistic that they can be successfully modelled as Kerr (or Schwarzschild) black holes.

The promising black-hole candidates can be divided into two classes: *Stellar black holes* with masses of a few (maybe up to 100) Solar masses, and *supermassive black holes* with millions or billions of Solar masses. Black holes with other masses are more speculative: *Mini-black-holes* with masses of several orders of magnitude less than a Solar mass could have come into existence shortly after the big bang, and *intermediate black holes* with several hundred or a few thousand Solar masses might be harboured e.g. in globular clusters. However, up to now we have no strong observational evidence for their existence. Therefore we discuss only the other two types.

7.1 Stellar black holes

(a) Cyg X-1

As the name indicates, Cyg X-1 is the first X-ray source that was detected in the constellation Cygnus (Swan). It is the brightest permanent source of hard X-rays in the sky.

X-ray sources cannot be observed with ground-based telescopes because (fortunately) our atmosphere is non-transparent for X-rays. The first observations of celestial X-ray sources were made with the help of Aerobee sounding rockets beginning in the year 1962. Cyg X-1 was detected in 1964. The Aerobees were ballistic rockets that could reach an altitude of about 250 km. After a flight of less than 10 minutes the payload fell back to the ground on a parachute.

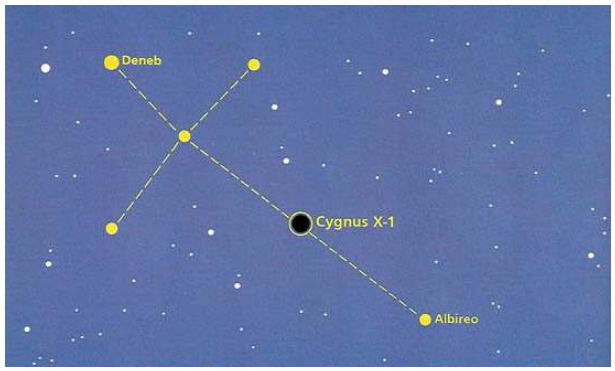

The X-ray observations were made at wavelengths from 1 to 15 Å with Geiger counters whose field of view swept over a stripe in the sky as the rocket rotated about its axis. This allowed only a rough localisation of the detected sources in the sky, so it ws not possible to decide whether there is an optical or radio source at the same position as Cyg X-1.

In the year 1970 the first X-ray satellite, Uhuru, was launched. ("Uhuru" is a Swahili word meaning "freedom".) It allowed to localise Cyg X-1 to within a few arcminutes which is still not accurate enough for deciding whether there is an optical (or radio) source at the same position. However, with the Uhuru satellite one observed time variations in the flux from Cyg X-1 on a time-scale of a little bit less than a second. As different parts of an emission region can show synchronised time variations only if they are causally connected, this means that the emission region of Cyg X-1 must be so small that light can travel through it in less than a second. This limited the diameter of the emission region of Cyg X-1 to less than 200 000 km. (For the sake of comparison, note that the diameter of our Sun is about 1 400 000 km!)

In the early 1970s the resolution of X-ray observations had improved sufficiently to localise Cyg X-1 to within an arcminute. Also, in the year 1971 a radio source was detected in the same area that showed variations on a similar time scale as the X-ray source Cyg X-1. This radio source could be located with an accuracy of about one arcsecond. This observation suggested that Cyg X-1 might be associated with an O star (a blue giant visible in the optical) with the catalogue number HDE 226868 that was within the error box of the radio observation. The spectral lines from this star show a redshift that varies periodically with a period of about 5.5 days. The obvious interpretation is that the star forms a binary system together with a partner; the periodic variation in the redshift comes from the Doppler effect when the star orbits about the barycentre of the binary system. The companion is not visible, neither in the optical nor in the radio. Moreover, it was observed that the intensity of the blue star varies with the same period as the redshift. The commonly accepted interpretation is that the star is not spherical but elongated in the direction towards the barycentre. In the course of one orbit it shows us sometimes a smaller and sometimes a bigger cross-sectional surface.

This indicates that the gravitational field of the compact companion has deformed the star and that there is a mass flow ("accretion flow") from the star onto the companion. The X-rays that we observe are produced when the accreted matter (gas or plasma) is strongly heated near the compact companion. The picture on the right shows an artist's impression of how the binary system may look like. (Actually, an observer would see a distorted image because of light bending, but these effects are ignored in the picture.)

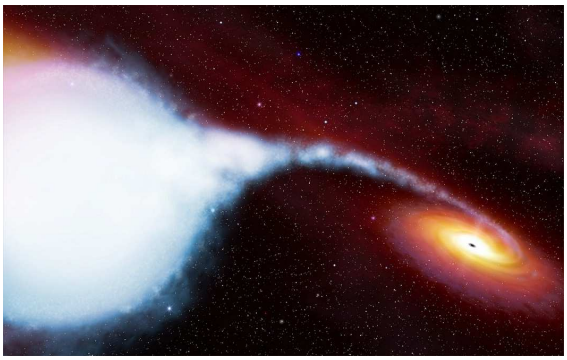

HDE 226868 is close enough for measuring its distance with the parallax method. One found that the system is about 2 kpc away from us. (For the sake of comparison, note that the centre of our Galaxy is at a distance of about 8 kpc from us.) With the distance known, one can combine the redshift measurements and other information on the orbits with stellar evolution models to determine the masses of the two companions. The up-to-date values average to 18 Solar masses for the blue star and 15 Solar masses for the compact companion, but there is still a rather big error margin. In 2021 a paper was published where the authors advocate a mass of 40 Solar masses for the blue star and more than 20 Solar masses for the compact companion. Recall that the latter has a diameter of less than 200 000 km, so it is inded a very compact object. It cannot be a white dwarf because there is an upper limit of about 1.4 Solar masses for a white dwarf. (This is the famous Chandrasekhar limit the discovery of which won S. Chandrasekhar the Nobel prize.) It cannot be a neutron star because also for a neutron star a mass of more than 10 Solar masses is out of the question. (The upper limit for the mass of a neutron star is not quite clear, because it depends strongly on the assumptions about the interior structure, but it cannot be much more than 3 Solar masses. The most massive neutron star we know has a mass of just a bit more than 2 Solar masses and most astrophysicists believe that this is close to the limit.) So a black hole is the most natural explanation. Other possible explanations (a boson star, a neutrino ball, a gravastar ..) have been suggested, but they are much more speculative.

Additional support for the black-hole hypothesis comes from the observation of "dying pulse trains" from the neighbourhood of Cyg X-1. These are X-ray signals that die down in exactly the way as one would expect if matter spirals towards an event horizon. By contrast, if matter hits a surface the emitted radiation does not die down but rather ends in a bright flash. This is strong evidence for the existence of an event horizon and the absence of a surface.

A black hole with 15 Solar masses has a Schwarzschild radius of about 45 km. At a distance of 2 kpc, the black hole associated with Cyg X-1 would cast a shadow with an angular diameter of less than 10^{-9} arcseconds. (Recall Synge's formula from p. 37 for the angular radius of the shadow of a Schwarzschild black hole which gives the correct order of magnitude also for a Kerr black hole.) This is far too small for observations within the foreseeable future. This is a pity because the shape of the shadow could give us important information on the spin of the black hole, recall the picture on p. 100. Up to now the spin of the black hole associated with Cyg X-1 is unknown. Observations with the X-ray satellite Chandra seem to indicate that the inner edge of the accretion disc is very close to the horizon which would imply that the black hole is almost extreme. (Recall that in the Schwarzschild limit, $a \to 0$, the ISCO of a Kerr black hole tends to $6m = 3r_+$ while for the extreme case, $a \to m$, it approaches $m = r_+$.) However, this is in disagreement with earlier papers where the authors have found indications for a slow rotation close to the Schwarzschild limit.

Cygnus X-1 was the subject of a wager between Stephen Hawking and Kip Thorne in 1974. Thorne was betting that the compact companion was a black hole, whereas Hawking said it was not. After a few years Hawking admitted that he had lost the bet and paid up (a one-year subscription of the magazine Penthouse) but claimed that he never really doubted that the companion was a black hole: He said that he took the opposite position just because he wanted to have the consolation of winning the bet in the unlucky case that the object turned out not to be a black hole.

Cyg X-1 is the oldest and best known candidate for a stellar black hole in an X-ray binary, but it is not the only one . There are more than a dozen further ones, with masses between 3 and 30 Solar masses. An incomplete list can be found on the Wikipedia page on "stellar black hole".

Further circumstantial evidence for the existence of stellar black holes comes from the observation of *gamma ray bursts*. The precise mechanism behind gamma ray bursts is not yet understood, but it is widely accepted that they are associated with the collapse of a neutron star to a black hole. Such a collapse could be caused by matter falling onto the neutron star from a companion star, thereby making the neutron star unstable, or from the merger of two neutron stars.

(b) The LIGO gravitational wave events

Further very strong evidence for the existence of stellar black holes comes from gravitational wave events observed since 2015. The first observations were made with the two LIGO detectors (Laser Interferometer Gravitational-Wave Observatory). Both detectors are located in the US, one at Hanford, Washington State, and the other at Livingston, Louisiana. Since 2021 there are four such detectors in operation: The two LIGO detectors were joined by Virgo in Italy and KAGRA in Japan. Most of the gravitational wave signals observed so far are believed to have been produced by a merger of two stellar black holes.

The LIGO, Virgo and KAGRA instruments are Michelson interferometers. The two LIGO instruments are the biggest ones with a geometric arm length of 4 kilometres. (The effective arm length is much bigger because the beams are reflected back and forth many times before going to the detector.) There is also a smaller instrument called GEO600 near Hannover in Germany with an arm length of 600 metres. It played a very important role for developing and testing the laser technology that was then incoporated into the bigger LIGO instruments. All these interferometric detectors work in the same fashion: An incoming gravitational wave would influence the distance between the mirrors and also the path of the light beam inside the interferometer. Both effects produce a change in the interference pattern, see the picture below. Several second-generation gravitational wave detectors are at the planning stage. In particular, a space-bound interferometer, LISA, with 5 million kilometres arm length may be launched in the early 1930s.

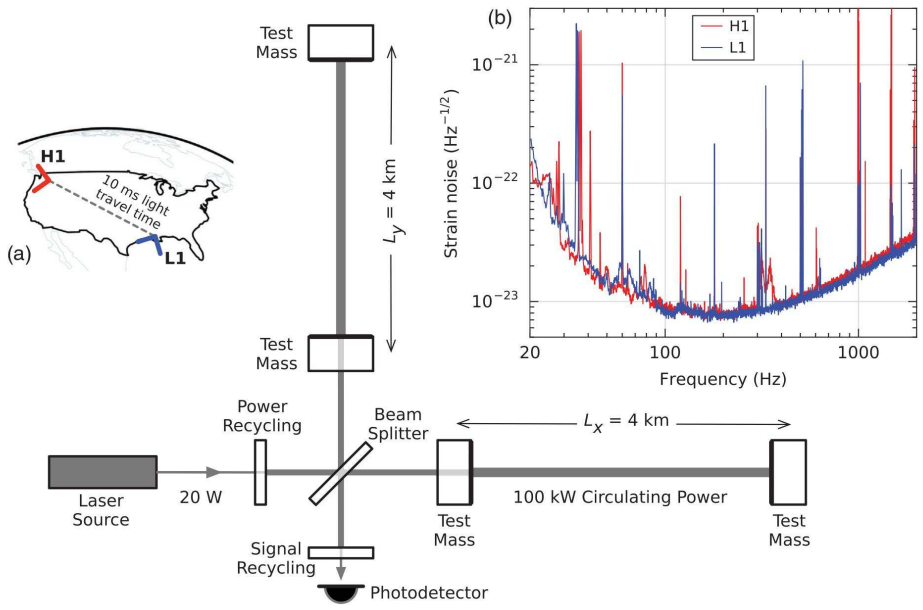

The two LIGO detectors underwent an upgrade and were relaunched in the late summer of 2015. In one of the very first runs after the upgrade, which was not even planned as a full science run but rather as a test, both LIGO detectors registered a signal on 14 September 2015 which perfectly matched the expectations of a gravitational wave coming from the merger of two black holes of about 30 Solar masses each. During the merger the incredibly high energy of 3 Solar masses times c^2 was emitted within a millisecond. After a very careful analysis the LIGO scientists announced the discovery not earlier than 11 February 2016 to the public. (The press conference can be watched e.g. on youtube, see https://www.youtube.com/watch?v=aEPIwEJmZyE.) The announcement made headlines around the world. A second event, again from the merger of two black holes, was detected on 26 December (boxing day) of 2015. By now, as of July 2022, with Virgo and KAGRA having come online, about 100 events have been registered. The majority was, most likely, produced by the merger of two stellar black holes. A few are probably produced by the merger of two neutron stars (which for a very short time formed an unstable neutron star which then collapsed to a black hole) and there are also a few events where possibly a black hole merged with a neutron star. Gravitational waves were predicted

by Albert Einstein, on the basis of his (linearised) theory of General Relativity in 1916. It took almost exactly 100 years until they were finally directly detected. *Indirect* evidence for their existence was provided by a binary pulsar whose energy loss was interpreted as due to gravitational radiation. This won Russell Hulse and Joe Taylor the physics Nobel prize already in 1993. Rainer Weiss, Kip Thorne and Barry Barish were awarded the physics Nobel prize in 2017 for their contributions to LIGO and the direct discovery of gravitational waves. In a sense, this was also a Nobel prize for the detection of black holes.

The direct discovery of gravitational waves is to be considered as the starting point for a "gravitational wave astronomy". It is often said, that it will provide us with a "second eye" (in addition to the "electromagnetic eye") for observing the universe.

The observation of the LIGO event from 14 September 2015 was published in a paper with more than 1000 authors, see B. Abbott et al., Phys. Rev. Lett. 116, 061102 (2016). The pictures in this section are taken from this paper.

As shown in the upper left panel of the figure on the preceding page, the distance between the two LIGO detectors equals $c/(10\,\mathrm{ms})$. Depending on the direction the gravitational wave comes from, the time at which the signal is detected at one detector should be between 0 and 10 ms after it is detected by the other. Only signals that are registered by both LIGO detectors within 10 ms are considered. In the case of GW150914 the time delay was 6.9 ms. The signal was observed over approximately 0.2 s. The upper right panel of the figure on the preceding page shows the sensitivity of the LIGO detectors, depending on the frequency of the incoming gravitational wave. The relevant LIGO observations were made at a frequency of 50 to 250 Hz. In this frequency range, the LIGO detectors are able to measure changes in the arm length of about a thousandth of a proton diameter.

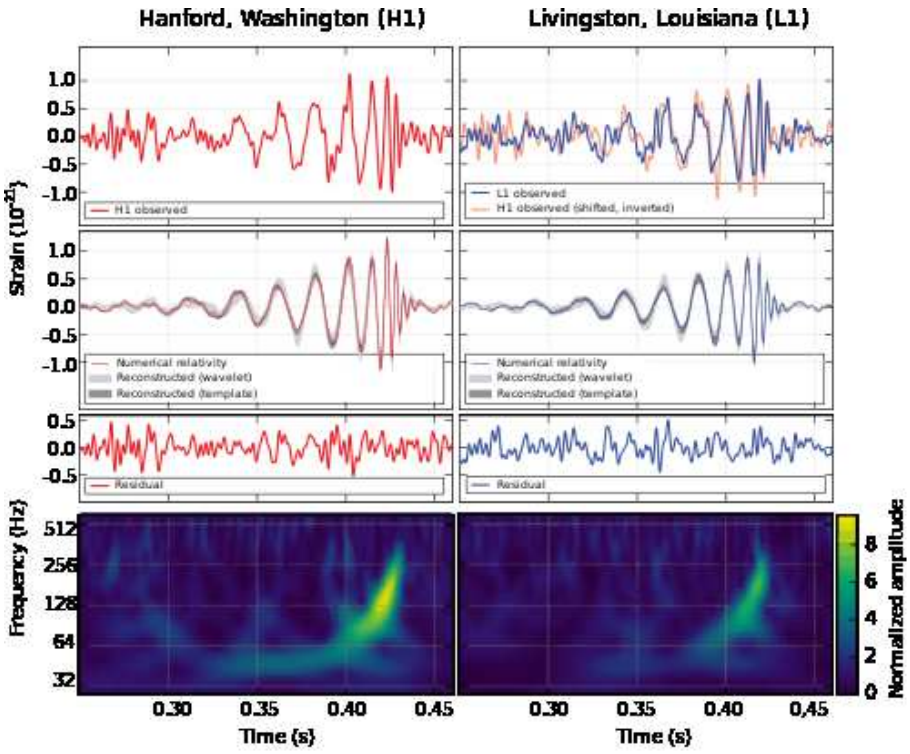

In the figure on the preceding page the first row shows the signals of GW150914 as they were received at Hanford (red) and Livingston (blue). The only manipulation is that frequencies outside of the sensitivity window of the LIGO detectors were filtered away. The observed signals were then compared to theoretically calculated wave-forms. Theorists have provided a collection of such wave-forms, for merging black holes and merging neutron stars with a large variety of parameters. The second row of the figure below shows the template that fits the observations best. It is a merger of two black holes with masses of $36\,M_\odot$ and $29\,M_\odot$, see the table below. Three phases are to be distinguished: The inspiral (which is periodic with an increasing amplitude), the merger (where the amplitude reaches its maximum) and the ringdown (where the amplitude strongly drops and the system becomes stationary again). The third row of the figure below shows the difference between the first and the second row which is to be interpreted as noise. Note that the ringdown is essentially drowned in the noise. As the difference between a merger of black holes (two horizons) and a merger of neutron stars (two surfaces) is significant only in the ringdown phase, one cannot really conclude from the observed wave-form that it is a black-hole merger. The assuredness that this event was indeed a black-hole merger comes mainly from the masses involved: It is believed that neutron stars cannot be much heavier than 3 Solar masses. The last row in the figure on the previous page shows the increase in frequency from about 50 Hz to about 250 Hz, i.e., the "chirp".

The location of the source in the sky is largely unknown: With only two detectors one can locate the source only to within an area that is as big as the constellation Orion. The location is in the Southern sky, i.e., the signal travelled through the body of the Earth, practically without being affected. The more gravitational wave detectors come online, the better the position of a source can be determined by way of triangulation. The table below gives the relevant data. We read that the merger took place far outside of our Galaxy, about 1.2×10^9 years ago. The equivalent of 3 Solar masses was converted into gravitational wave energy within less than a second. This corresponds to a radiated power that is more than the power radiated as electromagnetic waves by all visible sources in the Universe.

Primary black hole mass	$36^{+5}_{-4}\,M_\odot$
Secondary black hole mass	$29^{+4}_{-4}\,M_\odot$
Final black hole mass	$62^{+4}_{-4}\,M_\odot$
Final black hole spin $\lvert a\rvert/m$	$0.67^{+0.05}_{-0.07}$
Luminosity distance	$410^{+160}_{-180}\,\mathrm{Mpc}$
Source redshift z	$0.09^{+0.03}_{-0.04}$

7.2 Supermassive black holes

(a) The S stars near Sgr A^*

Already in the 1960s the British astronomers Donald Lynden-Bell and Martin Rees conjectured that our Galaxy harbours a black hole at its centre, and that the same is true for many other galaxies. At that time, this idea was highly speculative. By now, there is very good evidence that it is true.

The immediate neighbourhood of the centre of our Galaxy, which is in the direction of the constellation Sagittarius (Archer), cannot be observed with optical telescopes because it is hidden behind dust. In the infrared and in the radio, however, the dust is largely transparent, and the same is true on the other side of the optical spectrum in the X-ray. In the year 1974 a compact radio source was detected near the centre of our Galaxy which was called Sagittarius A^*, abbreviated Sgr A^*. Intensive observations of its neighbourhood began in the 1990s. Two groups studied the motion of a group of stars, the so-called S stars, that orbit the centre of our Galaxy with infrared cameras: A team from the Max Planck Institute for Extraterrestrial Physics (MPE) in Garching, headed by Reinhard Genzel, used the VLT in Chile, while a team from the University of California at Los Angeles (UCLA), headed by Andrea Ghez, used the Keck telescope in Hawaii. The S stars have angular distances of about 0.1 to 0.5 arcseconds from the centre of our Galaxy and one of them, the star S2, needs not more than 15 years for a revolution. The picture below shows its orbit as it was determined by the MPE group.

The observations of the MPE group and the UCLA group are in very good agreement. All S stars were found to describe perfect Kepler ellipses around a common centre (seen in perspective). From the orbits one could deduce the mass of the central object to be 4.1×10^6 Solar masses. The distance of the galactic centre from us is about 8 kpc. This implies that the S stars orbit at a distance of more than 1000 Schwarzschild radii which explains why the deviations from Kepler ellipses are small. Only in 2017 was it possible to measure, for the star S2, the relativistic pericentre precession.

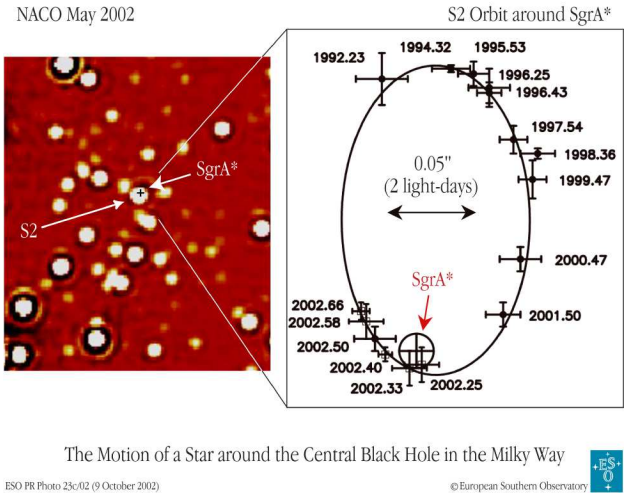

There is only a very moderate amount of X-ray radiation from the centre of our galaxy. If the central mass had a surface, a large part of the luminosity, in particular in the X-ray, would be emitted when accreted matter hits the surface. However, this kind of radiation is not observed. This is strong evidence for the conjecture that there is a black hole at the centre of our Galaxy.

In the year 2012 an object was observed near the centre of our galaxy in the infrared that was interpreted as a gas cloud and denoted G2. It was expected that, because of the tidal forces, G2 would disintegrate when passing through its pericentre and that the fragments would be swallowed by the black hole, emitting strongly in the X-ray regime when being accelerated towards the centre.

Nothing like that happened. G2 has gone through its pericentre in 2014 without any spectacular events. It is now widely believed that there is a star at the centre of G2 which keeps the matter together so that it will not be ripped apart by the tidal forces. The picture shows an artist's impression of the orbit of G2 (red) and, for the sake of comparison, the orbits of several S stars (blue).

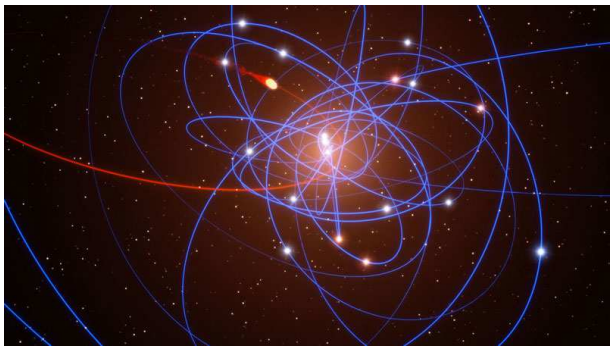

In the year 2016 a new beam combiner called GRAVITY went into operation with the VLT. With this new instrument it is possible to see infrared stars, and other objects orbiting the centre of our galaxy, with angular distances of less than 0.01 arcseconds. It was already mentioned that, with the help of this instrument, a pericentre precession of stars orbiting the centre of our Galaxy has been observed.

If our galaxy harbours a black hole at its centre, then it is very likely that the same is true of most, if not all, other galaxies. A particularly interesting candidate is the object at the centre of M87 (i.e., number 87 in the Messier catalogue) in the constellation Virgo (virgin). M87 is much more active than the centre of our own Galaxy. In partucular, M87 features a spectacular jet. It was the first jet of a galactic nucleus that was ever detected, namely already in 1918 by Heber Curtis. In analogy to Sgr A^*, the radio source at the centre of M87 is sometimes called M87*. It is at a distance of about 17 Mpc which is more than three orders of magnitude farther away than Sgr A^*. However, as its mass is about 5×10^9 Solar masses, the mass-to-distance ration isn't much smaller than for Sgr A^*.

(b) The shadows of Sgr A^* and M87*

If the object at the centre of our galaxy is a black hole, then it casts a shadow that is big enough for being observed with present instruments. A mass of 4.1×10^6 Solar masses corresponds to a Schwarzschild radius of $r_S = 12 \times 10^6$ km. If this value is inserted into Synge's formula (151) for the shadow, together with $r_O = 8$ kpc, one finds an angular diameter of the shadow of about 53 microarcseconds. This is resolvable with present day Very Long Baseline Interferometry (VLBI), using radio telescopes on different continents. The second biggest shadow is the one of the black hole (candidate) at the centre of the galaxy M87 with approximately 40 microarcseconds. The shadows of all other known black-hole candidates are smaller by several orders of magnitude.

The Event Horizon Telescope is a project under US leadership aiming at observing the shadow of Sgr A^* and of M87*. There is a sub-project, called the BlackHoleCam, which is financed by the European Union. At present (as of July 2022) the observations are done at 1.3 mm wavelength (i.e, in the far infrared) with various telescopes, see p. 41, and it is planned to observe in the future at submillimetre wavelengths; this would further reduce the scattering effects which are washing out the shadow.

The first pictures of the shadow of M87* were released to the public in April 2019, and the first pictures of Sgr A* were released to the public in May 2022, see p. 42. In both cases the data were taken in April 2017, but the processing and the evaluation took several years. In particular in the case of Sgr A* the data analysis was very difficult because the image changes within hours, whereas for the much heavier black hole in M87 it is quite stable over a day or two.

In principle, the shadow could provide us with important information about the spin of the object: If the observer is in the equatorial plane, or at least not at a very high inclination, then the shape of the observed shadow gives full information about the spin. Unfortunately we are observing M87* from a very high inclination (almost from the bottom side) and, apparently and surprisingly, the same seems to be true for Sgr A*. Therefore, the fact that the shadow is

circular to a high degree doesn't tell us much about the spin. From the fact that M87 has a big jet we suspect that the black hole at its centre must be spinning fast: The most effective process for launching a jet is the Blandford-Znajek process which asumes that the power for the jet comes from the angular momentum of a central black hole. In the case of Sgr A* we have no clear information about the spin of the black hole associated with this radio source.

We emphasise again that the shadow is not an image of the horizon but rather of the photon sphere or, in the case of a rotating black hole, of the photon region. Therefore, an observation of the shadow is not an ultimate proof that there is a black hole, i.e., an object with an event horizon. However, both in the case of M87* and in the case of Sgr A* all observations are in perfect agreement with the assumption that there is a Kerr black hole associated with this radio source. It is not impossible but very difficult to come up with an alternative model that concentrates the corresponding mass within a few Schwarzschild radii without a shining surface. All such alternative models are more exotic, and much more speculative, than a black hole.

8 Black-hole theorems

In this chapter we give a brief overview of three kinds of black-hole theorems, the socalled thermodynamical laws of black holes, the uniqueness (or no-hair) theorems, and the singularity theorems.

8.1 Black hole thermodynamics

There is a formal analogy between the laws of thermodynamics and black-hole physics. This analogy was discovered by Jacob Bekenstein when he was a PhD student with John Wheeler in Princeton. Major contributions were made by Stephen Hawking who originally had opposed Bekenstein's ideas. It is now widely believed that the analogy is not only formal but that the black-hole analogues of temperature and entropy are indeed associated with a physical temperature and a physical entropy.

For understanding the basic ideas of black hole thermodynamics we need to know what the "surface gravity" of a black hole is. Of course, this notion is well known from Newtonian gravity. There the surface gravity of a gravitating body is just the acceleration experienced at its surface by a test particle. For the Earth, the surface gravity is 9.8 m/s^2. By analogy, one would try to define the surface gravity of a black hole as the modulus of the 4-acceleration a test particle experiences at the horizon. We will now calculate this quantity for the simple case of a Schwarzschild black hole and we will find that, unfortunately, it turns out to be infinite.

As we want to evaluate certain expressions on the horizon, we have to consider the Schwarzschild metric in coordinates in which the metric is regular at the horizon. We choose the ingoing Eddington-Finkelstein coordinates $(t', r, \vartheta, \varphi)$ in which the metric reads

$$g = -\Big(1 - \frac{r_S}{r}\Big)c^2 dt'^2 + \frac{2r_S c}{r}\, dr\, dt' + \Big(1 + \frac{r_S}{r}\Big)dr^2 + r^2\big(d\vartheta^2 + \sin^2\vartheta d\varphi^2\big) \tag{400}$$

with

$$r_S = 2m = \frac{2GM}{c^2}\,, \tag{401}$$

recall (43). A static observer (i.e., an observer at constant (r, ϑ, φ) has four-velocity

$$U = \alpha \partial_{t'} \tag{402}$$

where α is determined by the condition that

$$-c^2 = g(U,U) = \alpha^2 g_{t't'} = -\alpha^2 c^2 \Big(1 - \frac{r_S}{r}\Big)\,, \tag{403}$$

i.e.,

$$\alpha = \frac{1}{\sqrt{1 - \dfrac{r_S}{r}}}\,. \tag{404}$$

We want to calculate the acceleration of such an observer, i.e., the thrust that has to be provided for keeping the observer in the static position,

$$a^\rho \partial_\rho = \nabla_U U = \nabla_{(\alpha\partial_{t'})}(\alpha\partial_{t'}) = \alpha\Big(\alpha \nabla_{\partial_{t'}}\partial_{t'} + \big(\partial_{t'}\alpha\big)\partial_{t'}\Big) = \alpha^2 \nabla_{\partial_{t'}}\partial_{t'} \tag{405}$$

where we have used in the last step that α depends only on r but not on t'. The most obvious way of determining the coefficients a^ρ is to express $\nabla_{\partial_{t'}}\partial_{t'}$ with the Christoffel symbols in the Eddington-Finkelstein coordinates. However, there is a more convenient way: We insert both sides of (405) into $g\big(\cdot, \partial_\sigma\big)$ which results in

$$a^\rho g_{\rho\sigma} = \alpha^2 g\big(\nabla_{\partial_{t'}}\partial_{t'}, \partial_\sigma\big) = \alpha^2\Big(\partial_{t'} g\big(\partial_{t'}\partial_\sigma\big) - g\big(\partial_{t'}, \nabla_{\partial_{t'}}\partial_\sigma\big)\Big)$$

$$= \alpha^2\Big(\partial_{t'} g_{t'\sigma} - g\big(\partial_{t'}, \nabla_{\partial_\sigma}\partial_{t'}\big)\Big) = \alpha^2\Big(0 - \frac{1}{2}\partial_\sigma g\big(\partial_{t'}, \partial_{t'}\big)\Big) = -\frac{\alpha^2}{2}\partial_\sigma g_{t't'}\,. \tag{406}$$

We evaluate this equation successively for $x^\sigma = \vartheta, \varphi, t', r$:

$$a^\vartheta g_{\vartheta\vartheta} = 0 \quad \Longrightarrow \quad a^\vartheta = 0\,, \tag{407}$$

$$a^\varphi g_{\varphi\varphi} = 0 \quad \Longrightarrow \quad a^\varphi = 0\,, \tag{408}$$

$$a^{t'} g_{t't'} + a^r g_{rt'} = 0 \quad \Longrightarrow \quad a^{t'} = a^r \frac{r_S \cancel{c}}{r \cancel{c}^2\Big(1 - \dfrac{r_S}{r}\Big)}\,, \tag{409}$$

$$a^{t'} g_{t'r} + a^r g_{rr} = \frac{\alpha^2}{2} c^2 \frac{r_S}{r^2}\,. \tag{410}$$

Inserting (409) into (410) yields

$$a^r \frac{r_S}{r\cancel{c}\Big(1 - \dfrac{r_S}{r}\Big)} \frac{r_S \cancel{c}}{r} + a^r\Big(1 + \frac{r_S}{r}\Big) = c^2 \frac{r_S}{2r^2\Big(1 - \dfrac{r_S}{r}\Big)}\,,$$

$$\cancel{a^r r_S^2} + a^r r^2\Big(1 - \frac{\cancel{r_S^2}}{\cancel{r^2}}\Big) = c^2 \frac{r_S}{2}\,,$$

$$a^r = \frac{c^2 r_S}{2r^2}\,. \tag{411}$$

Then (409) gives us the remaining coefficient of the acceleration

$$a^{t'} = \frac{c^{\not 2} r_S}{2r^2}\frac{r_S}{r\not{\left(1-\frac{r_S}{r}\right)}}\,, \tag{412}$$

hence

$$a^\rho \partial_\rho = a^{t'}\partial_{t'} + a^r \partial_r = \frac{c r_S^2}{2r^3\left(1-\frac{r_S}{r}\right)}\partial_{t'} + \frac{c^2 r_S}{2r^2}\partial_r\,. \tag{413}$$

Therefore, the modulus of the acceleration is

$$\sqrt{g_{\rho\sigma}a^\rho a^\sigma} = \sqrt{(a^{t'})^2 g_{t't'} + (a^r)^2 g_{rr} + 2a^{t'}a^r g_{t'r}} =$$

$$\sqrt{-\frac{c^2 r_S^4}{4r^6\left(1-\frac{r_S}{r}\right)^{\not 2}}c^{\not 2}\not{\left(1-\frac{r_S}{r}\right)} + \frac{c^4 r_S^2}{4r^4}\left(1+\frac{r_S}{r}\right) + \frac{2cr_S^2}{2r^3\left(1-\frac{r_S}{r}\right)}\frac{c^2 r_S}{2r^2}\frac{r_S c}{r}}$$

$$= \frac{c^2 r_S\sqrt{-\not{r}_S^{\not 2} + r^2\left(1-\frac{\not{r}_S^{\not 2}}{\not{r}^2}\right) + \not{2}\not{r}_S^{\not 2}}}{2r^3\sqrt{1-\frac{r_S}{r}}} = \frac{c^2 r_S}{2r^2\sqrt{1-\frac{r_S}{r}}}\,. \tag{414}$$

For $r_S \ll r$ we can neglect r_S/r in comparison to 1, hence

$$\sqrt{g_{\rho\sigma}a^\rho a^\sigma} \approx \frac{c^2 r_S}{2r^2} = \frac{c^{\not 2}\not{2}m}{\not{2}r^2} = \frac{GM}{r^2}\,, \tag{415}$$

i.e., in this approximation what is required to hold the observer at constant (r,ϑ,φ) is just the Newtonian acceleration. However, in the limit $r \to r_S$ we get

$$\sqrt{g_{\rho\sigma}a^\rho a^\sigma} \to \infty\,, \tag{416}$$

i.e., an infinite thrust is necessary for holding the observer at the horizon. Clearly, this is related to the fact that the horizon is lightlike, so a timelike curve cannot be tangent to it. In order to get a finite expression that characterises the strength of the gravitational field at the horizon one uses, instead of the derivative with respect to proper time which is encoded into the notion of 4-acceleration, the derivative with respect to coordinate time. This brings in an additional redshift factor,

$$\frac{d\tau}{dt} = \sqrt{1-\frac{r_S}{r_0}} \tag{417}$$

and the surface gravity of a Schwarzschild black hole becomes

$$\kappa = \lim_{r\to r_S}\sqrt{1-\frac{r_S}{r}}\,\frac{c^2 r_S}{2r^2\sqrt{1-\frac{r_S}{r}}} = \frac{c^2}{2r_S} = \frac{c^2}{4m} = \frac{c^4}{4GM}\,. \tag{418}$$

As proper time for an observer on a t-line is the same as coordinate time for $r \to \infty$, one often says that κ is the limit for $r \to r_S$ of the "acceleration with respect to an observer at infinity".

We will now demonstrate that the surface gravity κ of a Schwarzschild black hole can be rewritten in another way that allows generalisation beyond the Schwarzschild case. The horizon can be characterised as the hypersurface where the Killing vector field

$$K = K^\mu \partial_\mu = \frac{1}{c}\partial_{t'} \tag{419}$$

becomes lightlike. On this hypersurface, the differential of the function

$$\Phi = -g_{\mu\nu} K^\mu K^\nu \,, \tag{420}$$

$d\Phi = \partial_\mu \Phi dx^\mu$, is a multiple of the covector field $K_\mu dx^\mu = g_{\mu\nu} K^\nu dx^\mu$. We will now show how the factor of proportionality is related to the surface gravity κ.

Claim: For a Schwarzschild black hole, the surface gravity $\kappa = c^2/(2r_S)$ satifies

$$\partial_\mu \Phi\Big|_{r=r_S} = \frac{2\kappa}{c^2} K_\mu\Big|_{r=r_S} \tag{421}$$

where Φ and K_μ are defined as above.
Proof: From

$$\Phi = -g_{\mu\nu} K^\mu K^\nu = -g_{\mu\nu} \frac{1}{c^2} \delta^\mu_{t'} \delta^\nu_{t'} = -g_{t't'} \, \frac{1}{c^2} = 1 - \frac{r_S}{r} \tag{422}$$

we calculate

$$\partial_\mu \Phi = \delta^r_\mu \frac{r_S}{r^2} \to \delta^r_\mu \frac{1}{r_S} \tag{423}$$

for $r \to r_S$. On the other hand,

$$K_\mu = g_{\mu\nu} K^\nu = g_{\mu t'} \frac{1}{c} = \delta^{t'}_\mu g_{t't'} \frac{1}{c} + \delta^r_\mu g_{rt'} \frac{1}{c} = -\delta^{t'}_\mu c\Big(1 - \frac{r_S}{r}\Big) + \delta^r_\mu \frac{r_S}{r} \to \delta^r_\mu \tag{424}$$

for $r \to r_S$. So the claim is equivalent to

$$\delta^r_\mu \frac{1}{r_S} = \frac{2\kappa}{c^2} \delta^r_\mu \tag{425}$$

which is indeed true, because $\kappa = c^2/(2r_S)$. □

Note that the Killing vector field K that generates the horizon is defined only up to a constant scalar factor. We have chosen this factor such that $\Phi = -g(K,K) \to 1$ for $r \to \infty$. This fixes the Killing vector field uniquely.

We have thus found a characterisation of the surface gravity that can be generalised to all other black holes where the horizon is generated by a Killing vector field (i.e., where it is a socalled "Killing horizon"). This includes in particular the Kerr spacetime. We will now determine, with this method, the surface gravity for a Kerr black hole with $0 < a^2 < m^2$.

Also in this case we have to work in coordinates in which the metric is regular at the (outer) horizon. We choose the (generalised) ingoing Eddington-Finkelstein coordinates $(\tilde{t}, \tilde{r}, \tilde{\vartheta}, \tilde{\varphi})$ that are related to the Boyer-Lindquist coordinates $(t, r, \vartheta, \varphi)$ by

$$c\, d\tilde{t} = c\, dt + \frac{2mr}{\Delta}\, dr \,, \quad d\tilde{r} = dr \,, \quad d\tilde{\vartheta} = d\vartheta \,, \quad d\tilde{\varphi} = d\varphi + \frac{a}{\Delta}\, dr \tag{426}$$

recall (316). As the duality condition

$$dx^\mu(\partial_\nu) = \partial_\nu x^\mu = \delta^\mu_\nu \tag{427}$$

has to hold in both coordinate systems, the Gaussian basis vector fields transform according to

$$\partial_{\tilde{t}} = \partial_t\,, \quad \partial_{\tilde{\varphi}} = \partial_\varphi\,, \quad \partial_{\tilde{r}} = \partial_r - \frac{2mr}{c\Delta}\partial_t - \frac{a}{\Delta}\partial_\varphi\,, \quad \partial_{\tilde{\vartheta}} = \partial_\vartheta\,. \tag{428}$$

The Killing vector field that generates the outer horizon is

$$K = \frac{1}{c}\big(\partial_t + \Omega_H\partial_\varphi\big) = \frac{1}{c}\big(\partial_{\tilde{t}'} + \Omega_H\partial_{\tilde{\varphi}}\big) \tag{429}$$

where

$$\Omega_H \;=\; \frac{c\,a}{r_+^2 + a^2} \;=\; \frac{c\,a}{2mr_+}\,, \quad r_+ = m + \sqrt{m^2 - a^2}\,, \tag{430}$$

recall (394). The Killing vector field K changes from timelike to spacelike when the horizon at $r = r_+$ is crossed from the outside to the inside. At the horizon this vector field is lightlike and tangent to the horizon. With the help of this Killing vector field K we define the surface gravity κ of a Kerr black hole by the condition

$$\partial_\mu\Phi\big|_{r=r_+} = \frac{2\kappa}{c^2}K_\mu\big|_{r=r_+} \tag{431}$$

where

$$\Phi = -g(K,K)\,. \tag{432}$$

Again, we have normalised the Killing vector field such that $\Phi \to 1$ for $r \to \infty$. In the following calculation we make use of (428) and we read the metric coefficients in the Boyer-Lindquist coordinates from (301). We first calculate the left-hand side of (431):

$$\Phi = -g(K,K) = -\frac{1}{c^2}g\big(\partial_{\tilde{t}} + \Omega_H\partial_{\tilde{\varphi}}, \partial_{\tilde{t}} + \Omega_H\partial_{\tilde{\varphi}}\big) = -\frac{1}{c^2}g\big(\partial_t + \Omega_H\partial_\varphi, \partial_t + \Omega_H\partial_\varphi\big)$$

$$= \frac{1}{c^2}\big(-g_{tt} - 2\Omega_H g_{t\varphi} - \Omega_H^2 g_{\varphi\varphi}\big) = 1 - \frac{2mr}{\rho^2} + 2\Omega_H\frac{2mr}{\rho^2 c}a\sin^2\vartheta - \frac{\Omega_H^2}{c^2}\sin^2\vartheta\Big(r^2 + a^2 + \frac{2mr}{\rho^2}a^2\sin^2\vartheta\Big)$$

$$= 1 - \frac{2mr}{\rho^2} + 2\Omega_H\frac{2mr}{\rho^2 c}\,a\sin^2\vartheta - \frac{\Omega_H^2}{\rho^2 c^2}\sin^2\vartheta\Big(\big(\Delta + 2mr\big)\big(\Delta + 2mr - a^2\sin^2\vartheta\big) + 2mra^2\sin^2\vartheta\Big)$$

$$= \frac{1}{\rho^2}\Big(\Delta + \cancel{2mr} - a^2\sin^2\vartheta - \cancel{2mr} + \frac{4mr}{c}\Omega_H a\sin^2\vartheta - \frac{\Omega_H^2}{c^2}\sin^2\vartheta\big(\Delta^2 + 4mr\Delta + 4m^2r^2 - \Delta a^2\sin^2\vartheta\big)\Big)$$

$$= \frac{1}{\rho^2}\Big(\Delta - a^2\sin^2\vartheta + \frac{2r}{r_+}\,a^2\sin^2\vartheta - \frac{a^2}{4m^2r_+^2}\sin^2\vartheta\big(\Delta^2 + 4mr\Delta + 4m^2r^2 - \Delta a^2\sin^2\vartheta\big)\Big)\,. \tag{433}$$

Making use of the fact that Φ depends only on $\tilde{r} = r$ and $\tilde{\vartheta} = \vartheta$, we now calculate the partial derivatives of Φ with respect to the (generalised) Eddington-Finkelstein coordinates.

$$\partial_{\tilde{t}}\Phi = \partial_t\Phi = 0\,, \tag{434}$$

$$\partial_{\tilde{\varphi}}\Phi = \partial_\varphi\Phi = 0\,, \tag{435}$$

$$\partial_{\tilde{r}}\Phi = \partial_r\Phi + 0 = \rho^2\Phi\,\partial_r\frac{1}{\rho^2} + \frac{1}{\rho^2}\,\partial_r\big(\rho^2\Phi\big) = \rho^2\Phi\,\partial_r\frac{1}{\rho^2}$$
$$+\frac{1}{\rho^2}\Big(2(r-m)+\frac{2}{r_+}\,a^2\sin^2\vartheta-\frac{a^2}{4m^2r_+^2}\,\sin^2\vartheta\big(4\Delta(r-\cancel{m})+\cancel{4m\Delta}+8mr(r-\cancel{m})+\cancel{8m^2r}-2(r-m)a^2\sin^2\vartheta\big)\Big) \tag{436}$$

$$\Longrightarrow\quad \partial_{\tilde{r}}\Phi\big|_{r=r_+} = 0 + \frac{1}{(r_+^2+a^2\cos^2\vartheta)}\Big(2(r_+-m)+\frac{2}{r_+}\,a^2\sin^2\vartheta-\frac{2a^2\sin^2\vartheta}{m}+\frac{(r_+-m)}{2m^2r_+^2}a^4\sin^4\vartheta\Big)$$
$$= \frac{2(r_+-m)}{(r_+^2+a^2\cos^2\vartheta)}\Big(1-\frac{a^2\sin^2\vartheta}{mr_+}+\frac{a^4\sin^4\vartheta}{4m^2r_+^2}\Big) = \frac{2(r_+-m)\big(2mr_+-a^2\sin^2\vartheta\big)^2}{(r_+^2+a^2\cos^2\vartheta)4m^2r_+^2} \tag{437}$$

$$\partial_{\tilde{\vartheta}}\Phi = \partial_\vartheta\Phi = \rho^2\Phi\,\partial_\vartheta\frac{1}{\rho^2} + \frac{1}{\rho^2}\,\partial_\vartheta\big(\rho^2\Phi\big)$$
$$= \rho^2\Phi\,\partial_\vartheta\frac{1}{\rho^2} + \frac{2\sin\vartheta\cos\vartheta}{\rho^2}\Big(-a^2+\frac{2r}{r_+}a^2-\frac{a^2}{4m^2r_+^2}(\Delta^2+4mr\Delta+4m^2r^2)+\frac{\Delta a^4\sin\vartheta}{2m^2r_+^2}\Big) \tag{438}$$

$$\Longrightarrow\quad \partial_{\tilde{\vartheta}}\Phi\big|_{r=r_+} = 0 + \frac{2a^2\sin\vartheta\cos\vartheta}{(r_+^2+a^2\cos^2\vartheta)}\big(-1+2-1\big) = 0\,. \tag{439}$$

We now turn to the right-hand side of (431):

$$K_{\tilde{t}} = g(K,\partial_{\tilde{t}}) = g(K,\partial_t) = \frac{1}{c}\Big(g_{tt}+\Omega_H g_{t\varphi}\Big) = \frac{1}{c}\Big(-c^2+\frac{2mrc^2}{\rho^2}-\frac{ca}{2mr_+}\frac{2mr}{\rho^2}ca\sin^2\vartheta\Big)$$
$$= \frac{c}{\rho^2}\Big(-r^2-a^2\cos^2\vartheta+2mr-\frac{r}{r_+}a^2\sin^2\vartheta\Big) = \frac{c}{\rho^2}\Big(-\Delta+a^2\sin^2\vartheta-\frac{a^2r}{r_+}\sin^2\vartheta\Big) \tag{440}$$

$$\Longrightarrow\quad K_{\tilde{t}}\big|_{r=r_+} = 0\,, \tag{441}$$

$$K_{\tilde{\varphi}} = g(K,\partial_{\tilde{\varphi}}) = g(K,\partial_\varphi) = \frac{1}{c}\Big(g_{t\varphi}+\Omega_H g_{\varphi\varphi}\Big)$$
$$= \frac{1}{c}\Big\{-\frac{2mr}{\rho^2}ca\sin^2\vartheta+\frac{ca}{2mr_+}\Big(\sin^2\vartheta(r^2+a^2)+\frac{2mr}{\rho^2}a^2\sin^4\vartheta\Big)\Big\}$$
$$= \frac{\sin^2\vartheta}{\rho^2}\Big\{-2mra+\frac{a}{2mr_+}\Big((r^2+a^2)(r^2+a^2\cos^2\vartheta)+2mra^2\sin^2\vartheta\Big)\Big\}$$
$$= \frac{\sin^2\vartheta}{\rho^2}\Big\{-2mra+\frac{a}{2mr_+}\Big((\Delta+2mr)(r^2+a^2\cos^2\vartheta)+2mra^2\sin^2\vartheta\Big)\Big\}$$

$$= \frac{\sin^2\vartheta}{\rho^2}\Big\{ -2mra + \frac{a\Delta}{2mr_+}(r^2+a^2\cos^2\vartheta) + \frac{ar}{r_+}(\Delta+2mr)\Big\} \tag{442}$$

$$\Longrightarrow \quad K_{\tilde\varphi}\big|_{r=r_+} = \frac{\sin^2\vartheta\big(-2mr_+a+2mr_+a\big)}{r_+^2+a^2\cos^2\vartheta} = 0\,, \tag{443}$$

$$K_{\tilde r} = g(K,\partial_{\tilde r}) = \frac{1}{c}g\Big(\partial_t+\Omega_H\partial_\varphi, \partial_r - \frac{2mr}{c\Delta}\partial_t - \frac{a}{\Delta}\partial_\varphi\Big)$$

$$= \frac{1}{c}\Big\{ -\frac{2mr}{c\Delta}g_{tt} - \frac{a}{\Delta}g_{t\varphi} + \Omega_H\Big(-\frac{2mr}{c\Delta}g_{t\varphi} - \frac{a}{\Delta}g_{\varphi\varphi}\Big)\Big\}$$

$$= \frac{2mr}{\cancel{c^2}\Delta}\cancel{c^2}\Big(1-\frac{2mr}{\rho^2}\Big) + \frac{a}{\cancel{c}\Delta}\frac{2mr}{\rho^2}\cancel{c}a\sin^2\vartheta + \frac{\cancel{c}\,a}{\cancel{c}2mr_+}\left(\frac{2mr}{\cancel{c}\Delta}\frac{2mr}{\rho^2}\cancel{c}a\sin^2\vartheta - \frac{a}{\Delta}\sin^2\vartheta\Big(r^2+a^2+\frac{2mr}{\rho^2}a^2\sin^2\vartheta\Big)\right)$$

$$= \frac{2mr}{\Delta\rho^2}\Big(r^2+a^2\cos^2\vartheta - 2mr + a^2\sin^2\vartheta\Big) + \frac{a^2\sin^2\vartheta}{2mr_+\Delta\rho^2}\Big(2mr\big(2mr - a^2\sin^2\vartheta\big) - \rho^2(r^2+a^2)\Big)$$

$$= \frac{2mr}{\rho^2} + \frac{a^2\sin^2\vartheta}{2mr_+\Delta\rho^2}\Big(2mr\big(-\Delta+r^2+a^2-a^2\sin^2\vartheta\big) - \rho^2(r^2+a^2)\Big)$$

$$= \frac{1}{\rho^2}\Big(2mr + \frac{a^2\sin^2\vartheta}{2mr_+\cancel{\Delta}}\big(-2mr\cancel{\Delta} - \rho^2\cancel{\Delta}\big)\Big)$$

$$= \frac{1}{\rho^2}\Big\{2mr - \frac{a^2\sin^2\vartheta}{2mr_+}\Big(r^2+a^2\cos^2\vartheta+2mr\Big)\Big\}$$

$$= \frac{1}{\rho^2}\Big\{2mr - \frac{a^2\sin^2\vartheta}{2mr_+}\Big(\Delta - a^2\sin^2\vartheta + 4mr\Big)\Big\} \tag{444}$$

$$\Longrightarrow \quad K_{\tilde r}\big|_{r=r_+} = \frac{4m^2r_+^2 + a^4\sin^2\vartheta - 4mr_+a^2\sin^2\vartheta}{(r_+^2+a^2\cos^2\vartheta)2mr_+} = \frac{\big(2mr_+ - a^2\sin^2\vartheta\big)^2}{(r_+^2+a^2\cos^2\vartheta)2mr_+} \tag{445}$$

$$K_{\tilde\vartheta} = \frac{1}{c}\,g(\partial_{\tilde t}+\Omega_H\partial_{\tilde\varphi},\partial_{\tilde\vartheta}) = \frac{1}{c}\,g(\partial_t+\Omega_H\partial_\varphi,\partial_\vartheta) = 0\,. \tag{446}$$

So the condition (431) is equivalent to

$$\frac{2(r_+-m)\big(2mr_+ - a^2\sin^2\vartheta\big)^2}{(r_+^2+a^2\cos^2\vartheta)4m^2r_+^2} = \frac{2\kappa}{c^2}\,\frac{\big(2mr_+ - a^2\sin^2\vartheta\big)^2}{(r_+^2+a^2\cos^2\vartheta)2mr_+}\,, \tag{447}$$

so the surface gravity of a Kerr black hole is

$$\kappa = \frac{c^2(r_+-m)}{2mr_+} = \frac{c^2\sqrt{m^2-a^2}}{2m(m+\sqrt{m^2-a^2})}\,. \tag{448}$$

We will now establish the analogy between black-hole theory and thermodynamics. First we need to know what is the analogon to the equilibrium state space. If we restrict to Kerr black holes, then there are two parameters, m and a, both with the dimension of a length, so the state space is two-dimensional. This is analogous e.g. to a gas which has also a two-dimensional state space, coordinatised e.g. with the entropy S and the volume V.

To have black holes witrh two horizons, we restrict the parameters m and a according to

$$m > 0\,, \quad a^2 < m^2 \tag{449}$$

so that we have an outrer horizon at $r_+ = m + \sqrt{m^2 - a^2}$. The inner horizon at $r_- = m - \sqrt{m^2 - a^2}$ will play no role in the following.

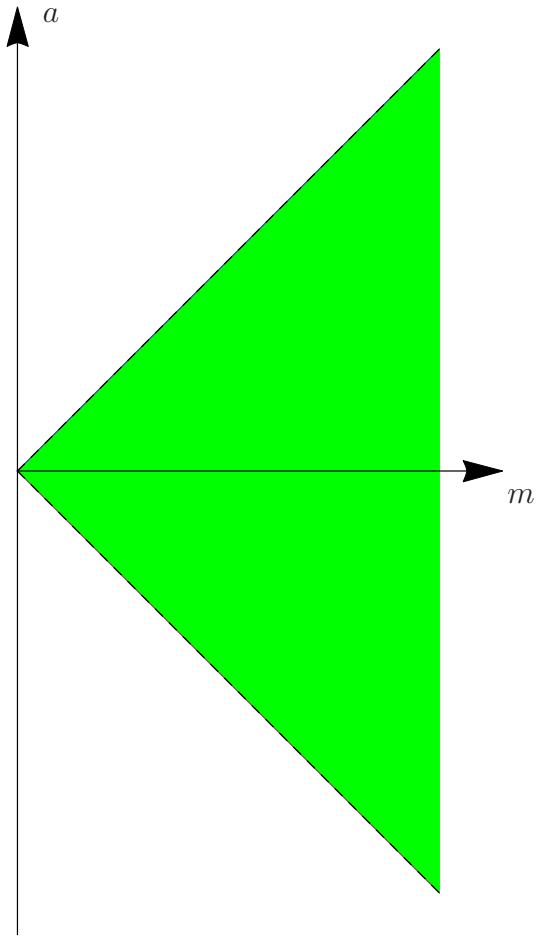

The set of all such Kerr black holes fill the interior of an infinite wedge (green in the picture) in the $m - a-$plane. This is the state space of Kerr black holes. The boundary of this wedge (dashed in the picture) corresponds to the extreme black holes with $a^2 = m^2$. The naked-singularity case ($a^2 > m^2$) is not covered.There is no "thermodynamics of naked singularities".

In ordinary thermodynamics we have five relevant variables on the state space, namely the temperature T, the entropy S, the pressure p, the volume V and the internal energy U. It is our goal to define five analogous state space functions for black holes and then to investigate whether the following well-known laws of thermodynamics hold for black holes.

0^{th} law: For a system in equilibrium the temperature is a constant.

1^{st} law: $dU = TdS - pdV$.

2^{nd} law: In a closed system the entropy cannot decrease, $\delta S \geq 0$.

3^{rd} law: $T = 0$ cannot be reached, by any procedure, in finitely many steps.

We have given the 3^{rd} law here in Nernst's version of 1912. There is also another version, often called the Planck-Nernst law, which says that the entropy S approaches zero if T approaches zero. However, it is known that the Planck-Nernst law does not hold for all materials, so it is not universal.

For a Kerr black hole we need five functions of a and m which can serve as the analogues of T, S, p, V and U. There are the following candidates:

- the surface gravity

$$\kappa = \frac{c^2(r_+ - m)}{2mr_+} = \frac{c^2\sqrt{m^2 - a^2}}{2m(m + \sqrt{m^2 - a^2})}\,, \tag{450}$$

- the area of the horizon

$$A = 8\pi m r_+ = 8\pi m\big(m + \sqrt{m^2 - a^2}\big)\,, \tag{451}$$

  recall Problem 1 of Worksheet 10,

- the angular velocity of the horizon

$$\Omega_H = \frac{ca}{2mr_+} = \frac{ca}{2m(m + \sqrt{m^2 - a^2})}\,, \tag{452}$$

- the mass

$$M = \frac{c^2 M}{G}\,, \tag{453}$$

- the spin

$$J = \frac{c^3 ma}{G}\,. \tag{454}$$

For setting up an analogy with thermodynamics, one associates:

temperature $T = \dfrac{\hbar}{2\pi ck}\,\kappa$ ($\kappa =$ surface gravity)

entropy $S = \dfrac{kc^3}{4\hbar G}\,A$ ($A =$ area of the horizon)

pressure $p \mathrel{\hat{=}} -\,\Omega_H$ ($\Omega_H =$ angular velocity of the horizon)

volume $V \mathrel{\hat{=}} J$ ($J =$ spin)

internal energy $U = c^2 M$ ($M =$ mass)

Here we have introduced, in addition to c and G which occur naturally in general relativity, the Planck constant $\hbar$ and the Boltzmann konstant k which is necessary to make sure that T and S have the correct dimensions. Note that the four laws remain unchanged if we multiply T with a positive numerical factor and divide S by the same factor, so the factors we have chosen seem ambiguous at the moment. Also note that p has not the dimension of a pressure and V has not the dimension of a volume, but this is to be expected because we are considering a gas just as an example. We could equally well consider another thermodynamical system with a two-dimensional state space, e.g. a magnetisable material where the analogue of V is the magnetisation M and the analogue of p is the magnetic field strength $-B$. So the only thing to be required is that the product of the analogue of p and the analogue of V should give a quantity with the dimension of an energy, and this is the case.

We now look at the laws one by one and check if their analogues are true for black holes.

The analogue of the 0^{th} law says that the surface gravity of a stationary black hole is a constant. This is indeed true for Kerr black holes. We emphasise again that this result is non-trivial: As in the Kerr case the horizon is not a "round sphere", recall Worksheet 10, it would have been very natural to assume that the surface gravity depends on the latitudinal coordinate ϑ

We now turn to the 1^{st} law. To that end we calculate

$$T\,dS = \frac{c^2}{8\pi G}\kappa\,dA = \frac{c^2}{\cancel{8\pi}\,G}\,\frac{c^2\sqrt{m^2-a^2}}{2m\big(m+\sqrt{m^2-a^2}\big)}\cancel{8\pi}\,d\big(m(m+\sqrt{m^2-a^2})\big)$$

$$= \frac{c^4\sqrt{m^2-a^2}}{2Gm(m+\sqrt{m^2-a^2})}\left(\big(m+\sqrt{m^2-a^2}\big)dm + m\Big(dm + \frac{m\,dm - a\,da}{\sqrt{m^2-a^2}}\Big)\right)$$

$$= \frac{c^4\sqrt{m^2-a^2}}{2Gm(m+\sqrt{m^2-a^2})}\Big(\big(m+\sqrt{m^2-a^2}\big)dm + \frac{m\big(\sqrt{m^2-a^2}+m\big)}{\sqrt{m^2-a^2}}\,dm - \frac{m\,a\,da}{\sqrt{m^2-a^2}}\Big)$$

$$= \frac{c^4}{2Gm}\Big(\sqrt{m^2-a^2}\,dm + m\,dm - \frac{m\,a\,da}{m+\sqrt{m^2-a^2}}\Big)\,. \tag{455}$$

$$-p\,dV = \Omega_H dJ = \frac{ca}{2m(m+\sqrt{m^2-a^2})}\,\frac{c^3}{G}\,d(ma) = \frac{c^4 a}{2Gm(m+\sqrt{m^2-a^2}}\,\big(m\,da + a\,dm\big)\,. \tag{456}$$

Hence

$$T\,dS - p\,dV = \frac{c^4}{2Gm}\Big(\sqrt{m^2-a^2}\,dm + m\,dm - \cancel{\frac{m\,a\,da}{m+\sqrt{m^2-a^2}}} + \frac{a\,\big(\cancel{m\,da} + a\,dm\big)}{m+\sqrt{m^2-a^2}}\Big)$$

$$= \frac{c^4}{2Gm(m+\sqrt{m^2-a^2})}\Big(\big(m\sqrt{m^2-a^2}+m^2-\cancel{a^2}\big)\,dm + m\big(m+\sqrt{m^2-a^2}\big)\,dm + \cancel{a^2\,dm}\Big)$$

$$= \frac{c^4}{\cancel{2}\,G\,m\,\cancel{(m+\sqrt{m^2-a^2})}}\cancel{2}\,\cancel{\big(m\sqrt{m^2-a^2}+m^2\big)}\,dm = \frac{c^4}{G}\,dm\,. \tag{457}$$

As

$$dU = c^2 dM = \frac{c^4}{G}dm\,, \tag{458}$$

this proves that the 1^{st} law is indeed true. This result does not look very deep. One might have the impression that such a kind of analogy can be always constructed if one plays around sufficiently long with the available quantities. However, in 1974 Stephen Hawking showed, using concepts from quantum field theory on a curved background, that (even Schwarzschild) black holes can radiate: If one considers e.g. a quantised Klein-Gordon field on the Schwarzschild background, pair creation in the domain of outer communication may produce a field with negative energy that moves into the black hole and a field with positive energy that escapes to infinity. Hawking showed that, for an observer sufficiently far outside, the latter shows a Planck spectrum with the above-given temperature $T = \dfrac{\hbar}{2\pi ck}\,\kappa$ which is often called the *Hawking*

temperature. Whereas the analogy with the 1st law determined the temeprature only up to a numerical factor that remained undetermined, from the Planck spectrum the temperature can be read uniquely. Hawking's result showed that the analogy between the surface gravity and a temperature is more than a coincidence: The surface gravity is associated with a physical temperature that can actually be measured, at least in principle. Note, however, that the Hawking temperature of a Schwarzschild black hole, $T = \hbar c/(8km) = \hbar c^3/(8kGM)$, has the mass in the denominator. Therefore, for a supermassive and even for a stellar black hole this temperature is very, very low. Correspondingly, these black holes suffer a measurable mass loss only on very long time-scales. Actually, it takes more than the age of the universe until such a black hole has lost a measurable fraction of its mass. Therefore, Hawking radiation can be expected to be actually observed only with mini-black-holes whose existence is still speculative. However, there are several claims that Hawking radiation has actually been observed in the laboratory by way of *analogue graity* experiments. The idea is to do experiements with some kind of materials (fluids, dielectrics, etc.) which are described by equations that are formally the same as equations that hold for black holes. In particular, Jeff Steinhauer [Nature 12, 959 (2016)] has claimed that his group has observed Hawking radiation in an analogue experiment with Bose-Einstein condensates. This claim is still the matter of a vivid debate.

We now turn to the 2nd law. Even before the analogy to thermodynamics was brought forward, Stephen Hawking [Phys. Rev. Lett. 26, 13 (1971)] had proven a theorem which is often called the "area theorem". It says that under certain assumptions the horizon area of a black hole cannot decrease. It was this observation that brought Jacob Bekenstein to the idea of associating the horizon area with an entropy. The proof of the area theorem is too involved for being given here; a good source for background material on the area theorem and on the entire subject of black-hole thermodynamics is the Living Review by Robert Wald [The Thermodynamics of Black Holes. Living Rev. Relativ. 2001, 4(1) 6, http://www.livingreviews.org/lrr-2001-6]. The validity of the 2nd law had to be re-examined after the discovery of Hawking radiation. During the process of radiating a black hole loses mass. As the horizon area of a Schwarzschild black hole equals $A = 16\pi m^2 = 16\pi G^2 M^2/c^4$, this implies that A decreases as well, so the 2nd law is violated. (The reason why Hawking's area theorem implicitly excludes Hawking radiation is in the fact that one of the assumptions on which the area theorem is based is an energy condition. Roughly speaking, it is assumed that the considered black-hole spacetime is a solution of Einstein's field equation with an energy-momentum tensor with non-negative energy density. Clearly, in the presence of Hawking radiation this assumption is violated because Hawking radiation requires negative energies.) Actually, it should not come as a surprise that the entropy of a black hole may decrease if it is radiating: Also in ordinary thermodynamics the entropy of a system may drecrease if it is not closed. A radiating black hole swallows matter (with negative energy), so it is not closed. Bekenstein was indeed successful in establishing a version of the 2nd law that includes Hawking radiation. To that end he defined a total entropy that is composed of the above-mentioned entropy of the black hole and an appropriately defined entropy of the environment with the outgoing radiation.

In ordinary thermodynamics there is also a way of defining the entropy in the language of information theory. Leonard Susskind, who is best known for his pioneering contributions to string theory, and others have shown that a similar interpretation of the above-defined black-hole entropy is possible as well. In particular, Susskind developed a method of how to actually *calculate* the entropy of a black hole with methods from string theory. Susskind described in

a popular book, entitled "The black hole war", his controversy with Stephen Hawking on the question of whether information is lost in a black hole. In technical terms, this controversy is related to the question of whether the time evolution of a black hole can be described by a unitary operator as is usually assumed in quantum mechanics. In a bet against John Preskill, Stephen Hawking and Kip Thorne (for this time on the same side) had opined in 1997 that the answer is "no". Hawking conceded in 2004, but Thorne never did. Obviously, all these considerations are to some extent based on speculations, because they make use of a hypothetical quantum gravity theory (based e.g. on string theory) which up to now does not exist in a mathematically precise and generally accepted version.

The question of whether an analogue of the 3rd law holds for black holes is still a matter of debate. It is clear that the Planck-Nernst version is *not* satisfied: For Kerr black holes the limit $T \to 0$ corresponds to $\kappa \to 0$, i.e, to $m^2 - a^2 \to 0$. In this limit $A \to 8\pi m^2 \neq 0$, i.e., the entropy does not go to zero. However, the above-quoted Nernst 1912 version of the 3rd law may have an analogue. There are some partial results to the effect that, under certain conditions, $T = 0$ cannot be reached, i.e., the black hole cannot become extremal. E.g., Kip Thorne [Astrophys. J. 191, 507 (1974)] found that, under certain assumptions, the spin parameter of a black hole that swallows mass and angular momentum from its environment is limited by $|a| \leq 0.998m$.

8.2 Black hole uniqueness theorems ("no hair theorems")

We have studied in this course, among other things, the following black-hole spacetimes:

- Schwarzschild (mass M)
- Reissner-Nordström (mass M, charge Q)
- Kerr (mass M, angular momentum J)

There is also a charged version of the Kerr metric,

- Kerr-Newman (mass M, angular momentum J, charge Q)

The Kerr-Newman metric, which was found by Ted Newman and collaborators shortly after the discovery of the Kerr metric, has the same form (301) as the Kerr metric. The only difference is in the Δ which now contains an additional term proportional to the square of the charge.

We have to ask ourselves whether these three parameters, M, J and Q, characterise a stationarily rotating charged bFlack hole uniquely, or if there are other types of such black holes which require additional parameters for their description. Actually, one should not expect that these three parameters are sufficient: Before undergoing gravitational collapse, a gravitating body may have any combination of (mass, angular momentum and charge) multipole moments. Why should one expect that, after gravitational collapse has taken place and the object has settled down as a stationarily rotating black hole, all the higher-order multipole moments should be uniquely determined by M, J and Q? However, this is exactly what one found: It was proven, step by step, between the late 1960s and the mid 1980s by several scientists, including Werner Israel (for non-rotating black holes), David Robinson (for rotating uncharged black holes) and Pavel Mazur (for rotating charged black holes), that a black hole must be a Kerr-Newman black hole, uniquely characterised by M, J and Q, provided that some conditions are satisfied: The spacetime should be stationary and asymptotically flat, it should be a solution of the Einstein-Maxwell equations, it should be analytic and there should be an

event horizon that satisfies a regularity condition. For a precise formulation of this uniqueness theorem and a detailed guide to the proof see Theorem 3.3 in P. Chruściel, J. Costa, M. Heusler[Stationary black holes: Uniqueness and beyond, Living Rev. Relativity 15 (2012) 7 , `http://www.livingreviews.org/lrr-2012-7`]. Other variants of the theorem include energy conditions and/or conditions that make sure that the horizon has spherical topology.

The black-hole uniqueness theorem is also known as the "no-hair theorem". Here one refers to all properties which are not determined by M, J and Q as to "hairs", and then the theorem says that a stationary electrovacuum black hole has no hairs. The name "no-hair theorem" was made popular by John Wheeler but Wheeler himself indicated that it was coined by his PhD student Jacob Bekenstein.

If one allows, in addition to gravity and electromagnetism, other interactions, i.e., if one gives the black hole e.g. a scalar charge or a Yang-Mills charge, then there is no no-hair theorem. Actually, one needs infinitely many parameters for characterising e.g. a black hole with scalar charge. Details can be found in the above-mentioned Living Review by Chruściel, Costa and Heusler.

Most people believe that for the supermassive and stellar black holes that actually exist in Nature the electric charge plays no role, and that this is all the more true for scalar charges, Yang-Mills charges and so on. (However, we don't really know this for sure.) Then the no-hair theorem says that these black holes should be properly described by the Kerr metric. Of course, this is true only as long as we neglect the influence on the gravitational field of all matter around the black hole, i.e. only as long as we assume that the vacuum Einstein field equation holds (outside of the horizon). Matter around the black hole would give a deviation of the (mass and angular momentum) multipoles from the Kerr multipoles. Such "distorted black holes" are under detailed investigation. However, this is to be understood as considering small corrections. The no-hair theorem gives very strong support to the assumption that the black holes that actually exist in Nature are very well described by the Kerr metric. We have already emphasised that to date this assumption is in agreement with all observations Therefore, a good knowledge of the properties of Kerr black holes (which include Schwarzschild black holes as a special case) is of paramount importance for a thorough understanding of the theory of black holes. In this course we have tried to lay the foundations for such a good knowledge.

8.3 The singularity theorem of Roger Penrose

In 1965 Roger Penrose proved a mathematical theorem for which he got 50 % of the 2020 Physics Nobel Prize. It was the first time that the Physics Nobel Prize was given for a mathematical result. Penrose's theorem was the first of three *singularity theorems*. The second one was proven by Stephen Hawking in 1967 and the third one by Penrose and Hawking together in 1969. Whereas Penrose's 1965 theorem is of relevance to black holes, Hawking's 1967 theorem is of relevance to cosmology. The 1969 theorem resulted from an attempt to formulate one theorem that covers the black-hole situation and the cosmological situation simultaneously. However, the 1969 theorem does not cover either of the earlier theorems as a special case. If one is interested in the gravitational collapse that leads to a black hole, Penrose's 1965 theorem is the most relevant one. Therefore, we will restrict to it in the following. All three theorems

(in a slightly reformulated fashion, and also changing the numbering) are discussed and (almost completely) proven in the monograph by S. Hawking and G. Ellis [The Large-Scale Structure of the Universe, Cambridge UP, 1973)]. An insightful discussion of the singularity theorems can also be found in the textbook by R. Wald [General Relativity, Chicago UP, 1984].

It is important to put the singularity theorems into historic perspective. Before Penrose presented his result, a *generic* gravitational collapse had not been investigated. There was the pioneering work by Oppenheimer and his PhD student Snyder which we have discussed earlier in this course: This was about the gravitational collapse of a spherically symmetric ball of dust. It was found that the collapse ended, after a finite time, in a singularity. Here the term "singularity" means that the mass density and some curvature invariants become infinite, so an observer near this singularity would be ripped apart by infinitely strong tidal forces. The Oppenheimer-Snyder result was not usually considered as particularly dramatic: It was widely believed that the formation of such a singularity was a consequence of the highly idealised assumptions. Most people expected that a star that is *not* perfectly spherically symmetric and *not* a dust would not end up in such a singular state. What Penrose proved was that this expectation was wrong.

For formulating Penrose's theorem we need some terminology. Firstly, and most importantly, we have to clarify how Penrose defined a singularity. It would certainly be desirable to define a spacetime as singular if some curvature invariants become infinite. Such "curvature singularities" occur in all the black-hole spacetimes we have discussed in this course, at $r = 0$ in the spherically symmetric black-hole spacetimes and at the ring $(r = 0, \vartheta = \pi/2)$ in the Kerr spacetime. Unfortunately, until now no one was able to prove that such a curvature singularity forms under generic conditions during gravitational collapse. What Penrose proved was the formation of a weaker kind of singularities. His definition of a singularity refers to incompleteness of geodesics, i.e., to the situation that along a geodesic the affine parameter does not run over all of $\mathbb{R}$:

Definition: A spacetime (M, g) is *singular* if it is not extendable and if there is at least one timelike or lightlike geodesic that is incomplete.

Here the condition of being not extendable means that the spacetime is not a proper subset of some bigger spacetime. Clearly, this condition is necessary because otherwise one could always produce incomplete timelike or lightlike geodesics just by removing points from a perfectly nice spacetime such as e.g. Minkowski spacetime. Probably everybody will agree that incompleteness of a timelike geodesics, where incompleteness means that proper time does not run over all of $\mathbb{R}$, indicates some kind of singularity: If the worldline ends for an observer at a finite proper time, either in the past indicating an initial singularity or in the future indicating an end singularity, this is certainly something disturbing. The situation is maybe not quite so dramatic in the lightlike case: As an affine parameter along a lightlike geodesic cannot be identified with a directly measurable quantity, one might be skeptical about calling incompleteness of a lightlike geodesic a "singularity". Unfortunately, for the theorem it was not possible to restrict to the timelike case.

The theorem is based on three hypotheses. The first one is an "energy condition", i.e., it requires the energy-momentum tensor of the spacetime to have a certain property. The following terminology is used.

Definition: Assume that on a spacetime (M, g) Einstein's field equation $R_{\mu\nu} - (R/2)g_{\mu\nu} + \Lambda g_{\mu\nu} = \kappa T_{\mu\nu}$ holds.

(a) One says that the *weak energy condition* is satisfied if

$$T_{\mu\nu}U^\mu U^\nu \geq 0 \text{ for all } U^\mu \text{ with } g_{\mu\nu}U^\mu U^\nu < 0\,. \tag{459}$$

(b) One says that the *null energy condition* is satisfied if

$$R_{\mu\nu}K^\mu K^\nu \geq 0 \text{ for all } K^\mu \text{ with } g_{\mu\nu}K^\mu K^\nu = 0\,. \tag{460}$$

Clearly, the weak energy condition expresses the fact that all observers measure a non-negative energy density. This is believed to be true for all ordinary matter, i.e., for all matter celestial bodies such as stars are made of. If the weak energy condition holds, then by continuity we also have $T_{\mu\nu}K^\mu K^\nu \geq 0$ for all lightlike vectors. By Einstein's field equation, this implies that the null energy condition holds. So the weak energy condition, which is assumed to hold for all ordinary matter, implies the validity of the null energy condition.

The second hypothesis uses the following notion.

Definition: A subset S of a spacetime is called a *Cauchy surface* if every inextendable timelike curve intersects S exactly once. A spacetime is called *globally hyperbolic* if it admits a Cauchy surface.

The standard example of a Cauchy surface is a hypersurface $t =$ constant in Minkowski spacetime (in standard inertial Minkowski coordinates (ct, x, y, z)), so Minkowski spacetime is globally hyperbolic. Note, however, that not every inextendable spacelike hypersurface in Minkowski spacetime is a Cauchy surface: The hyperboloid $ct = \sqrt{a^2 + x^2 + y^2 + z^2}$ (with a constant $a > 0$) is an inextendable and spacelike hypersurface, but it is not a Cauchy surface; there are timelike curves, asymptotically approaching the light cone $ct = \sqrt{x^2 + y^2 + z^2}$ from below, that do not insersect it. The Kruskal extension of the Schwarzschild spacetime is globally hyperbolic as well: The horizontal cross-section through the middle of the Carter-Penrose diagram on p.17 (which gives a snapshot of the socalled Einstein-Rosen bridge) is a Cauchy surface. By contrast, the regions I and II alone of this diagram (which are covered by the ingoing Eddington-Finkelstein coordinates) do not admit a Cauchy surface, i.e., they are not globally hyperbolic. Note that a Cauchy surface need not be a (smooth) submanifold. However, the following has been proven: If a spacetime admits a Cauchy surface, then it admits a Cauchy surface that is a smooth 3-dimensional spacelike submanifold.

The relevance of this notion becomes clear if one investigates partial differential equations such as the classical wave equation $g^{\mu\nu}\nabla_\mu\nabla_\nu\phi = 0$ on a spacetime: It turns out that existence and uniqueness of a solution to this equation is guaranteed if initial data on a Cauchy surface are prescribed. If a spacetime does not admit a Cauchy surface, such an existence-and-uniqueness theorem does not hold, i.e., the initial-value problem is not well posed.

The third hypothesis uses a notion that was already discussed for the Schwarzschild spacetime and in the Oppenheimer-Snyder collapse, recall in particular Worksheet 7.

Definition: A *closed trapped surface* is a 2-dimensional spacelike submanifold of a spacetime that is diffeomorphic to the 2-sphere S^2 for which both families of orthogonal lightlike directions converge.

To understand this notion we have to recall that the orthocomplement of a 2-dimensional spacelike submanifold is 2-dimensional with signature $(+-)$ at each point. Therefore, there are precisely two lightlike directions in this orthocomplement. In Minkowski spacetime one family of these lightlike directions is diverging and the other one is converging, which corresponds to the natural idea of interpreting the first one as outgoing and the other one as ingoing. We have already seen, however, that in the region $r < 2m$ of a Schwarzschild spacetime for a sphere ($r = \text{constant}, t = \text{constant}$) both families go in the direction of decreasing r, i.e., both families are converging. For spheres with this property Penrose has coined the term "closed trapped surface". Of course, closed trapped surfaces are beyond our ordinary geometric intuition.

Penrose has introduced the term *apparent horizon* for the boundary of the region where closed trapped surfaces exist. In the Schwarzschild spacetime the aparent horizon coincides with the event horizon. We have seen, however, that this is not always true: In the Oppenheimer-Snyder collapse the apparent horizon is different from the event horizon, recall again Worksheet 7. In any case, the presence of closed trapped surfaces indicates the existence of some kind of horizon.

We are now ready to formulate Penrose's singularity theorem.

Theorem (R. Penrose, 1965): Assume that in a spacetime (M, g) the following three hypotheses are satisfied:

(a) The null energy condition holds.
(b) There exists a non-compact Cauchy surface.
(c) There exists a closed trapped surface.

Then there is an incomplete lightlike geodesic.

Note that the hypotheses of this theorem guarantee only the existence of an incomplete *lightlike* geodesic; all timelike geodesics may be complete.

The crucial points are that no symmetry is assumed and that the energy-momentum tensor can be much more general than a dust, it just has to satisfy the null energy condition. Roughly speaking, the theorem expresses the fact that the gravitational collapse of a star leads to a singularity if (a) the star consists of ordinary matter, (b) the state of the star and its surrounding at one instant of time determines this state at every time (i.e., no unpredictable interference comes in from somewhere else), and (c) the collapse has reached a certain stage, indicated by the formation of some kind of horizon. The fact that the Cauchy surface is assumed to be non-compact may be interpreted as saying that the star is isolated: It is very well possible that our universe as a whole admits a *compact* Cauchy surface; such "closed" world models, where the spatial topology of our universe is a 3-sphere or a 3-torus, are seriously considered. However, one would not expect the global topology of the universe to have an effect on the gravitational collapse of a star.

According to the official wording, 50 % of the 2020 Physics Nobel Prize was given to Roger Penrose "for the discovery that black hole formation is a robust prediction of the general theory of relativity". With all due respect, we have to emphasise that this wording is misleading. Penrose's theorem is not about the formation of a black hole; it is about the formation of a singularity inside a black hole. The fact that a black hole is forming is not a result, it is part of the hypotheses, namely by assuming the existence of a closed trapped surface.